

# DIPLOMARBEIT

## Master Thesis

### **Integral Abutment Bridge Design With Thin-Walled Prestressed Precast Bridge Girders**

ausgeführt zum Zwecke der Erlangung des akademischen Grades  
eines Diplom-Ingenieurs/ einer Diplom-Ingenieurin  
unter der Leitung von

O.Univ. Prof. Dr. Johann Kollegger

unter der Mitarbeit von  
Dip.Ing David Wimmer

E212

Institut für Tragkonstruktionen

eingereicht an der Technischen Universität Wien  
Fakultät für Bauingenieurwesen

von

Omar Yerena Rascon  
1028260  
Burgstraße 19/1/13  
3400 Klosterneuburg

Wien, am

Unterschrift

## *Acknowledgement*

Throughout the process of writing my thesis I have had much help from my family, especially from my wife Marlene. My sister, and my parents have always kept me motivated and I hope this project makes them understand why I decided to be so far away from them.

No thesis would be possible without the talent and support of an advisor; therefore, I would also like to thank David for his patience and help given to me during this process.

The Institute of Structural Engineering at the Vienna University of Technology led by professor Kollegger allowed me to work closely in many projects, allowing me to widen my horizons when it comes to structural engineering in every day life. Being able to travel to Obergurgl Tirol to build an ice-structure was one of the highlights of academic time here in Vienna.

Finishing my studies while working full time was very challenging but with support and patience I was able to accomplish it. I hereby also thank my co-workers and my bosses at Raunicher + Partner ZT for being so supportive for me to finish my studies.

## ***Abstract***

Bridge construction has always been part of structural engineering, and has been evolving throughout the years. New construction technologies have been discovered to better use materials and construction techniques. Precast concrete is one of these evolving techniques that are being utilized more and more nowadays. The motivation behind this project is the use of prestressed precast concrete as a realistic replacement to composite construction of bridges.

An existing composite overpass bridge, between the Austrian states of Upper Austria and Salzburg, is taken as a starting point to find out if it is possible to build a bridge with an equivalent bending stiffness with use of thin-walled prestressed precast bridge girders. These bridge girders allow the slenderness of the bridge to stay almost unchanged while decreasing the heavy weights having to be moved around during the construction of the bridge.

The structural analysis of the bridge was carried out by first analyzing a 2-dimensional model to better approximate the prestress needed on each construction phase. Additionally a 3-D analysis was performed on a more accurate model to give the final internal forces with help of the software RFEM from Dlubal and with an excel spreadsheet programed to find the internal stresses on the girders of the structure.

This research illustrates the plausibility of using prestressed precast concrete as a technique in order to build an overpass bridge with a span of ca. 47 m. The design was achieved by modeling the construction of the bridge in 5 construction phases. These phases help illustrate the internal forces at different points on the girders and the bridge's slab due to self weight as well as the prestressing loads being applied on the built in tendons.

The research performed for this project is an addition to ongoing research on prestressed precast bridge construction at the Vienna University of Technology, but it already shows great potential to use prestress precast concrete in order to build structures as slender and stiff such as composite structures.

---

## TABLE OF CONTENTS

<b>1</b>	<b>INTRODUCTION .....</b>	<b>1</b>
<b>2</b>	<b>THEORETICAL BACKGROUND .....</b>	<b>4</b>
2.1	INTEGRAL BRIDGES .....	4
2.1.1	<i>Advantages and Limitations of Integral abutment bridges [8] [9] .....</i>	<i>7</i>
2.2	PRECAST AND PRESTRESSES .....	12
2.3	THIN-WALLED PRECAST PRESTRESSED BRIDGE GIRDERS [2] .....	16
<b>3</b>	<b>APPROACH.....</b>	<b>24</b>
3.1	CONSTRUCTION PHASES .....	24
3.1.1	<i>Construction phase 1 – Transportation and Assembly.....</i>	<i>25</i>
3.1.2	<i>Construction Phase 2 – Redirection Saddles .....</i>	<i>28</i>
3.1.3	<i>Construction Phase 3 Main Prestress .....</i>	<i>30</i>
3.1.4	<i>Construction Phase 4.....</i>	<i>32</i>
3.1.5	<i>Construction Phase 5 (Load Model 1) .....</i>	<i>32</i>
<b>4</b>	<b>LOADS.....</b>	<b>33</b>
4.1	SELF-WEIGHT DISTRIBUTION AND MODELING: .....	34
4.1.1	<i>Abutment and Deck Slab.....</i>	<i>34</i>
4.1.2	<i>Roadbed .....</i>	<i>35</i>
4.1.3	<i>Edge Beams and Sidewalks (Barriers) .....</i>	<i>36</i>
4.2	LOAD MODEL 1 (LIVE LOADS) .....	36
<b>5</b>	<b>PRE-MODELING .....</b>	<b>39</b>
5.1	SOFTWARE MODELING .....	41
5.2	TWO-DIMENSIONAL MODEL EQUIVALENT CROSS-SECTION .....	43
5.3	THREE-DIMENSIONAL MODEL PRESTRESSED CROSS-SECTION .....	44
5.4	FALSEWORK LOADS SUPERPOSITION .....	45
5.5	EUROCODE .....	46
<b>6</b>	<b>ANALYSIS .....</b>	<b>47</b>
6.1	TWO-DIMENSIONAL MODELS .....	47
6.1.1	<i>Construction Phase 1 Assembly / Construction and Self-weight .....</i>	<i>48</i>
6.1.2	<i>Construction Phase 2 Prestressing redirection and in-situ concrete. ....</i>	<i>50</i>
6.1.3	<i>Construction Phase 3 Main Prestressing and in-situ concrete .....</i>	<i>52</i>



---

6.1.4	Construction Phase 4 Final Prestressing .....	54
6.1.5	Construction Phase 5 (Load Model 1) .....	56
6.2	THREE-DIMENSIONAL MODEL.....	58
6.2.1	Construction Phase 1.....	60
6.2.2	Construction Phase 2.....	62
6.2.3	Construction Phase 3.....	64
6.2.4	Construction Phase 4.....	67
6.2.5	Construction Phase 5 (Load Model 1) .....	70
6.2.6	Calculation of Tendons for each Construction Phase 3D Model.....	73
6.3	FALSEWORK ANALYSIS .....	76
6.4	STRESS COMPARISON (5 PHASES VS. FALSEWORK AND CREEP).....	81
6.5	ULTIMATE LIMIT STATE ANALYSIS.....	89
<b>7</b>	<b>SUMMARY AND CONCLUSIONS.....</b>	<b>90</b>
	<b>WORKS CITED.....</b>	<b>91</b>
	<b>LIST OF TABLES AND FIGURES.....</b>	<b>93</b>
<b>8</b>	<b>APPENDICES.....</b>	<b>96</b>
8.1	APPENDIX 1 (2D STRESS ANALYSIS) .....	97
8.2	APPENDIX 2 (3D STRESS ANALYSIS) .....	98
8.3	APPENDIX 3 (FALSEWORK STRESS ANALYSIS) .....	99
8.4	CREEP COEFFICIENT .....	141
8.5	EFFECTIVE FLANGE WIDTH $B_{EFF}$ .....	145
8.6	ULTIMATE LIMIT STATE ANALYSIS OF BEAMS .....	147
8.6.1	Midspan Center Beam Reinforcement Analysis .....	147
8.6.2	Longitudinal Reinforcement in girders.....	159
8.6.3	Shear Reinforcement.....	160
8.6.4	Slab Reinforcement: .....	161

# 1 Introduction

This master's thesis explores the possibility of building an integral bridge, which already exists, with use of prestressed thin-walled precast beams. The existing overpass integral bridge, located on the A1 Westautobahn in the Austrian city of Seewalchen, was built with steel beams and a concrete deck slab (Figure 1).

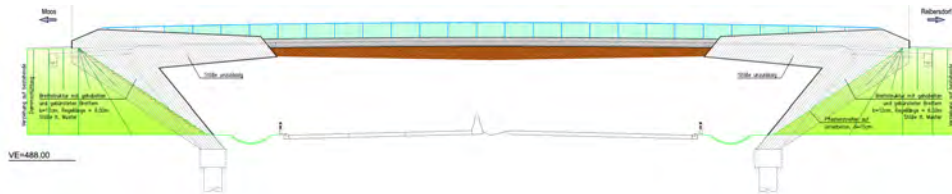


Figure 1: Existing Overpass bridge on the A1 Autobahn in Austria [1]

This thesis explores a different approach to designing an already built overpass integral abutment bridge on the A1 Westautobahn in Austria by making use of thin-walled precast prestressed bridge girders.

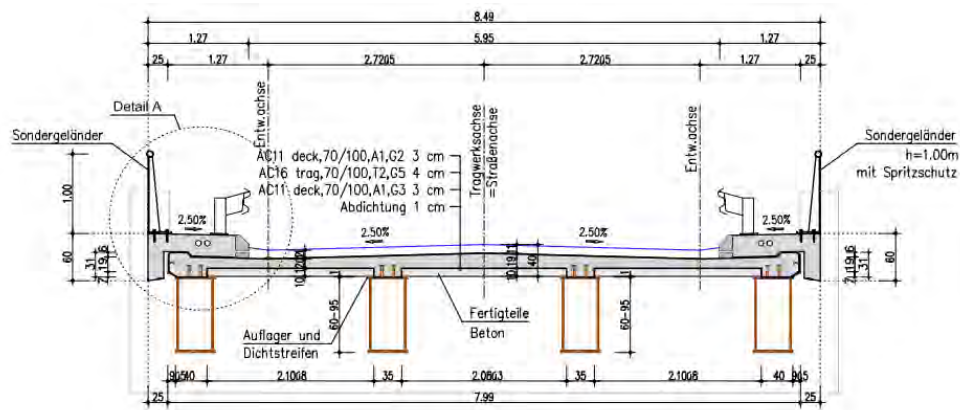


Figure 2: Composite Integral Bridge Cross-Section.

The previous figure (Figure 2) illustrates the cross-section of the already built composite integral bridge. This cross-section has a very slender design limited mostly only to composite construction; this thesis explores the possibility of using the advantages of precast and prestressed concrete construction in order to achieve

concrete bridge with a comparable slenderness. In future chapters the subject of prestress precast concrete will be explored more in depth to help understand the advantages of using these construction techniques. And most importantly, the research done at the institute for structural engineering of the Vienna University of Technology on thin-walled prestressed precast bridge girders is the design foundation on which this project is built on.

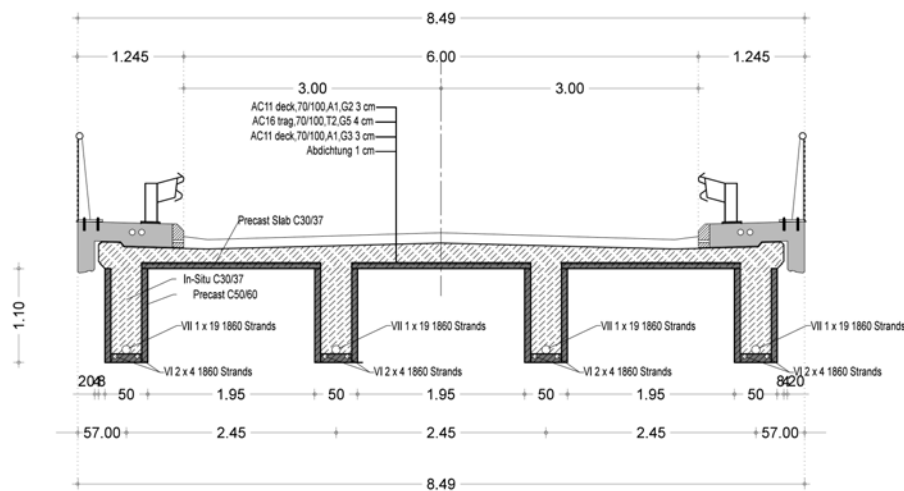


Figure 3: Reinforced Concrete Integral Bridge Cross-Section.

The thin-walled girders (see chapter 2.3 for design theory) replace the steel girders as illustrated in Figure 3. The work in this thesis explains the design needed in order to achieve a slender yet strong concrete construction. The design of the bridge was performed with help of finite element method software analysis of 2D and 3D models. These models simulate the construction of a bridge in construction phases. The construction phases are used in order to simulate the different stresses and internal forces resulting from the different steps involved in bridge design.

The approach taken in this thesis is to first define and give a theoretical background of the different construction methods used to design the already built overpass integral bridge. These methods are the following three:

- Integral Abutment Bridges
- Precast and Prestress
- Thin-walled Precast Prestressed Bridge Girders

What is it implied when mentioning the term integral bridge / integral abutment bridge? This definition is looked at from different sources, which all conclude in the same definition for these type of bridges.

The scope of this thesis is very wide and it is based mainly on the use of prestress and precast concrete. These two techniques are the main source of inspiration for the bridge construction methodology reported in this thesis. Therefore, it is imperative to define and explore different uses of prestress and precast in other projects

The last theoretical background is given on the suggested approach to build a similar integral bridge to replace the composite system used in the bridge with use of thin-walled precast prestressed bridge girders developed by the Research Center of Structural Concrete of the Vienna University of Technology [2] [3] [4]. The development of thin-walled precast beam structures is also explored in the following chapter to better understand the methodology used to design the already built overpass integral bridge.

The theoretical backgrounds for the construction methods considered in this thesis are very important to better understand this project. Additionally, it is also imperative to understand what loading was considered while designing the bridge. The software models used are also well documented in the following chapters of this thesis. The software model chapter explores the different methods used to analyze the bridge's loads and stresses being a 2-Dimensional and a 3-Dimensional analysis of the bridge.

The analysis chapter explores all the results of stress curves of the bridge's girders for both the 2D and 3D analysis, and includes the additional analysis for the ultimate limit state. Additional information to this chapter, such as the complete printouts of internal loads and stress curves for the 2D and 3D models is located in the Appendices of this thesis.

Lastly, the summary and conclusions chapter of this thesis discusses the results from the finite element models and calculations done throughout this investigation.

## ***2 Theoretical Background***

### ***2.1 Integral Bridges***

To first understand the construction advantage and disadvantages of integral bridges it is imperative to first define and explain what integral bridges are. There are many definitions from different sources of which types of bridges may be considered as integral bridges, here are some of these definitions:

An integral bridge may be defined as having no expansion joints or sliding bearings, the deck is continuous across the length of the bridge. Integral bridges are alternatively referred to as integral abutment bridges, jointless bridges, integral bent bridges and rigid-frame bridges. Semi-integral or integral backwall bridges typically have sliding bearings, but no expansion joints [5].

Integral abutment bridges can be described as bridges generally built with their superstructures integral with the abutments, and without expansion or contraction joints for the entire length of the superstructure. The abutments, being cast integral with the superstructure, avoid expansion joints and movement bearings that otherwise require regular maintenance [6].

As defined by Burke Jr., integral bridges refer to single- or multi-span continuous bridges without movable deck joints at the superstructure/abutment interface [7], being normally supported by embankments with sub-type abutments on flexible piles [8].

Integral bridges have been around for many years but in recent years their use has been more popular in the construction of new bridges as well as the refurbishment of old ones because of its advantages. The work done in this project reflects the use of an integral abutment bridge with a span of approximately 47 m. Figuring out what is the maximum length of integral bridges has been a subject widely explored by many researchers and engineers because of the advantages of building bridges with this type of techniques.

In traditional bridges, the use of expansion joints, roller supports, abutment bearings and other structural releases to account for cyclic thermal expansion and contraction, creep and shrinkage. The use of all these joints has over the years proven to be expensive to design, build, and maintain. During the 1960 when speed and traffic loads were significantly higher, problems with joints emerged. The continuous maintenance and replacement of expansion joints has been a big problem in many of the current bridges. In order to avoid the problems created by expansion joints, lack of maintenance and also high manufacturing costs, the use of integral abutment bridges has been beneficial in the construction of new and replacement bridges.

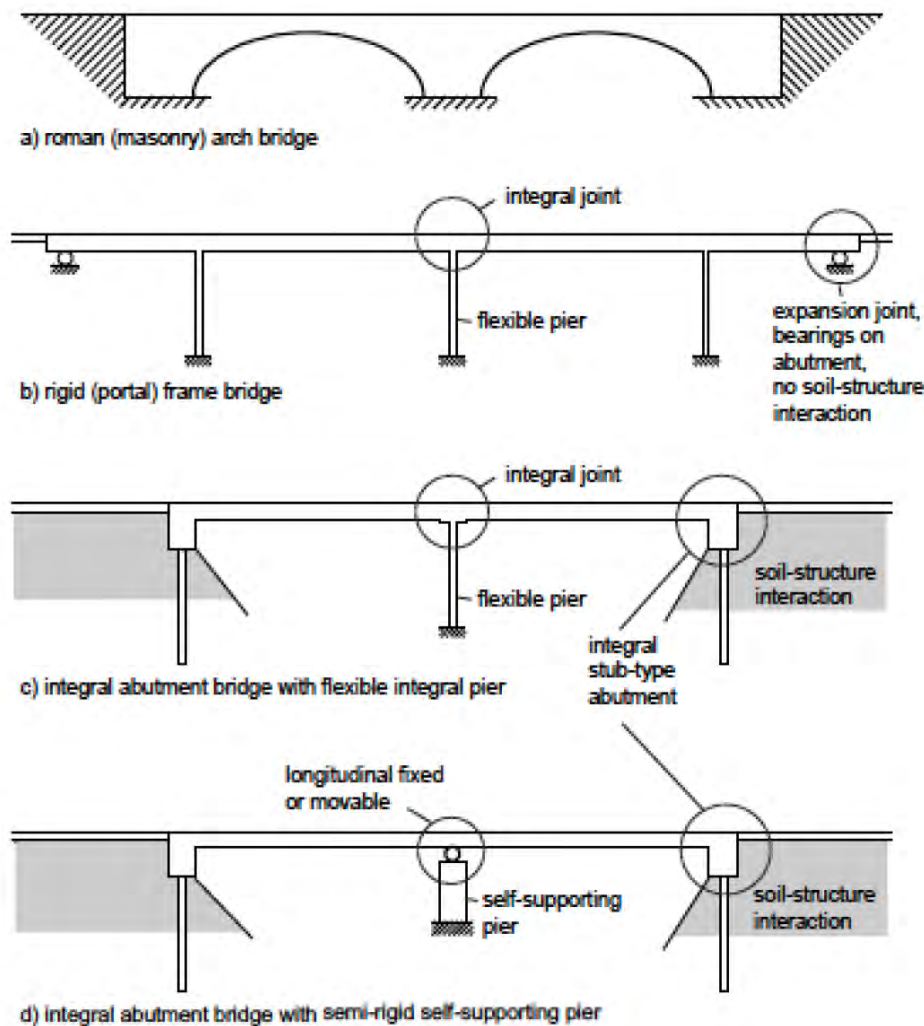
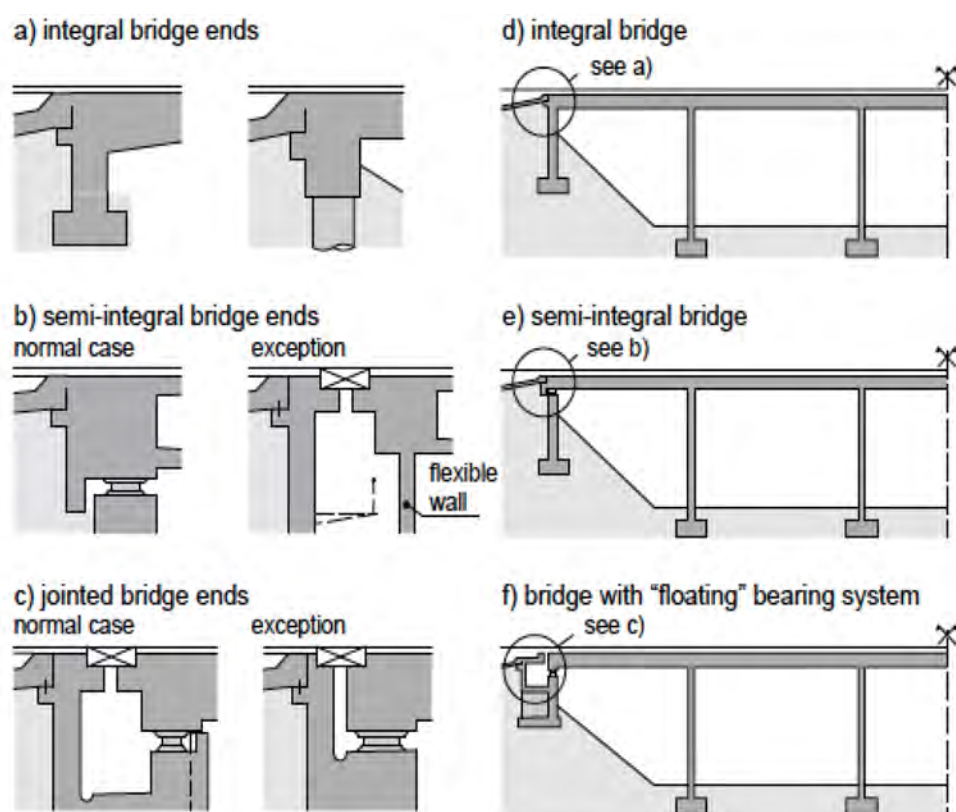


Figure 4: Comparison of Integral Abutment Bridge to other Jointless Bridges [8]

The use of jointless bridges is illustrated in Figure 4, and it shows how the roman (masonry) arch bridge type has existed for now centuries. The idea of not having to replace parts and reduce maintenance is one of the improvements in bridge construction. [9]



detailing of deck and piers detailing of bridge ends	deck monolithic (jointless)		deck with joint(s)
	all piers monolithic with deck or no piers	pier(s) with bearings or joints (top/bottom)	("gerber"-type joint, joint over piers, ...)
both bridge ends integral	integral bridge		jointed bridge
one bridge end semi-integral, other bridge end integral or semi-integral		semi-integral bridge	
at least one bridge end jointed (= with expansion joint)		"floating" bearing system (1)	

(1) both bridge ends with expansion joint and sliding bearings (longitudinally movable).

Figure 5: Integral Bridges according to the Swiss Federal Roads Office [8]

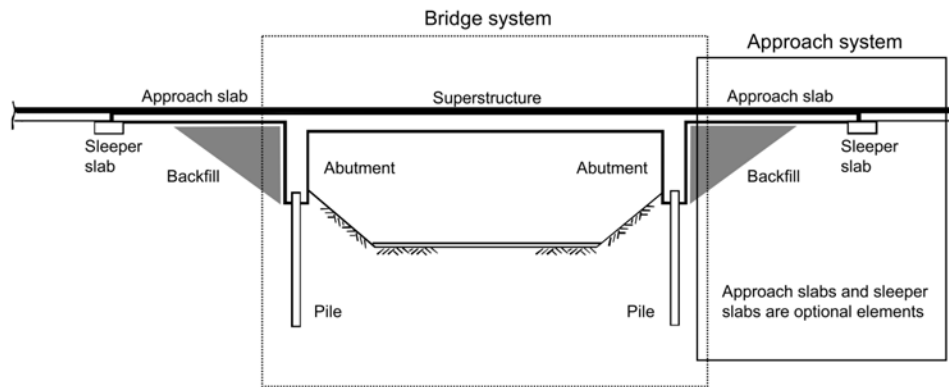


Figure 6: Simplified Geometry of an Integral Abutment Bridge [9].

### 2.1.1 Advantages and Limitations of Integral abutment bridges [8] [9]

Integral bridges are nowadays growing in popularity in rural and urban highways because of their many advantages. Originally, as a reaction to the destructive effects of leaking movable deck joints and massive pavement pressures, it became very clear that this type of bridge construction has more advantages and fewer limitations than the classical bridge construction with joints.

#### Advantages

##### Reduced Substructure Cost

First and foremost, multiple span integral bridges with embankments and pile supported stub-type abutments are composite structures. Whereas single span jointed bridges with wall-type abutments must be designed to support embankments, continuous multiple span integral bridges on the other hand are built compositely with embankments and are supported by them. For jointed bridges, expensive wall-type abutments and abutment foundations are needed to support embankments. Integral abutment bridges receive much of their longitudinal and lateral support from embankments.

##### No Bearing and Joints

One of the most noticeable differences is the lack of bearings and deck joints in integral bridges. Not only does this result in savings in initial costs, the absence of joints and bearings will reduce maintenance efforts. This is an important benefit



because presently available deck joint sealing devices have such short effective service lives.

### Simplified Construction

The simple characteristics of integral bridges make for rapid and economical construction. For example, there is no need to construct cofferdams, make footing excavations, place backfill, remove cofferdams, prepare bridge seats, place bearings, backwalls, and deck joints. Instead, integral construction generally results in just four concrete placement days. After the embankments, piles, and pile caps have been placed and deck stringers erected, deck slabs, continuity connections, and approach slabs can follow in rapid succession. In extreme cases, some multiple span integral bridges have been completed with just two concrete placement days; one for the structure itself, and one for the approach slabs.

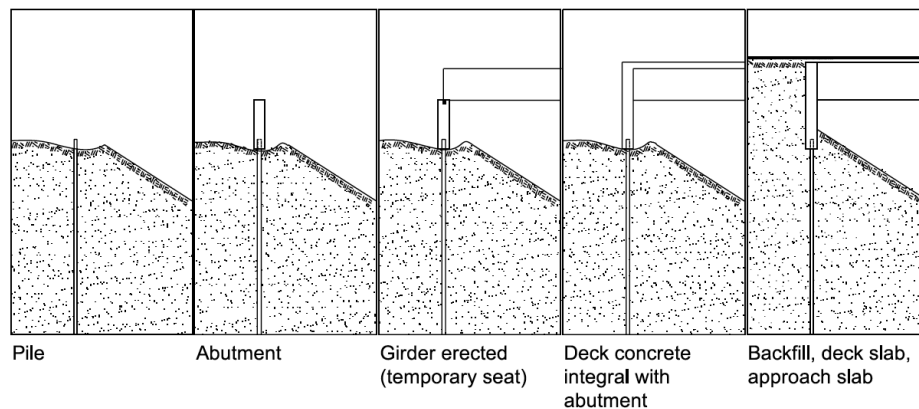


Figure 7: Typical construction phases of integral abutments. [8]

### Minimized Deterioration

The most obvious reason why integral bridges have become so popular, especially with transportation departments located in and above the Snow Belt, is their outstanding resistance to deicing chemical corrosion and deterioration. Since these bridges do not have movable deck joints at abutments (Figure 8), deck drainage contaminated by deicing chemicals cannot penetrate bridge deck slabs and adversely affect the primary bridge members.

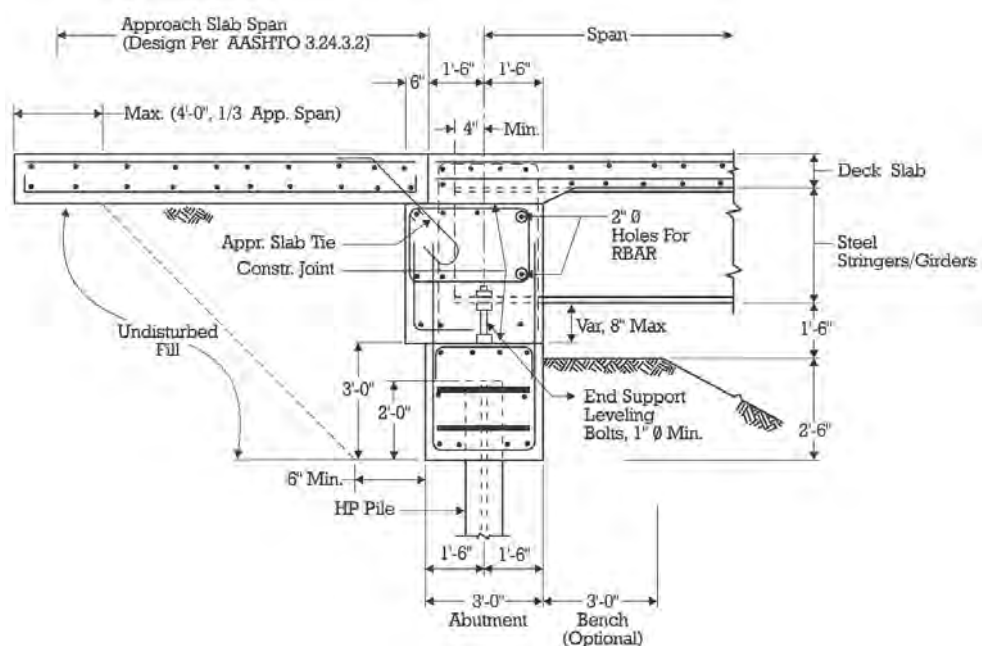


Figure 8: Integral abutment. [10]

### Simplified Bridge Replacement

When using multiple span integral bridges to replace single span structures with wall-type abutments, the great adaptability of integral bridges allows them to span across existing foundations, thus avoiding the need to remove them. Since small bridges are usually replaced in 50-year cycles, use of integral bridges with their simple pile foundations will considerably simplify future bridge replacements. Also, the more durable integral bridges should help to increase the serviceable bridge age and extend replacement cycles by two or more decades.

### Extraordinary Resistance

One of the most important attributes of integral bridges, an attribute that is seldom recognized, is their substantial reserve strength capacity. The integrity of their unified structural system makes them extremely resistant to the potentially damaging effects of illegal super-loads; pressures generated by the restrained growth of jointed rigid pavements, earthquakes, and debris-laden flood flows.

### Secondary Effects

Like most of their jointed bridge counterparts, integral bridges are subjected to secondary effects due to shrinkage, creep, thermal gradients, differential settlement, and differential deflections. They are also subjected to passive pressure effects when abutment backfill is compressed during superstructure elongation, and

to pavement relief joint pressures when moisture and sustained high temperatures trigger pavement growth. The stress levels generated by these secondary effects are generally understood but as yet not well quantified. However, they can be controlled and be provided for to such an extent that except for continuity connections at supports, they usually need not be considered when designing short single span or multiple span continuous bridges less than 300 feet long (ca. 90 m). This simplification is possible because design specifications usually permit higher stresses when secondary stresses (shrinkage, creep, passive pressure, etc.) are combined with primary stresses (dead load, live load, and impact) to determine maximum allowable service stresses. Also, it should be emphasized that the secondary effects do not alter the ultimate load capacity of the structure.

#### Limitations

##### Design of Continuous Spans

Although the characteristics of integral bridges provide many design simplifications, their unified structural system does require the design of continuous spans for multiple span bridges. However, with the help of computer programs and design aids, the extra effort of designing continuous spans can be minimized. With the development of State standard designs for a wide range of three and four span continuous bridges, even this extra effort can be further minimized.

##### Approach Slabs

Integral bridges should be provided with approach slabs to prevent vehicular traffic from consolidating backfill adjacent to abutments, to eliminate live load surcharging of backfill, and to minimize the adverse effect of consolidating backfill and approach embankments on movement of vehicular traffic. For bridges with closed decks (curbs, barriers, etc.), approach slabs should be provided with curbs to confine and carry deck drainage across backfill to the approaches and prevent erosion, or saturation and freezing of the backfill. Because of the continual cyclic movement of integral bridges, approach slabs must be anchored to the bridges; otherwise, continual bridge movement and joint infiltration will shift slabs toward flexible approach pavement, away from abutments and off the approach slab seats.

### Joints off the Bridge

Cycle control joints, joints which facilitate longitudinal cycling of bridges and approach slabs, should be provided between approach slabs and approach pavement. For the shortest bridges, the usual pavement expansion joint should be sufficient. For longer bridges, however, specially designed cycle control joints should be devised and provided.

### Pile Loading

One primary concern expressed about the construction of integral bridges with pile supported flexible abutments is the uncertainty about abutment pile flexural stresses. However, for typical two and three span bridges, the amount of thermal movement is less than an inch. Consequently, these stresses generally can be ignored. For longer bridges, actual bridge performance has shown that high pile flexural stresses do not adversely affect bridge performance.

### Buoyancy and Uplift.

Care must be exercised when using integral bridges for stream crossings because most deck type integral bridges are buoyant. Consequently, for those bridges with superstructures that can become submerged, air vents must be provided through the top of beam webs, and anchorage to piers should be considered. For multiple span bridges with short end-spans, deck slab concrete for the end-spans must be placed first to prevent end-span uplift during deck slab placement. Once constructed, however, integral bridges are more resistant to end-span uplift than their continuous end-jointed bridge counterparts since the substantial weight of integral abutments provides the necessary uplift restraint, even for end-to-center span length ratios down to 0.5 and below.

### Embankments

Since integral bridges receive significant support from embankments, such bridges should be built only in conjunction with stable, well-consolidated embankments. Consequently, integral bridge embankments must be constructed first to ensure that embankments and sub-foundation soils are consolidated and stabilized before the flexible pier and abutment piles are driven.

## 2.2 *Precast and Prestress*



Figure 9: Walnut Lane Memorial Bridge in Philadelphia [11].

The single most important event leading to the launching of the precast/prestressed concrete industry in North America was the construction in 1950 of the famed Walnut Lane Memorial Bridge Figure 9. By the time of construction there was little published information and there was a total lack of experience with linear prestressing in the US. [12].

The existence of precast is somehow the proof needed to see that it is a very innovative construction type. In global terms, the market share of precast 'grey' frames' (structural concrete with no architectural qualities') is probably around 5 percent of the multistory business. However, for precast structures with an integrated facade or other decorative features, the global market share is closer to 15 %, being as high as 70 % in the colder climates and/or where site labor is expensive. [13]

In some cases the use of precast concrete may not be as cost effective, such case is when labor is not expensive, for example, where local labor policies demand high levels of unskilled site labor, heavy concrete prefabricates create the potential for new safety hazards due to transportation, handling and temporary stability. Similarly in countries with a strong steel industry and widespread education in steelwork design, the popular opinion is that precast cannot compete with structural steelwork frames.

According to the PCI design book for Precast and Prestressed Concrete [12] precast in PCI certified plants ensures the manufacture of high quality architectural and structural products. Precasting also facilitates production of a wide variety of shapes and sizes, and the use of prestressing substantially extends the span capability of products. Similarly, prestressing, defined by ACI as “...internal stresses (that) have been introduced to reduce potential tensile stresses in concrete resulting from loads,” can be used to enhance structural capabilities of a concrete member. These capabilities enable architects and engineers to achieve highly innovative and economically competitive buildings and other structures.

The following are examples of some of the unique features of precast and prestressed concrete:

- Construction speed.
- Plant-fabrication quality control.
- Fire resistance and durability.
- With prestressing: greater span-to-depth ratios, more controllable performance, less material usage.
- With architectural precast concrete: wide variety of highly attractive surfaces, shapes, finishes and colors.
- Thermal and acoustical control.
- All weather construction.

While precast and prestressed concrete can be manufactured in a variety of customized sizes and shapes, maximum economy is achieved by using the common products that have evolved in the industry. Some of the most prevalent products can be seen in Figure 10, this figure also illustrates how the use of thin-walled precast is not widely used, making this research very relevant in the construction industry.

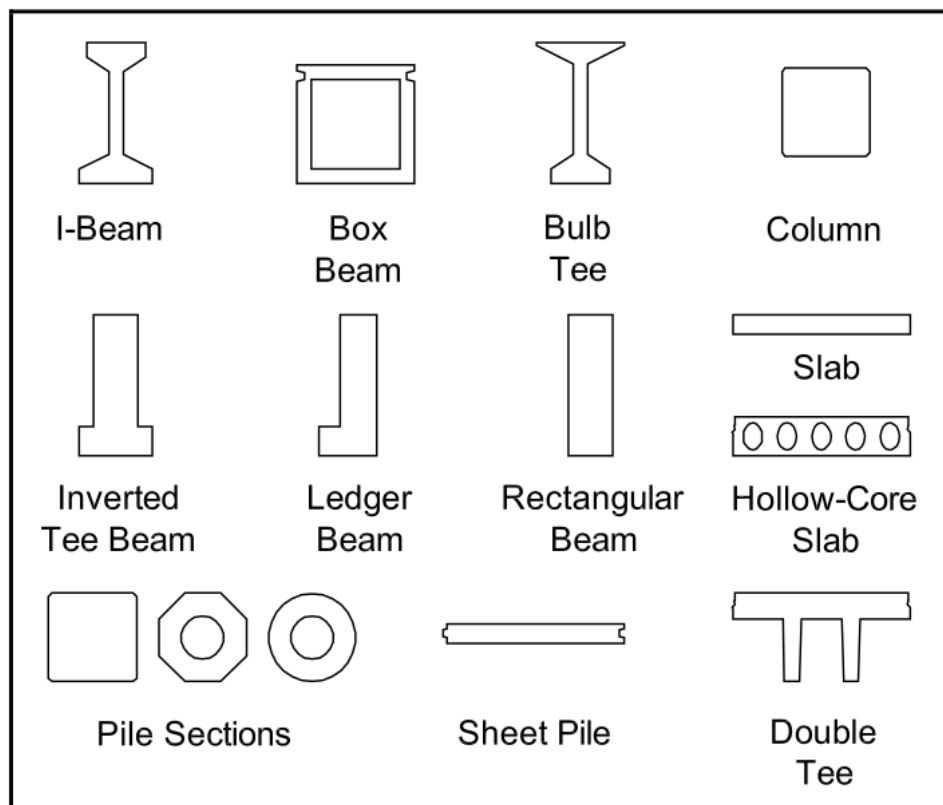


Figure 10: Common precast and prestressed concrete products. [12]

The main goal of Prestressing structures is to cover the internal stresses caused by the loading effects. Working against the stresses that appear during the serviceability limit state and through prestressing avoidance of larger cracks is possible.

During the normal use of a bridge, internal forces appear. These internal forces can be resisted by the use of prestressing methods. The addition of prestress to a bridge girder for example would not create additional strength to the structure but it makes the structure stiffer and helps the structure to take the stresses created during the serviceability limit state. By prestressing the concrete structure cracks can be almost altogether avoided or in some cases just minimized to appear within the normed limits. [14] [15]

There are three types of Prestressing:

- Prestressing with immediate bonding
- Prestressing with late bonding
- Prestressing without bonding (internal and also external)

Figure 11 illustrates the steps required to prestress a structure while using a center-hole jack.

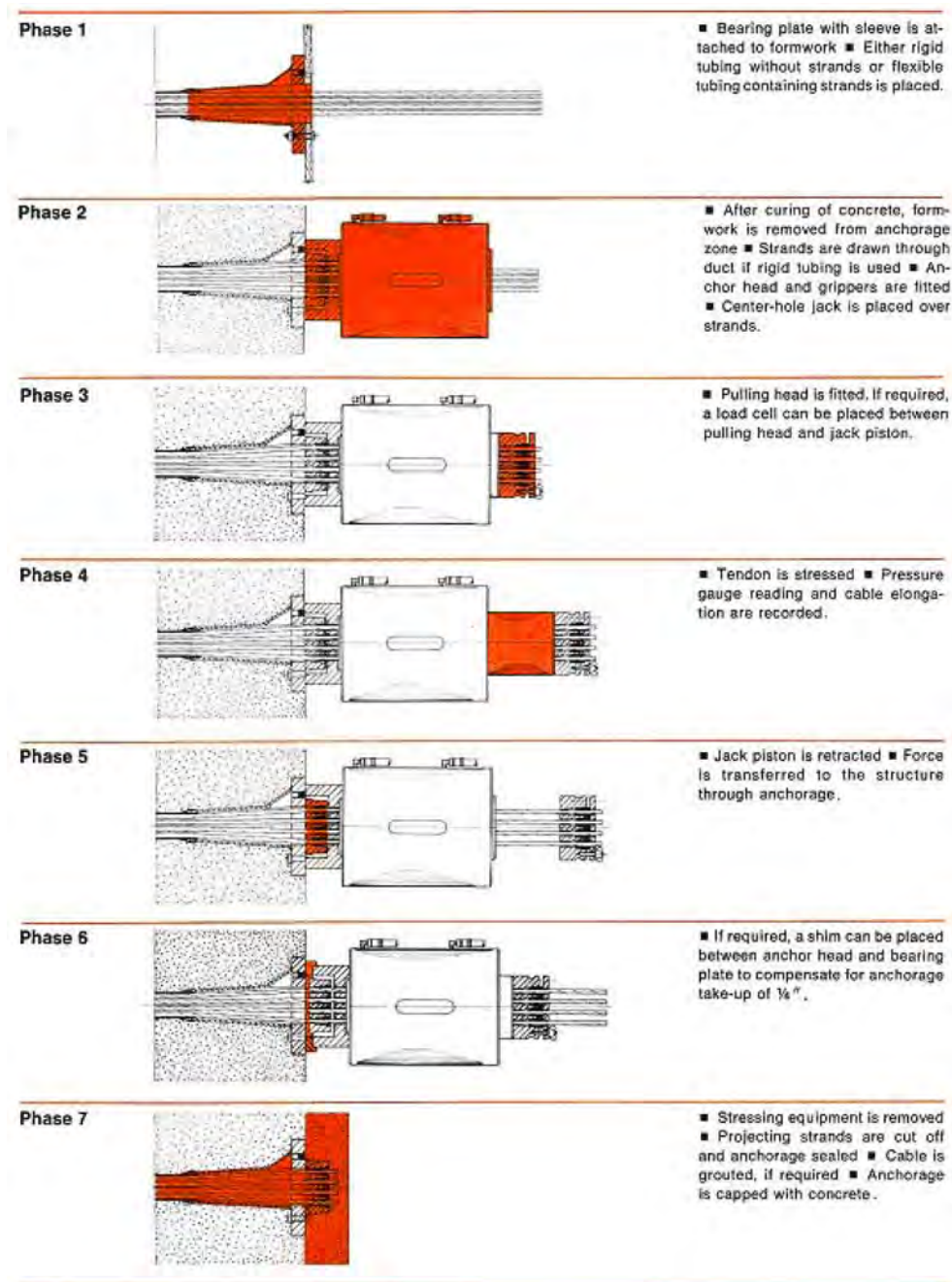


Figure 11: Complete jacking sequence VSL corporation [16]



### **2.3 *Thin-Walled Precast Prestress Bridge Girders [2]***

A research project conducted at the Institute for Structural Engineering at the Vienna University of Technology applied the known technologies lattice-girders floor slabs and double-wall elements in order to implement them in bridge construction and civil engineering. This research makes use of semi-precast elements of 5-7 cm thick to use them as formwork to subsequently add in-situ concrete and creates a bridge girder. The objective of this research was to create precast girders, which could be then transported and erected easily by common transportation and lifting equipment. These girders could then be used as formwork reducing considerably the use of formwork and scaffolding.

One of the biggest advantages of this method is that much of necessary reinforcement as well as the prestress tendons can be built into the girder at the precast production plant, reducing construction time at the site as well as reducing the times the roads have to be closed or rerouted. Additionally, weather stops being a factor needed to be taken into consideration when casting concrete at a precast plant with controlled environment, therefore achieving higher concrete quality.

The connection between the roadway slab and the girders is achievable with conventional connecting reinforcement and avoids the need to use expensive welded-on head-bolt dowels, which composite steel-concrete requires. All these advantages show that reinforced concrete can start being successfully used in bridge construction instead of steel and composite concrete-steel, which are usually used for slender girder bridges.

Two production methods were examined in the course of this research producing one 30-meter girder from each one of them. The methods were the following:

- Conventional lattice-girder floor slabs with strong base plate
- [17]Double-wall elements (Manufactured in a fully automated rotary production system)

The first manufacturing method made use of conventional lattice-girder floor slabs and a base plate as seen in Figure 12. These precast floor plates with a thickness between 5 and 7 cm were manufactured using a conventional method. The plates were placed on a formwork table to serve as wall elements and stirrup reinforcement was then installed at the bottom end of the slabs to supply the plates with a concrete base of about 10 to 20 cm thick. In order to obtain a stiff cross-section during the construction phase, a horizontal system of reinforcing bars was welded to the upper side. Additional tendons for prestressing can be built into the cross-section at the required height and location. The maximum transportation length of this type of girders is 38 meters, but shorter girders may also be assembled together on site by means of continuous tendons. This construction method can be chosen for bridge structures with spans between 20 and 50 meters.



Figure 12: Conventional lattice-girder floor slab. [2]

The second production method makes use of double-wall elements, further increasing the degree of prefabrication and minimizing the complexity of the work during manufacturing. This method eliminates the use of lattice-girders floor slabs. The elements were manufactured on a fully automated rotary precast bed. The sidewalls were cast first and then rotated into an upright position where a 10 to 20 cm thick slab was cast as the floor of the girder. Figure 13 illustrates the rotary formwork table, which was used to cast the sidewalls of the girder, there it can be seen that one side is cast first, then the whole cage is rotated to cast the other sidewall and then the floor slab is cast.



Figure 13: Double-wall element Rotary table. [2]

The process limits the maximal width of the double-wall elements to 50 cm. This width limitation also limits the use of this type of girders for short span bridges, since the width limits the amount of tendons that fit in the cross-section.

Both girders were tested at a large scale to provide insights on how to speed-up the production and improve the structural properties of this new type of construction.



Figure 14: Complete double-wall element bridge girder. [2]

Based on the results obtained from research projects performed to this date, it can be seen that the use of precast floor plates or double-wall elements is technically possible and represents a cost-efficient alternative for the construction of bridges and civil engineering structures. This type of construction represents an advancement for concrete bridges with short spans.

Compared to steel girders, considerable cost-savings can be gained just by reducing the weight that needed to be lifted during the construction phase.

The through-shaped precast concrete components compared to the prestressed concrete girders, have the advantage of having of considerably less weight, while having the same load

bearing capacity, therefore allowing concrete to be considered for construction of structures previously limited only to steel construction. The research on thin-walled precast prestressed girders is an ongoing project at the Institute for Structural Engineering at Vienna University of Technology with opportunity to improvements and innovation in the following years. [2]



The use of KAP-STEEL-Waves as a replacement to lattice girders is a new advancement for the constructing of thin-walled precast girders.



Figure 15: Double Wall Element (DWE) [17]

The use of the double-wall is increasing rapidly, because it substitutes cast-in-place concrete walls. This type of construction is not only used for the high surface quality, but also because of the exact production- and quality control as well as the quick construction process. Double walls are widely used in construction nowadays because of the high cost effectiveness and quality, and also because of its flexibility, it can be used for industrial, and commercial buildings, basement walls, floor walls, staircase walls fire-protection walls, and many other uses, such as bridge girders. This flexibility allows a real use of double walls on construction as a replacement to cast-in place concrete walls.

The thin-walled girders share a very similar design to double-walled elements therefore; these new technology may also be utilized

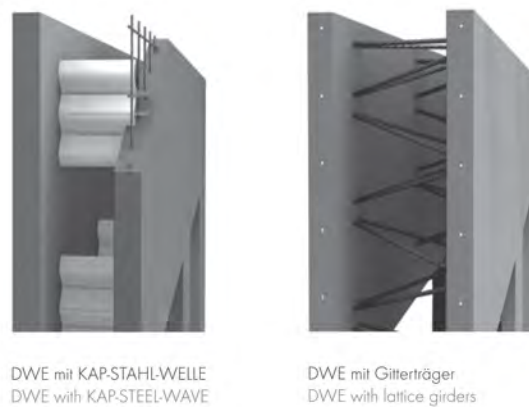


Figure 16: Double Wall View with KAP Steel [17].

The incorporation of the KAP-Steel-Waves during the construction of the double-wall has revolutionized the industry. The KAPPEMA technology further enhances the usability of the double wall. The wall system, manufactured with the new innovative KAP-Wave elements, optimizes the handling during the onsite production, and simplifies the everyday production and for the first time, it allows changes during the installation of the double wall. The disadvantages of conventional lattice girders are solved through the use of the KAP-STEEL-WAVE.

The wave, in connection with form rods made out of high-quality steel, withstand high extraction forces, to overcome shear forces as well as to secure the join compounds. Therefore, high amount of casting pressure can be absorbed.

With the conventional DWE-System the lattice girders remain in the reinforcement layers, serving at the same time as a spacers and consequently influencing the wall thickness.

Heavy concrete shells result from the use of conventional lattice girders, but the KAPPEMA system does not need the usual 17 mm, specified by most construction standards, to have enough pullout strength.

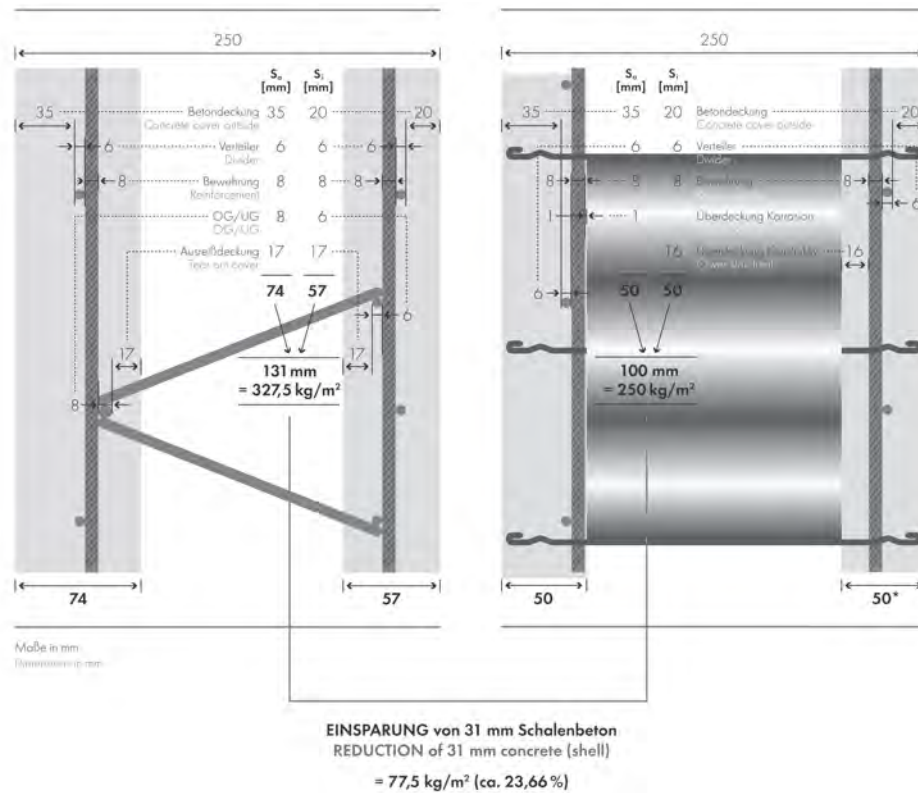


Figure 17: Image comparing lattice girders and KAP Steel

The KAP-STEEL-WAVE is very transportable and easy to install. The waves can be stacked on EUR-pallets weighing approximately 300 kg for 700 m² of Double-Wall-Elements. The Waves are then installed during casting every 80 cm. The use of these Wave elements is much simpler than the lattice girders because the Waves are very light, maneuverable and easy to store.



Figure 18: Image of Horizontal formwork table + EUR-pallet

The KAP-STEEL-WAVE system is used as a replacement of lattice girders because of its many advantages. The main advantage of the KAP system is the location of the waves because it allows a more adequate position of the prestressed ducts. On the other hand, the lattice girder were always on the way and had to be cut or repositioned in order to allow the prestressing ducts to be placed into position, adding time and effort to the construction of the beams.



Figure 19: Formwork table for production of Double-Wall-Elements (DWE)



### 3 Approach

#### 3.1 Construction Phases

For the modeling of this bridge 4 construction phases were considered with an additional phase being the Load Model 1 modeled after the load model 1 found in the Eurocode [18]. These five construction phases were chosen in order to gradually increase the weight of the bridge as well as the amount of prestress on the bridge main beams. With the equivalent bending stiffness cross-section it was possible to start pre-dimensioning the bridge's properties.

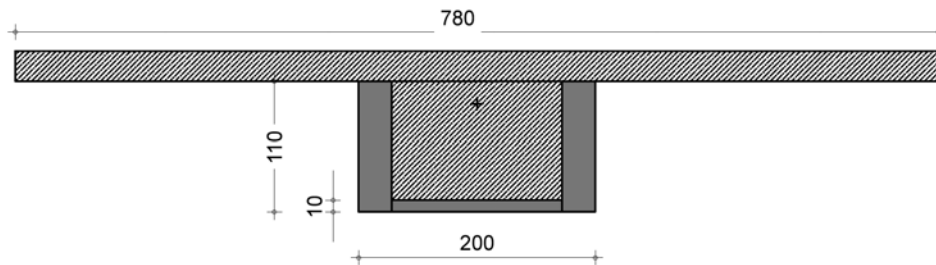


Figure 20: 2D Model Equivalent Cross-Section.

The equivalent cross-section seen in Figure 20 was used to calculate the bending moments due to self-weight and prestresses as well as the normal forces due to prestresses.

A very important requirement for the design of the bridge was to have compression stresses throughout the structure (on the top and bottom of the beams) in order to avoid tensile cracks on the concrete during the construction process. The compressive stresses on the bridge beams were required to stay within a specific stress range in order to not be over compressed and to not have any tensile stresses.

### 3.1.1 Construction phase 1 – Transportation and Assembly

The first construction phase consisted on having the precast concrete beam with already prestressed tendons built into it. These prestresses were large enough to fight back the deformations due to the precast beam's self-weight and any additional deformations due to lifting the beams, as well as to have additional prestress for the next construction phases. These prestresses allow the beams to be lifted and put into place without suffering deformations due to self-weight.

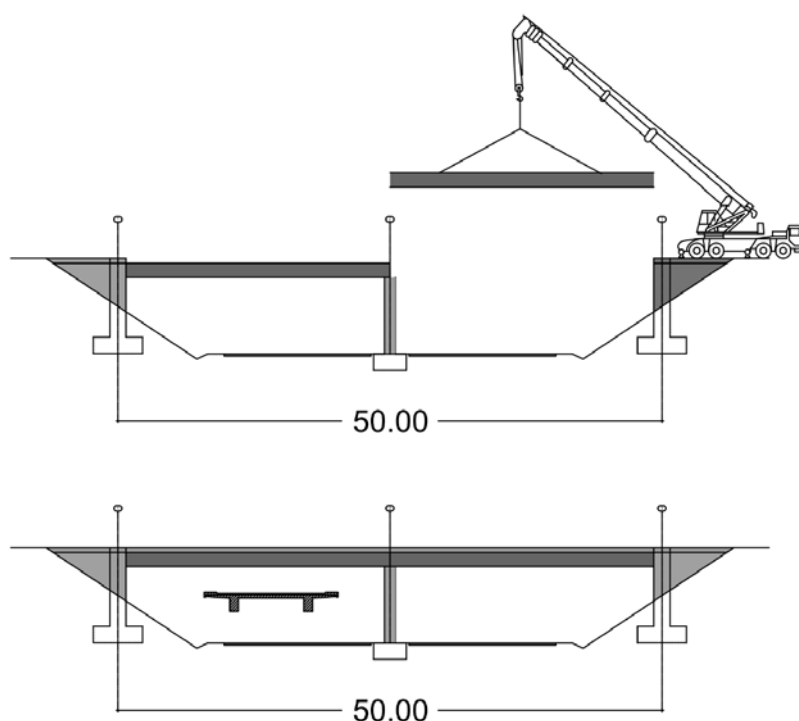


Figure 21: Example of Transportation and Assembly of a 2 span girder bridge. [2]

Once the precast prestressed beams are placed onto the abutments there is no access to the prestress tendons, therefore the first prestress loads in the beams has to be large enough to resist the self-weight of the precast beam as well as the additional weight due to the in-situ concrete. Because of the fact that the prestressed tendons inside of the precast are not accessible after being mounted on the abutments, the prestresses were positioned as close to the edge as possible to increase the tensile strength of the beam. The prestress load for the construction

phase was chosen based on the self-weight of the precast beam plus the self-weight of construction phase 2, this prestress load has to be large enough to keep all stresses in the beam in compression. The prestressed tendons are located at the bottom of the precast beam at the midspan and once they reach the redirection saddles the tendons then are anchored at the height of the center of mass of the precast beam.

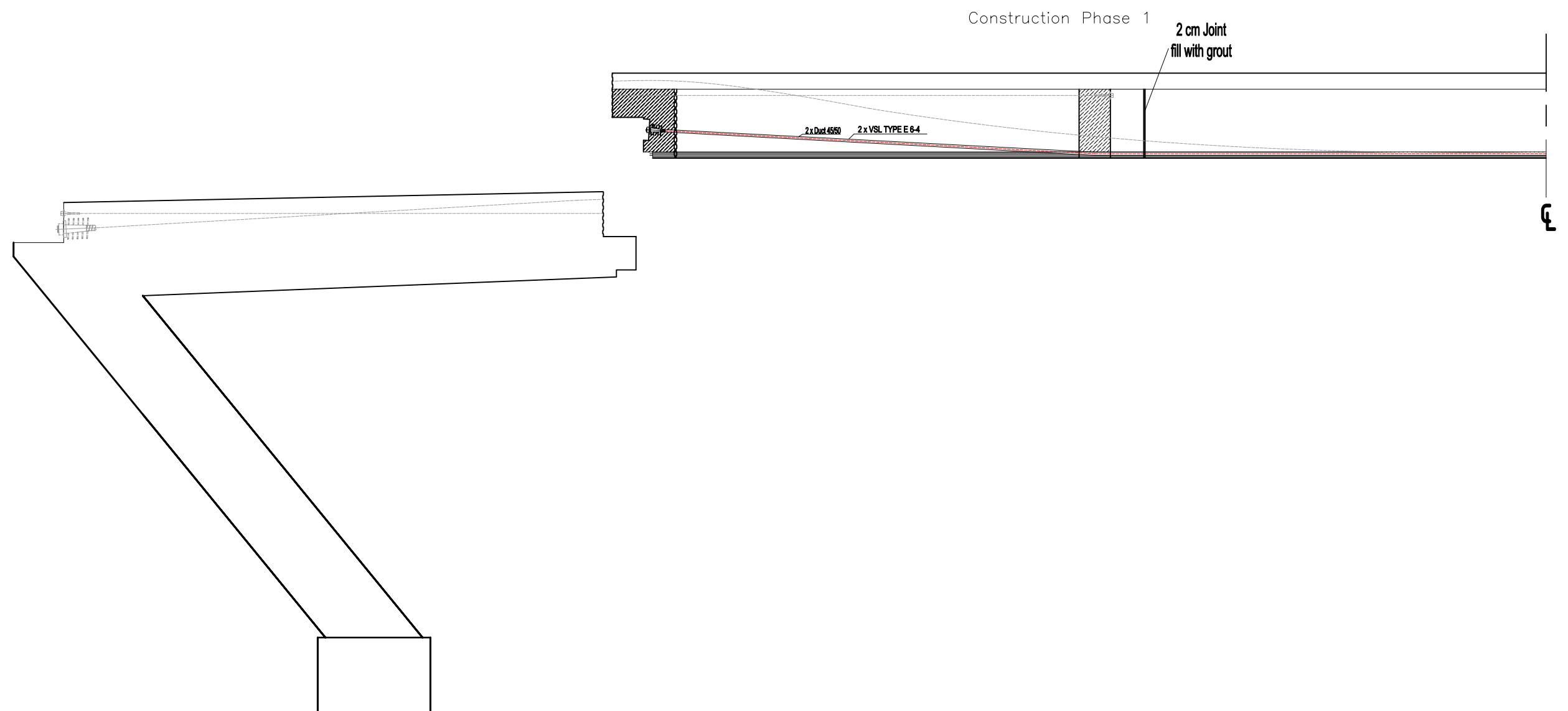


Figure 22: Tendons position Construction Phase 1

### **3.1.2 Construction Phase 2 – Redirection Saddles**

The second construction phase happens after the beams have been already mounted on the abutments and in situ concrete starts being poured inside of the precast. Additionally, to the construction phase 1 prestress, a second prestress is applied. This second prestress is applied from the redirection point in the beam into the abutment. This prestress acts as a direct connection between the abutment and the beam, turning the statically determinate system into a statically indeterminate system. The system being statically indeterminate is the main difference between this construction phase and the previous one. As seen in (Figure 23) the tendons are located from a redirection point on the beam to the beginning of the abutment. By having rigid connections to the abutments the bridge is considered to be an integral bridge.

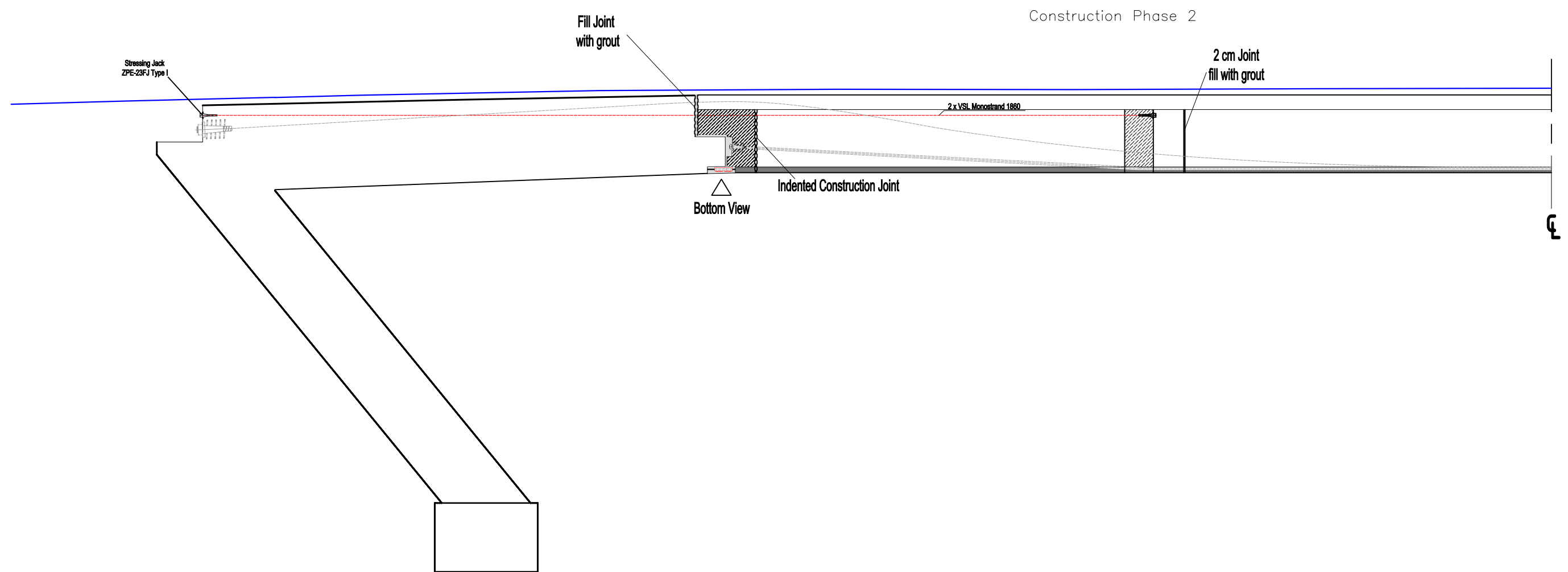


Figure 23: Tendons Position Construction Phase 2.

### ***3.1.3 Construction Phase 3 Main Prestress***

The third construction phase is vital for the bridge's design because the largest prestressing load is applied during this phase, here the beam's cross-section is already complete and is being loaded with the next pour of concrete being the bridge slabs, the roadbed, and the barriers (including sidewalks). These loads being applied on the completed beams are the final self-weight loads of the bridge, which completes the cross-section of the bridge. Here the prestress load is applied onto tendons situated in key locations of the beams. The prestressed tendons are located at the bottom on the midspan of the beam and come out of the top of the beams closer to the abutments. This location is chosen because the beams are in tension at the bottom of the midspan of the beam and are also in tension at the top of the beam at the abutments. The prestressed tendons follow a very smooth parabolic curve avoiding any stress peaks.

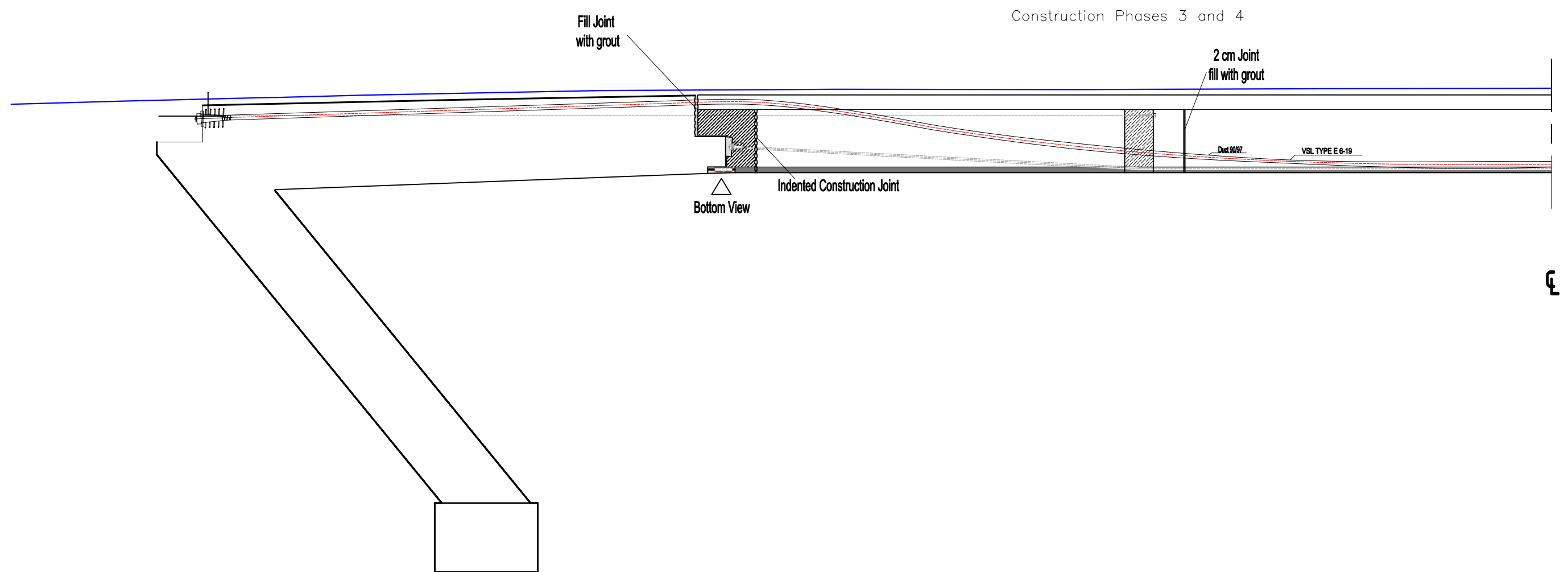


Figure 24: Tendons Position Construction Phase 3 and 4.



#### **3.1.4 Construction Phase 4**

The final construction phase takes part in an already complete cross-section of the bridge. This last construction phase includes no self-weight load but only adds a prestress load on the main tendons to guarantee compressive stresses throughout the bridge as well as to reduce the deformations of the fully loaded bridge.

#### **3.1.5 Construction Phase 5 (Load Model 1)**

This construction phase consists on the Load Model 1 loading according to the Eurocode (see Loading chapter for load distribution diagrams). [18] This loading case consists of distributed loads as well as point loads. These loads were included in the software analysis by creating one load case only for the distributed loads applied on the lanes and the point loads were applied differently. The point loads, as seen previously in the loading chapter, are four point loads applied simulating the axial loads of a vehicle driving on top of the bridge. These four point loads are then reapplied 1.2 m apart from the previous ones, and a load case is created for each one of these groups of point loads. From these load cases a load combination is then created in the RFEM software model in order to calculate the internal forces from the governing load, which are then used find the stresses.

## 4 *Loads*

The bridge loads were applied to the 2-D and 3-D software models as distributed line loads. This is an approximation used in order to simplify the pre-analysis. The loads applied to the bridge structure are divided into two main categories, dead and live loads. In order to apply the loads correctly onto the simplified model, all loads were calculated from the existing bridge geometry. This was done by multiplying the specific weight with the cross-sectional area for each part of the structure.

Both, dead and live loads were applied as following:

The dead loads considered for the software model were the self-weight of the different parts of the structure, such as, the abutment plus deck slab, the roadbed, and the edge beams. These dead loads were applied on the software model separately i.e. a load case was created for each one of these three previously described parts of the bridge. This was done in order to be able to make quick geometrical adjustments on the structure.

## 4.1 Self-weight distribution and modeling:

### 4.1.1 Abutment and Deck Slab

The abutment load was calculated from the following geometry in Figure 25.

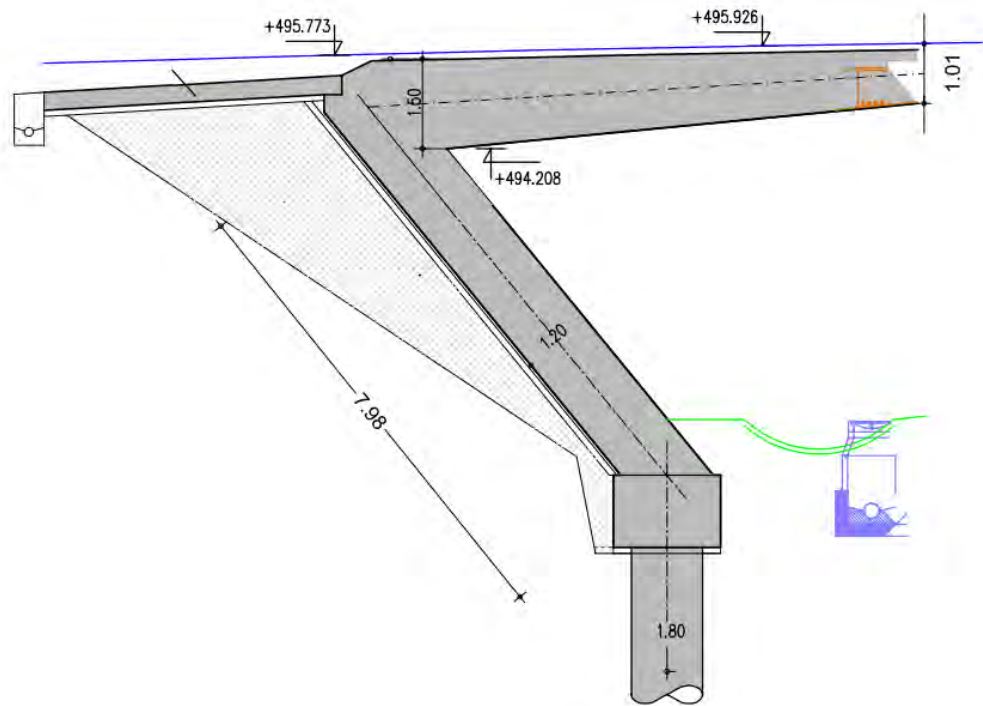


Figure 25: Abutment Measurements

The geometry of the existing bridge was taken as guide to dimension the reinforced concrete bridge. To calculate the distributed load to be applied in the FEM model, the cross-sectional area, which in this case is always the 7.8 m width times the thickness of the elements, is multiplied with the specific weight of concrete.

$$\begin{aligned}
 \gamma_c &= 25 \text{ kN/m}^3 \\
 &= 1.2 \text{ m} \cdot 7.8 \text{ m} \cdot 25 \frac{\text{kN}}{\text{m}^3} = 243 \text{ kN/m} \\
 &= 1.5 \text{ m} \cdot 7.8 \text{ m} \cdot 25 \frac{\text{kN}}{\text{m}^3} = 292 \text{ kN/m} \\
 &= 1.0 \text{ m} \cdot 7.8 \text{ m} \cdot 25 \frac{\text{kN}}{\text{m}^3} = 195 \text{ kN/m}
 \end{aligned}$$

The geometry of the deck slab made it a not so straightforward task to calculate the cross-sectional area. Therefore an excel calculation was used to calculate the area.

$$\gamma_c = 25 \text{ kN/m}^3$$

$$\text{Area} = 2 \text{ m}^2$$

$$\text{Deck slab} = 2 \text{ m}^2 \cdot 25 \frac{\text{kN}}{\text{m}^3} = 292 \text{ kN/m}$$

#### 4.1.2 Roadbed

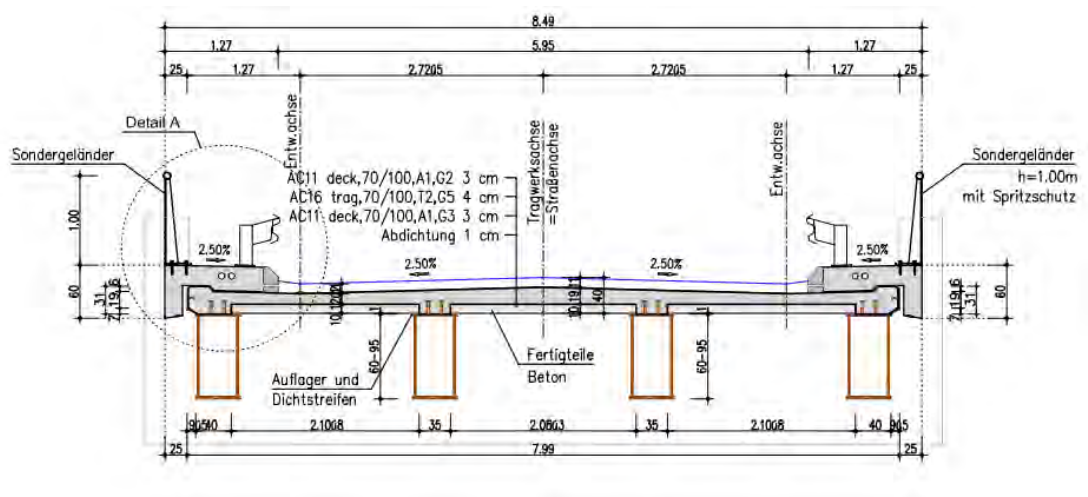


Figure 26: Composite Bridge Cross-section

The distributed load on the roadbed was calculated according to the value  $\gamma = 24 \text{ kN/m}^3$  found in EN 1991-1-1:2002 [19]. The roadbed has a constant height and width of 11 cm and 6 m respectively.

$$\gamma_{\text{roadbed}} = 24 \text{ kN/m}^3$$

$$g_{\text{roadbed}} = 0.11 \text{ m} \cdot 5.95 \text{ m} \cdot \frac{24 \text{ kN}}{\text{m}^3} = 15.7 \text{ kN/m}$$

### 4.1.3 Edge Beams and Sidewalks (Barriers)

The loads for the edge beams and sidewalks (Barriers) were calculated the same way as the other bridge parts, first exact measurements were taken from bridge's cross-section to be able to calculate the area to then be able to multiply it with concrete's specific weight

$$\gamma_{concrete} = 25 \text{ kN/m}^3$$

$$g_{barriers} = 0.686 \text{ m}^2 \cdot \frac{25 \text{ kN}}{\text{m}^3} = 17.15 \text{ kN/m}$$

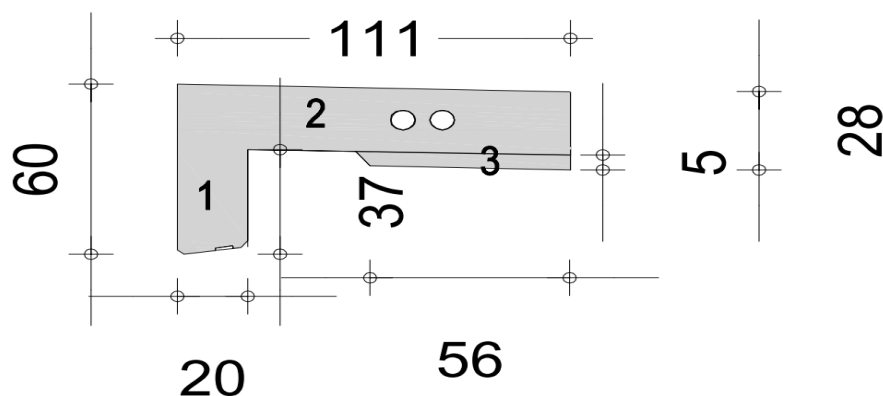


Figure 27: Edge Beam Measurements

## 4.2 Load Model 1 (Live Loads)

The live loads applied to the structure were taken as the load model 1 described in the Eurocode EN 1991-2-2002 [18]. The load model 1 (LM 1) specifies a specific load for each car-axle, and these loads were calculated by using the additional module moving loads in RFEM. The double-axle system is called a tandem system. The live loads are applied as axle loads as seen in Figure 28. The axle loads of  $Q=300 \text{ kN}$  are applied on each axle of the main lane (Lanes are defined to have a 3 m width), and  $Q=200 \text{ kN}$  for the secondary lane with a 1.2 m axle spacing. These live loads were applied simultaneously in the FEM model in order to satisfy the LM 1. In order to find the governing load case, load cases was

created for each moving load across the entire length of the bridge starting at one end of the bridge and increasing every two meters until the end of the bridge.

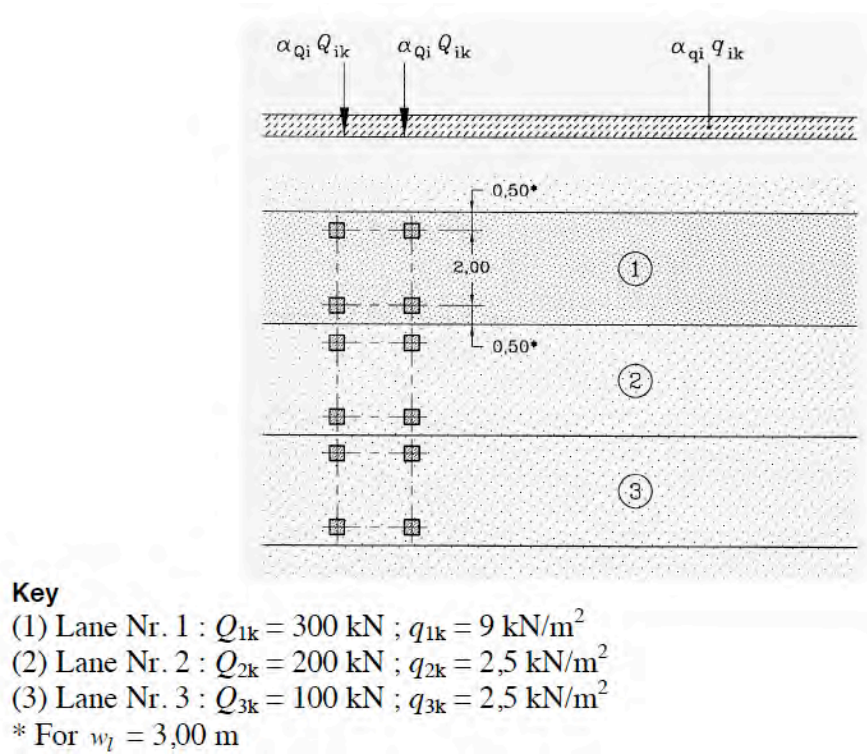


Figure 28: Load Model 1 Axle Load Distribution [18]

Figure 28 illustrates the distribution of the axle loads with the tire spacing for the main and secondary lanes, as well as the uniformly distributed load (UDL). Figure 29 and illustrates how the UDL was calculated for the 2D Model and how the UDL load was applied to the RFEM 3D Model.

$$UDL = 2 \cdot \left( 1.109 \text{ m} \cdot 2.5 \frac{\text{kN}}{\text{m}^2} \right) + \left( 3 \text{ m} \cdot 9 \frac{\text{kN}}{\text{m}^2} \right) + \left( 3 \text{ m} \cdot 2.5 \frac{\text{kN}}{\text{m}^2} \right) \approx 40.10 \text{ kN/m}$$

Additionally to the uniformly distributed load, the axle loads from the load model 1 were applied on the 2D model as movable loads throughout the whole length of the abutments and the bridge's span. The point loads may be seen in

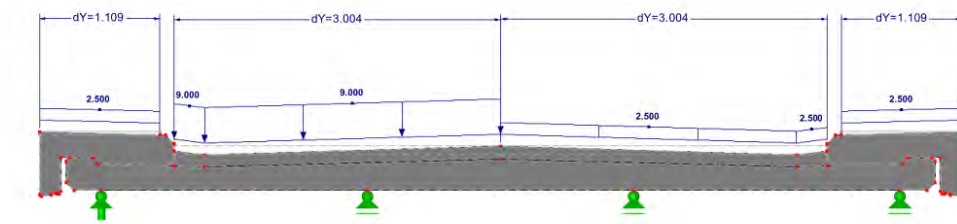


Figure 29: Load Model 1 Load Distribution illustrated with RFEM [18]

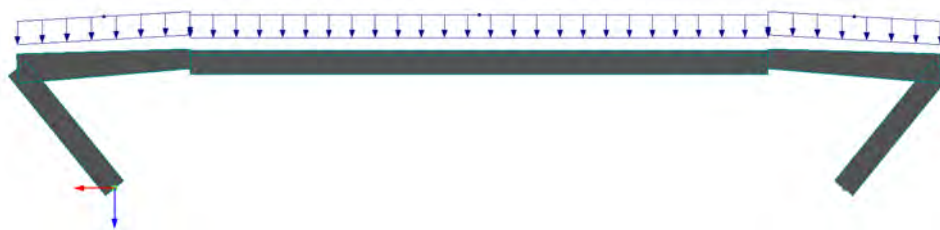


Figure 30: UDL (40 kN/m) on the RFEM 2D Model [18]

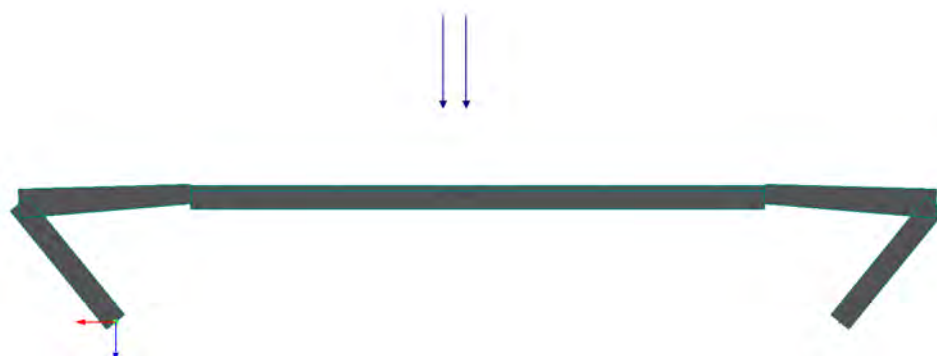


Figure 31: Load Model 1 Movable Axle loads (300 and 200) kN with 1.2 m axle spacing) in RFEM 2D model [18]

## 5 Pre-modeling

The task at hand was to model an existing steel concrete bridge consisting of steel beams and concrete slabs and roadbed, with a bridge consisting of prestressed precast bridge beams. The motivation for this model was to illustrate that a prestressed thin-walled precast beam could potentially replace a steel beam Figure 26 in the construction of a bridge.

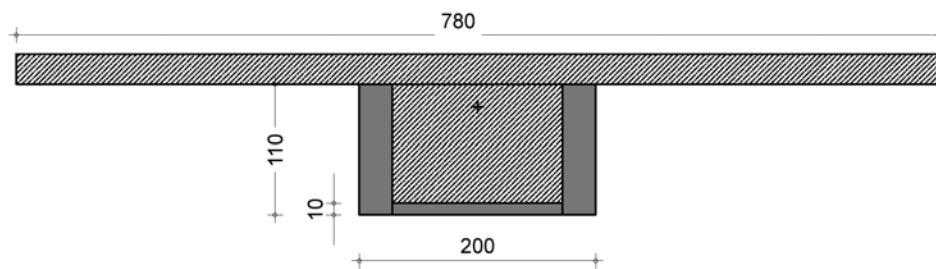


Figure 32: Equivalent cross-section

To do a pre-analysis model of the existing structure, an equivalent cross-section of the bridge seen in Figure 32 above had to be calculated and from this equivalent cross-section a 3D model was then used to create the following final cross-section.

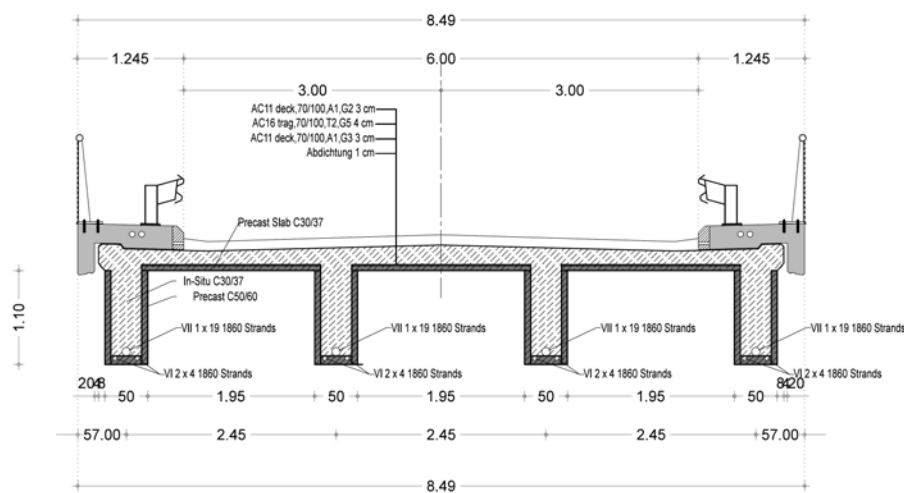


Figure 33: Reinforced Concrete final cross-section



The first step to calculate an equivalent cross section (2D Model) was to use the actual shape of the steel concrete bridge (Figure 26) and then figure out the dimensions of it this is illustrated in Figure 32.

Once the final shape of the bridge was chosen to be four 1.1 m high 0.50 m wide beams, a 2D model for analysis was prepared with help of the software RFEM from Dlubal. This software gives the user the freedom to either calculate the self-weight of a structure based on the properties of the cross-section these being material type and shape, but it also allows the user to input a predefined value for the self-weight. The latter option was the one chosen to use in order to calculate the self-weight of the bridge. This was done in order to calculate the center of gravity and the moment of inertia externally with use of an excel spreadsheet to be able to double check the values calculated automatically by the software RFEM as well as to optimize the geometry of the beams. A calculation of the center of gravity as well as the moment of inertia was performed and can be seen in the Appendix 1. The moment of inertia values calculated by the software were the same as the ones calculated externally with the excel spreadsheet.

The internal forces were all calculated with the software RFEM because of the complexity of the system, the end system was chosen to be a statically indeterminate system, which would make hand calculations tedious and very prone to mistakes. Although the end system was a statically indeterminate system, the first phase of the analysis was actually a statically determinate system and the calculation of the internal forces was performed by hand with help of construction tables, at the end these values were used only to compare accurateness of the software results, but the hand calculations are found in the Appendix 1.

---

## 5.1 *Software Modeling*

As mentioned before, the software used to analyze and calculate the internal forces of the integral bridge at hand was RFEM 4.10.2680 from the software company Dlubal. This software offers the end-user different possibilities to analyze two-dimensional as well as three-dimensional models.

RFEM makes use of load cases (LC), load groups (LG), as well as load combinations (CO). These three different types of loadings help the user model more accurately the loads acting on a structure. The software also has the possibility of calculating the self-weight of the structure by itself, or allowing the user to input a define load. This freedom allows the user to calculate and double-check the loads externally, which is the case of this report. The software has also built in algorithms and theories that accurately simulate real end results.

In order to better approximate reality, two different types of models of the integral bridge were created. The first model was a 2-D model of an equivalent cross-section, this cross-section allowed for a simple pre-dimensioning of the required prestresses. The second model was a 3-D model that more accurately approximated the cross-section of the bridge. Included in the 3-D software model were four beams with the final cross-section of the bridge. Therefore, for the 3-D analysis an individual calculation was performed for each of the beam's internal forces. These two models, were the core that allowed the calculation of internal forces, but the stresses were not calculated with RFEM but with excel. Therefore, all the data from the internal forces was exported to an excel spreadsheet where all the stress formulas in all the desired locations of the cross-section of the beam.

The excel spreadsheet made use of the data calculated with RFEM for the 2-D and 3-D models for each one of the construction phases; the internal forces calculated by RFEM were the moment due to self-weight and the normal force and moments due to the prestress load. These internal forces were exported for the entire 28.8 m length of the bridge with a spacing of 1.2 m between each value. Therefore the bridge was divided into 24 ( $28.8 \text{ m} / 1.2 = 24$ ) even parts and these values were used on the excel analysis to calculate and plot the stresses on the entire beam allowing a better visual understanding of the stresses inside of the bridge.

The stresses were calculated in the 2D analysis only for the top of the top and bottom of the beam. The stresses were calculated at all points of contact between the precast beam and the in-situ concrete. The stresses were calculated as following:

$$\sigma_{i,c} = \frac{M_{self-weight}}{S_i} + \frac{N_P}{A_c} + \frac{M_P}{S_i}$$

$\sigma_{i,c}$	Concrete stress at a specific height in the bridge's beam.
$M_{self-weight}$	Moment due to self-weight load applied on each construction phase.
$S_i$	Elastic section modulus at the specified height.
$N_P$	Normal force due to prestress load applied on each construction phase.
$A_c$	Concrete cross-sectional area at each construction phase.
$M_P$	Moment due to prestress load applied on each construction phase.

The stresses were calculated for every construction phase at different locations of the beam. The chosen locations to calculate the stresses were the following:

#### Abutment or support

This location is where the beam connects to the abutment and it is located at the beginning and at the end of the bridge's beams, this location was important to take into consideration because the stresses were always very high being that the bridge beams have a rigid connection to the abutment from the prestressed on the second construction phase.

#### Redirection of the tendons

This is located 7.2 m from the beginning of the bridge's girder and 7.2 m from the other end of the bridge's girder. This location includes the change of direction of the prestressed tendons inside of the initial thin-walled precast beam (redirection saddle). In this part of the bridge are also located the tendons for the second construction phase. Therefore, it was interesting to calculate the stresses in this location as well.

### Midspan

Stresses located at the midspan of the bridge were also calculated and taken into consideration for the dimensioning of the required prestress loads required to keep compressive stresses throughout the bridge.

## 5.2 *Two-Dimensional Model Equivalent Cross-Section*

The 2-D model included the previously mentioned equivalent cross-section. This equivalent cross-section approximates the bridge as having only one large beam underneath the bridge slab, hence simulating all four of the bridge's beams. This was done in order to simplify the analysis of the bridge's internal forces and to easily export the data to excel for faster analysis. This model helped as a pre-dimensioning basis and its results were later used to dimension the 3-D model.

For the 2-D analysis, the stresses were calculated at the top of the beam as well as at the bottom for all three locations mentioned previously (support, redirection, and midspan). Calculating the stresses for the top and the bottom of the bridge's beam is vital to be able to understand and illustrate which parts of the bridge are under compressive or tensile stress. Additionally, stress curves were plotted to better illustrate the progression of the stresses throughout the bridge's length.



Figure 34: 2D Model RFEM.

### 5.3 *Three-Dimensional Model Prestressed Concrete Cross-Section*

This model was the final and more accurate approximation of the actual bridge's cross-section. The analysis was more in-depth compared to the 2-D model, because the stresses were calculated in various locations of the cross-section as well as for all construction phases. From the internal forces calculated with the 3-D model, more specific stresses were calculated. The stress analysis of the 3-D model differentiates the stresses in the pre-cast beam from the stresses of the in-situ concrete at any relevant location. Therefore, the stresses of the overall structure can be looked at more specifically as well as more accurately. These stresses are vital to understand if the whole structure is under tension or compression; therefore, internal forces were calculated at significant locations of the beam (i.e. top and bottom of the pre-cast beams as well as for the top and bottom of the in-situ concrete).



Figure 35: 3D Model RFEM.

### 5.4 Falsework Loads Superposition

In addition to modeling the bridge with 2D and 3D models, the stresses were also calculated with a third model with the same methodology as the other two. This third model makes the assumption that the entire bridge girder is cast all at once into an onsite falsework with all the prestress tendons built into it, that is, the entire loads of the bridge are superimposed onto one construction phase. The stresses on this falsework model reflect the internal stresses acting on the structure and this was done in order to compare the stresses with the stresses of the fourth construction phase (3D Model). The resulting stresses calculated with this model help determine the stresses of a final stage taking into consideration the concrete creep coefficient of the entire cross-section. This model simulates the calculation of the difference in internal restraint forces through creep. More information about the calculation of stresses and the creep factor can be found in section 6.3 and the Appendix.

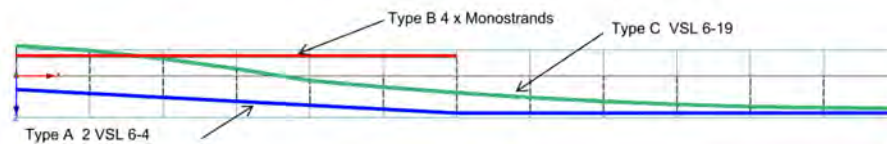


Figure 36: Tendon Layout for Falsework Phase.

## 5.5 Eurocode

### Limitation of concrete Stress

According to the EN 1992-1-1:2004 5.10.2.2

- P Local concrete crushing or splitting at the end of pre- and post-tensioned members shall be avoided.
- Local concrete crushing or splitting behind post-tensioning anchors should be avoided in accordance with the relevant European Technical Approval.
- The strength of concrete at application of or transfer of prestress should not be less than the minimum value defined in the relevant European Technical Approval.
- If prestress in an individual tendon is applied in steps, the required concrete strength may be reduced. The minimum strength  $f_{cm}(t)$  at the time  $t$  should be  $k_4$  [%] of the required concrete strength for full prestressing given in the European Technical Approval. Between the minimum strength and the required concrete strength for full prestressing, the prestress may be interpolated between  $k_5$  [%] and 100% of the full prestressing.

Note: The values of  $k_4$  and  $k_5$  for use in a Country may be found in its National Annex. The recommended values are 50 and 30 respectively.

- (5). The concrete compressive stress in the structure resulting from the prestressing force and other loads acting at the time of tensioning or release of prestress, should be limited to:

$$\sigma_c = 0.6 f_{ck}(t)$$

For pretensioned elements the stress at the time of transfer of prestress may be increased to  $k_6 f_{ck}(t)$ , if it can be justified by tests or experience that longitudinal cracking is prevented.

Note: The value of  $k_6$  for use in a Country may be found in its Annex. The recommended value is 0.7.

If the compressive stress permanently exceeds  $0.45 f_{ck}(t)$  the non-linearity of creep should be taken into account

## 6 *Analysis*

The model of the structure was first done in a 2D representation of the bridge to find the initial pre-dimensions, which helped do a more accurate representation of the structure in a 3D model.

These two model types were then loaded with the appropriate dead and live loads to represent the overpass bridge at hand. Once the pre-dimensioning was set, a third model (falsework structure), also 3-dimensional (defined in the last chapter), was created with all the pre-stresses from the construction phases in order to calculate the final internal forces necessary to calculate the required reinforcement and stress details.

### 6.1 *Two-Dimensional Models*

Four different construction phases and a live-load phase (construction phase 5) were considered for the modeling of the bridge in order to reduce deformations and to keep all internal stresses within the values specified in the Eurocode standards.

The 2-D Model assumes an equivalent cross-section, which sums all 4 beams of the bridge into one large wide beam. This is an accurate approximation because the center of gravity and the total cross-sectional area remain unchanged. This allows for an easier software model for the pre-dimension process of the total structure. The main goal of the four construction phases is to be able to load the structure with enough prestress in order for the whole structure to be under compression, the limits for these stresses are the ones described previously in the Eurocode chapter of this Thesis. For the first four construction phases the maximum stress should not exceed  $0.45 f_{ck}(t)$  and the stresses during the load model 1 loading should not exceed  $0.60 f_{ck}(t)$ . The construction phases were used to calculate the internal forces of the structure (normal forces and bending moments) from the self-weight and pre-stressing loading cases.

All relevant printouts and calculations for the 2-D model are located on the Appendix 1 of this report.



### 6.1.1 Construction Phase 1 Assembly / Construction and Self-weight

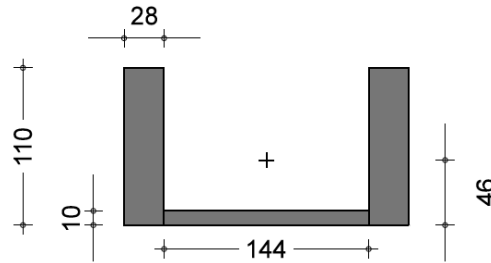


Figure 37: 2D Equivalent cross-section construction phase 1.

The first construction phase of the bridge is considered to be when the pre-fabricated C50/60 strength concrete beams are ready to be moved from the location of fabrication to the construction site. The two dimensional beam is modeled with tendons built into the bottom of the structure allowing the structure to be pre-stressed. These prestressed tendons allow the beam to be lifted and moved around without exceeding maximum stresses defined in the Eurocode chapter of this report.

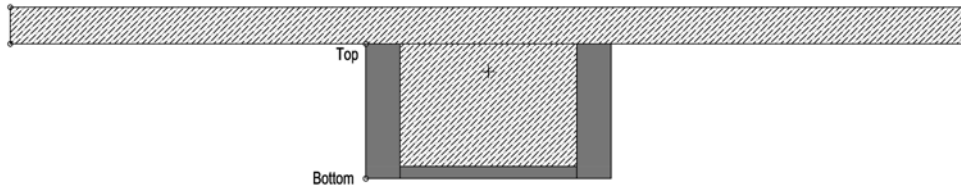


Figure 38: 2D Model Stress Locations.

Figure 38 shows the location on the beam where the stresses were calculated for the first three construction phases. The last two construction phases have in addition to the top and bottom stresses, the stresses on the very top of the bridge slab. These stresses were not plotted in the following stress plots because they are not relevant for the predesign. The stresses were calculated more into detail with help of the 3D model analysis.

$$\sigma_{max} = -2.01 \frac{MN}{m^2} < f_{ctm} = 4.1 \frac{MN}{m^2}$$

$$\sigma_{min} = -12.05 \frac{MN}{m^2} < 0.45 \cdot f_{ck} = -22.5 \frac{MN}{m^2}$$

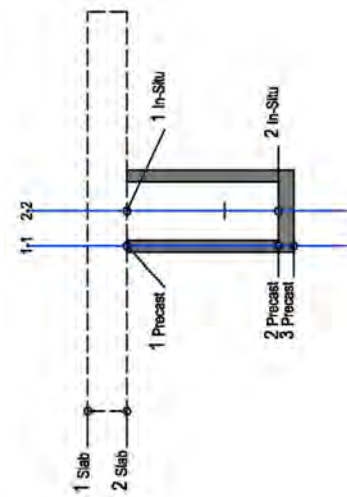
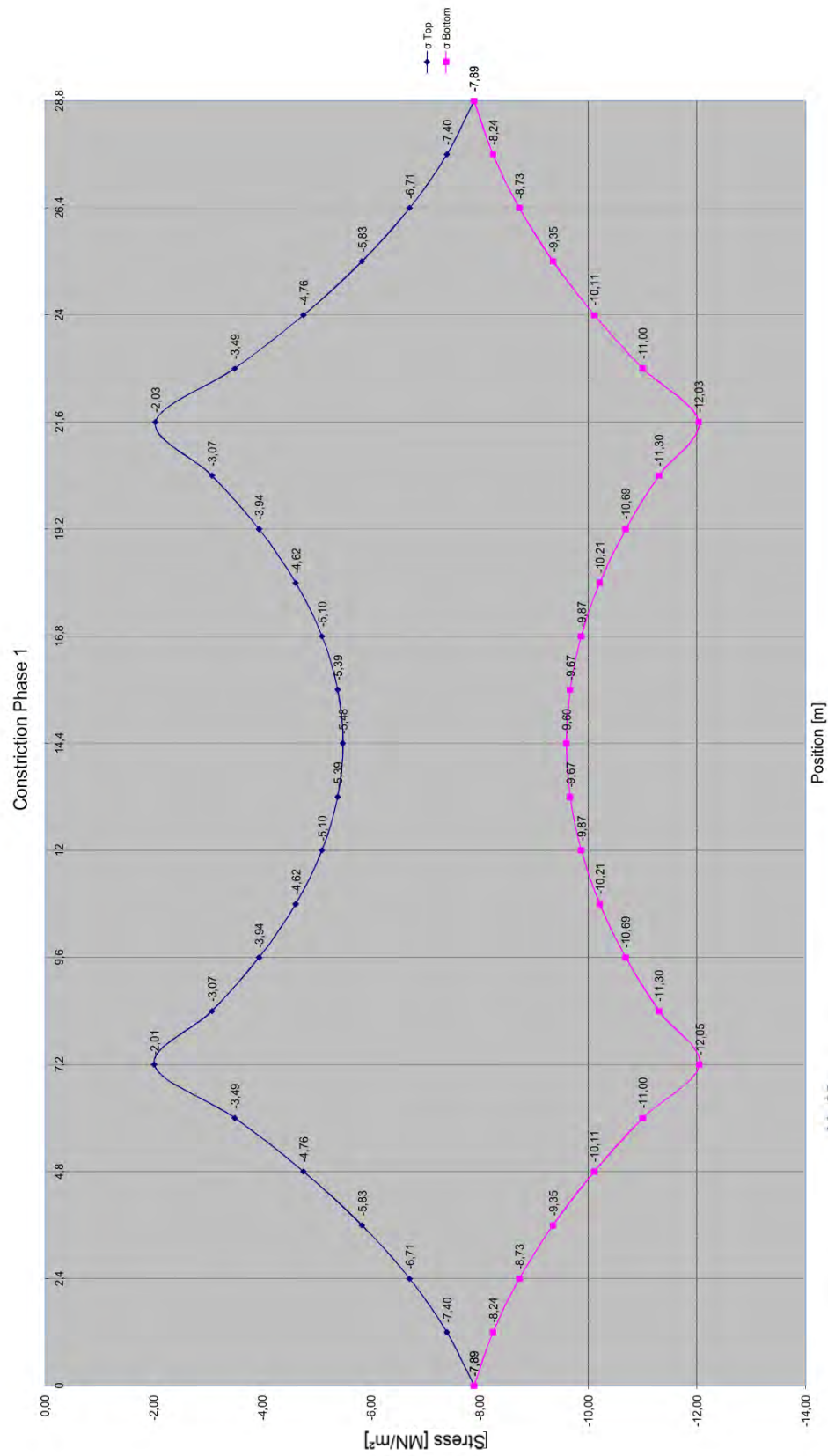


Figure 39: 2D Analysis Stresses Construction Phase 1.

### 6.1.2 Construction Phase 2 Prestressing redirection and in-situ concrete

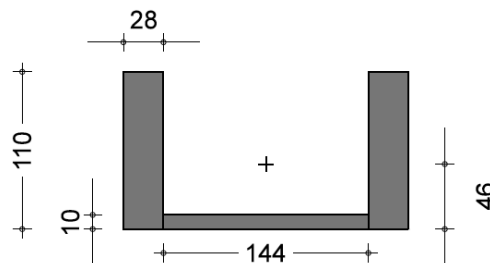


Figure 40: 2D Equivalent cross-section construction phase 2.

The second constitution phase is taken to be when the bridge's beam is already mounted in position on the abutments. At this point the prestressed tendons from the first construction phase are not accessible anymore because of where they are supported on the abutments. Therefore the bridge's system requires additional prestressed tendons that run from the redirection point on the beam (defined earlier) all the way to the beginning of the abutments on both sides respectively. The prestressed tendons in this construction phase fix the beams to both ends turning the system from a statically determinate into a statically indeterminate structure. This system change is clearly reflected in the graphical representation of the moments for both self-weight and prestress.

$$\sigma_{max} = 4.49 \frac{MN}{m^2} > f_{ctm} = 4.1 \frac{MN}{m^2} \text{ additional reinforcement considered}$$

$$\sigma_{min} = -18.89 \frac{MN}{m^2} < 0.45 \cdot f_{ck} = -22.5 \frac{MN}{m^2}$$

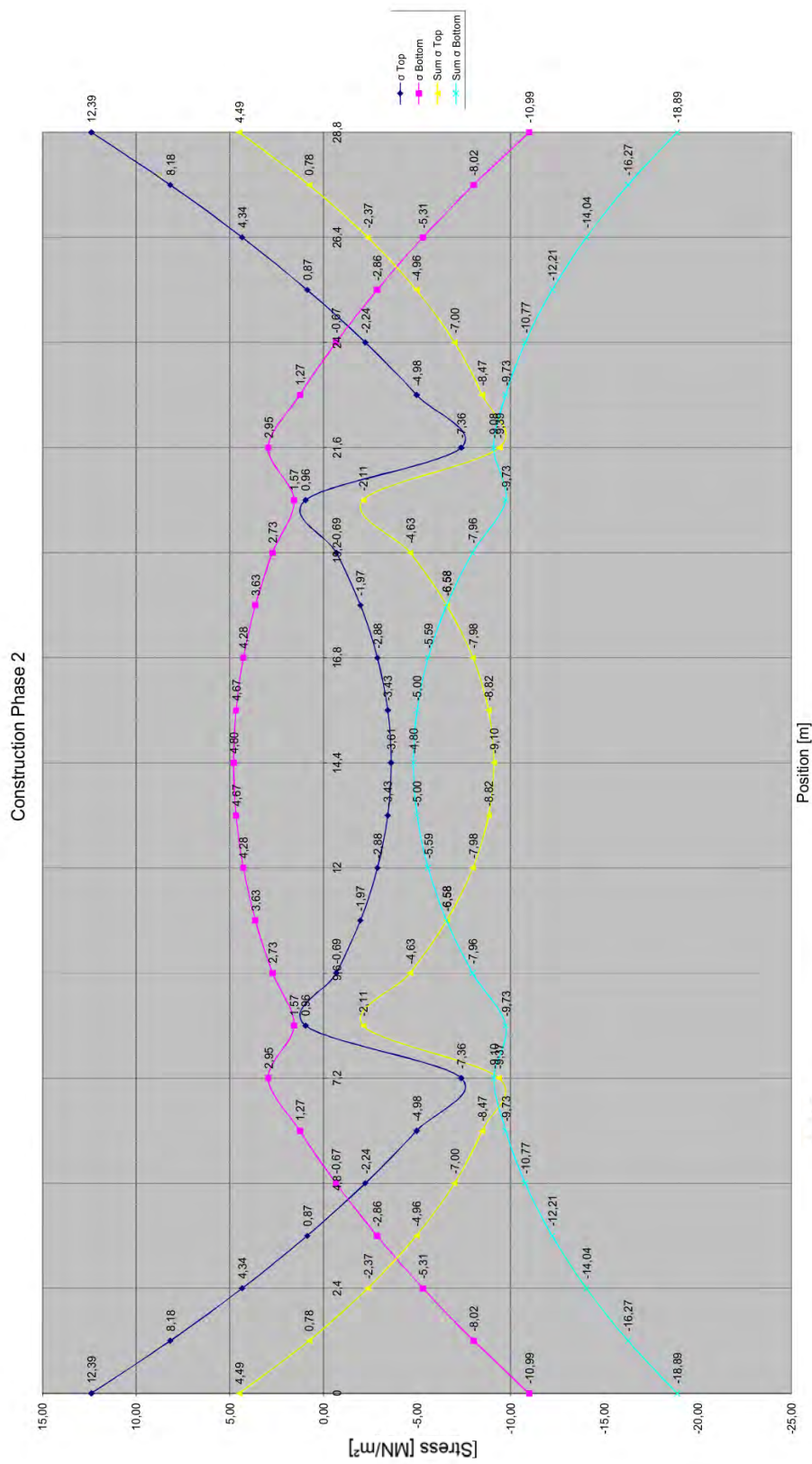


Figure 41: 2D Analysis Stresses Construction Phase 2.

### 6.1.3 Construction Phase 3 Main Prestressing and in-situ concrete

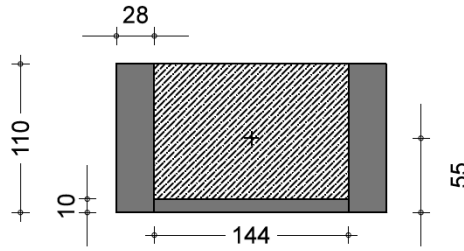


Figure 42: 2D Equivalent cross-section construction phase 3.

During this construction phase the main tendons of the bridge's cross-section are prestressed. The largest prestress takes place during this phase, therefore, the location of the main tendons was very critical in order to reinforce the structure in places where it is more necessary. The location of the tendons as seen in Appendix 1 was chosen to follow this path because in the midspan it is clear the structure is under tension stresses at the bottom of the beam and compression on the top, therefore the tendons are located as low as possible to reinforce the structure's tensile area. On the supports the tensile stresses are located on the top of the beam, therefore, the tendons are located as high as possible to cover as much of the tensile area of the beam with reinforcement. The geometry of the beam acts as the boundary condition for the location of the tendons. As illustrated in Figure 33 (Cross-section of midspan phase 3) the tendon is located at the lowest point possible on the pre-cast beam, this location is also convenient while laying down the tendons, because it doesn't require any additional construction, it just sits on the bottom of the precast beam. The tendons' location at the support and redirection were as high as possible to reinforce the beam's tensile area. In consequence, the tendons' location at the support was chosen to stick out of the top of the beam but still be within the lower portion of the bridge's slab.

$$\sigma_{max} = -5.17 \frac{MN}{m^2} < f_{ctm} = 4.1 \frac{MN}{m^2}$$

$$\sigma_{min} = -19.68 \frac{MN}{m^2} < 0.45 \cdot f_{ck} = -22.5 \frac{MN}{m^2}$$

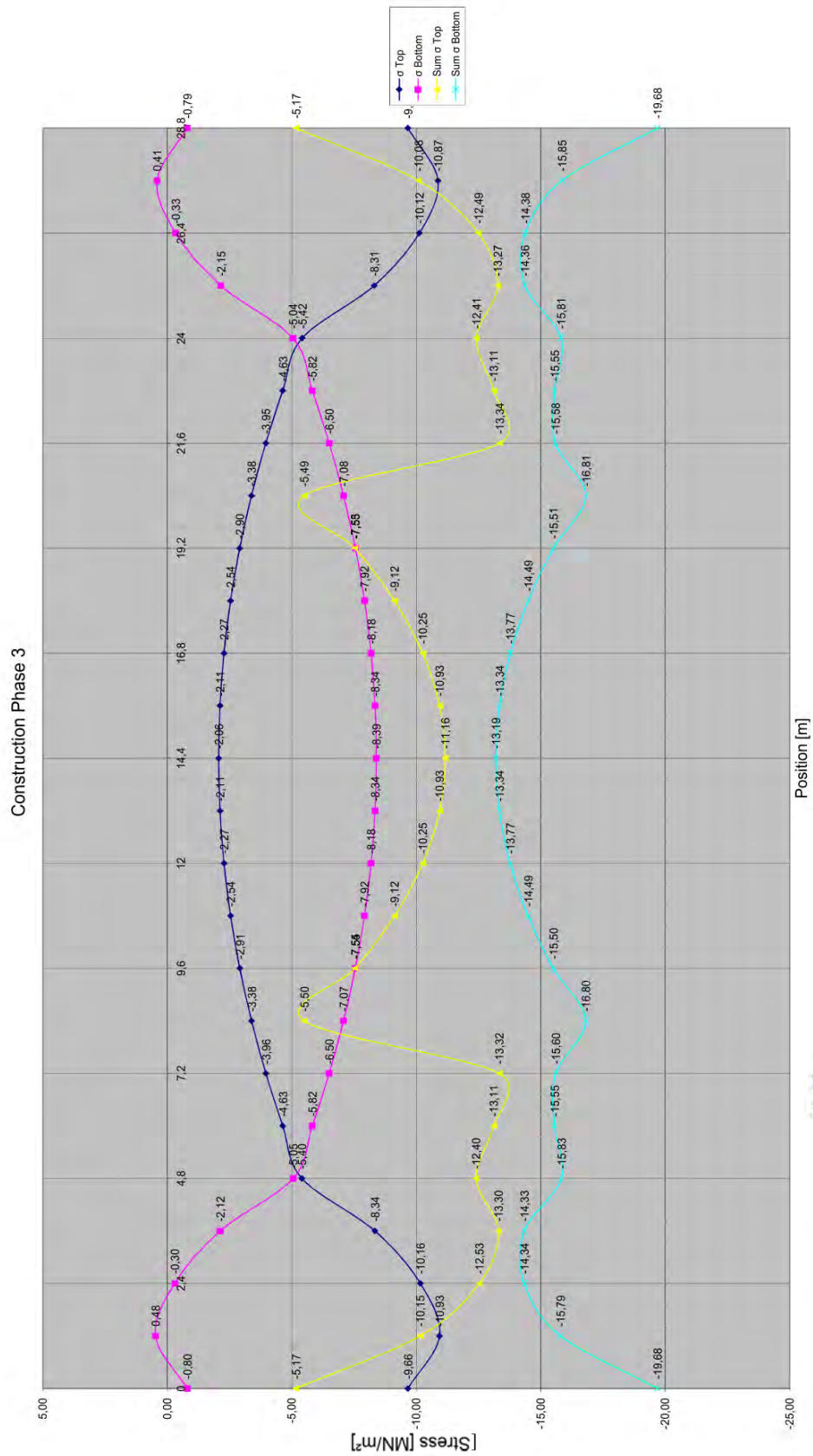


Figure 43: 2D Analysis Stresses Construction Phase 3.

#### 6.1.4 Construction Phase 4 Final Prestressing

The final construction phase takes place when complete cross-section of the bridge is already completed and then the final prestress is applied on the main tendons; this allows the structure to increase the pre-stresses in order to stay within the specified limits.

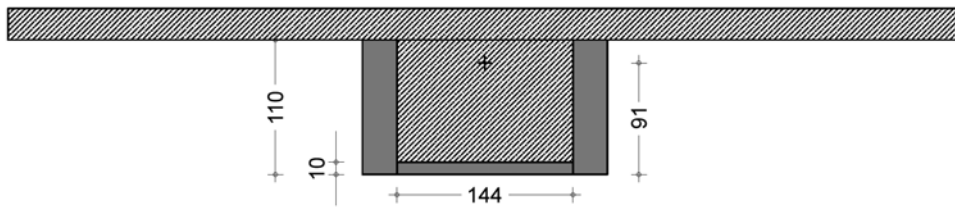


Figure 44: 2D Equivalent cross-section construction phase 4

$$\sigma_{max} = -5.85 \frac{MN}{m^2} < f_{ctm} = 4.1 \frac{MN}{m^2}$$

$$\sigma_{min} = -18.56 \frac{MN}{m^2} < 0.45 \cdot f_{ck} = -22.5 \frac{MN}{m^2}$$



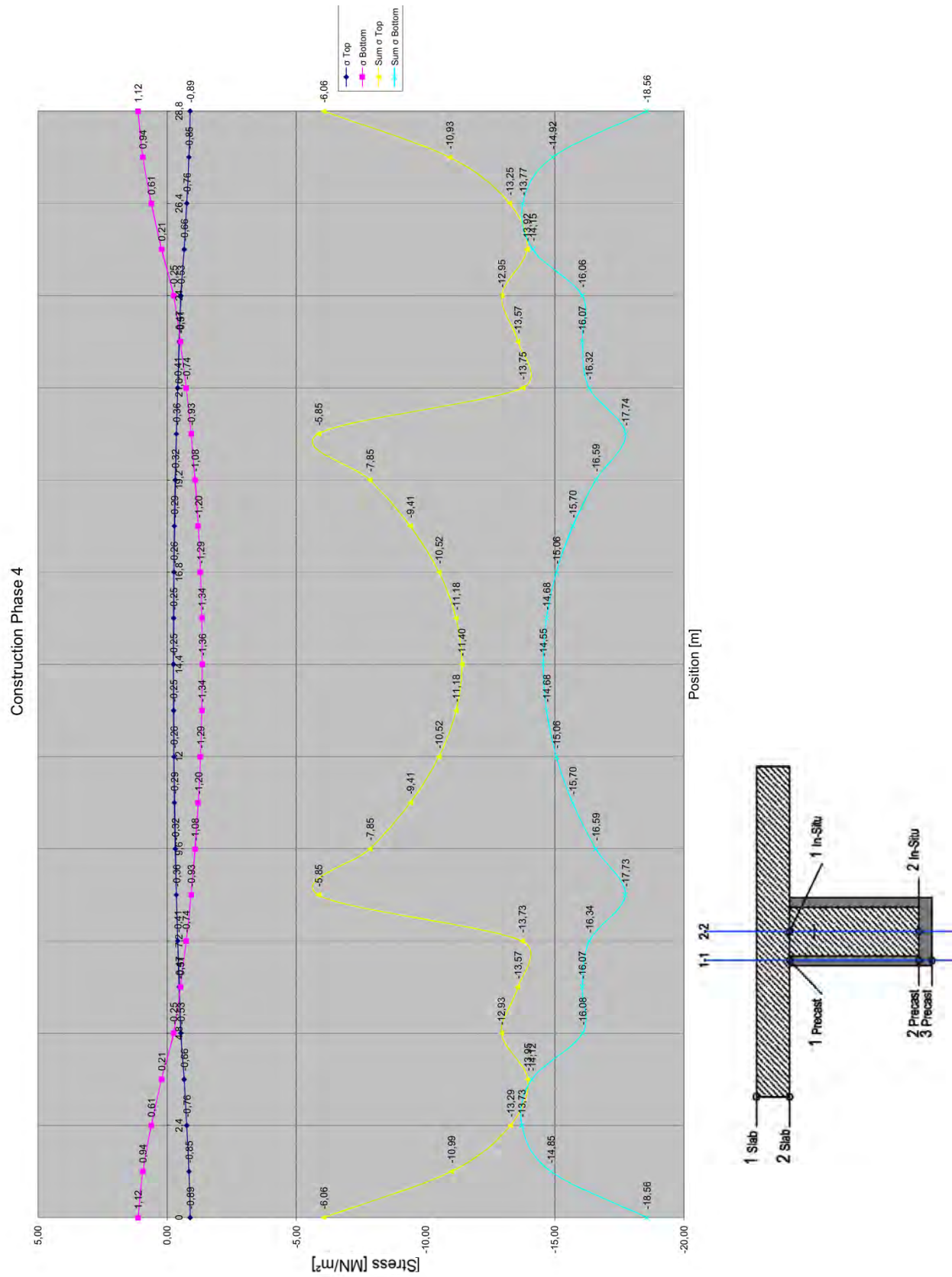


Figure 45: 2D Analysis Stresses Construction Phase 4.



### 6.1.5 Construction Phase 5 (Load Model 1)

The distributed and point loads described in the Load Model 1 of the Eurocode [18] were applied to a model of the system with a complete cross-section. The internal forces calculated on this model were used to analyze the stresses in the structure for this phase, the following graph illustrates the stresses of the phase, for this phase, the Eurocode allows the stresses to be  $0.60 f_{ck}$ , as seen in the figure the stresses are within the specified limit.

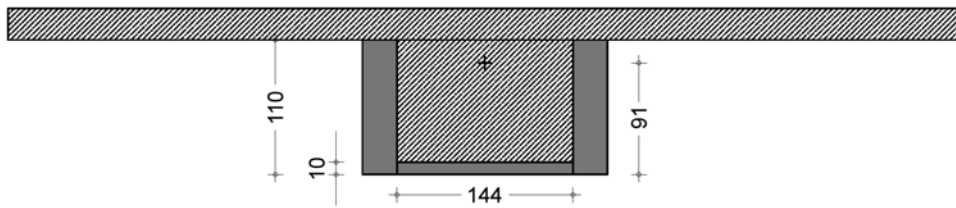


Figure 46: 2D Equivalent cross-section Load Model 1

$$\sigma_{max} = -4.75 \frac{MN}{m^2} > f_{ctm} = 4.1 \frac{MN}{m^2} \text{ additional reinforcement considered}$$

$$\sigma_{min} = -27.14 \frac{MN}{m^2} < 0.60 \cdot f_{ck} = -30 \frac{MN}{m^2}$$

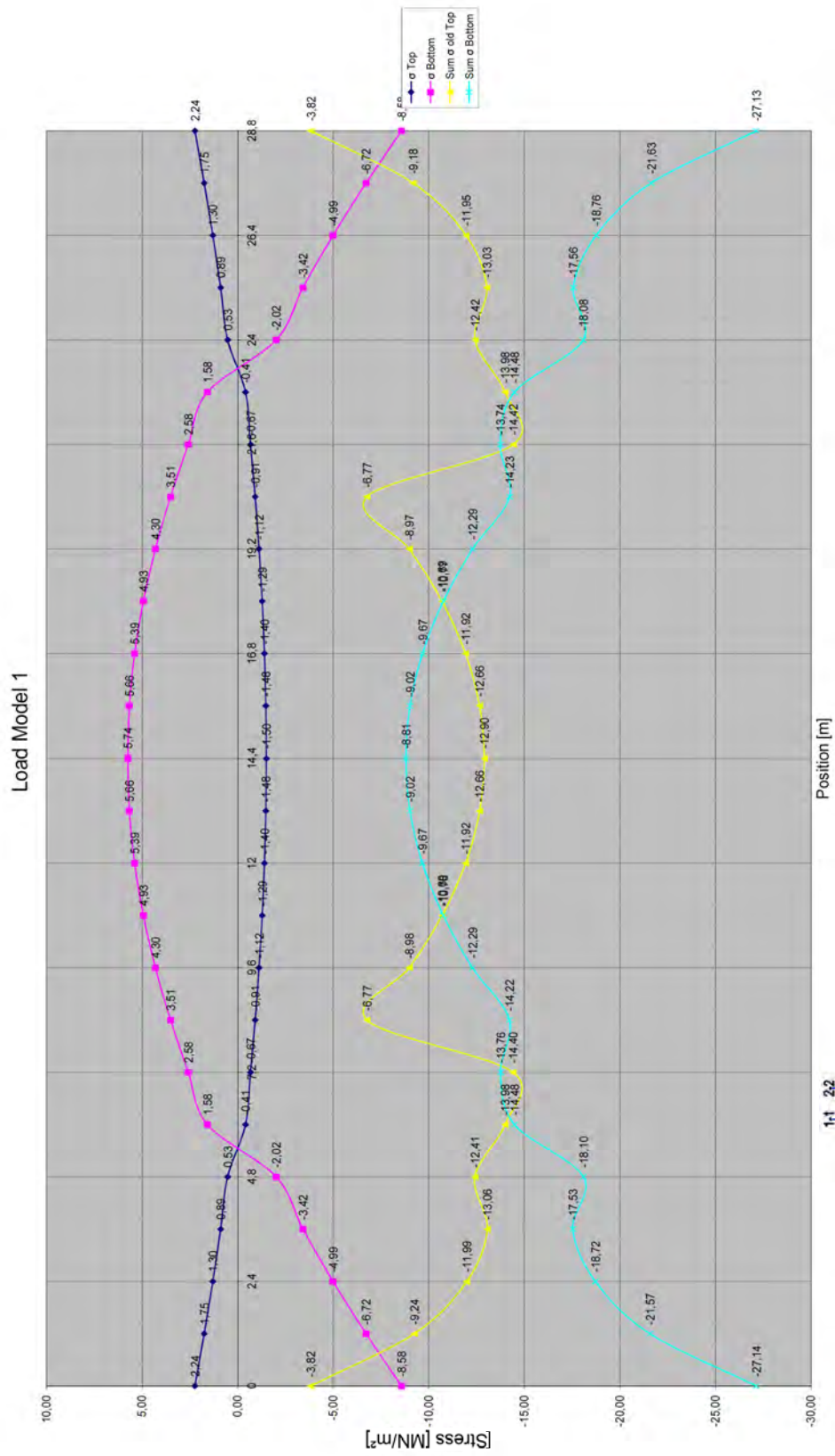


Figure 47: 2D Analysis Stresses Load Model 1.

## 6.2 *Three-Dimensional Model*

The prestressed tendons calculated in the 2D model were then applied to a 3D cross-section of the bridge to then calculate the stresses in the same manner done previously. The tendons were modeled on each beam of the 3D cross-section as a steel member with a very small cross-section with an axial load representing the prestress being applied on the beam. The amount of prestress being allocated to each beam was calculated with help of the excel spreadsheets, which helped visualize as well as analyze the optimum amount of prestress. This analysis is in the form of stress curves found in Appendix 2. The different stress curve plots for all four-construction phases and the live load phase (load model 1) were used to find the optimum amount of prestress staying within the allowable ranges.

Complementary analysis was performed on all three important locations of the beams (support, redirection and midspan) in order to find out if additional reinforcement was needed to satisfy the ultimate limit state. This analysis may be found in the Appendix 3.

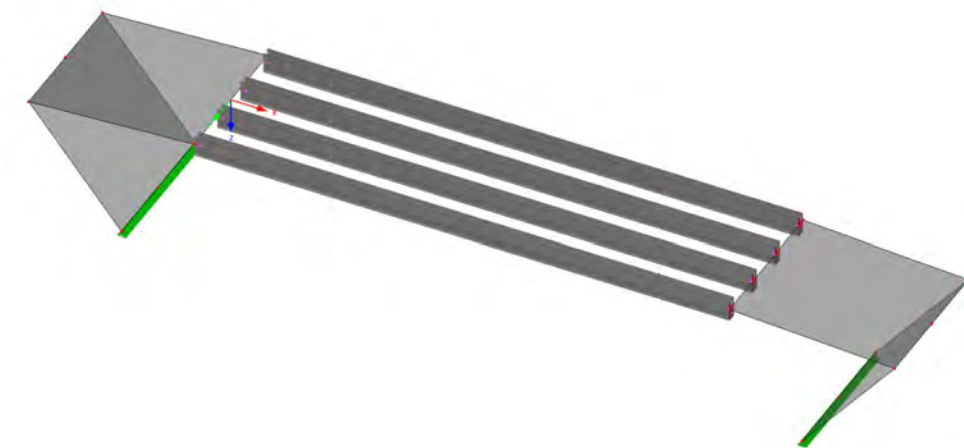


Figure 48: 3D Model Overview from RFEM.

The following figure (Figure 49) illustrates the location on the beam's cross-section where the stresses were calculated for all of the five construction phases. The stresses in these locations govern the design of the bridge girder because of its crucial location. The locations of contact between precast and in-situ concrete were inspected to see if tensile stresses existed, tensile stresses are not favorable for the design during the construction phases.

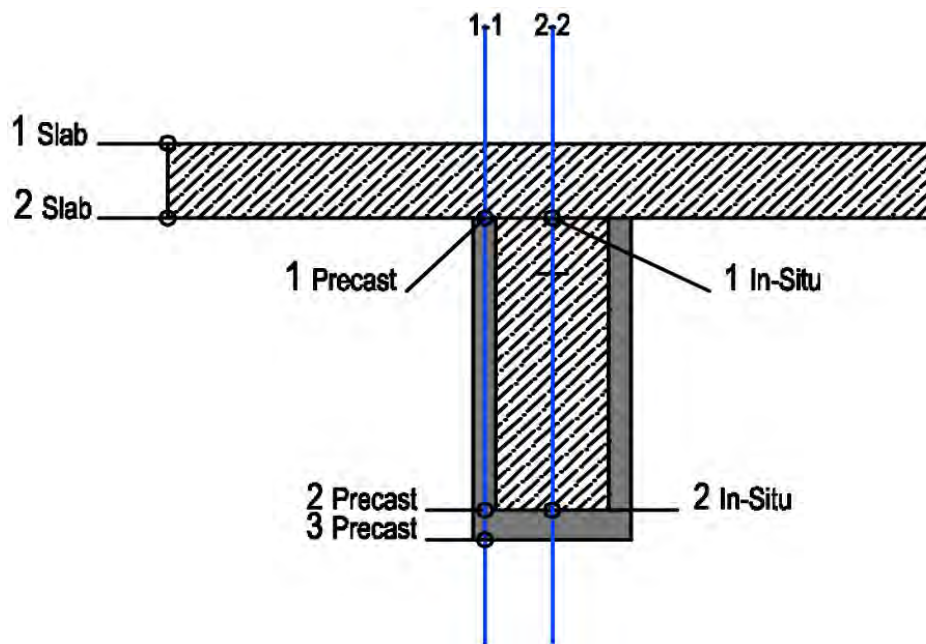


Figure 49: Location of Stress Points in Cross-Section.

### 6.2.1 Construction Phase 1

The first prestress load allows the precast beams to be moved to the construction site without being deformed while being transported and assembled, additionally, this initial prestress also helps the structure to resist some of the construction loads being applied during the construction phases. In the RFEM software model an initial support for the abutments is taken into consideration in order to keep the beams in the right position at the time the beams are placed into position. These additional supports are necessary to keep the abutments in an upright position while the beams are being hoisted into position. The bridge's structural system at this point is statically determinate, because it is not yet fixed at both ends to the abutments. Since all the prestressing for this phase happens elsewhere, there is no access to the tendons in order to modify the stresses.

As seen in the following figures the tendons are located at different locations to reinforce the beam's tensile areas. The loads applied on the structure to calculate the stresses were self-weight (MN) on each beam and the prestress on the tendons. The amount of prestress applied during this construction phase was calculated to be 1.5 MN for each beam.

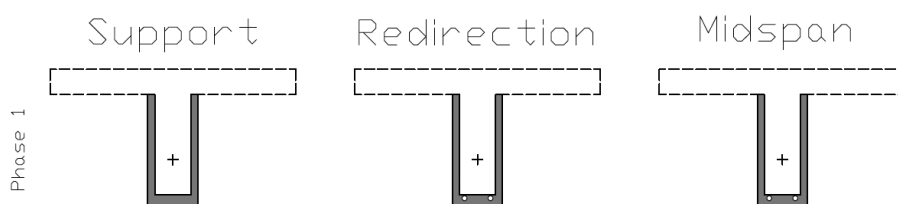


Figure 50: Cross-section sketches for construction phase 1.

$$\sigma_{max} = -2.00 \frac{MN}{m^2} < f_{ctm} = 4.1 \frac{MN}{m^2}$$

$$\sigma_{min} = -12.05 \frac{MN}{m^2} < 0.45 \cdot f_{ck} = -22.5 \frac{MN}{m^2}$$

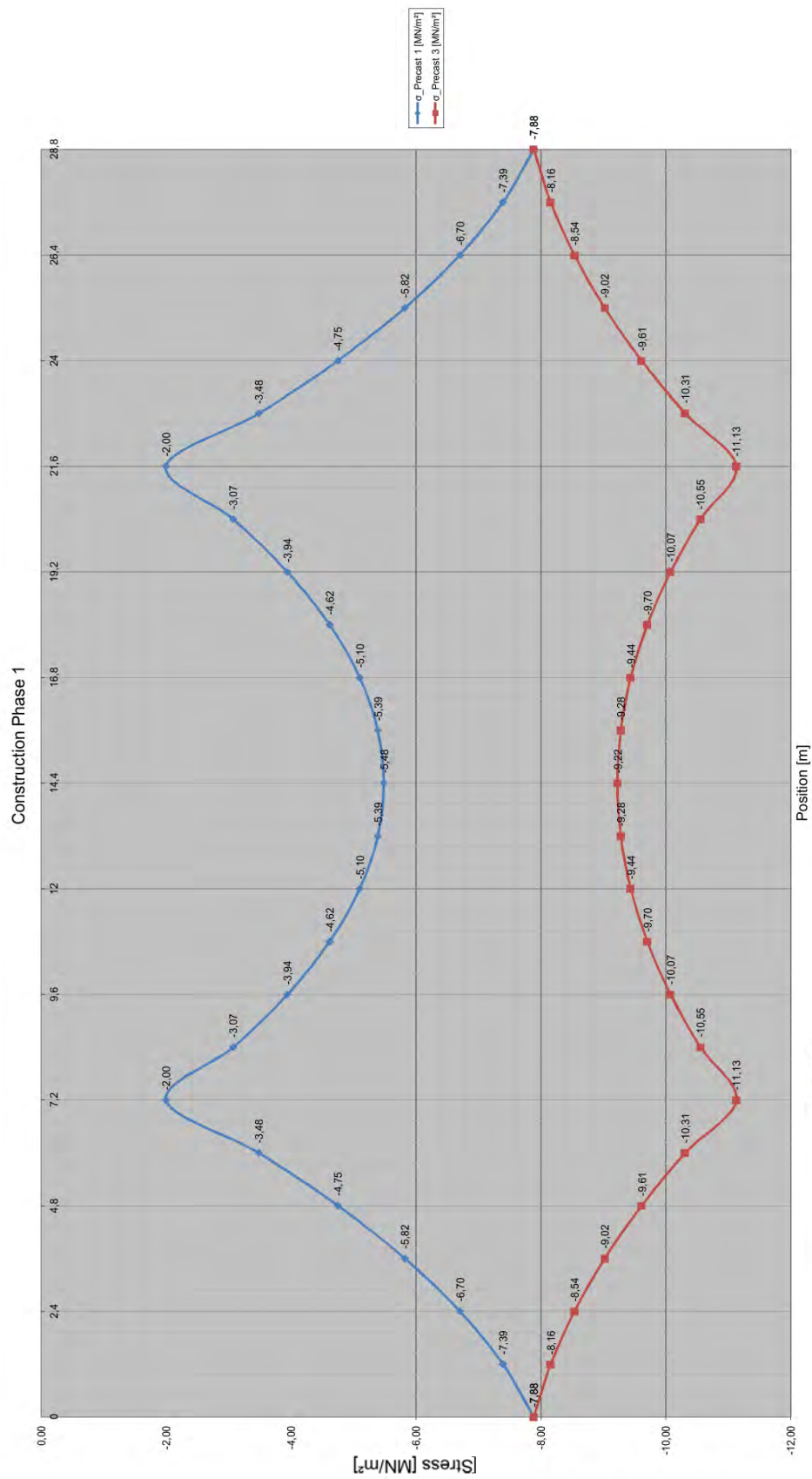


Figure 51: 3D Analysis Stresses Construction Phase 1.

### 6.2.2 Construction Phase 2

During the second construction phase additional tendons are added to the beams at a height of 1 meter as seen in Figure 52 to be able to connect the beams to the abutments and avoid all types of joints. These tendons connect the abutments to the beam from the edge of the abutment to the redirection location of the beam. With the addition of these tendons the system is no longer statically determinate but it is then statically indeterminate. The software RFEM takes into account the change in system and automatically calculates the correct internal forces. The self-weight considered in this phase was 9 kN/m on each beam and 0.25 MN prestress.

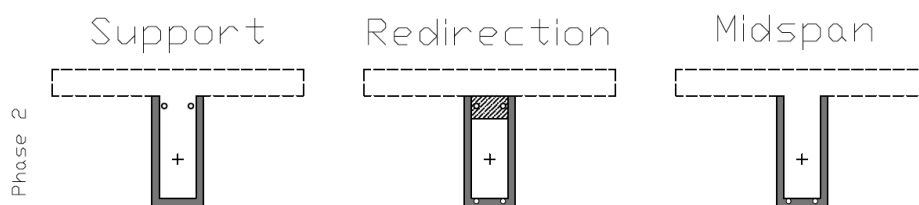


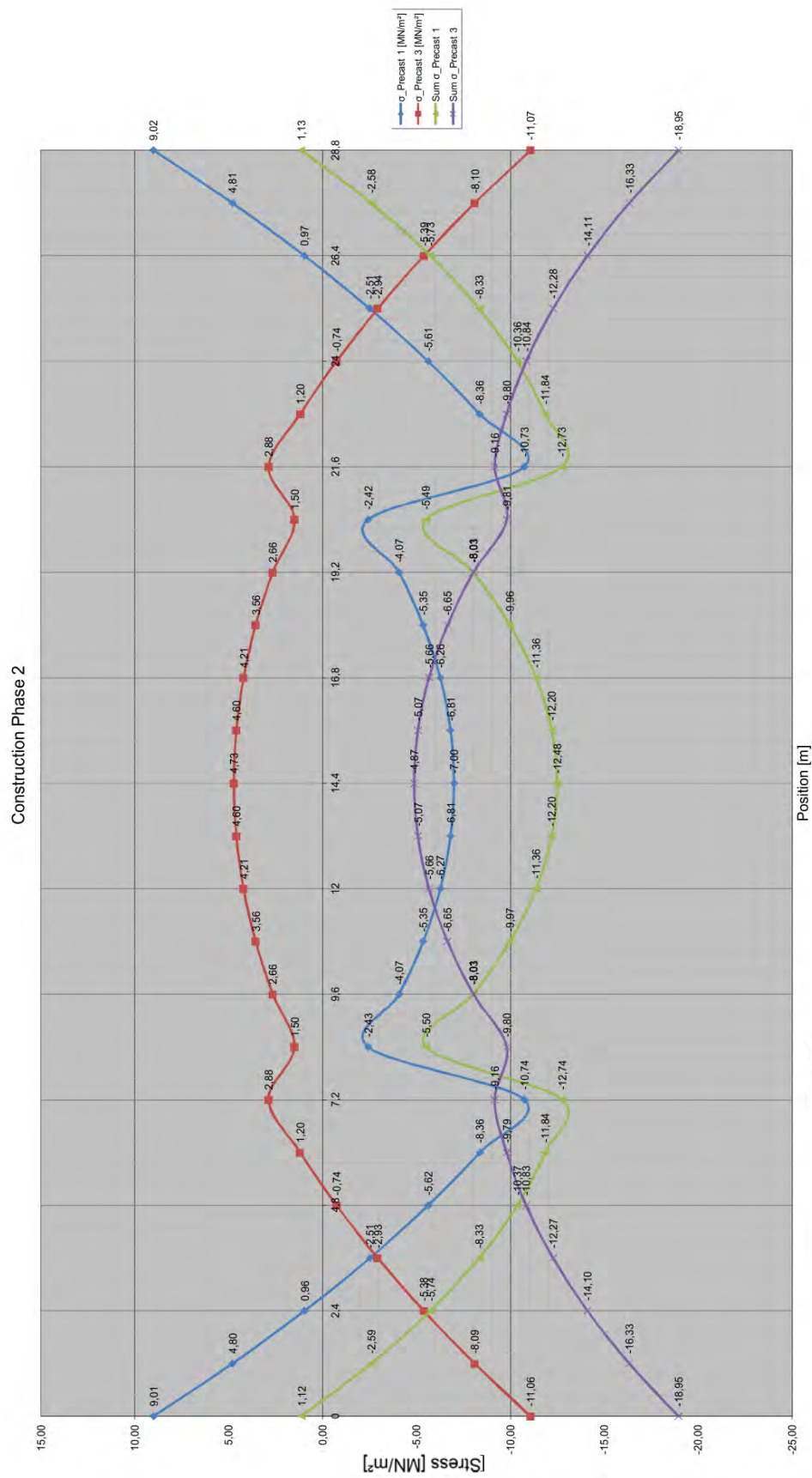
Figure 52: Cross-section sketches for construction phase 2.

#### Monostrands

The prestress from this construction phase is applied to eight monostrands (two per girder) situated from the redirection points of the girder all the way to the end of the abutment. These monostrands are anchored on the redirection construction and are prestressed at the end of the abutment.

$$\sigma_{max} = 1.13 \frac{MN}{m^2} < f_{ctm} = 4.1 \frac{MN}{m^2}$$

$$\sigma_{min} = -18.95 \frac{MN}{m^2} < 0.45 \cdot f_{ck} = -22.5 \frac{MN}{m^2}$$





### 6.2.3 Construction Phase 3

The largest amount of prestress is applied during this phase therefore it has the largest amount of tendons. These tendons are prestressed with 2.875 MN and are positioned throughout the entire length of the beam (see Figure 54). The tendons' location is imperative to maintain the entire beam under compressive stresses. Therefore, the tendons from this construction phase are laid where the beams largest tensile stresses would show up. Additional tendons are put into the same duct in order to be later prestressed during construction phase 4.

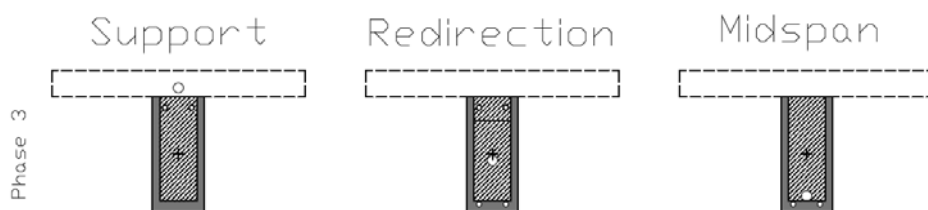


Figure 54: Cross-section sketches for construction phase 3.

#### Hole spacing

For this construction phase the hole spacing was taken to be the following:

During this construction phase all 19 tendons are prestressed to 89% of their capacity, leaving the rest 11% for the next phase.

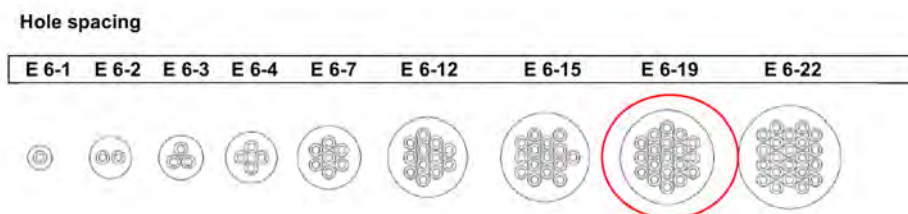


Figure 55: Hole spacing for 19 tendons. [20]

$$\sigma_{max} = 1.29 \frac{MN}{m^2} < f_{ctm} = 4.1 \frac{MN}{m^2}$$

$$\sigma_{min} = -19.13 \frac{MN}{m^2} < 0.45 \cdot f_{ck} = -22.5 \frac{MN}{m^2}$$

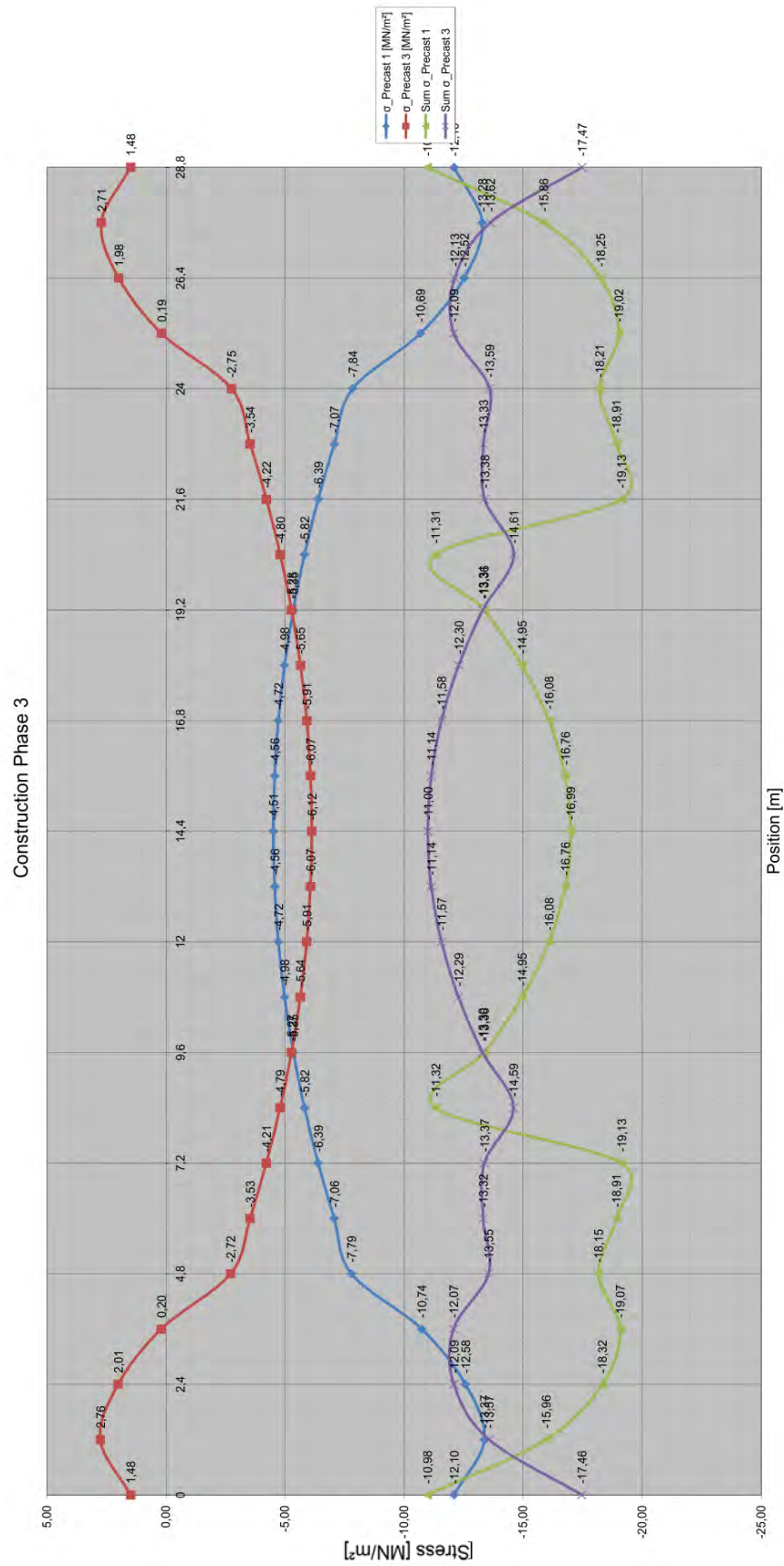
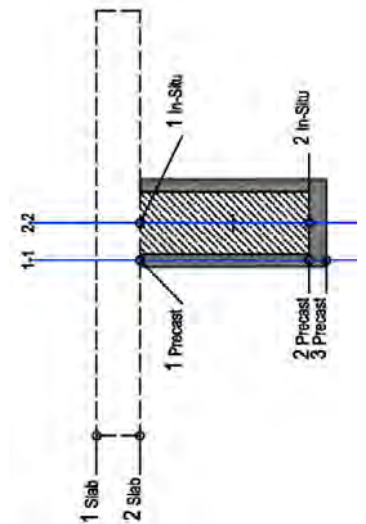


Figure 56: 3D Analysis Stresses Construction Phase 3.



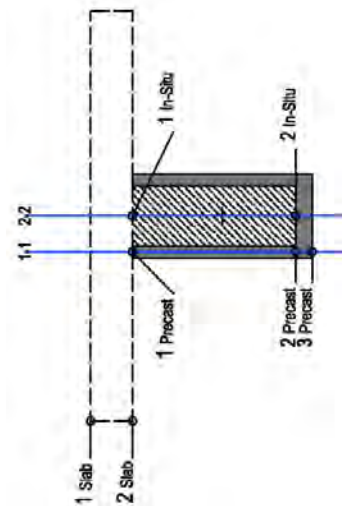
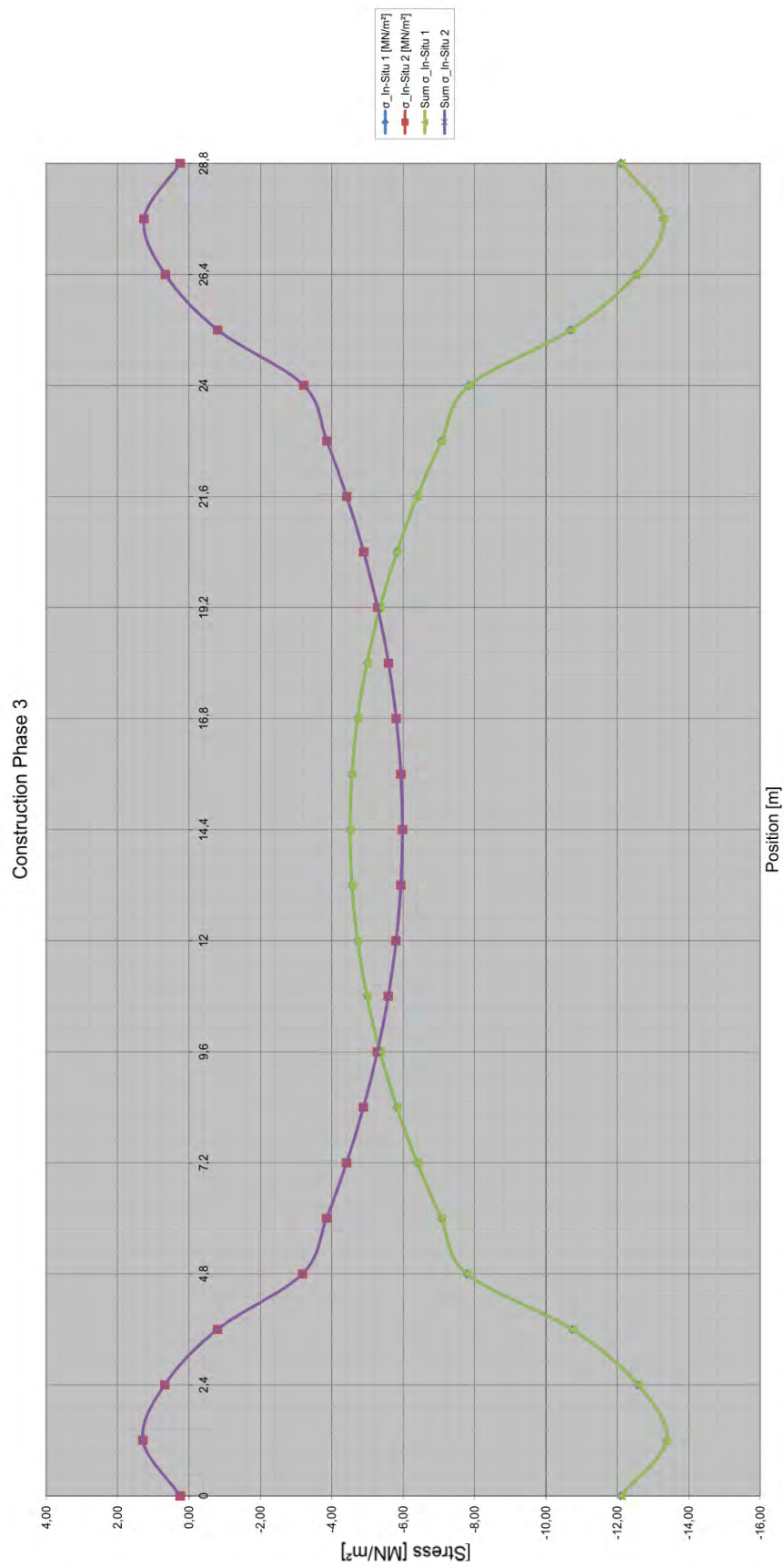


Figure 57: 3D Analysis In-Situ Concrete Stresses Construction Phase 3.

#### 6.2.4 Construction Phase 4

During this construction phase the last prestressing occurs because the complete cross-section is by now finished. All dead loads have been applied to the previous construction phases, and therefore most stresses have already been taken into account. As mentioned before, the tendons share the same duct as the tendons in the third construction phase but are prestressed at a later time. This last prestress of 0.50 MN, on each girder, is then applied to the completed cross-section, which has no extra self-weight loading, allowing the in-situ concrete as well as the precast beams to get more compressive stresses.

Additionally, a surface was introduced into the software model in order to simulate the bridge slab. The software model RFEM has an option (Ribs) to embed members into surfaces to better simulate the interaction between surface and members. Therefore, the internal forces calculated with the model simulate reality more accurately than by just superimposing the results.

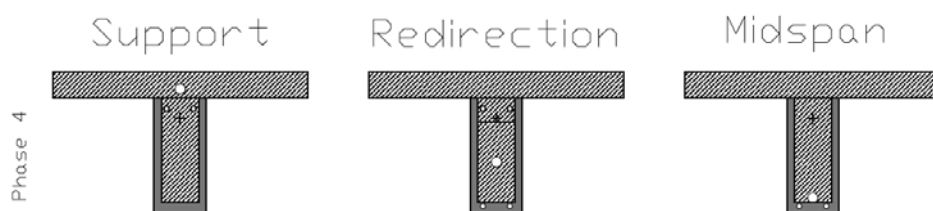


Figure 58: Cross-section sketches for construction phase 4.

#### Hole Spacing

During this phase, the last 11% of the tendon's capacity are prestressed in order to achieve 100% prestress on all 19 tendons.

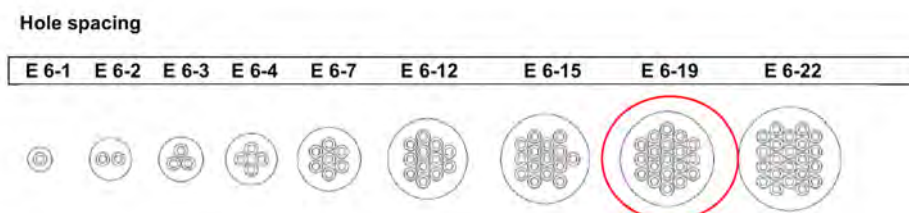


Figure 59: Hole spacing for 19 tendons. [20]

$$\sigma_{max} = 1.75 \frac{MN}{m^2} < f_{ctm} = 4.1 \frac{MN}{m^2}$$

$$\sigma_{min} = -19.61 \frac{MN}{m^2} < 0.45 \cdot f_{ck} = -22.5 \frac{MN}{m^2}$$

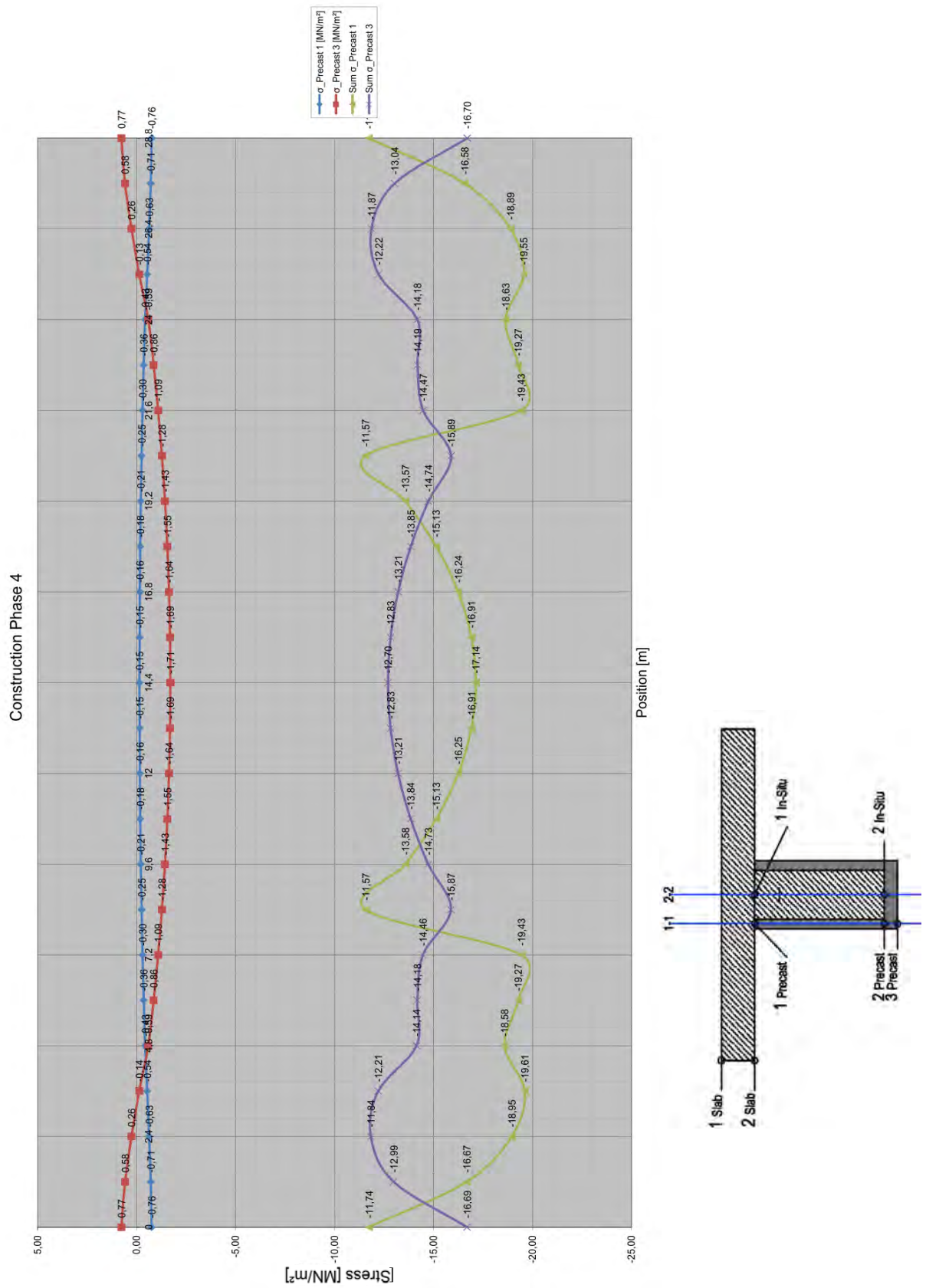


Figure 60: 3D Analysis Stresses Construction Phase 4.



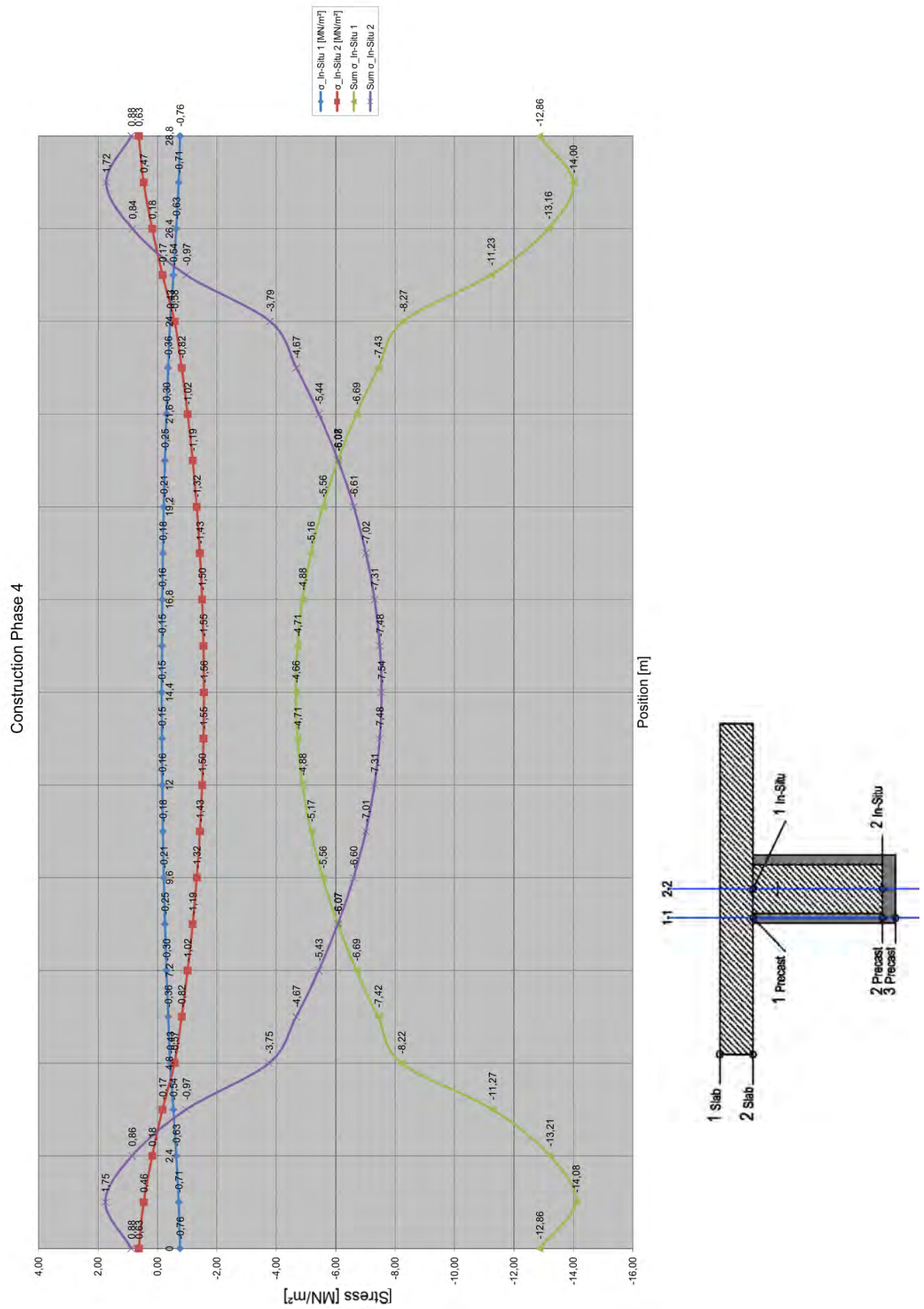


Figure 61: 3D Analysis In-Situ Concrete Stresses Construction Phase 4.

During the previous construction phase (No. 4), it can be seen that the stresses at 2.4 m away from the support location surpass the limit of  $0.45 \cdot f_{ck} = 13.5 \text{ MN/m}^2$ . The stress at this point is  $14.08 \text{ MN/m}^2$ , which is about 4% more than the allowable stress value. This stress is located at the top surface of the in-situ concrete. When looking into the stresses taking the creep value into account, it can be seen that the final stress at this point is actually lower. Therefore, the stress is taken into consideration but no further action is required.

### 6.2.5 Construction Phase 5 (Load Model 1)

This construction phase, as mentioned before, consists of the loading live loading applied on the structure according to the load model 1 [18]. Therefore, the loads applied to this phase are only the live loads specified in load model 1. This phase doesn't include any self-weight loading or prestressing.

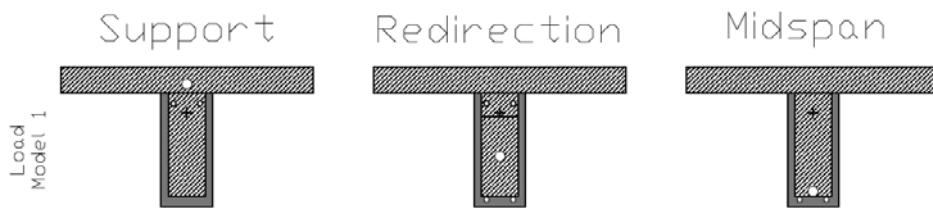


Figure 62: Cross-section sketches for Load Model 1.

$$\sigma_{max} = 4.23 \frac{\text{MN}}{\text{m}^2} > f_{ctm} = 4.1 \frac{\text{MN}}{\text{m}^2} \text{ additional reinforcement considered}$$

$$\sigma_{min} = -22.43 \frac{\text{MN}}{\text{m}^2} < 0.60 \cdot f_{ck} = -30.0 \frac{\text{MN}}{\text{m}^2}$$

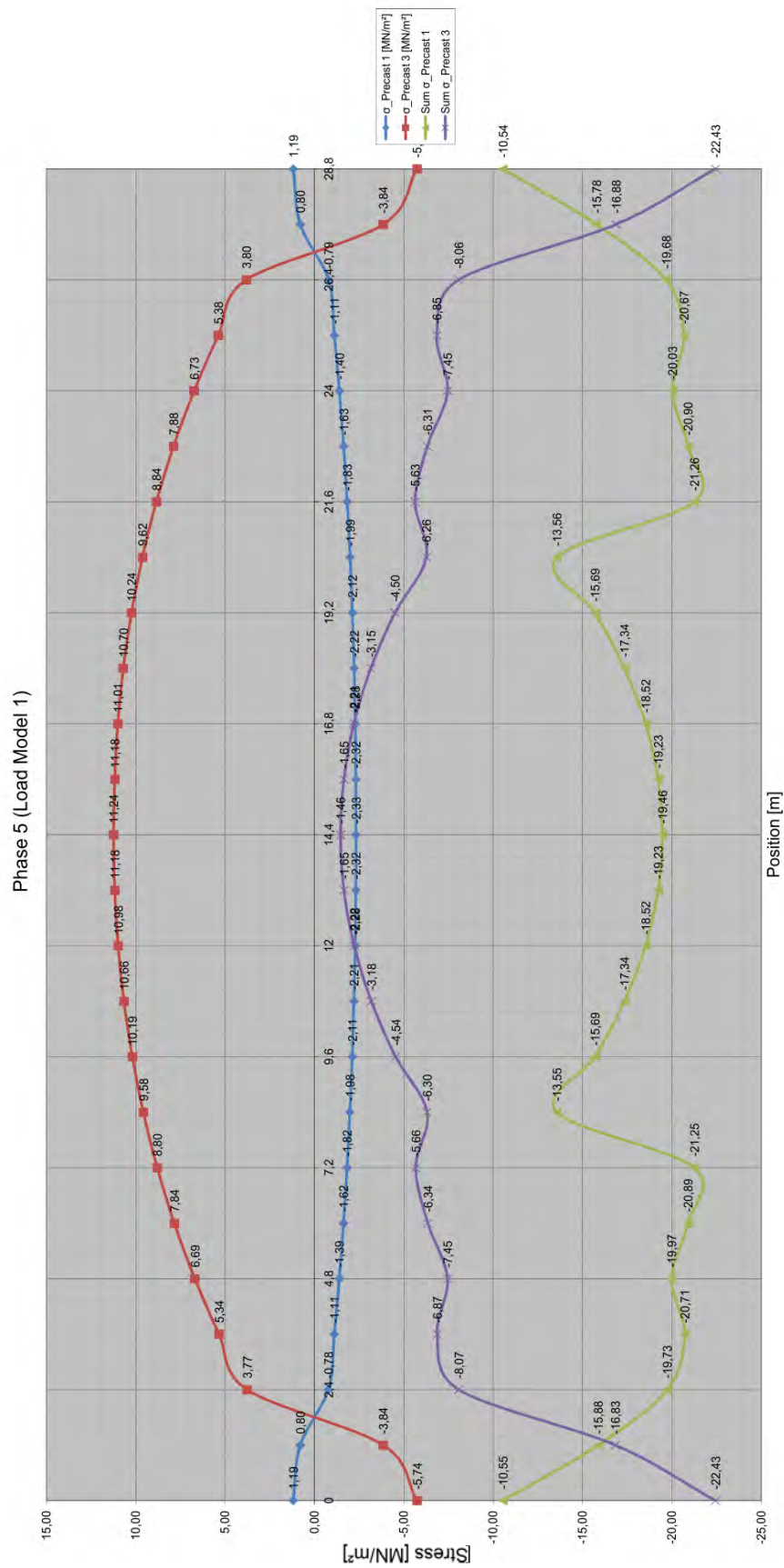
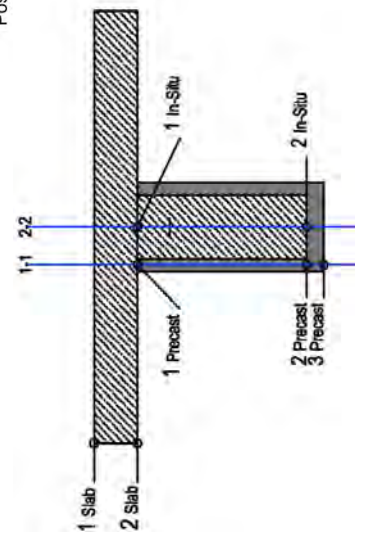


Figure 63: 3D Analysis Stresses Load Model 1.





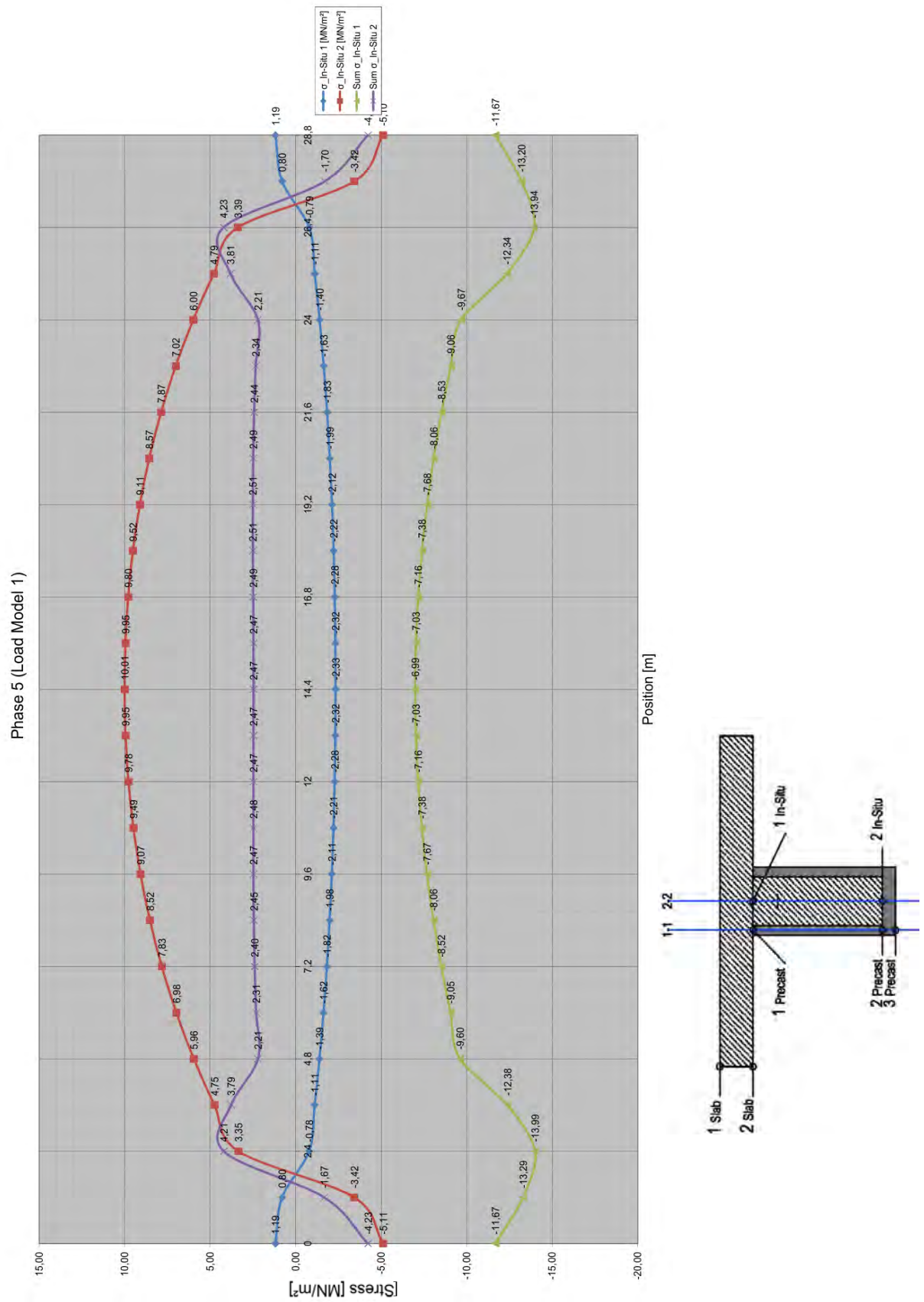


Figure 64: 3D Model In-Situ Concrete Stresses Load Model 1.

### 6.2.6 Calculation of Tendons for each Construction Phase 3D Model

The previous chapter illustrates how much prestress is applied on each construction phase. This section calculates the number of strands needed in order to satisfy the stresses calculated for each of the construction phases. This was done according to European Technical Approval No. ETA-06/0006

$$P_{max} = A_p \sigma_{p,mo}$$

$$n = \frac{P_{max}}{\sigma_{p,mo} \cdot A_{p,i}}$$

$$n = \frac{P_{max}}{0.7 \cdot 1860 \frac{N}{mm^2} \cdot 150 mm^2}$$

Determining the number of tendons necessary for each beam on each construction phase were determined from the stress applied to each construction phase in both the 2D and 3D analysis. The final amount of pretensioning

Table 1: Tendons for each Construction Phase

Construction Phase	$P_{max}$	Nr. Tendons
1	$\frac{6 MN}{4} = 1.5 MN$	$n = 7.68 \approx 8$
2	$\frac{2 MN}{4} = 0.5 MN$	$n = 2.56 \approx 4$
3	$\frac{11.5 MN}{4} = 2.87 MN$	$n = 14.72 \approx 15$
4	$\frac{2 MN}{4} = 0.5 MN$	$n = 2.56 \approx 4$

The diameter of the ducts containing the tendons was also calculated with the same European Technical Approval Ducting 2.2.1. But the final duct diameter sizes were taken from the table in page 59 of the ETA-06/0006. Tendons in construction phases 3 and 4 share the same duct, but are prestressed at different times as mentioned before.

Table 2: Duct Diameter for each Construction Phase

Phase	Strands [-] $A_P$ [mm <sup>2</sup> ]	$\varnothing_{int}/\varnothing_{ext}$ [mm]
1	n = 4 strands $A_P=600$ mm <sup>2</sup>	$\varnothing$ 45/50
2	n = 2 strands $A_P=300$ mm <sup>2</sup>	$\varnothing$ 40/45
3 and 4	n = 19 strands $A_P=2850$ mm <sup>2</sup>	$\varnothing$ 90/97

The prestressed tendons used in the bridge design were calculated from the excel spreadsheet found in Appendix 1 and Appendix 2, which calculates the stresses in the construction phases in order to determine the amount of prestress necessary to keep the bridge's stresses within the allowable norm values.

The following figure (Figure 65) illustrates the type of tendons and its position (not to scale) inside of the girders.

# Prestress Locations Construction Phases

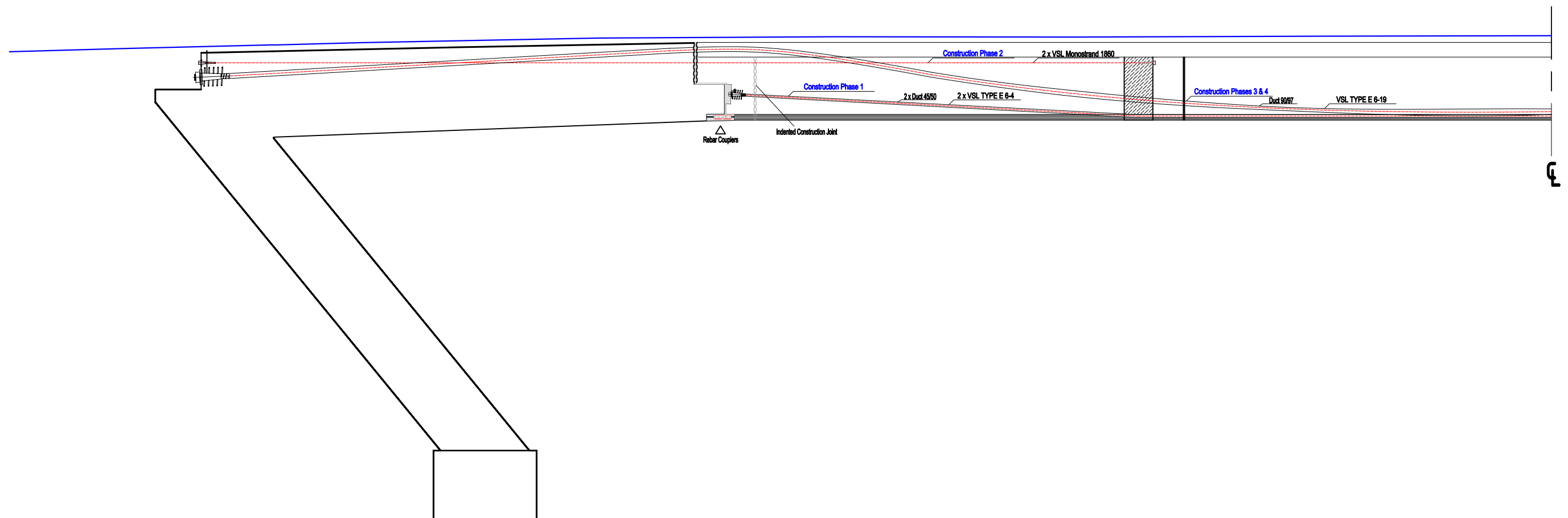


Figure 65: Tendon Layout for all Construction Phases.

### 6.3 Falsework Analysis

As mentioned in the previous chapter, an analysis was performed on a model simulating the construction of the bridge being performed all with one single construction phase. This falsework analysis was performed to find the stresses at the same locations as with the 3D analysis consisting of 4 construction phases plus the load model 1 phase. Therefore, the stresses were calculated with the same excel calculation. In the following figures (Figure 66, Figure 67, Figure 68, and Figure 69) one can see the stress distribution on the specific locations of the cross-section. The complete Excel analysis can be found in the Appendix 8.3. These stress curves illustrate how larger tensile stresses appear compared to the 4 Phase analyses. This falsework construction model helped the analysis of the internal stresses to then compare them to the stresses calculated with the 4th construction phase's analysis. This was done to be able to compare how the restraint forces inside of the structure change due to creep.

The falsework analysis as mentioned before, assumes all the prestresses as well as the loading due to self-weight are applied all at once. The prestresses taken into consideration were the ones at  $t=0$  to then compare them to the stresses calculated previously from the construction phases 4 and 5 (LM1). The stresses were calculated and plotted on the same excel spreadsheets in order to compare the stresses on the same locations of the girders.

The following section illustrates the cross-sectional stresses for the analysis consisting of 5 phases as well as the analysis for the falsework

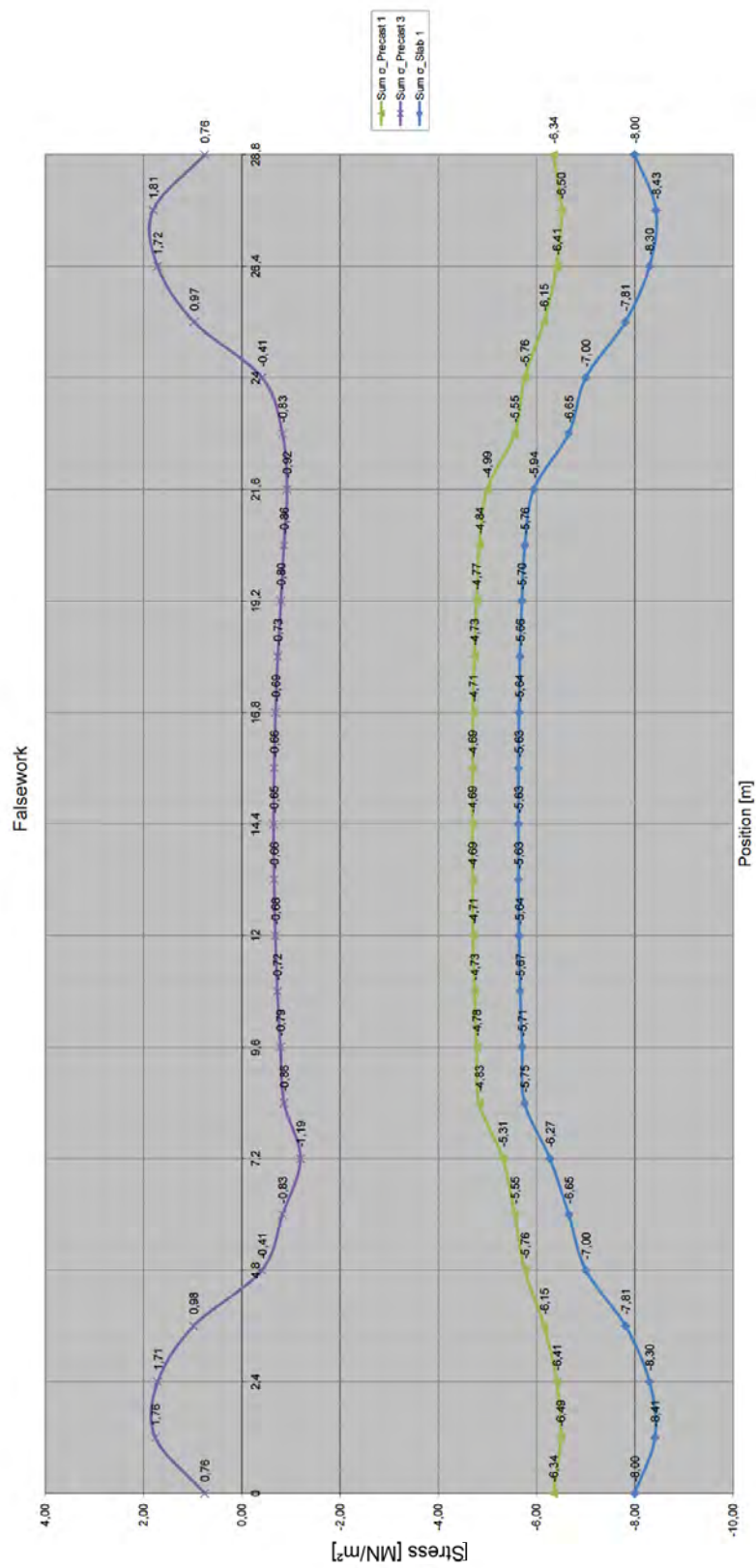
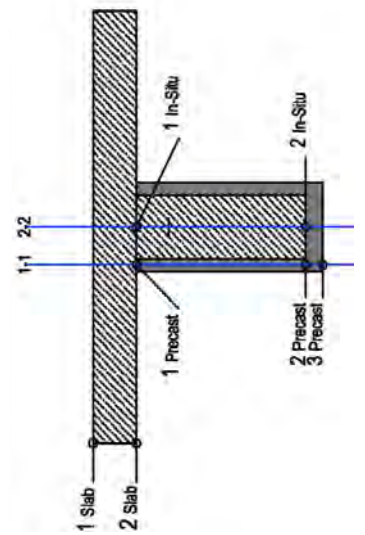


Figure 66: Falsework Stresses



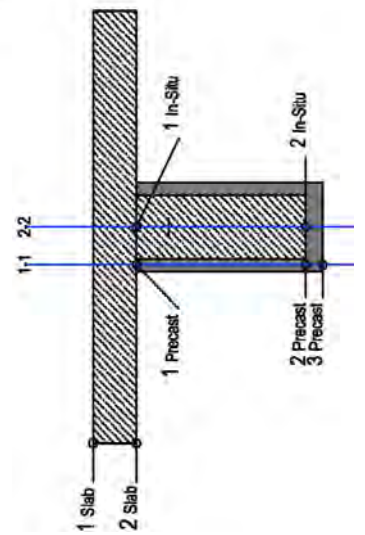
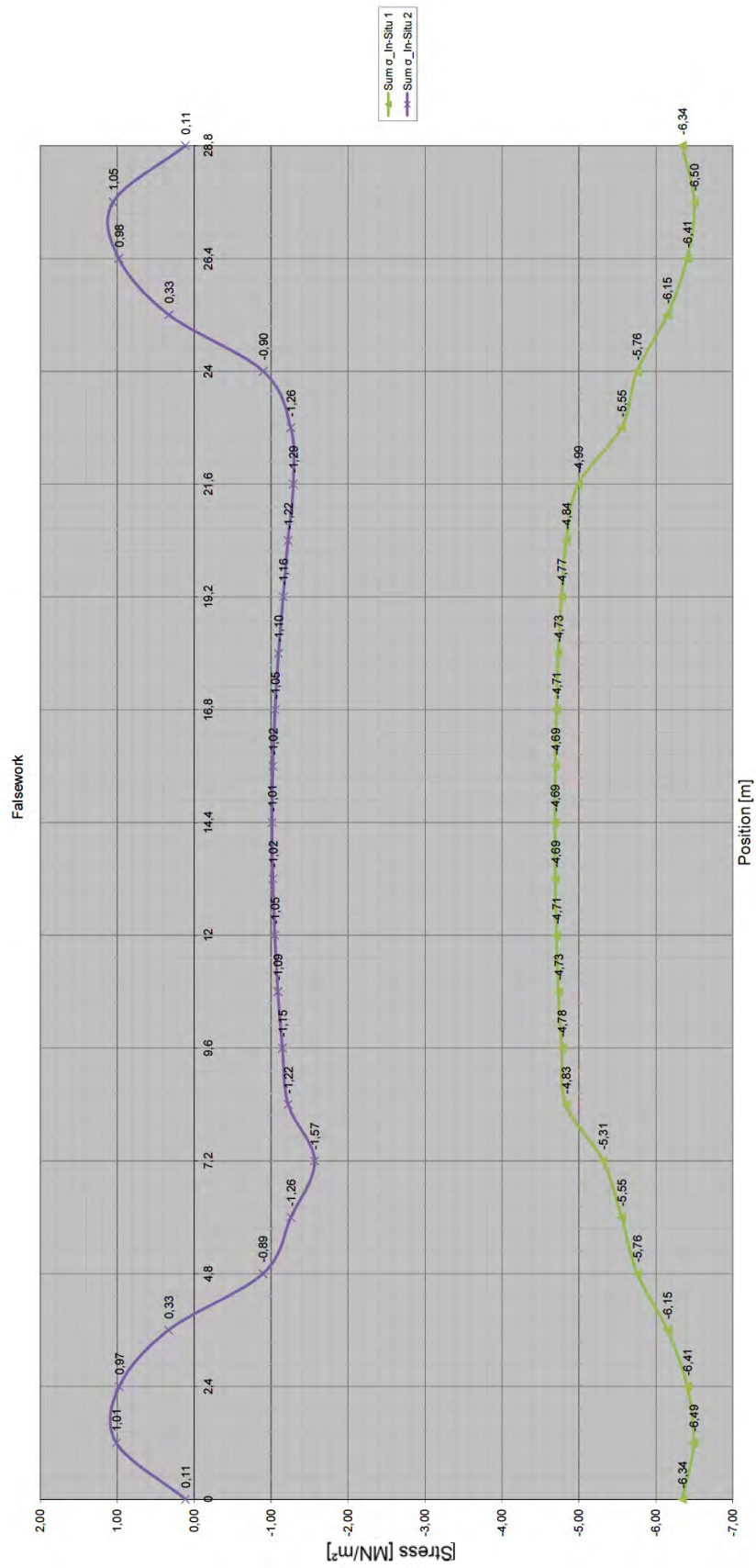


Figure 67: Falsework Stresses



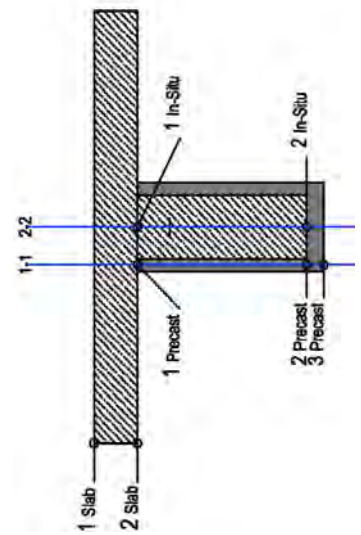
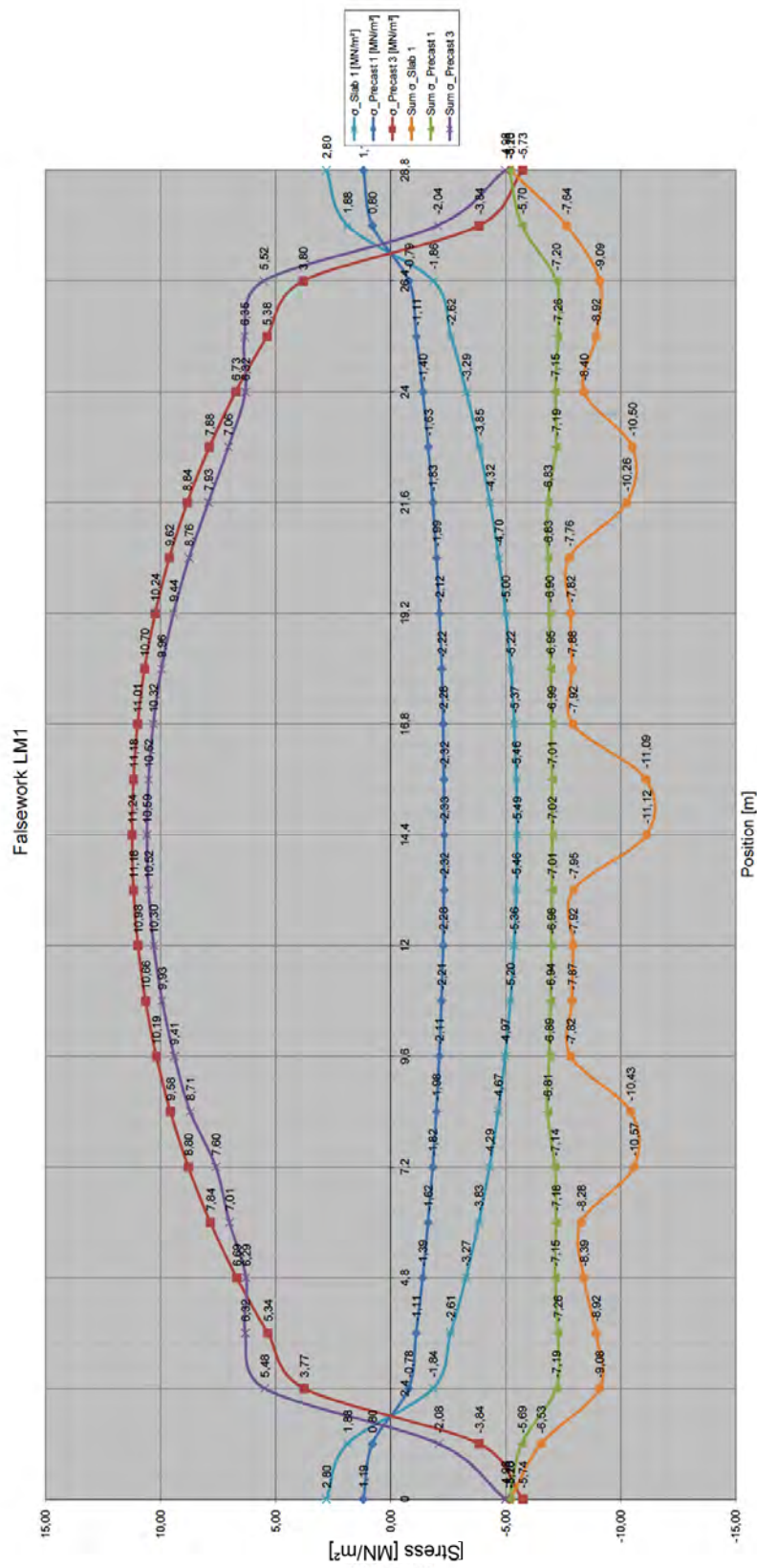


Figure 68: Falsework Stresses Load Model 1.



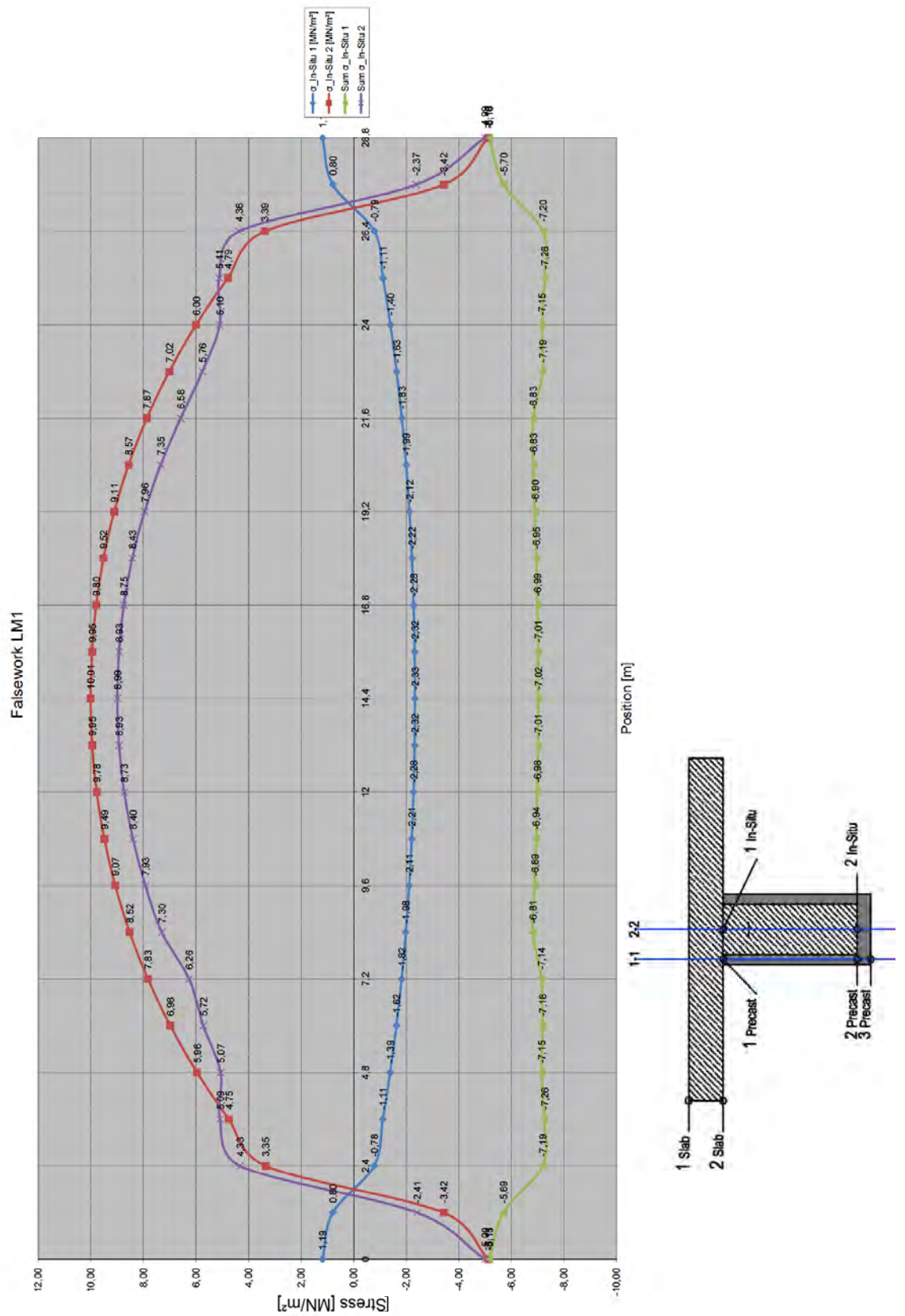


Figure 69: Falsework Stresses Load Model 1.

#### 6.4 Stress Comparison (5 Phases vs. Falsework and Creep)

Precast concrete members are subject to air-drying as soon as they are removed from molds or form. During exposure to the atmosphere, the concrete slowly loses some of its original water causing a shrinkage volume change to occur. [12]

When concrete is subjected to a sustained load, the deformation may be divided into two parts the first on being an elastic deformation which occurs immediately, and the second being a time-dependent deformation which begins immediately and continues at a decreasing rate over time. This time-dependent deformation is called creep. [12]

Creep and shrinkage strains vary with relative humidity, volume-surface ratio (or ratio of area to perimeter), level of sustained load including prestress, concrete strength at time of load application, and location of steel reinforcement, and other characteristics of the material and design. When high strength concretes are used, different values of shrinkage and creep may be needed. The joints between recast members typically are detailed to relieve such strains. [12]

The volume changes due to temperature variations can be positive (expansion) or negative (contraction), while volume changes from shrinkage and creep are only negative. [12]

According to the EN 1992-1-1 when the compressive stress of concrete at age  $t_0$  exceeds the value of  $0,45 f_{ck}(t_0)$  then creep non-linearity should be considered, therefore, during the stress analysis the stresses were kept under  $0,45 f_{ck}(t_0)$  to avoid considering non-linearity. Such a high stress can occur as a result of pretensioning, e.g. in precast concrete members at tendon level. [21]

The following formula was used to calculate the stresses at a later time taking the creep coefficient for the entire cross-section and the stresses from the falsework and the construction phases.

$$\sigma(t) = \sigma_B + (\sigma_L - \sigma_B) \cdot \frac{\varphi_{o\ Total}}{1 + \chi \cdot \varphi_{o\ Total}}$$

The following stress plots illustrate the cross-sectional stresses for the 3D analysis with construction phases, the falsework analysis, and a stress approximation using an analysis taking the creep coefficient into consideration, which can be found in section 8.4.

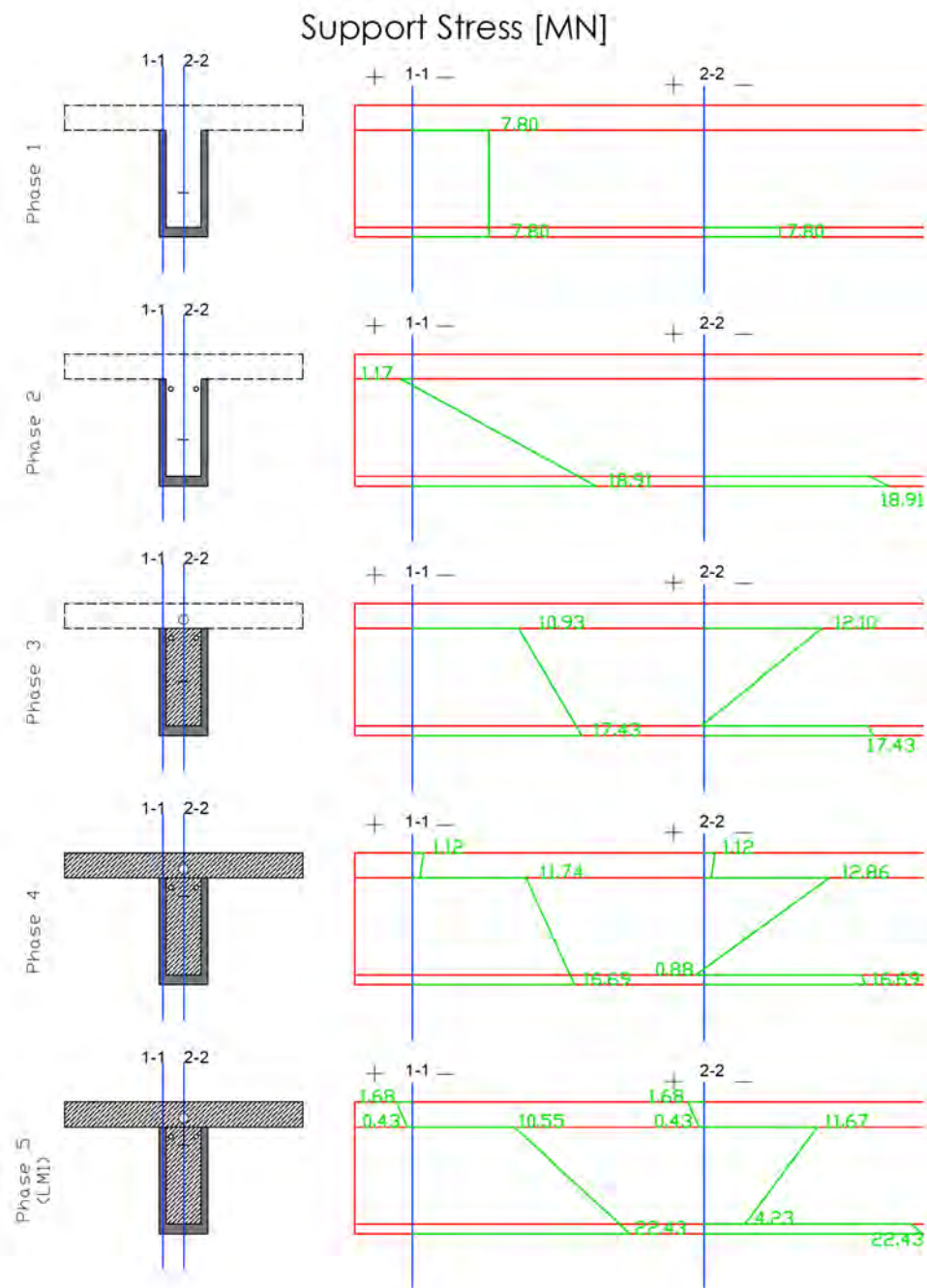


Figure 70: Stresses for all Construction Phases at the Support

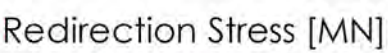


Figure 71: Stresses for all Construction Phases at Redirection Location

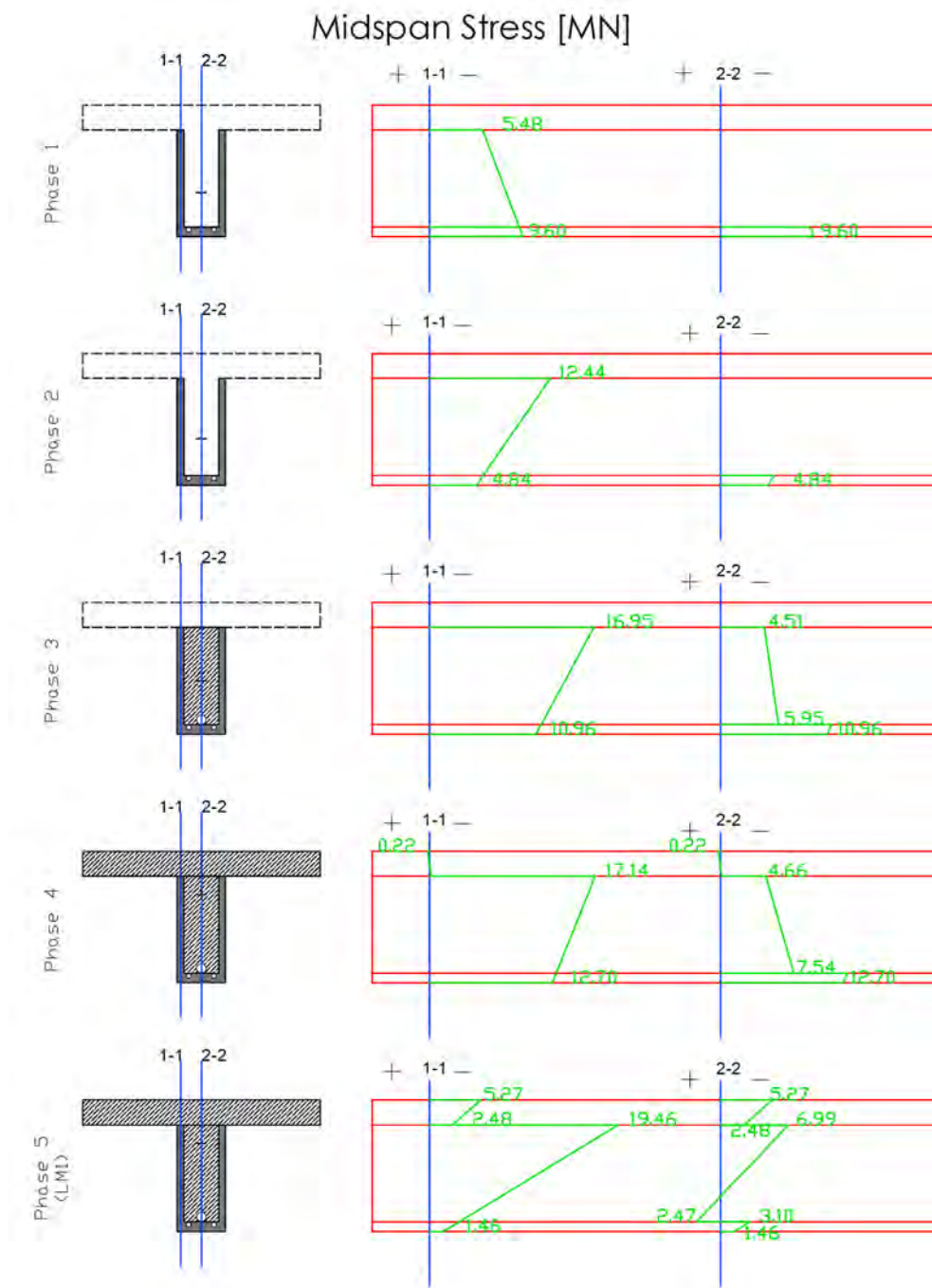


Figure 72: Stresses for all Construction Phases at Midspan.



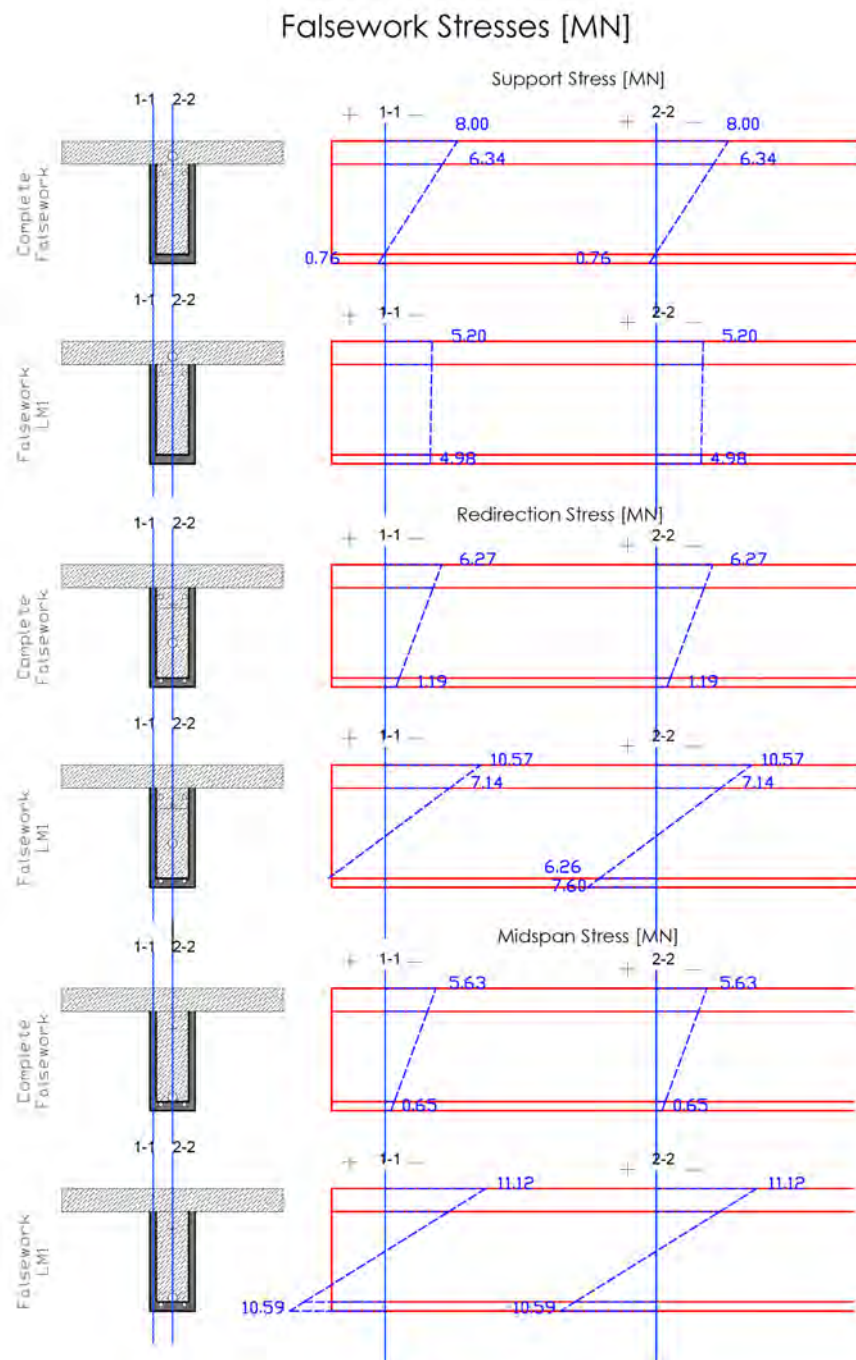


Figure 73: Falsework Stresses at Support, Redirection and Midspan locations.

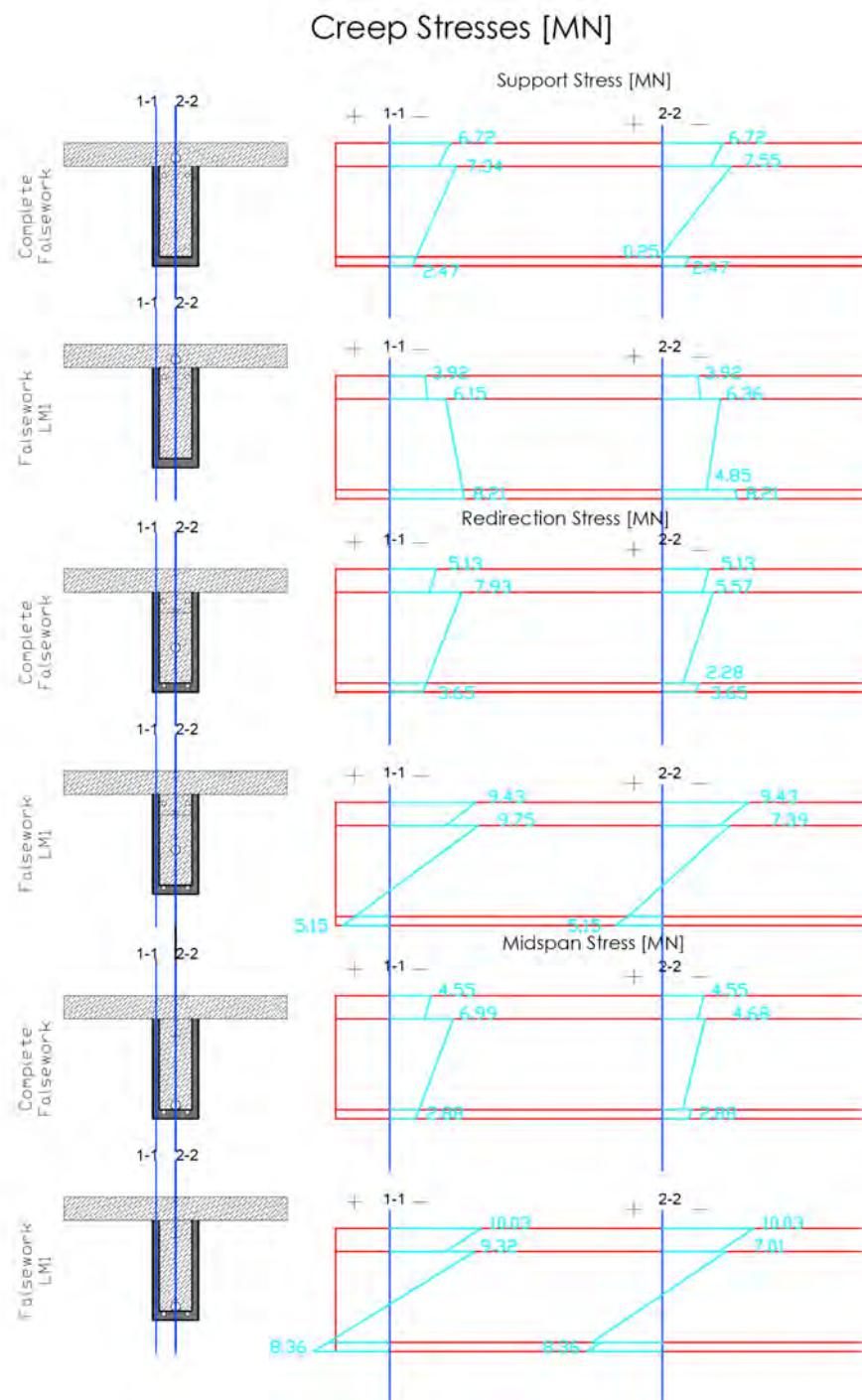


Figure 74: Creep Stresses at Support, Redirection and Midspan locations.

### Support Stress Comparison [MN]

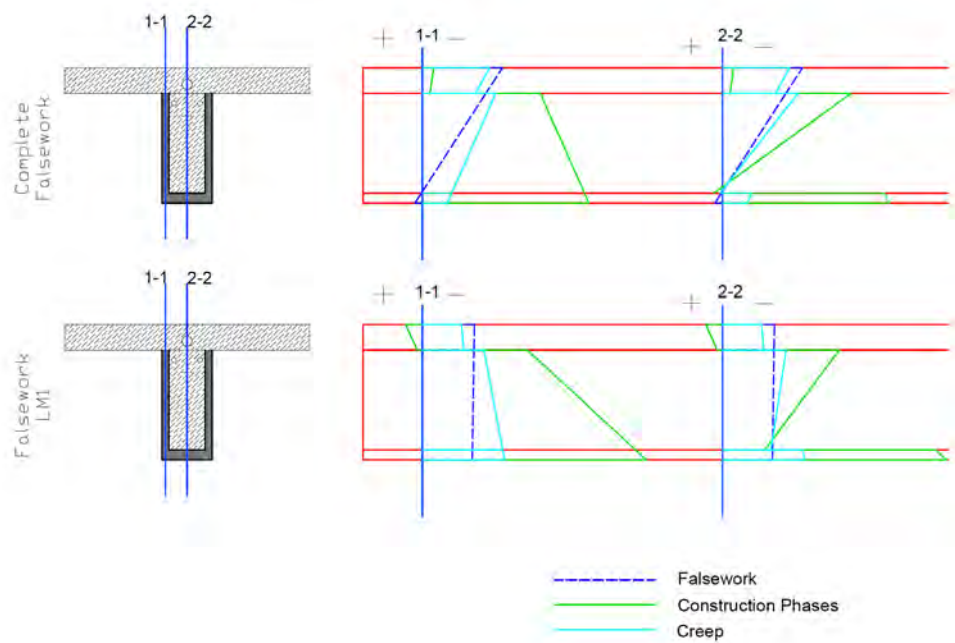


Figure 75: Stress Comparison at Support.

### Redirection Stress Comparison [MN]

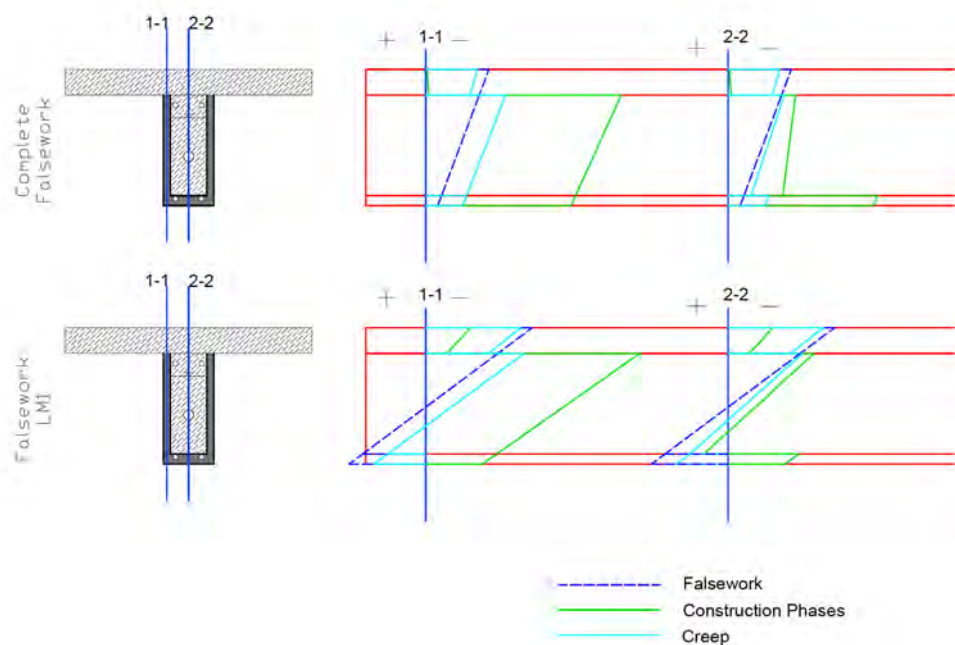


Figure 76: Stress Comparison at Redirection Location.



## Midspan Stress Comparison [MN]

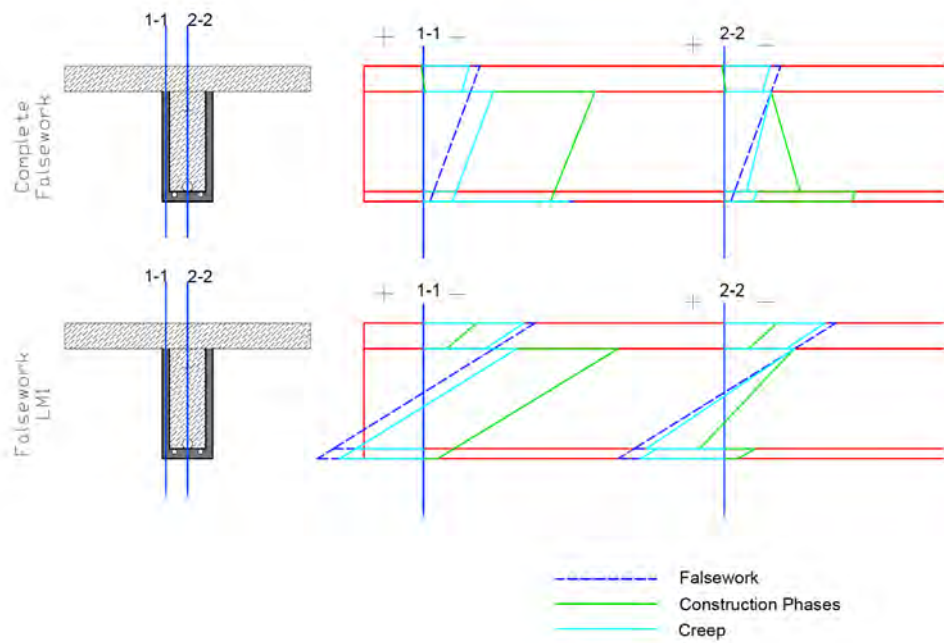


Figure 77: Stress Comparison at Midspan.

### 6.5 *Ultimate Limit State Analysis*

In order to finalize the analysis of the complete bridge girders, an ultimate limit state analysis of the structure was performed to find the reinforcement needed for all locations of the bridge. A more extended analysis for each of the three main locations (support, redirection, and midspan) can be located in Appendix Section 8.6.

Longitudinal Reinforcement:

4 Ø 26

Shear Reinforcement:

Ø 16/15

Slab Reinforcement:

Ø10/15

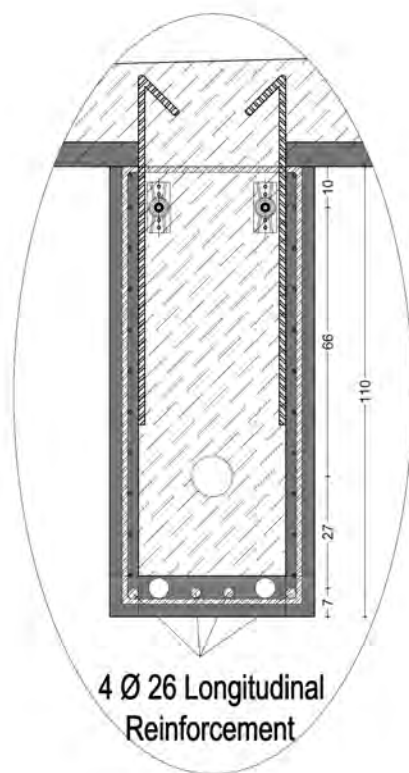


Figure 78: Typical Girder Cross-Section with Reinforcement.

## ***7 Summary and Conclusions***

This research illustrates the plausibility of building bridge with use of precast prestress thin wall girders. These girders built similarly to double wall elements, are slender and may realistically be used to build bridges previously limited to composite construction methods.

The construction phases' method used in order model and design the bridge helped better approximate how the bridge would really be built. The use of construction phases allowed the design to take considerations in advance in order to save construction time if the bridge were to be built as well as to simplify the design as much as possible.

Being able to build such a slender bridge with an equivalent bending stiffness to that of a composite bridge is big advantage, because a monolithic construction consisting of only one material type is easier to handle. Additionally, the way this bridge was designed it allows construction to happen without much additional formwork on site. An approximate 77% of the bridge is in-situ concrete; meaning only 33% of the weight has to be transported as an already built structure, reducing logistic problems. Additionally, the precast girders and slabs act as formwork reducing the construction time as well as the time the road needs to be closed. These advantages justify and allow concrete to be used as a material to build slender structures.

As mentioned before, this research is an ongoing project at the Vienna University of Technology where different innovative techniques are being explored in order to give another perspective to concrete construction methods.

## Works Cited

- [1] ASFINAG Autobahn Service GmbH Nord, Bestandsuebersichtsplan A1 Westautobahn, 2010.
- [2] David Wimmer, "Thin-walled precast concrete girders for bridge construction and civil engineering," *BFT INTERNATIONAL Concrete Plant + Precast Technology*, Aug. 2013.
- [3] David Wimmer, "Dissertation," TU Wien, Phd Thesis 2014.
- [4] Benjamn Kromoser, "Brueckenbau mit duennwandigen Fertigteilern Grossversuch zur Herstellung und zum Torsionswirkungsverhalten," TU Wien, MSc. Thesis 2011.
- [5] R.J. Lock, "Integral Bridge Abutments," Schofield Centre, M.Eng Project Report 2002.
- [6] John Connal. (2004) Integral Abutment Bridges - Austalian and US Practice. [Online]. <http://www.bridgeforum.org>
- [7] Burk Jr M.P., *The Design of Integral Concrete Bridges.*: Concrete International.
- [8] Lan Cheng, "On the Performance of Super-Long Integral Abutment Bridges - Parametric Analyses and Design Optimization," University of Trento,.
- [9] S Arsoy, J.M Duncan, and R.M Barker, "The Behavior of Integral Abutment Bridges," *FHWA/VTRC 00-CR3*, 1999.
- [10] Martin P. Burke, "Why Integral Bridges?," *Steel Bridges; News and Information from the Steel Bridge Gorum*, Fall 1993.
- [11] Pierce Bounds. (2013) wikipedia.org. [Online]. <http://memory.loc.gov/pnp/habshaer/pa/pa1700/pa1791/photos/355813pv.jpg>
- [12] PCI Industry Handbook Committee, *PCI Design Handbook, Precast and Prestressed Concrete*, 6th ed. Chicago: PCI, 2004.
- [13] Kim Elliot, *Precast Concrete Structures*. Oxford: Elsevier, 2002.
- [14] Johann Kollegger, *Skriptum Betonbau 1.*, 2010.
- [15] Johann Kollegger, *Skriptum Betonbau 2.*, 2010.
- [16] State of California, *Prestressed Manual: A guide for field inspection of Cast-*

---

*in-place post-tensioned structures*. California: DoT California, 2005.

- [17] bvt rausch. (2013, Dec.) BVT Rausch. [Online].  
[http://www.bvtrausch.com/english/kap\\_steel\\_wave.htm](http://www.bvtrausch.com/english/kap_steel_wave.htm)
- [18] European Committee for Standardization, *EN 1991-2, Eurocode 1: Actions on structures - Part 2: Traffic loads on bridges*.
- [19] European Committee for Standardization, *EN 1991-1-1, Eurocode 1 Actions on Structures - Part 1-1 General actions - Densities, self-weight, imposed loads for buildings*., 2002.
- [20] European Technical Approval, *No. ETA-06/0006*.
- [21] European Committee for Standardization, *EN 1992-1-1, Eurocode 2: Design of concrete structures Part 1-1: General rules and rules for buildings*.
- [22] Greg Shafer. (2013) *Innovative Methods of Concrete Bridge Design*. Document.

## *List of Tables and Figures*

Figure 1: Existing Overpass bridge on the A1 Autobahn in Austria [1].....	1
Figure 2: Composite Integral Bridge Cross-Section. ....	1
Figure 3: Reinforced Concrete Integral Bridge Cross-Section. ....	2
Figure 4: Comparison of Integral Abutment Bridge to other Jointless Bridges [8]..	5
Figure 5: Integral Bridges according to the Swiss Federal Roads Office [8] .....	6
Figure 6: Simplified Geometry of an Integral Abutment Bridge [9]. ....	7
Figure 7: Typical construction phases of integral abutments. [8].....	8
Figure 8: Integral abutment. [10] .....	9
Figure 9: Walnut Lane Memorial Bridge in Philadelphia [11]. ....	12
Figure 10: Common precast and prestressed concrete products. [12] .....	14
Figure 11: Complete jacking sequence VSL corporation [16] .....	15
Figure 12: Conventional lattice-girder floor slab. [2] .....	17
Figure 13: Double-wall element Rotary table. [2] .....	18
Figure 15: Double Wall Element (DWE) [17] .....	20
Figure 16: Double Wall View with KAP Steel [17]. ....	21
Figure 17: Image comparing lattice girders and KAP Steel .....	22
Figure 18: Image of Horizontal formwork table + EUR-pallet .....	22
Figure 19: Formwork table for production of Double-Wall-Elements (DWE) .....	23
Figure 20: 2D Model Equivalent Cross-Section. ....	24
Figure 21: Transportation and Assembly of a 2 span girder bridge. [2] .....	25
Figure 22: Tendons position Construction Phase 1 .....	27
Figure 23: Tendons Position Construction Phase 2. ....	29
Figure 24: Tendons Position Construction Phase 3 and 4. ....	31
Figure 25: Abutment Measurements .....	34
Figure 26: Composite Bridge Cross-section .....	35
Figure 27: Edge Beam Measurements .....	36
Figure 28: Load Model 1 Axle Load Distribution [18] .....	37
Figure 29: Load Model 1 Load Distribution illustrated with RFEM [18] .....	38
Figure 30: UDL (40 kN/m) on the RFEM 2D Model [18] .....	38
Figure 31: Load Model 1 Movable Axle loads (300 and 200) kN with 1.2 m axle spacing) in RFEM 2D model [18].....	38
Figure 32: Equivalent cross-section.....	39
Figure 33: Reinforced Concrete final cross-section.....	39

---

Figure 33: Reinforced Concrete final cross-section.....	39
Figure 34: 2D Model RFEM.....	43
Figure 35: 3D Model RFEM.....	44
Figure 36: Tendon Layout for Falsework Phase.....	45
Figure 37: 2D Equivalent cross-section construction phase 1.....	48
Figure 38: 2D Model Stress Locations. ....	48
Figure 39: 2D Analysis Stresses Construction Phase 1. ....	49
Figure 40: 2D Equivalent cross-section construction phase 2. ....	50
Figure 41: 2D Analysis Stresses Construction Phase 2. ....	51
Figure 42: 2D Equivalent cross-section construction phase 3. ....	52
Figure 43: 2D Analysis Stresses Construction Phase 3. ....	53
Figure 44: 2D Equivalent cross-section construction phase 4.....	54
Figure 45: 2D Analysis Stresses Construction Phase 4. ....	55
Figure 46: 2D Equivalent cross-section Load Model 1.....	56
Figure 47: 2D Analysis Stresses Load Model 1.....	57
Figure 48: 3D Model Overview from RFEM. ....	58
Figure 49: Location of Stress Points in Cross-Section. ....	59
Figure 50: Cross-section sketches for construction phase 1. ....	60
Figure 51: 3D Analysis Stresses Construction Phase 1. ....	61
Figure 52: Cross-section sketches for construction phase 2. ....	62
Figure 53: 3D Analysis Stresses Construction Phase 2. ....	63
Figure 54: Cross-section sketches for construction phase 3. ....	64
Figure 55: Hole spacing for 19 tendons. [20] .....	64
Figure 56: 3D Analysis Stresses Construction Phase 3. ....	65
Figure 57: 3D Analysis In-Situ Concrete Stresses Construction Phase 3.....	66
Figure 58: Cross-section sketches for construction phase 4. ....	67
Figure 59: Hole spacing for 19 tendons. [20] .....	67
Figure 60: 3D Analysis Stresses Construction Phase 4. ....	68
Figure 61: 3D Analysis In-Situ Concrete Stresses Construction Phase 4.....	69
Figure 62: Cross-section sketches for Load Model 1. ....	70
Figure 63: 3D Analysis Stresses Load Model 1.....	71
Figure 64: 3D Model In-Situ Concrete Stresses Load Model 1.....	72
Figure 65: Tendon Layout for all Construction Phases. ....	75
Figure 66: Falsework Stresses.....	77
Figure 67: Falsework Stresses.....	78

---

Figure 68: Falsework Stresses Load Model 1.....	79
Figure 69: Falsework Stresses Load Model 1.....	80
Figure 70: Stresses for all Construction Phases at the Support.....	82
Figure 71: Stresses for all Construction Phases at Redirection Location .....	83
Figure 72: Stresses for all Construction Phases at Midspan. ....	84
Figure 73: Falsework Stresses at Support, Redirection and Midspan locations. ....	85
Figure 74: Creep Stresses at Support, Redirection and Midspan locations. ....	86
Figure 75: Stress Comparison at Support. ....	87
Figure 76: Stress Comparison at Redirection Location. ....	87
Figure 77: Stress Comparison at Midspan. ....	88
Figure 78: Typical Girder Cross-Section with Reinforcement. ....	89
 Table 1: Tendons for each Construction Phase.....	 73
Table 2: Duct Diameter for each Construction Phase.....	74



## 8 *Appendices*

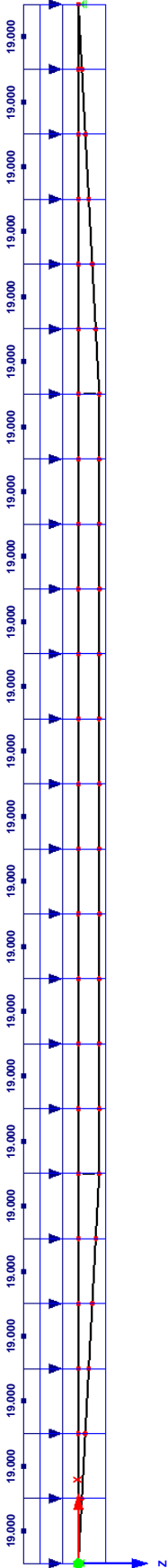
Project: RFEM

Structure: Phase\_1 2D

■ LC1: SELF WEIGHT CONSTRUCTION PHASE 1

LC1: Self Weight

Against Y-direction

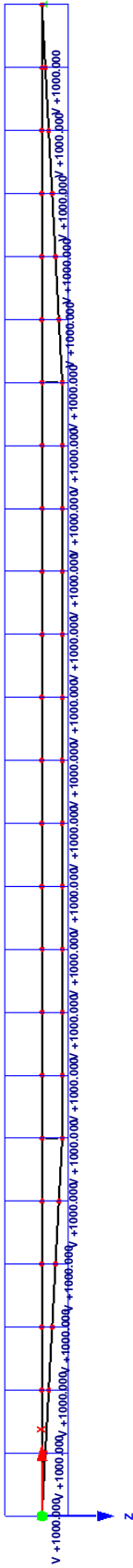


3.00 [m]

■ LC2: PRE-STRESS CONSTRUCTION PHASE 1

LC2: Pre-Stress

Against Y-direction



3.00 [m]

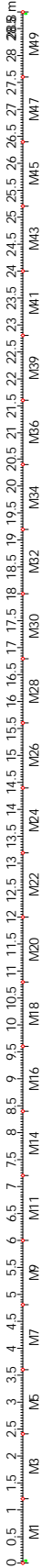
■ RESULT DIAGRAMS FOR CONTINUOUS MEMBERS - SM1

RFEM

LC1: Self Weight

Deformation - u

	x	y	u
	[m]	[m]	[mm]
max	14.400		54.3
min	--		--

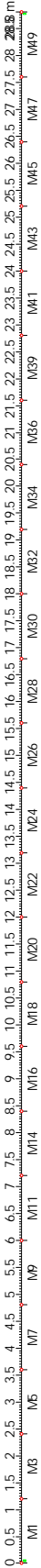


RFEM

LC1: Self Weight

Internal forces - M-y

	x	y	M-y
	[m]	[m]	[kNm]
max	14.400		1969.90
min	--		--



RFEM

LC1: Self Weight

Internal forces - N

	x	y	N
	[m]	[m]	[kN]
max	--		--
min	7.200		0

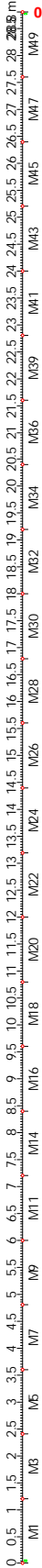


RFEM

LC1: Self Weight

Internal forces - V-z

	x	y	V-z
	[m]	[m]	[kN]
max	0.000		273.60
min	28.800		-273.60



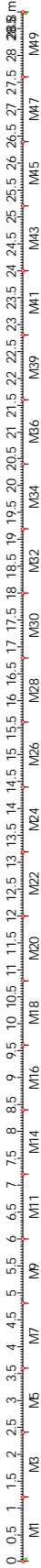
■ RESULT DIAGRAMS FOR CONTINUOUS MEMBERS - SM1

RFEM

LC2: Pre-Stress

Deformation - u

	x	u
	[m]	[mm]
max	14.400	11.7
min	--	--

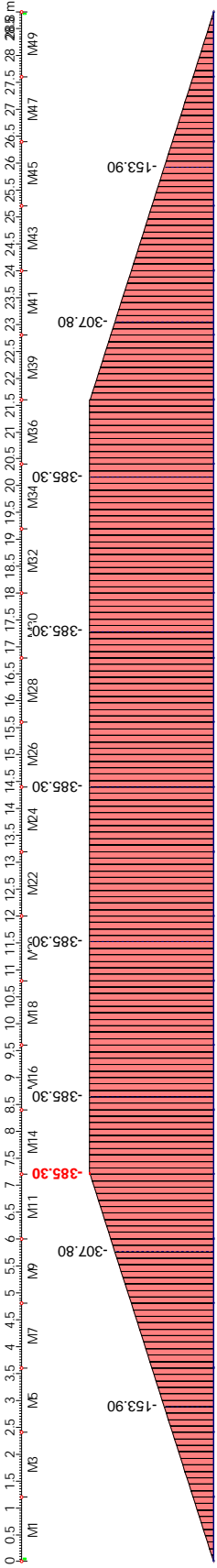


RFEM

LC2: Pre-Stress

Internal forces - M-y

	x	M-y
	[m]	[kNm]
max	--	-385.30
min	7.200	-385.30

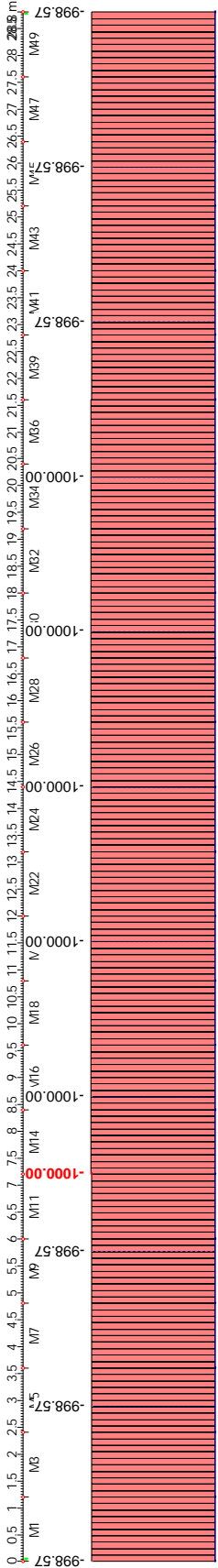


RFEM

LC2: Pre-Stress

Internal forces - N

	x	N
	[m]	[kN]
max	--	-1000.00
min	7.200	-1000.00

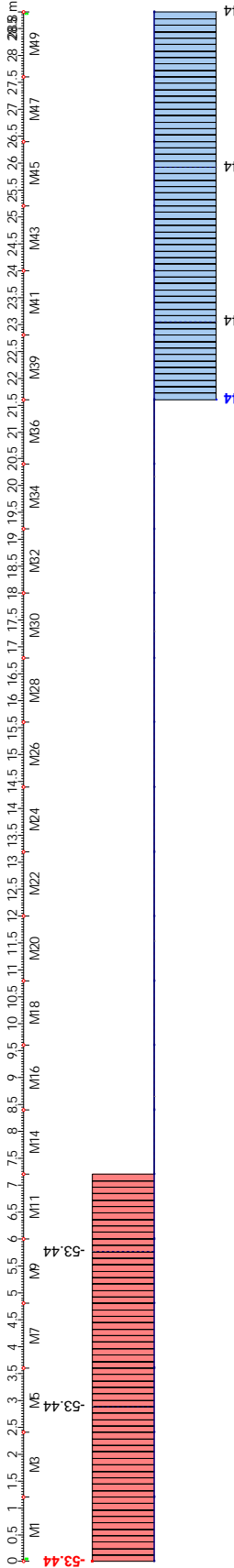


RFEM

LC2: Pre-Stress

Internal forces - V-z

	x	V-z
	[m]	[kN]
max	21.600	53.44
min	0.000	-53.44



Phase 1

Factor		6		Stresses												Concrete Stress Top				Concrete Stress Bott					
P [MN]	Self Weight	Pre-Stress	N	M.p	Stress P	Self Weight	Pre-Stress	Moment stress	Self Weight	Pre-Stress	Moment stress	Self Weight	Pre-Stress	Moment stress	Self Weight	Pre-Stress	Self Weight	Self Weight	Summ	Self Weight	Self Weight	Summ	σ Bottom		
x	M.g	-6000,00	-6000,00	-384,78	0,00	σ o(M.g)	σ o(P/A)	σ o(M.p)	σ u(M.g)	σ u(P/A)	σ u(M.p)	σ u(M.g)	σ u(P/A)	σ u(M.p)	σ oc(M.g)	σ oc(P/A)	σ uc(M.g)	σ uc(M.g)	σ Top	σ Top	σ Bottom	σ Bottom	σ Bottom		
0	0,00	-6000,00	-6000,00	-384,78	0,00	0,00	-7894,74	0,00	0,00	-7894,74	0,00	0,00	-7894,74	0,00	0,00	-7894,74	0,00	0,00	-7,89	-7,89	-7,89	-7,89	-7,89		
1,2	314,64	-6000,00	-6000,00	-769,50	-1154,28	-2219,18	-7894,74	2713,88	1567,01	-7894,74	2713,88	1567,01	-7894,74	2713,88	-2,22	-7894,74	1,22	1,22	-7,40	-7,40	-8,24	-8,24	-8,24		
2,4	601,92	-6000,00	-6000,00	-1154,28	-1154,28	-4245,38	-7894,74	5427,33	2997,76	-7894,74	5427,33	2997,76	-7894,74	5427,33	-4,25	-7894,74	2,34	2,34	-6,71	-6,71	-8,73	-8,73	-8,73		
3,6	861,84	-6000,00	-6000,00	-1539,00	-1923,78	-6078,61	-7894,74	8141,21	4292,25	-7894,74	8141,21	4292,25	-7894,74	8141,21	-6,08	-7894,74	3,35	3,35	-5,83	-5,83	-9,35	-9,35	-9,35		
4,8	1094,40	-6000,00	-6000,00	-1923,78	-1923,78	-7718,88	-7894,74	10854,67	5450,47	-7894,74	10854,67	5450,47	-7894,74	10854,67	-7,72	-7894,74	4,25	4,25	-4,76	-4,76	-10,11	-10,11	-10,11		
6	1299,60	-6000,00	-6000,00	-2311,80	-2311,80	-9166,16	-7894,74	13568,55	6472,43	-7894,74	13568,55	6472,43	-7894,74	13568,55	-9,17	-7894,74	5,05	5,05	-3,49	-3,49	-11,00	-11,00	-11,00		
7,2	1477,40	-6000,00	-6000,00	-2311,80	-2311,80	-10420,20	-7894,74	16305,28	7357,94	-7894,74	16305,28	7357,94	-7894,74	16305,28	-10,42	-7894,74	5,74	5,74	-2,01	-2,01	-12,05	-12,05	-12,05		
8,4	1627,90	-6000,00	-6000,00	-2311,80	-2311,80	-11481,69	-7894,74	16305,28	8107,48	-7894,74	16305,28	8107,48	-7894,74	16305,28	-11,48	-7894,74	6,33	6,33	-3,07	-3,07	-11,30	-11,30	-11,30		
9,6	1751,00	-6000,00	-6000,00	-2311,80	-2311,80	-12349,92	-7894,74	16305,28	8720,55	-7894,74	16305,28	8720,55	-7894,74	16305,28	-12,35	-7894,74	6,81	6,81	-3,94	-3,94	-10,69	-10,69	-10,69		
10,8	1846,80	-6000,00	-6000,00	-2311,80	-2311,80	-13025,60	-7894,74	16305,28	9197,67	-7894,74	16305,28	9197,67	-7894,74	16305,28	-13,03	-7894,74	7,18	7,18	-4,62	-4,62	-10,21	-10,21	-10,21		
12	1915,20	-6000,00	-6000,00	-2311,80	-2311,80	-13508,03	-7894,74	16305,28	9538,32	-7894,74	16305,28	9538,32	-7894,74	16305,28	-13,51	-7894,74	7,44	7,44	-5,10	-5,10	-9,87	-9,87	-9,87		
13,2	1956,20	-6000,00	-6000,00	-2311,80	-2311,80	-13797,21	-7894,74	16305,28	9742,52	-7894,74	16305,28	9742,52	-7894,74	16305,28	-13,80	-7894,74	7,60	7,60	-5,39	-5,39	-9,67	-9,67	-9,67		
14,4	1969,90	-6000,00	-6000,00	-2311,80	-2311,80	-13893,83	-7894,74	16305,28	9810,75	-7894,74	16305,28	9810,75	-7894,74	16305,28	-13,89	-7894,74	7,66	7,66	-5,48	-5,48	-9,60	-9,60	-9,60		
15,6	1956,20	-6000,00	-6000,00	-2311,80	-2311,80	-13797,21	-7894,74	16305,28	9742,52	-7894,74	16305,28	9742,52	-7894,74	16305,28	-13,80	-7894,74	7,60	7,60	-5,39	-5,39	-9,67	-9,67	-9,67		
16,8	1915,20	-6000,00	-6000,00	-2311,80	-2311,80	-13508,03	-7894,74	16305,28	9538,32	-7894,74	16305,28	9538,32	-7894,74	16305,28	-13,51	-7894,74	7,44	7,44	-5,10	-5,10	-9,87	-9,87	-9,87		
18	1846,80	-6000,00	-6000,00	-2311,80	-2311,80	-13025,60	-7894,74	16305,28	9197,67	-7894,74	16305,28	9197,67	-7894,74	16305,28	-13,03	-7894,74	7,18	7,18	-4,62	-4,62	-10,21	-10,21	-10,21		
19,2	1751,00	-6000,00	-6000,00	-2311,80	-2311,80	-12349,92	-7894,74	16305,28	8720,55	-7894,74	16305,28	8720,55	-7894,74	16305,28	-12,35	-7894,74	6,81	6,81	-3,94	-3,94	-10,69	-10,69	-10,69		
20,4	1627,90	-6000,00	-6000,00	-2311,80	-2311,80	-11481,69	-7894,74	16305,28	8107,48	-7894,74	16305,28	8107,48	-7894,74	16305,28	-11,48	-7894,74	6,33	6,33	-3,07	-3,07	-11,30	-11,30	-11,30		
21,6	1477,40	-6000,00	-6000,00	-2308,50	-2308,50	-10420,20	-7894,74	16282,00	7357,94	-7894,74	16282,00	7357,94	-7894,74	16282,00	-10,42	-7894,74	5,74	5,74	-2,03	-2,03	-12,03	-12,03	-12,03		
22,8	1299,60	-6000,00	-6000,00	-1923,78	-1923,78	-9166,16	-7894,74	13568,55	6472,43	-7894,74	13568,55	6472,43	-7894,74	13568,55	-9,17	-7894,74	5,05	5,05	-3,49	-3,49	-11,00	-11,00	-11,00		
24	1094,40	-6000,00	-6000,00	-1539,00	-1539,00	-7718,88	-7894,74	10854,67	5450,47	-7894,74	10854,67	5450,47	-7894,74	10854,67	-7,72	-7894,74	4,25	4,25	-4,76	-4,76	-10,11	-10,11	-10,11		
25,2	861,84	-6000,00	-6000,00	-1154,28	-1154,28	-6078,61	-7894,74	8141,21	4292,25	-7894,74	8141,21	4292,25	-7894,74	8141,21	-6,08	-7894,74	3,35	3,35	-5,83	-5,83	-9,35	-9,35	-9,35		
26,4	601,92	-6000,00	-6000,00	-769,50	-769,50	-4245,38	-7894,74	5427,33	2997,76	-7894,74	5427,33	2997,76	-7894,74	5427,33	-4,25	-7894,74	2,34	2,34	-6,71	-6,71	-8,73	-8,73	-8,73		
27,6	314,64	-6000,00	-6000,00	-384,78	-384,78	-2219,18	-7894,74	2713,88	1567,01	-7894,74	2713,88	1567,01	-7894,74	2713,88	-2,22	-7894,74	1,22	1,22	-7,40	-7,40	-8,24	-8,24	-8,24		
28,8	0,00	-6000,00	-6000,00	0,00	0,00	0,00	-7894,74	0,00	0,00	-7894,74	0,00	0,00	-7894,74	0,00	0,00	-7894,74	0,00	0,00	-7,89	-7,89	-7,89	-7,89	-7,89		
																		A [m²]	0,76					σ < 0,45 fck	22,50
																		Wo [m³]	-0,1418						
																		Wu [m³]	0,2008						
																		Wu c [m³]	0,2573						

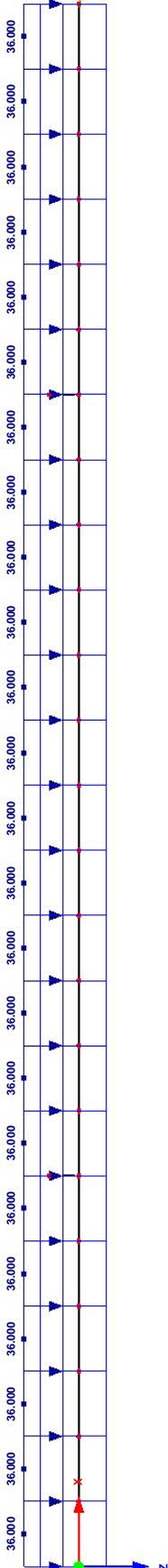
Project: RFEM

Structure: Phase 2 2D

■ LC1: SELF WEIGHT (In-Situ Concrete) Construction Phase 2

LC1: Self Weight (In-Situ Concrete)

Against Y-direction

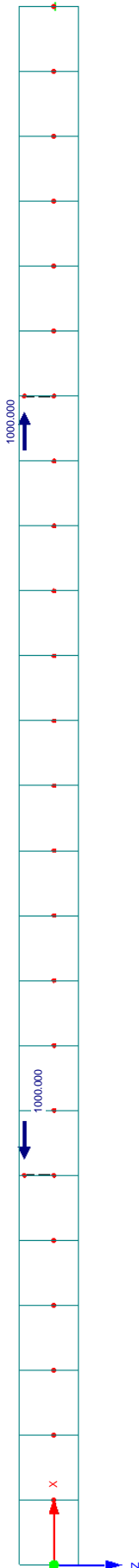


3.00 [m]

■ LC2: PRE-STRESS CONSTRUCTION PHASE 2

LC2: Pre-Stress

Against Y-direction



3.00 [m]

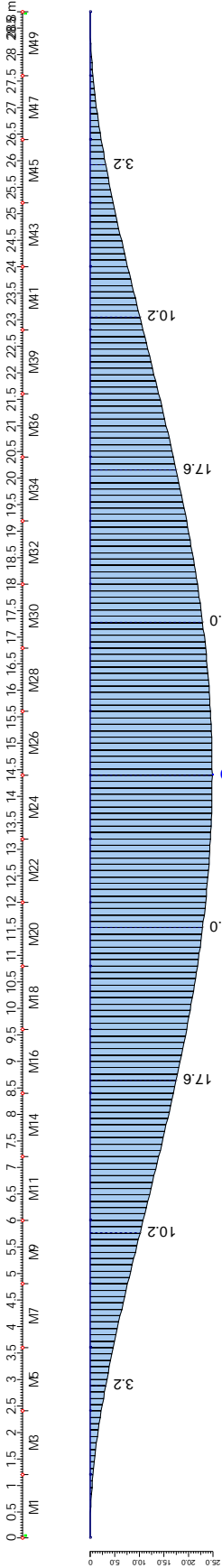
RESULT DIAGRAMS FOR CONTINUOUS MEMBERS - SM1

RFEM

LC1: Self Weight (In-Situ Concrete)

Deformation - u

x		u
[m]		[mm]
max	14.400	24.9
min	--	--

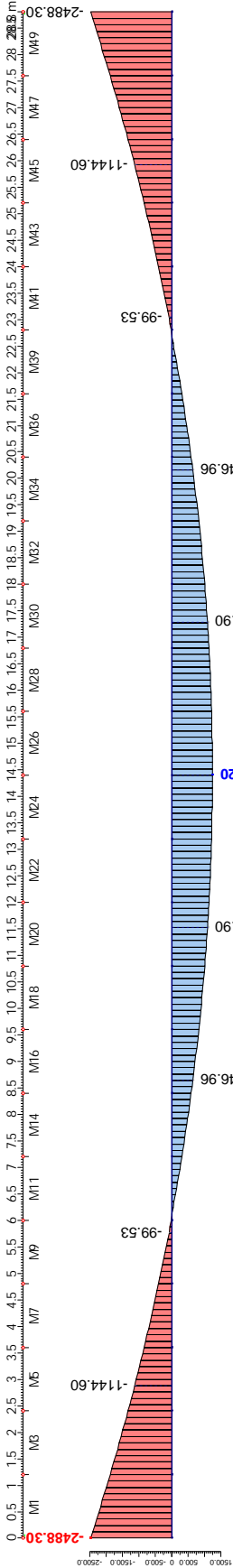


RFEM

LC1: Self Weight (In-Situ Concrete)

Internal forces - M-y

x		M-y
[m]		[kNm]
max	14.400	1244.20
min	0.000	-2488.30

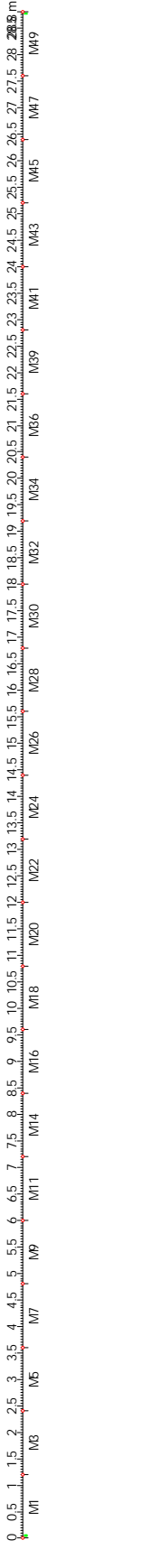


RFEM

LC1: Self Weight (In-Situ Concrete)

Internal forces - N

x		N
[m]		[kN]
max	--	--
min	--	--

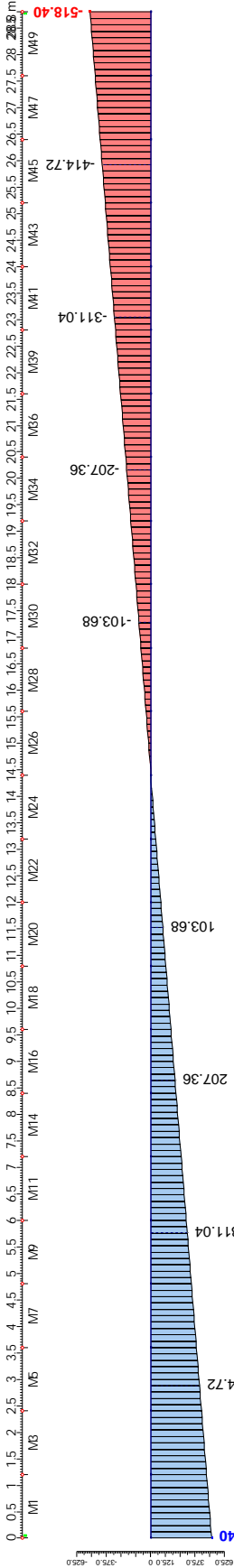


RFEM

LC1: Self Weight (In-Situ Concrete)

Internal forces - V-z

x		V-z
[m]		[kN]
max	0.000	518.40
min	28.800	-518.40



Project: RFEM

Structure: Phase 2 2D

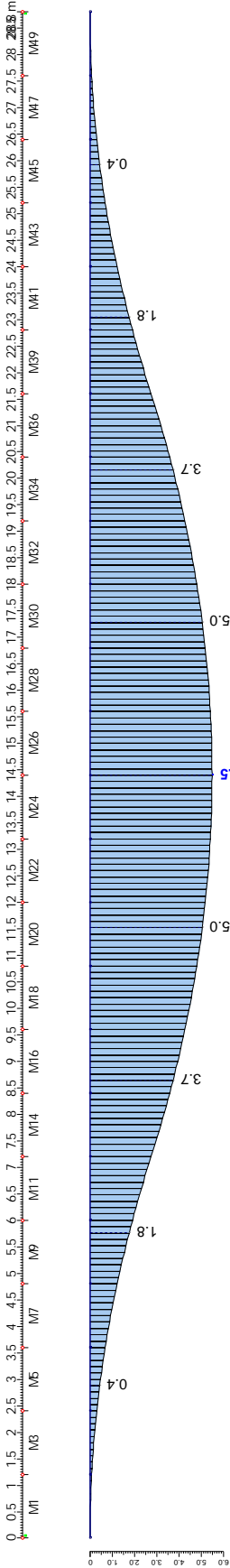
■ RESULT DIAGRAMS FOR CONTINUOUS MEMBERS - SM1

RFEM

LC2: Pre-Stress

Deformation - u

	x	u
	[m]	[mm]
max	14.400	5.5
min	--	--

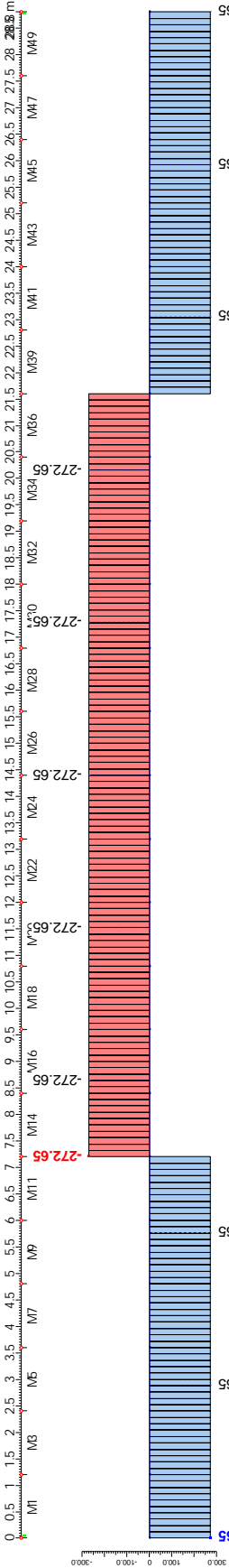


RFEM

LC2: Pre-Stress

Internal forces - M-y

	x	M-y
	[m]	[kNm]
max	0.000	272.65
min	7.200	-272.65

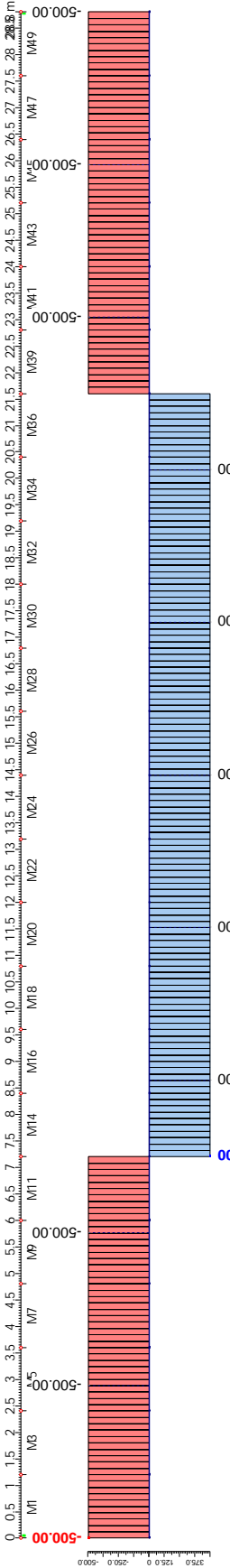


RFEM

LC2: Pre-Stress

Internal forces - N

	x	N
	[m]	[kN]
max	7.200	500.00
min	0.000	-500.00

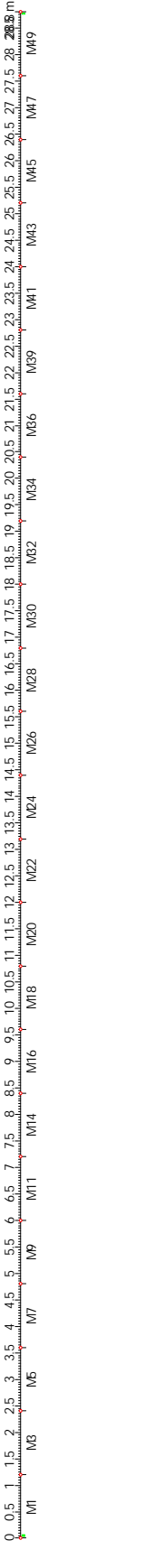


RFEM

LC2: Pre-Stress

Internal forces - V-z

	x	V-z
	[m]	[kN]
max	--	--
min	--	--





Phase 2

Phase 2			A [m²]		0.76		Wo [m³]		-0.1418		Wu [m³]		0.2008																																																																																																																																																																																																																																																																																																																																																																																																																																																																																																																																																																																																																																																																
Factor	P	Self Weight	Pre-Stress		Stresses		Concrete Stress Top		Concrete Stress Top		Concrete Stress Top		Concrete Stress Bott		σ < 0.45 fck																																																																																																																																																																																																																																																																																																																																																																																																																																																																																																																																																																																																																																																														
			M.g	N	M.p	σ	σ u(P/A)	σ u(M.p)	σ u(M.p)	σ u(P/A)	Pre-Stress	Moment_stress	Self Weight	σ u(M.g)		σ u(P/A)	Self Weight	σ u(M.g)	σ u(P/A)	Self Weight	σ u(M.g)	σ u(P/A)	Self Weight	σ u(M.g)	σ u(P/A)	Self Weight	σ u(M.g)	σ u(P/A)	Self Weight	σ u(M.g)	σ u(P/A)	Self Weight	σ u(M.g)	σ u(P/A)	Self Weight	σ u(M.g)	σ u(P/A)	Self Weight	σ u(M.g)	σ u(P/A)	Self Weight	σ u(M.g)	σ u(P/A)	Self Weight	σ u(M.g)	σ u(P/A)	Self Weight	σ u(M.g)	σ u(P/A)	Self Weight	σ u(M.g)	σ u(P/A)	Self Weight	σ u(M.g)	σ u(P/A)	Self Weight	σ u(M.g)	σ u(P/A)	Self Weight	σ u(M.g)	σ u(P/A)	Self Weight	σ u(M.g)	σ u(P/A)	Self Weight	σ u(M.g)	σ u(P/A)	Self Weight	σ u(M.g)	σ u(P/A)	Self Weight	σ u(M.g)	σ u(P/A)	Self Weight	σ u(M.g)	σ u(P/A)	Self Weight	σ u(M.g)	σ u(P/A)	Self Weight	σ u(M.g)	σ u(P/A)	Self Weight	σ u(M.g)	σ u(P/A)	Self Weight	σ u(M.g)	σ u(P/A)	Self Weight	σ u(M.g)	σ u(P/A)	Self Weight	σ u(M.g)	σ u(P/A)	Self Weight	σ u(M.g)	σ u(P/A)	Self Weight	σ u(M.g)	σ u(P/A)	Self Weight	σ u(M.g)	σ u(P/A)	Self Weight	σ u(M.g)	σ u(P/A)	Self Weight	σ u(M.g)	σ u(P/A)	Self Weight	σ u(M.g)	σ u(P/A)	Self Weight	σ u(M.g)	σ u(P/A)	Self Weight	σ u(M.g)	σ u(P/A)	Self Weight	σ u(M.g)	σ u(P/A)	Self Weight	σ u(M.g)	σ u(P/A)	Self Weight	σ u(M.g)	σ u(P/A)	Self Weight	σ u(M.g)	σ u(P/A)	Self Weight	σ u(M.g)	σ u(P/A)	Self Weight	σ u(M.g)	σ u(P/A)	Self Weight	σ u(M.g)	σ u(P/A)	Self Weight	σ u(M.g)	σ u(P/A)	Self Weight	σ u(M.g)	σ u(P/A)	Self Weight	σ u(M.g)	σ u(P/A)	Self Weight	σ u(M.g)	σ u(P/A)	Self Weight	σ u(M.g)	σ u(P/A)	Self Weight	σ u(M.g)	σ u(P/A)	Self Weight	σ u(M.g)	σ u(P/A)	Self Weight	σ u(M.g)	σ u(P/A)	Self Weight	σ u(M.g)	σ u(P/A)	Self Weight	σ u(M.g)	σ u(P/A)	Self Weight	σ u(M.g)	σ u(P/A)	Self Weight	σ u(M.g)	σ u(P/A)	Self Weight	σ u(M.g)	σ u(P/A)	Self Weight	σ u(M.g)	σ u(P/A)	Self Weight	σ u(M.g)	σ u(P/A)	Self Weight	σ u(M.g)	σ u(P/A)	Self Weight	σ u(M.g)	σ u(P/A)	Self Weight	σ u(M.g)	σ u(P/A)	Self Weight	σ u(M.g)	σ u(P/A)	Self Weight	σ u(M.g)	σ u(P/A)	Self Weight	σ u(M.g)	σ u(P/A)	Self Weight	σ u(M.g)	σ u(P/A)	Self Weight	σ u(M.g)	σ u(P/A)	Self Weight	σ u(M.g)	σ u(P/A)	Self Weight	σ u(M.g)	σ u(P/A)	Self Weight	σ u(M.g)	σ u(P/A)	Self Weight	σ u(M.g)	σ u(P/A)	Self Weight	σ u(M.g)	σ u(P/A)	Self Weight	σ u(M.g)	σ u(P/A)	Self Weight	σ u(M.g)	σ u(P/A)	Self Weight	σ u(M.g)	σ u(P/A)	Self Weight	σ u(M.g)	σ u(P/A)	Self Weight	σ u(M.g)	σ u(P/A)	Self Weight	σ u(M.g)	σ u(P/A)	Self Weight	σ u(M.g)	σ u(P/A)	Self Weight	σ u(M.g)	σ u(P/A)	Self Weight	σ u(M.g)	σ u(P/A)	Self Weight	σ u(M.g)	σ u(P/A)	Self Weight	σ u(M.g)	σ u(P/A)	Self Weight	σ u(M.g)	σ u(P/A)	Self Weight	σ u(M.g)	σ u(P/A)	Self Weight	σ u(M.g)	σ u(P/A)	Self Weight	σ u(M.g)	σ u(P/A)	Self Weight	σ u(M.g)	σ u(P/A)	Self Weight	σ u(M.g)	σ u(P/A)	Self Weight	σ u(M.g)	σ u(P/A)	Self Weight	σ u(M.g)	σ u(P/A)	Self Weight	σ u(M.g)	σ u(P/A)	Self Weight	σ u(M.g)	σ u(P/A)	Self Weight	σ u(M.g)	σ u(P/A)	Self Weight	σ u(M.g)	σ u(P/A)	Self Weight	σ u(M.g)	σ u(P/A)	Self Weight	σ u(M.g)	σ u(P/A)	Self Weight	σ u(M.g)	σ u(P/A)	Self Weight	σ u(M.g)	σ u(P/A)	Self Weight	σ u(M.g)	σ u(P/A)	Self Weight	σ u(M.g)	σ u(P/A)	Self Weight	σ u(M.g)	σ u(P/A)	Self Weight	σ u(M.g)	σ u(P/A)	Self Weight	σ u(M.g)	σ u(P/A)	Self Weight	σ u(M.g)	σ u(P/A)	Self Weight	σ u(M.g)	σ u(P/A)	Self Weight	σ u(M.g)	σ u(P/A)	Self Weight	σ u(M.g)	σ u(P/A)	Self Weight	σ u(M.g)	σ u(P/A)	Self Weight	σ u(M.g)	σ u(P/A)	Self Weight	σ u(M.g)	σ u(P/A)	Self Weight	σ u(M.g)	σ u(P/A)	Self Weight	σ u(M.g)	σ u(P/A)	Self Weight	σ u(M.g)	σ u(P/A)	Self Weight	σ u(M.g)	σ u(P/A)	Self Weight	σ u(M.g)	σ u(P/A)	Self Weight	σ u(M.g)	σ u(P/A)	Self Weight	σ u(M.g)	σ u(P/A)	Self Weight	σ u(M.g)	σ u(P/A)	Self Weight	σ u(M.g)	σ u(P/A)	Self Weight	σ u(M.g)	σ u(P/A)	Self Weight	σ u(M.g)	σ u(P/A)	Self Weight	σ u(M.g)	σ u(P/A)	Self Weight	σ u(M.g)	σ u(P/A)	Self Weight	σ u(M.g)	σ u(P/A)	Self Weight	σ u(M.g)	σ u(P/A)	Self Weight	σ u(M.g)	σ u(P/A)	Self Weight	σ u(M.g)	σ u(P/A)	Self Weight	σ u(M.g)	σ u(P/A)	Self Weight	σ u(M.g)	σ u(P/A)	Self Weight	σ u(M.g)	σ u(P/A)	Self Weight	σ u(M.g)	σ u(P/A)	Self Weight	σ u(M.g)	σ u(P/A)	Self Weight	σ u(M.g)	σ u(P/A)	Self Weight	σ u(M.g)	σ u(P/A)	Self Weight	σ u(M.g)	σ u(P/A)	Self Weight	σ u(M.g)	σ u(P/A)	Self Weight	σ u(M.g)	σ u(P/A)	Self Weight	σ u(M.g)	σ u(P/A)	Self Weight	σ u(M.g)	σ u(P/A)	Self Weight	σ u(M.g)	σ u(P/A)	Self Weight	σ u(M.g)	σ u(P/A)	Self Weight	σ u(M.g)	σ u(P/A)	Self Weight	σ u(M.g)	σ u(P/A)	Self Weight	σ u(M.g)	σ u(P/A)	Self Weight	σ u(M.g)	σ u(P/A)	Self Weight	σ u(M.g)	σ u(P/A)	Self Weight	σ u(M.g)	σ u(P/A)	Self Weight	σ u(M.g)	σ u(P/A)	Self Weight	σ u(M.g)	σ u(P/A)	Self Weight	σ u(M.g)	σ u(P/A)	Self Weight	σ u(M.g)	σ u(P/A)	Self Weight	σ u(M.g)	σ u(P/A)	Self Weight	σ u(M.g)	σ u(P/A)	Self Weight	σ u(M.g)	σ u(P/A)	Self Weight	σ u(M.g)	σ u(P/A)	Self Weight	σ u(M.g)	σ u(P/A)	Self Weight	σ u(M.g)	σ u(P/A)	Self Weight	σ u(M.g)	σ u(P/A)	Self Weight	σ u(M.g)	σ u(P/A)	Self Weight	σ u(M.g)	σ u(P/A)	Self Weight	σ u(M.g)	σ u(P/A)	Self Weight	σ u(M.g)	σ u(P/A)	Self Weight	σ u(M.g)	σ u(P/A)	Self Weight	σ u(M.g)	σ u(P/A)	Self Weight	σ u(M.g)	σ u(P/A)	Self Weight	σ u(M.g)	σ u(P/A)	Self Weight	σ u(M.g)	σ u(P/A)	Self Weight	σ u(M.g)	σ u(P/A)	Self Weight	σ u(M.g)	σ u(P/A)	Self Weight	σ u(M.g)	σ u(P/A)	Self Weight	σ u(M.g)	σ u(P/A)	Self Weight	σ u(M.g)	σ u(P/A)	Self Weight	σ u(M.g)	σ u(P/A)	Self Weight	σ u(M.g)	σ u(P/A)	Self Weight	σ u(M.g)	σ u(P/A)	Self Weight	σ u(M.g)	σ u(P/A)	Self Weight	σ u(M.g)	σ u(P/A)	Self Weight	σ u(M.g)	σ u(P/A)	Self Weight	σ u(M.g)	σ u(P/A)	Self Weight	σ u(M.g)	σ u(P/A)	Self Weight	σ u(M.g)	σ u(P/A)	Self Weight	σ u(M.g)	σ u(P/A)	Self Weight	σ u(M.g)	σ u(P/A)	Self Weight	σ u(M.g)	σ u(P/A)	Self Weight	σ u(M.g)	σ u(P/A)	Self Weight	σ u(M.g)	σ u(P/A)	Self Weight	σ u(M.g)	σ u(P/A)	Self Weight	σ u(M.g)	σ u(P/A)	Self Weight	σ u(M.g)	σ u(P/A)	Self Weight	σ u(M.g)	σ u(P/A)	Self Weight	σ u(M.g)	σ u(P/A)	Self Weight	σ u(M.g)	σ u(P/A)	Self Weight	σ u(M.g)	σ u(P/A)	Self Weight	σ u(M.g)	σ u(P/A)	Self Weight	σ u(M.g)	σ u(P/A)	Self Weight	σ u(M.g)	σ u(P/A)	Self Weight	σ u(M.g)	σ u(P/A)	Self Weight	σ u(M.g)	σ u(P/A)	Self Weight	σ u(M.g)	σ u(P/A)	Self Weight	σ u(M.g)	σ u(P/A)	Self Weight	σ u(M.g)	σ u(P/A)	Self Weight	σ u(M.g)	σ u(P/A)	Self Weight	σ u(M.g)	σ u(P/A)	Self Weight	σ u(M.g)	σ u(P/A)	Self Weight	σ u(M.g)	σ u(P/A)	Self Weight	σ u(M.g)	σ u(P/A)	Self Weight	σ u(M.g)	σ u(P/A)	Self Weight	σ u(M.g)	σ u(P/A)	Self Weight	σ u(M.g)	σ u(P/A)	Self Weight	σ u(M.g)	σ u(P/A)	Self Weight	σ u(M.g)	σ u(P/A)	Self Weight	σ u(M.g)	σ u(P/A)	Self Weight	σ u(M.g)	σ u(P/A)	Self Weight	σ u(M.g)	σ u(P/A)	Self Weight



Projekt: RFEM

Position: Phase\_3 2D

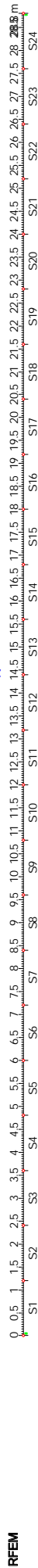
■ RESULT DIAGRAMS FOR CONTINUOUS MEMBERS - SM1



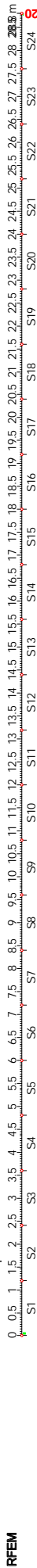
x	u
max	19.5
min	0



x	M-y
max	2868.50
min	-5737.00



x	N
max	0.000
min	0



x	V-z
max	1195.20
min	-1195.20

Projekt: RFEM

Position: Phase\_3 2D

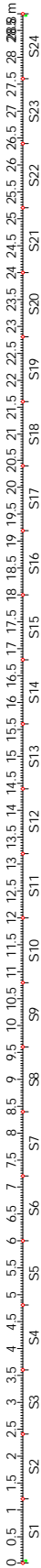
■ RESULT DIAGRAMS FOR CONTINUOUS MEMBERS - SM1

RFEM

LC2: Pre-Stress

Verformungen - u

	x	u
	[m]	[mm]
max	14.400	2.5
min	--	--

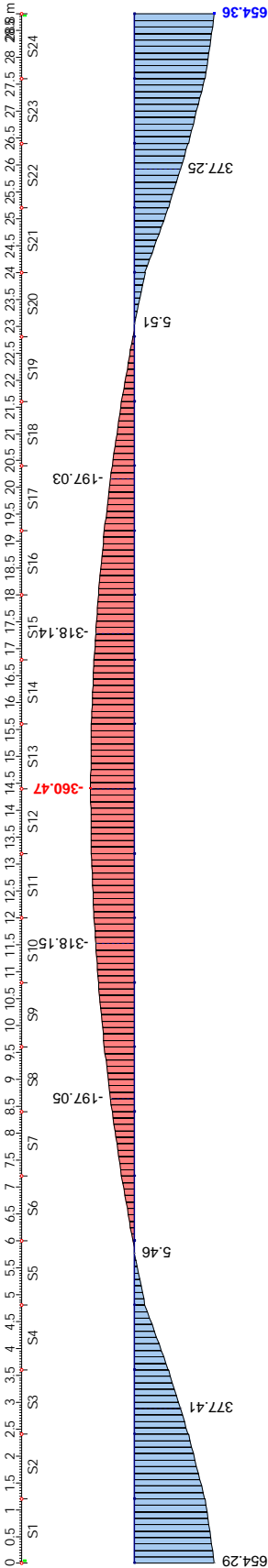


RFEM

LC2: Pre-Stress

Schnittgrößen - M-y

	x	M-y
	[m]	[kNm]
max	28.800	654.36
min	14.400	-360.47

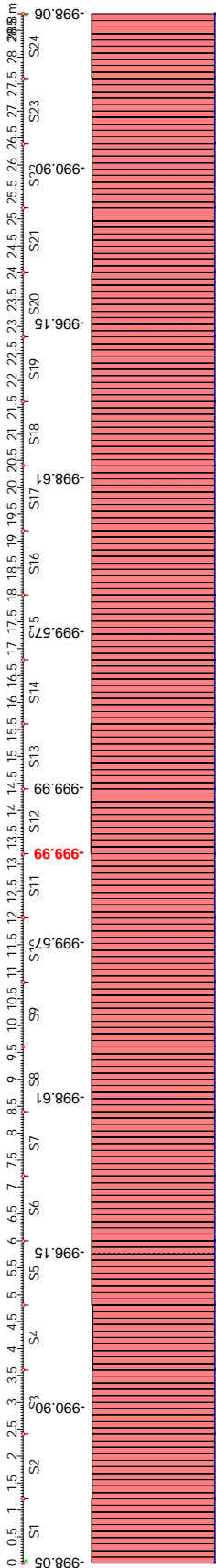


RFEM

LC2: Pre-Stress

Schnittgrößen - N

	x	N
	[m]	[kN]
max	--	--
min	13.200	-999.99

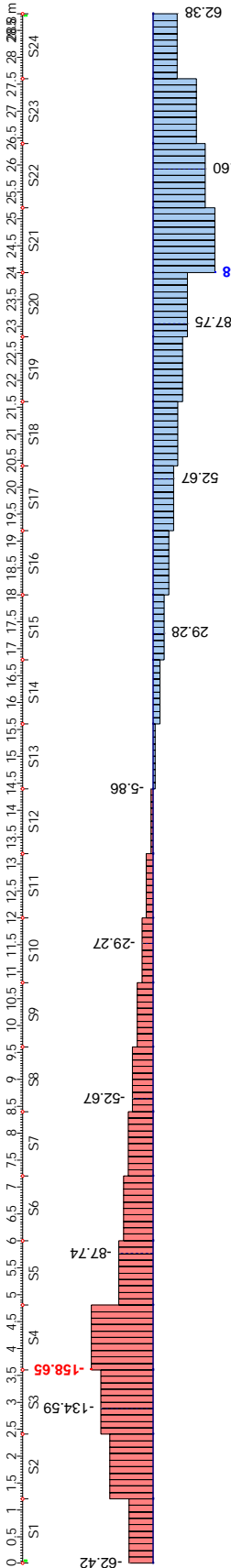


RFEM

LC2: Pre-Stress

Schnittgrößen - V-z

	x	V-z
	[m]	[kN]
max	24.000	158.48
min	3.600	-158.65





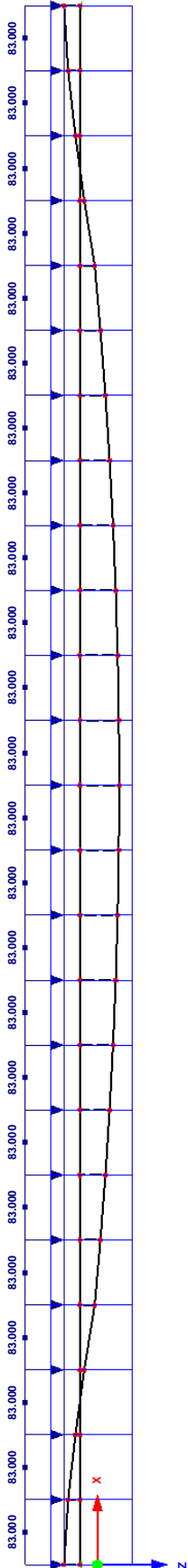
Project: RFEM

Structure: Phase 4 Prestress 2D

■ LF1: SELF WEIGHT (Deck Slabs + Edge Beams + Roadbed) Construction Phase 4

LC1: Self Weight (Deck Slabs + Edge Beams + Roadbed)

Against Y-direction

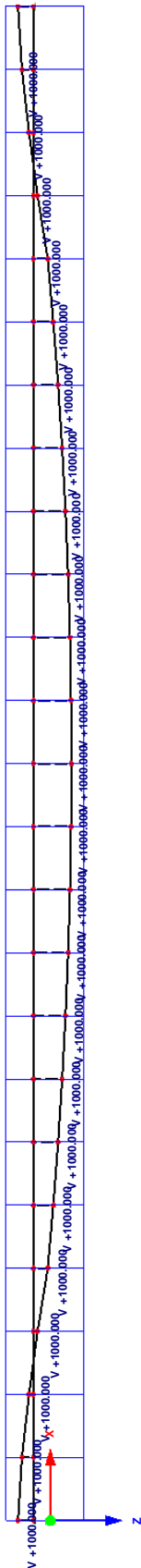


3.00 [m]

■ LF2: PRE-STRESS CONSTRUCTION PHASE 4

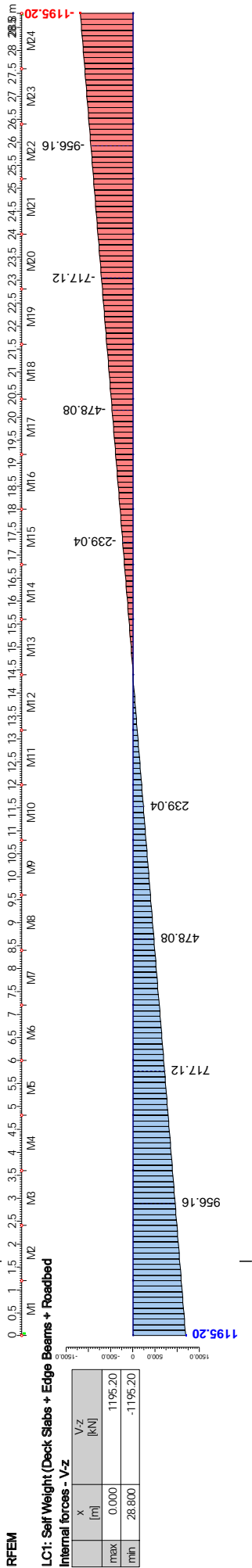
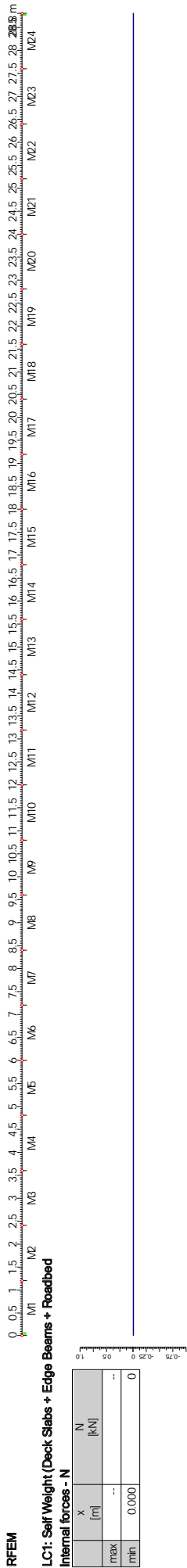
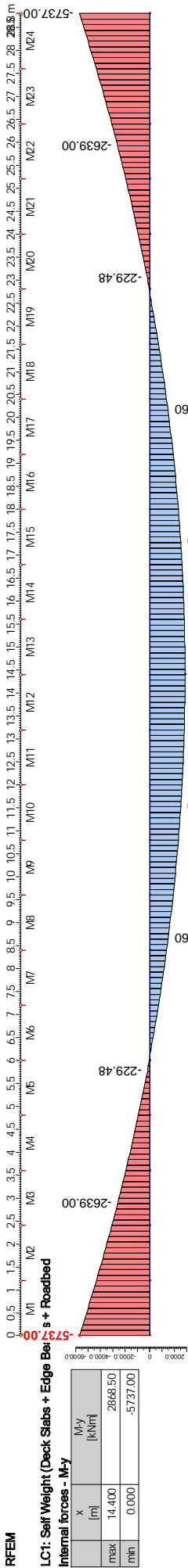
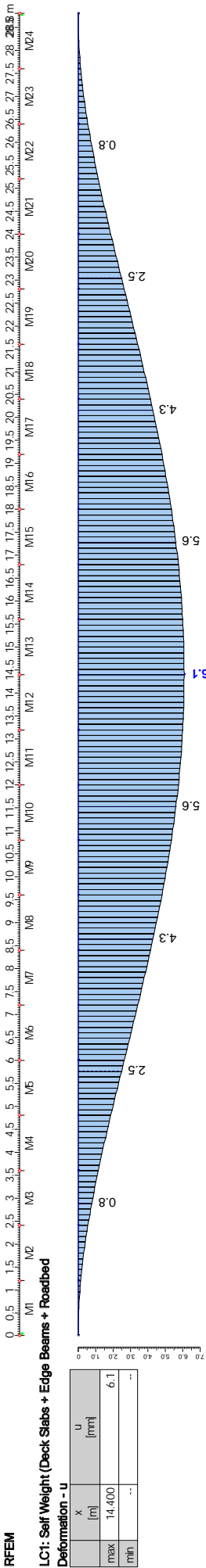
LC2: Pre-Stress

Against Y-direction



3.00 [m]

■ RESULT DIAGRAMS FOR CONTINUOUS MEMBERS - SM1



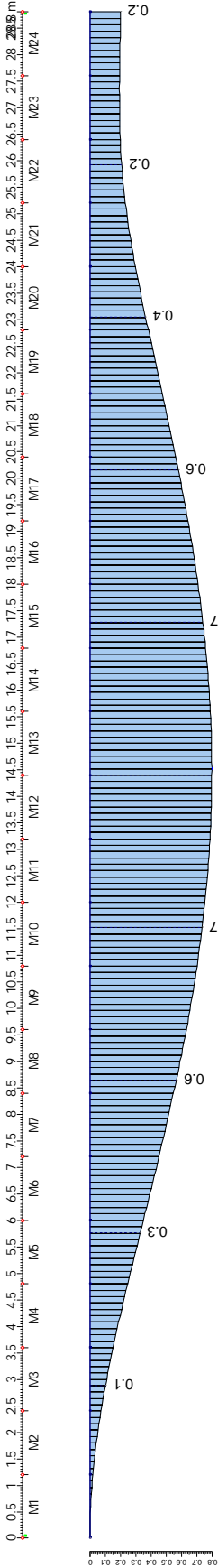
■ RESULT DIAGRAMS FOR CONTINUOUS MEMBERS - SM1

RFEM

LC2: Pre-Stress

Deformation - u

	x	u
	[m]	[mm]
max	14.520	0.8
min	--	--

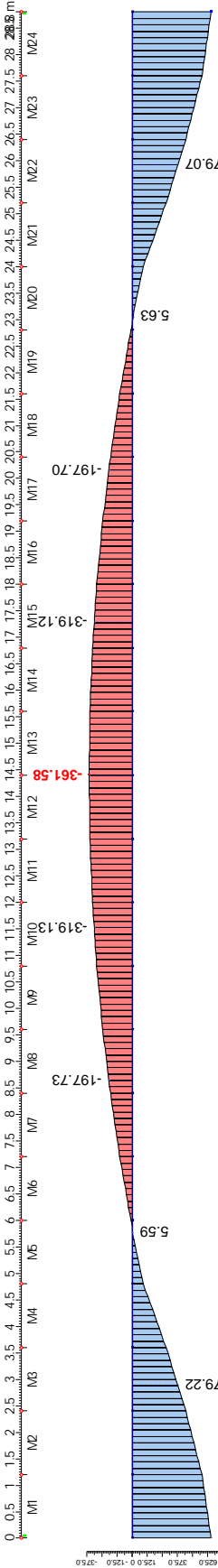


RFEM

LC2: Pre-Stress

Internal forces - M-y

	x	M-y
	[m]	[kNm]
max	28.800	653.87
min	14.400	-361.58

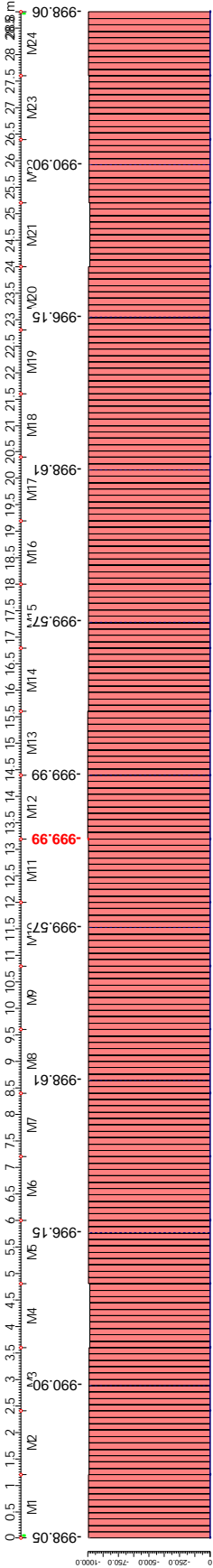


RFEM

LC2: Pre-Stress

Internal forces - N

	x	N
	[m]	[kN]
max	--	--
min	13.200	-999.99

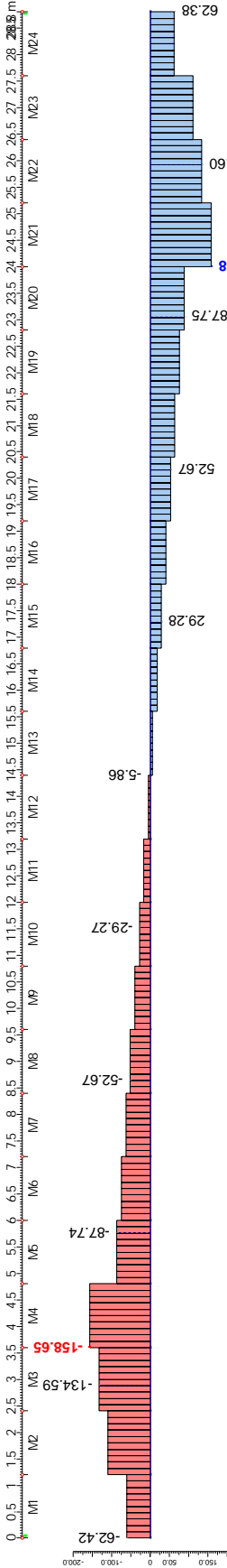


RFEM

LC2: Pre-Stress

Internal forces - V-z

	x	V-z
	[m]	[kN]
max	24.000	158.48
min	3.600	-158.65





## Phase 4a

Prestress Factor		2 Self-weight Factor				Stresses																
Self Weight		Pre-Stress		Stress P		Self Weight		Pre-Stress		Moment stress		Self Weight		Pre-Stress		Moment stress		Summ				
M_g	N	M_p	A [m²]	Wu [m³]	σ_o(M_g) [kN/m²]	σ_o(P/A) [kN/m²]	σ_o(M_p) [kN/m²]	σ_o(P/A) [kN/m²]	σ_o(M_p) [kN/m²]	σ_o(P/A) [kN/m²]	σ_u(M_p) [kN/m²]	σ_u(M_g) [kN/m²]	σ_u(M_p) [kN/m²]	σ_u(P/A) [kN/m²]	σ_u(M_p) [kN/m²]	σ_u(P/A) [kN/m²]	σ_u(M_p) [kN/m²]	σ_u(P/A) [kN/m²]	σ Top	σ Bottom	Sum σ Top	Sum σ Bottom
0	0.00	-2000.00	1307.60	4.20	-3.1393	0.8182	-476.19	-476.19	-416.53	-368.81	0.00	-476.19	-476.19	-476.19	-476.19	1598.24	1415.14	1598.24	-0.89	1.12	-6.06	-18.56
1.2	0.00	-2000.00	1157.80	4.20	-3.1393	0.8182	-476.19	-476.19	-382.81	-288.91	0.00	-476.19	-476.19	-476.19	-476.19	1415.14	1085.54	1415.14	-0.85	0.94	-10.99	-14.85
2.4	0.00	-2000.00	888.14	4.20	-3.1393	0.8182	-476.19	-476.19	-282.81	-198.91	0.00	-476.19	-476.19	-476.19	-476.19	1085.54	690.14	1085.54	-0.76	0.21	-13.29	-17.37
3.6	0.00	-2000.00	564.64	4.20	-3.1393	0.8182	-476.19	-476.19	-179.86	-139.86	0.00	-476.19	-476.19	-476.19	-476.19	690.14	225.43	690.14	-0.66	-0.25	-13.95	-14.12
4.8	0.00	-2000.00	184.44	4.20	-3.1393	0.8182	-476.19	-476.19	-58.75	-37.82	0.00	-476.19	-476.19	-476.19	-476.19	225.43	-13.57	225.43	-0.53	-0.51	-12.93	-16.08
6	0.00	-2000.00	-30.94	4.20	-3.1393	0.8182	-476.19	-476.19	9.86	68.23	0.00	-476.19	-476.19	-476.19	-476.19	-37.82	-261.79	-261.79	-0.47	-0.74	-13.57	-16.07
7.2	0.00	-2000.00	-214.18	4.20	-3.1393	0.8182	-476.19	-476.19	117.68	158.18	0.00	-476.19	-476.19	-476.19	-476.19	-261.79	-451.53	-451.53	-0.41	-0.93	-13.73	-16.34
8.4	0.00	-2000.00	-369.42	4.20	-3.1393	0.8182	-476.19	-476.19	158.18	189.72	0.00	-476.19	-476.19	-476.19	-476.19	-451.53	-606.95	-606.95	-0.36	-1.08	-5.85	-17.73
9.6	0.00	-2000.00	-496.58	4.20	-3.1393	0.8182	-476.19	-476.19	189.72	212.27	0.00	-476.19	-476.19	-476.19	-476.19	-606.95	-727.96	-727.96	-0.32	-1.20	-7.85	-16.59
10.8	0.00	-2000.00	-595.58	4.20	-3.1393	0.8182	-476.19	-476.19	212.27	225.82	0.00	-476.19	-476.19	-476.19	-476.19	-727.96	-814.47	-814.47	-0.29	-1.29	-9.41	-15.70
12	0.00	-2000.00	-666.36	4.20	-3.1393	0.8182	-476.19	-476.19	225.82	230.36	0.00	-476.19	-476.19	-476.19	-476.19	-814.47	-866.49	-866.49	-0.26	-1.34	-10.52	-15.06
13.2	0.00	-2000.00	-708.92	4.20	-3.1393	0.8182	-476.19	-476.19	230.36	235.82	0.00	-476.19	-476.19	-476.19	-476.19	-866.49	-883.89	-883.89	-0.25	-1.39	-11.18	-14.68
14.4	0.00	-2000.00	-723.16	4.20	-3.1393	0.8182	-476.19	-476.19	235.82	238.88	0.00	-476.19	-476.19	-476.19	-476.19	-883.89	-898.91	-898.91	-0.25	-1.36	-11.40	-14.55
15.6	0.00	-2000.00	-709.10	4.20	-3.1393	0.8182	-476.19	-476.19	238.88	242.38	0.00	-476.19	-476.19	-476.19	-476.19	-898.91	-914.91	-914.91	-0.25	-1.34	-11.18	-14.68
16.8	0.00	-2000.00	-666.72	4.20	-3.1393	0.8182	-476.19	-476.19	242.38	248.88	0.00	-476.19	-476.19	-476.19	-476.19	-914.91	-928.57	-928.57	-0.26	-1.29	-10.52	-15.06
18	0.00	-2000.00	-586.08	4.20	-3.1393	0.8182	-476.19	-476.19	248.88	258.38	0.00	-476.19	-476.19	-476.19	-476.19	-928.57	-947.71	-947.71	-0.29	-1.20	-9.41	-15.70
19.2	0.00	-2000.00	-497.20	4.20	-3.1393	0.8182	-476.19	-476.19	258.38	268.45	0.00	-476.19	-476.19	-476.19	-476.19	-947.71	-967.71	-967.71	-0.32	-1.08	-7.85	-16.59
20.4	0.00	-2000.00	-370.10	4.20	-3.1393	0.8182	-476.19	-476.19	268.45	278.89	0.00	-476.19	-476.19	-476.19	-476.19	-967.71	-987.71	-987.71	-0.36	-0.93	-5.85	-17.74
21.6	0.00	-2000.00	-214.88	4.20	-3.1393	0.8182	-476.19	-476.19	278.89	288.89	0.00	-476.19	-476.19	-476.19	-476.19	-987.71	-1007.71	-1007.71	-0.41	-0.74	-13.75	-16.32
22.8	0.00	-2000.00	-30.86	4.20	-3.1393	0.8182	-476.19	-476.19	288.89	298.89	0.00	-476.19	-476.19	-476.19	-476.19	-1007.71	-1027.71	-1027.71	-0.47	-0.51	-13.57	-16.07
24	0.00	-2000.00	184.52	4.20	-3.1393	0.8182	-476.19	-476.19	298.89	308.89	0.00	-476.19	-476.19	-476.19	-476.19	-1027.71	-1047.71	-1047.71	-0.53	-0.25	-12.95	-16.06
25.2	0.00	-2000.00	564.32	4.20	-3.1393	0.8182	-476.19	-476.19	308.89	318.89	0.00	-476.19	-476.19	-476.19	-476.19	-1047.71	-1067.71	-1067.71	-0.66	0.21	-13.92	-14.15
26.4	0.00	-2000.00	887.84	4.20	-3.1393	0.8182	-476.19	-476.19	318.89	328.89	0.00	-476.19	-476.19	-476.19	-476.19	-1067.71	-1087.71	-1087.71	-0.76	0.61	-13.25	-13.77
27.6	0.00	-2000.00	1158.04	4.20	-3.1393	0.8182	-476.19	-476.19	328.89	338.89	0.00	-476.19	-476.19	-476.19	-476.19	-1087.71	-1107.71	-1107.71	-0.85	0.94	-10.93	-14.92
28.8	0.00	-2000.00	1307.74	4.20	-3.1393	0.8182	-476.19	-476.19	338.89	348.89	0.00	-476.19	-476.19	-476.19	-476.19	-1107.71	-1127.71	-1127.71	-0.89	1.12	-6.06	-18.56

σ Max		< fctm	
σ min		< 0.45 fck	
		-5.85	-18.56

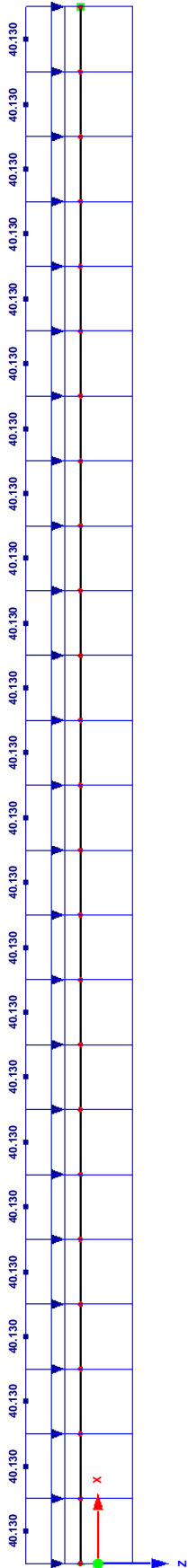
Project: RFEM

Structure: Phase 5\_LM1 2D

■ LC3: LM1 UDL (Construction Phase 5)

LC3: LM1 UDL

Against Y-direction

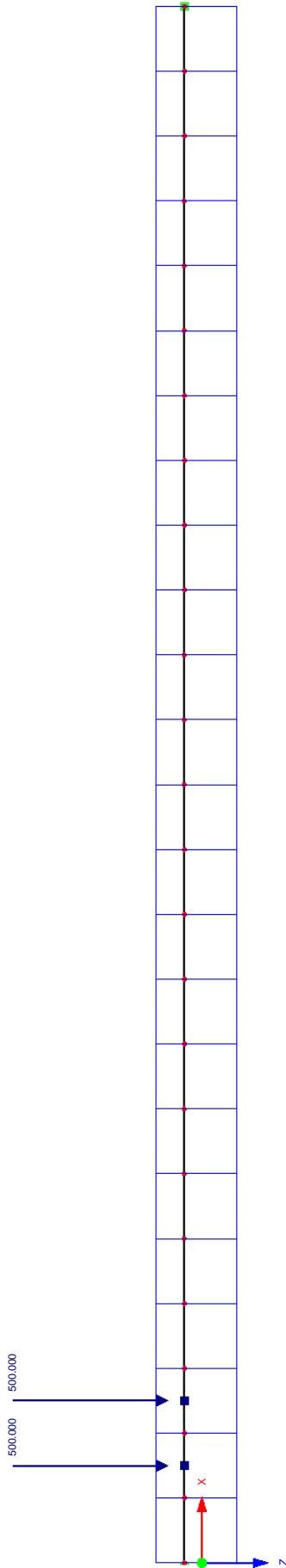


3.00 [m]

■ LC104: MOVING LOAD X = 1.800 M, CA1 (Construction Phase 5)

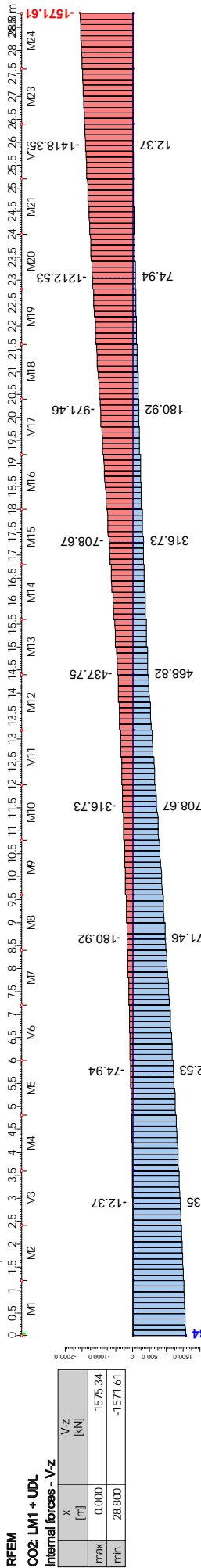
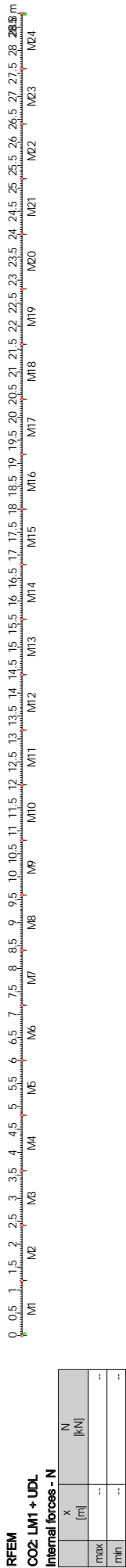
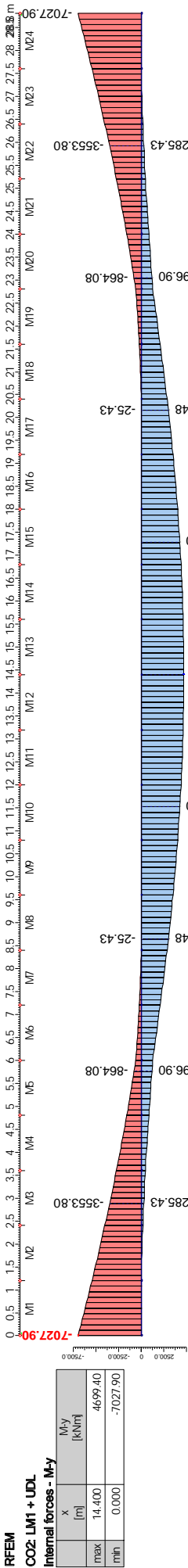
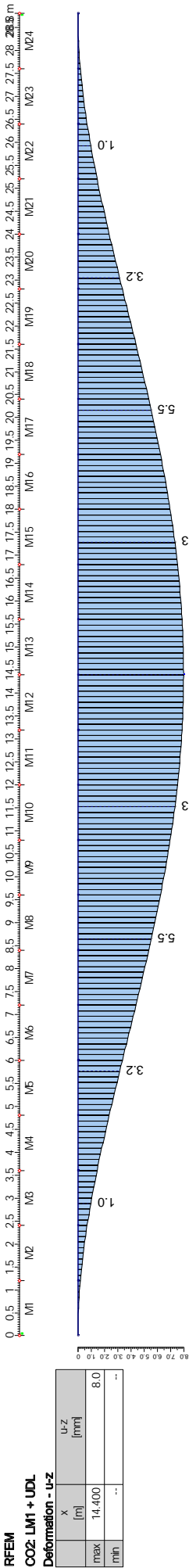
LC104: Moving Load x = 1.800 m, CA1

Against Y-direction



3.00 [m]

■ RESULT DIAGRAMS FOR CONTINUOUS MEMBERS - SM1



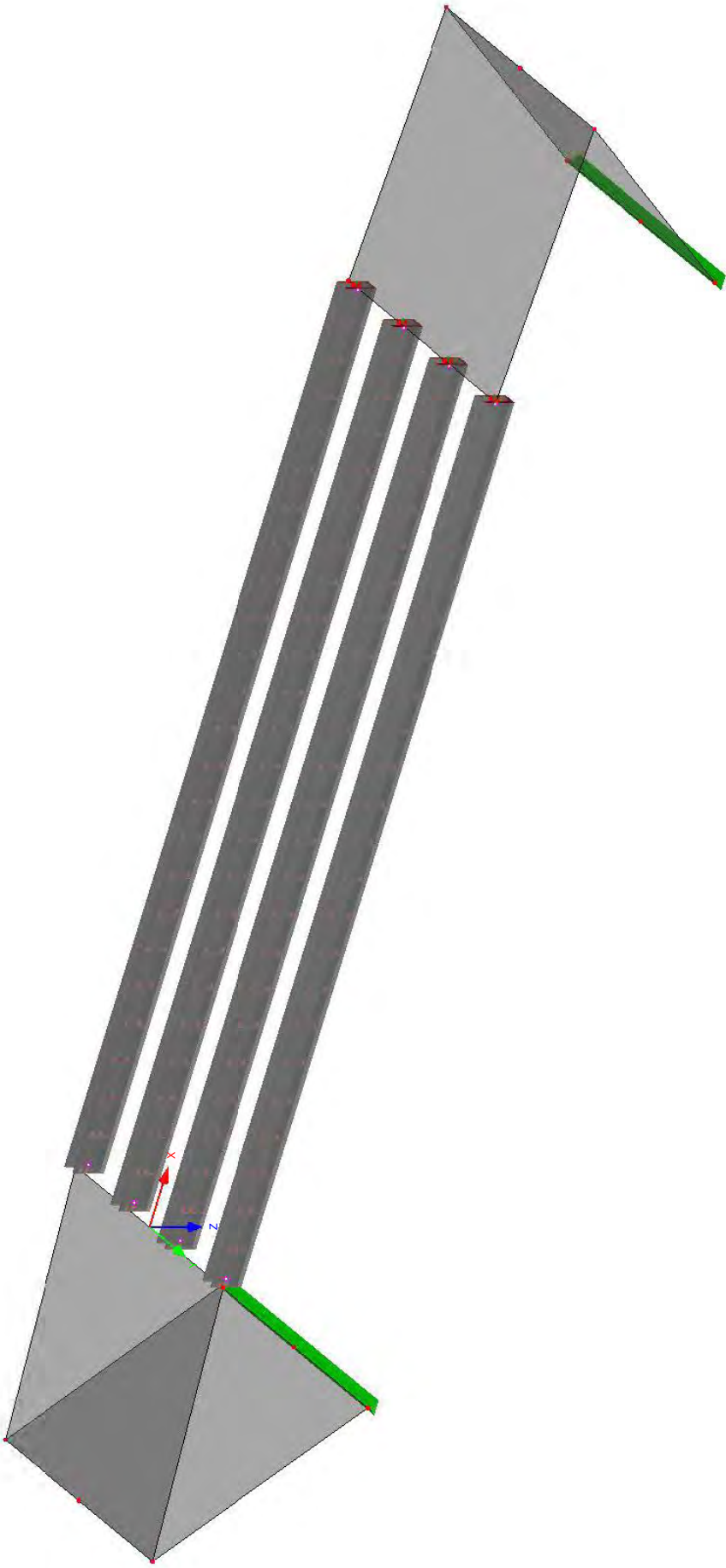


Structure: 3D\_Phase 1

Project: RFEM

■ STRUCTURE

Isometric



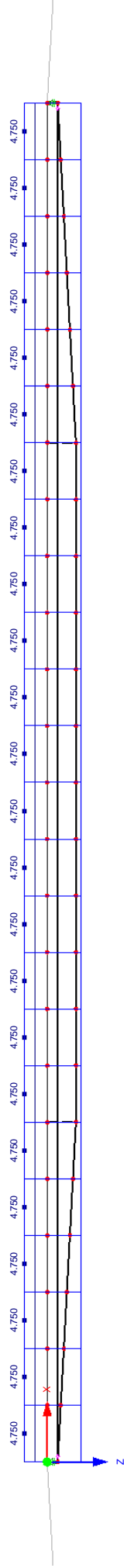
Project: RFEM

Structure: 3D\_Phase 1

■ LC1: SELF WEIGHT

LC1: Self Weight

Against Y-direction

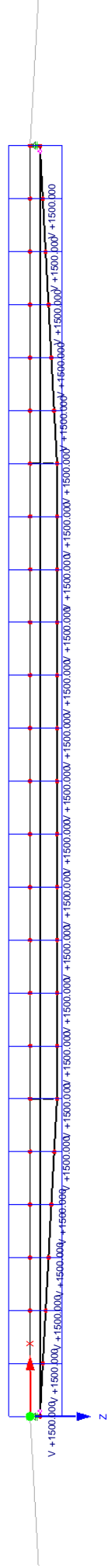


3.00 [m]

■ LC2: PRE-STRESS

LC2: Pre-Stress

Against Y-direction



3.00 [m]

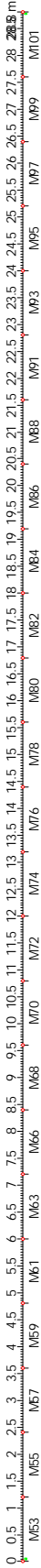
■ RESULT DIAGRAMS FOR CONTINUOUS MEMBERS - SM2

RFEM

LC1: Self Weight

Deformation - u

	x	u
	[m]	[mm]
max	14.400	54.3
min	--	--

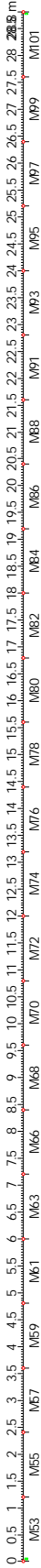


RFEM

LC1: Self Weight

Internal forces - M-y

	x	M-y
	[m]	[kNm]
max	14.400	492.48
min	--	--



RFEM

LC1: Self Weight

Internal forces - N

	x	N
	[m]	[kN]
max	0.000	421.80
min	--	--

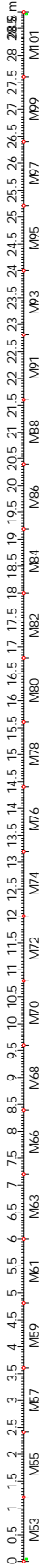


RFEM

LC1: Self Weight

Internal forces - V-z

	x	V-z
	[m]	[kN]
max	0.000	68.40
min	28.800	-68.40



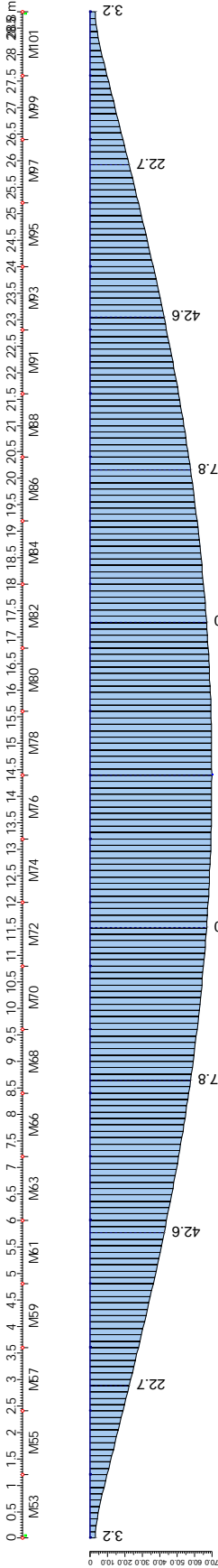
■ RESULT DIAGRAMS FOR CONTINUOUS MEMBERS - SM2

RFEM

LC2: Pre-Stress

Deformation - u

	x	y	z
	[m]	[m]	[mm]
max	14.400	70.1	
min	--	--	

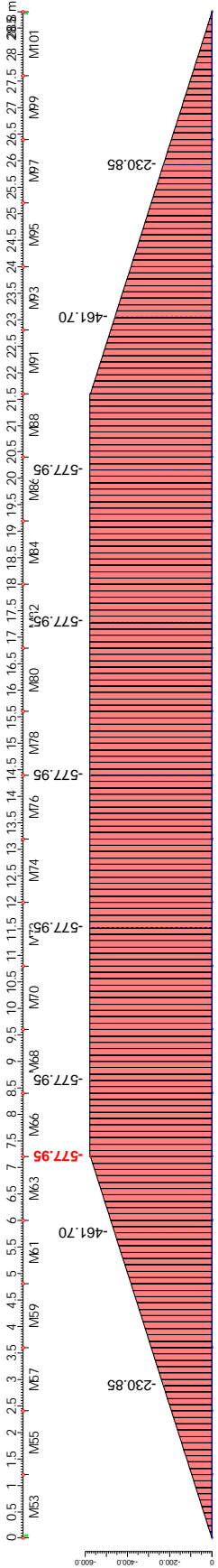


RFEM

LC2: Pre-Stress

Internal forces - M-y

	x	y	z
	[m]	[kNm]	
max	7.200	-577.95	
min			

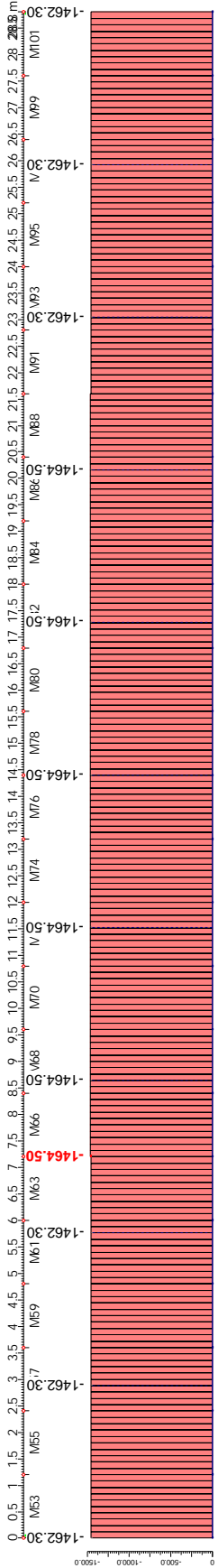


RFEM

LC2: Pre-Stress

Internal forces - N

	x	y	z
	[m]	[kN]	
max	--		
min	7.200	-1464.50	

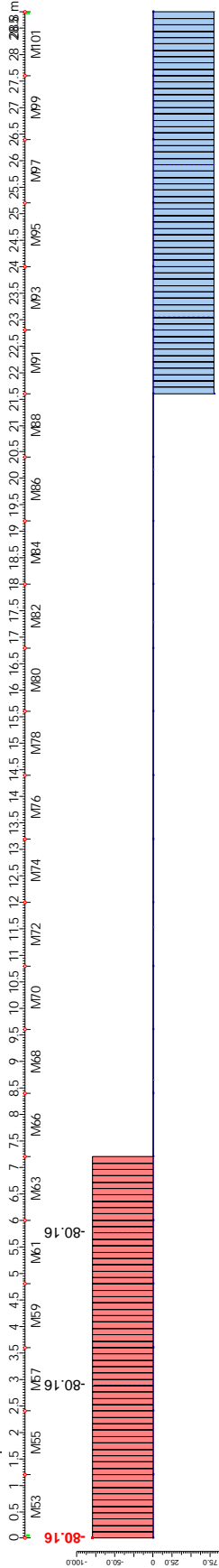


RFEM

LC2: Pre-Stress

Internal forces - V-z

	x	y	z
	[m]	[kN]	
max	21.600	80.16	
min	0.000	-80.16	



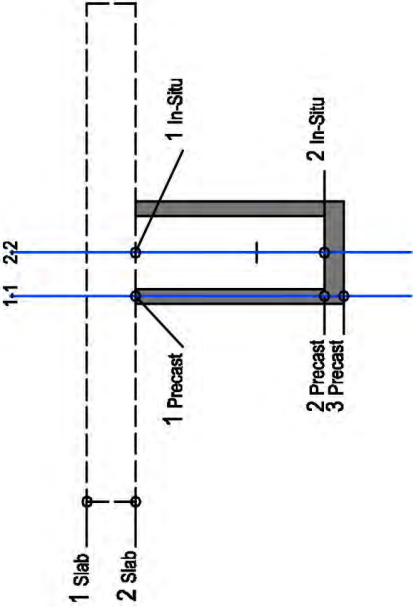


Phase 1

x	Factor		Stresses Phase 1																
	P [MN]		Pre-Stress		Stress P	Slab 1		Slab 2		In-Situ 1		In-Situ 2		Precast 1		Precast 2		Precast 3	
	Self Weight		M.g	N	M.p	σ Slab 1 [MN/m²]	σ Slab 2 [MN/m²]	σ Slab 2 [MN/m²]	σ Slab 2 [MN/m²]	σ In-Situ 1 [MN/m²]	σ In-Situ 1 [MN/m²]	σ In-Situ 2 [MN/m²]	σ In-Situ 2 [MN/m²]	σ Precast 1 [MN/m²]	σ Precast 2 [MN/m²]	σ Precast 2 [MN/m²]	σ Precast 3 [MN/m²]	σ Precast 3 [MN/m²]	
0		0.00	-1497.90	0.00	0.00	0.00	0.00	0.00	0.00	0.00	0.00	0.00	0.00	-7.88	-7.88	-7.88	-7.88	-7.88	
1.2		78.66	-1497.90	-96.19	0.00	0.00	0.00	0.00	0.00	0.00	0.00	0.00	0.00	-7.39	-8.23	-8.23	-8.16	-8.16	
2.4		150.48	-1497.90	-192.38	0.00	0.00	0.00	0.00	0.00	0.00	0.00	0.00	0.00	-6.70	-8.72	-8.72	-8.54	-8.54	
3.6		215.46	-1497.90	-288.56	0.00	0.00	0.00	0.00	0.00	0.00	0.00	0.00	0.00	-5.82	-9.34	-9.34	-9.02	-9.02	
4.8		273.60	-1497.90	-384.75	0.00	0.00	0.00	0.00	0.00	0.00	0.00	0.00	0.00	-4.75	-10.10	-10.10	-9.61	-9.61	
6		324.90	-1497.90	-480.94	0.00	0.00	0.00	0.00	0.00	0.00	0.00	0.00	0.00	-3.48	-10.99	-10.99	-10.31	-10.31	
7.2		369.36	-1497.90	-577.95	0.00	0.00	0.00	0.00	0.00	0.00	0.00	0.00	0.00	-2.00	-12.04	-12.04	-11.13	-11.13	
8.4		406.98	-1500.10	-577.95	0.00	0.00	0.00	0.00	0.00	0.00	0.00	0.00	0.00	-3.07	-11.30	-11.30	-10.55	-10.55	
9.6		437.76	-1500.10	-577.95	0.00	0.00	0.00	0.00	0.00	0.00	0.00	0.00	0.00	-3.94	-10.69	-10.69	-10.07	-10.07	
10.8		461.70	-1500.10	-577.95	0.00	0.00	0.00	0.00	0.00	0.00	0.00	0.00	0.00	-4.62	-10.21	-10.21	-9.70	-9.70	
12		478.80	-1500.10	-577.95	0.00	0.00	0.00	0.00	0.00	0.00	0.00	0.00	0.00	-5.10	-9.87	-9.87	-9.44	-9.44	
13.2		489.06	-1500.10	-577.95	0.00	0.00	0.00	0.00	0.00	0.00	0.00	0.00	0.00	-5.39	-9.67	-9.67	-9.28	-9.28	
14.4		492.48	-1500.10	-577.95	0.00	0.00	0.00	0.00	0.00	0.00	0.00	0.00	0.00	-5.48	-9.60	-9.60	-9.22	-9.22	
15.6		489.06	-1500.10	-577.95	0.00	0.00	0.00	0.00	0.00	0.00	0.00	0.00	0.00	-5.39	-9.67	-9.67	-9.28	-9.28	
16.8		478.80	-1500.10	-577.95	0.00	0.00	0.00	0.00	0.00	0.00	0.00	0.00	0.00	-5.10	-9.87	-9.87	-9.44	-9.44	
18		461.70	-1500.10	-577.95	0.00	0.00	0.00	0.00	0.00	0.00	0.00	0.00	0.00	-4.62	-10.21	-10.21	-9.70	-9.70	
19.2		437.76	-1500.10	-577.95	0.00	0.00	0.00	0.00	0.00	0.00	0.00	0.00	0.00	-3.94	-10.69	-10.69	-10.07	-10.07	
20.4		406.98	-1500.10	-577.95	0.00	0.00	0.00	0.00	0.00	0.00	0.00	0.00	0.00	-3.07	-11.30	-11.30	-10.55	-10.55	
21.6		369.36	-1497.90	-577.95	0.00	0.00	0.00	0.00	0.00	0.00	0.00	0.00	0.00	-2.00	-12.04	-12.04	-11.13	-11.13	
22.8		324.90	-1497.90	-480.94	0.00	0.00	0.00	0.00	0.00	0.00	0.00	0.00	0.00	-3.48	-10.99	-10.99	-10.31	-10.31	
24		273.60	-1497.90	-384.75	0.00	0.00	0.00	0.00	0.00	0.00	0.00	0.00	0.00	-4.75	-10.10	-10.10	-9.61	-9.61	
25.2		215.46	-1497.90	-288.56	0.00	0.00	0.00	0.00	0.00	0.00	0.00	0.00	0.00	-5.82	-9.34	-9.34	-9.02	-9.02	
26.4		150.48	-1497.90	-192.38	0.00	0.00	0.00	0.00	0.00	0.00	0.00	0.00	0.00	-6.70	-8.72	-8.72	-8.54	-8.54	
27.6		78.66	-1497.90	-96.19	0.00	0.00	0.00	0.00	0.00	0.00	0.00	0.00	0.00	-7.39	-8.23	-8.23	-8.16	-8.16	
28.8		0.00	-1497.90	0.00	0.00	0.00	0.00	0.00	0.00	0.00	0.00	0.00	0.00	-7.88	-7.88	-7.88	-7.88	-7.88	
					σ < 0.45 fck	13.50	13.50	13.50	13.50	13.50	13.50	13.50	13.50	22.50	22.50	22.50	22.50	22.50	

A [m²]	0.19
S_c.1 [m³]	-0.0354
S_c.2 [m³]	0.0643
S_c.3 [m³]	0.0502
S_c.4 [m³]	0.0000

σ Max	-2.00	σ Max	< fctm
σ min	-12.04	σ min	< 0.45 fck



Cross-Section 1			
Position	Support	Redirection	Midspan
Height	σ [MN/m²]	σ [MN/m²]	σ [MN/m²]
1 Slab	0.00	0.00	0.00
2 Slab	0.00	0.00	0.00
1 Precast	0.00	0.00	0.00
2 Precast	-7.88	-2.00	-5.48
3 Precast	-7.88	-11.13	-9.22

Cross-Section 2			
Position	Support	Redirection	Midspan
Height	σ [MN/m²]	σ [MN/m²]	σ [MN/m²]
1 Slab	0.00	0.00	0.00
2 Slab	0.00	0.00	0.00
1 In-Situ	0.00	0.00	0.00
2 In-Situ	0.00	0.00	0.00
2 Precast	-7.88	-11.13	-9.22
3 Precast	-7.88	-12.04	-9.60

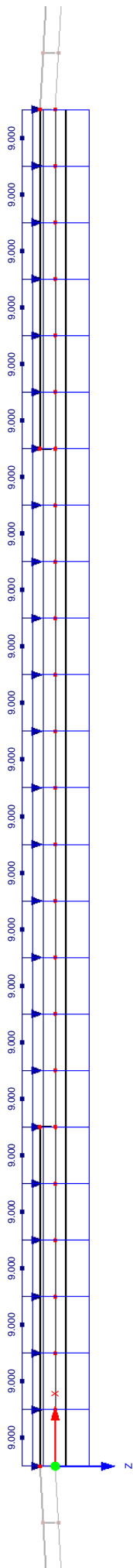
Project: RFEM

Structure: 3D\_Phase 2

■ LC1: SELF WEIGHT

LC1: Self Weight

Against Y-direction

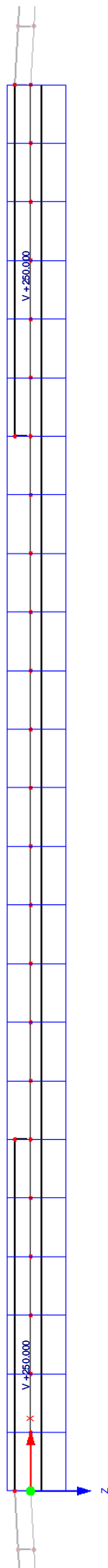


3.00 [m]

■ LC2: PRE-STRESS

LC2: Pre-Stress

Against Y-direction



3.00 [m]

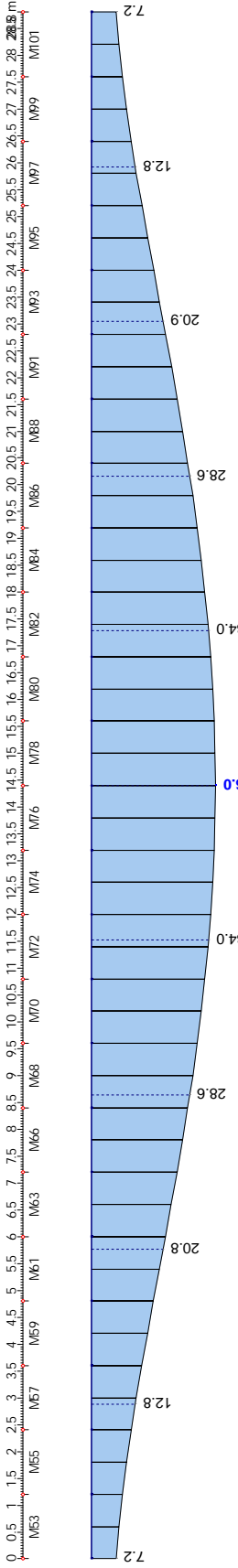
RESULT DIAGRAMS FOR CONTINUOUS MEMBERS - SM2

RFEM

LC1: Self Weight

Deformation - u

	x	y	z	u
	[m]	[m]	[m]	[mm]
max	14.400			36.0
min	--			--

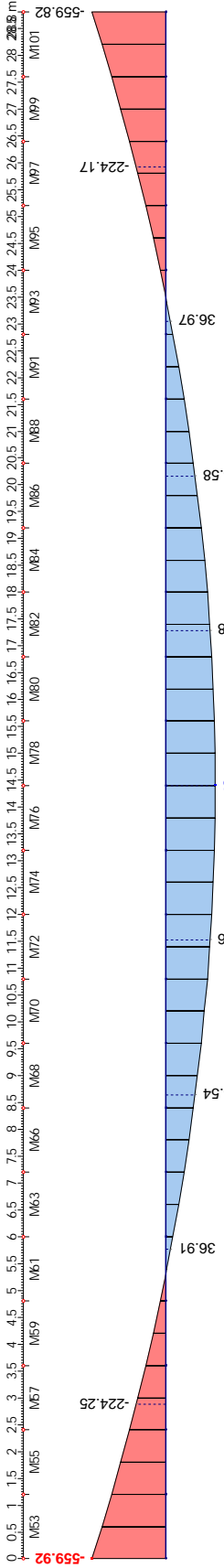


RFEM

LC1: Self Weight

Internal forces - M-y

	x	y	z	M-y
	[m]			[kNm]
max	14.400			373.25
min	0.000			-559.92

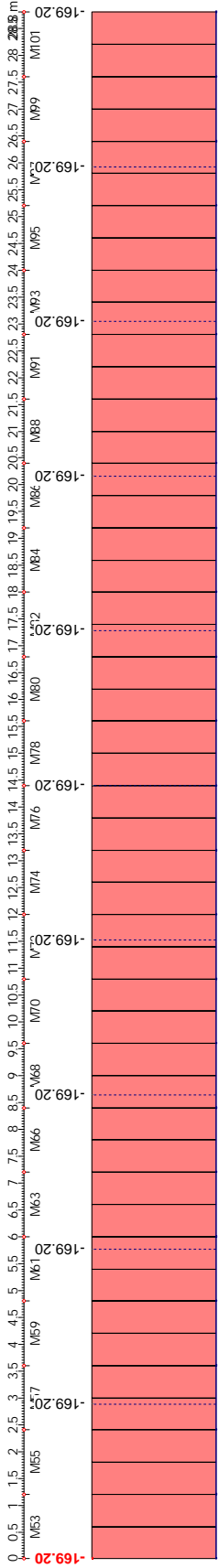


RFEM

LC1: Self Weight

Internal forces - N

	x	y	z	N
	[m]			[kN]
max	--			--
min	0.000			-169.20

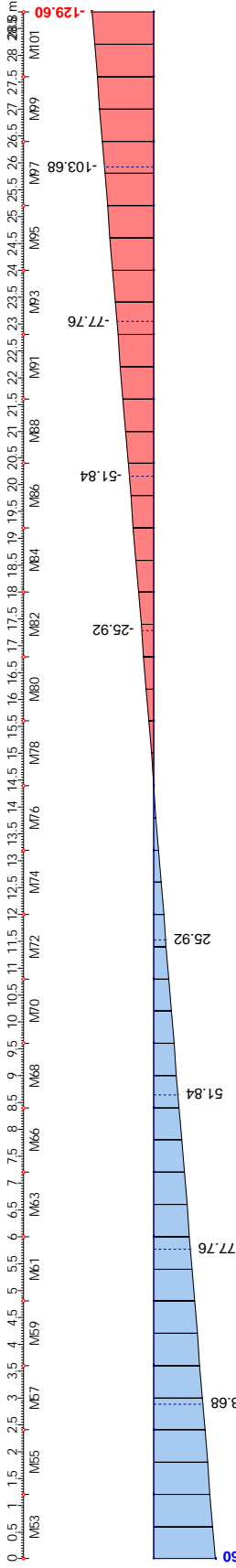


RFEM

LC1: Self Weight

Internal forces - V-z

	x	y	z	V-z
	[m]			[kN]
max	0.000			129.60
min	28.800			-129.60



Project: RFEM

Structure: 3D\_Phase 2

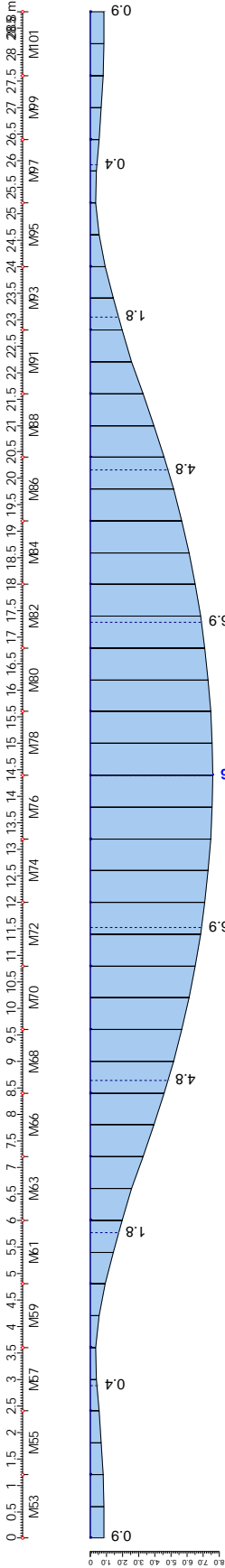
RESULT DIAGRAMS FOR CONTINUOUS MEMBERS - SM2

RFEM

LC2: Pre-Stress

Deformation - u

	x	u
	[m]	[mm]
max	14.400	7.6
min	--	--

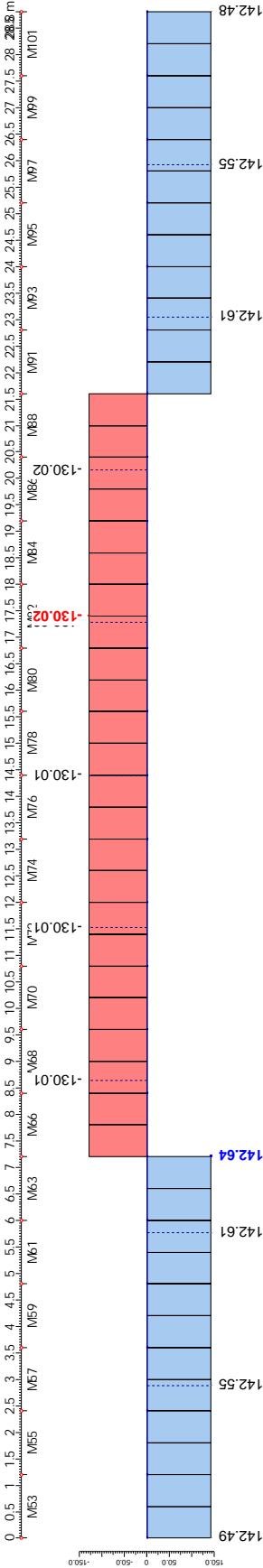


RFEM

LC2: Pre-Stress

Internal forces - M-y

	x	M-y
	[m]	[kNm]
max	7.200	142.64
min	17.400	-130.02

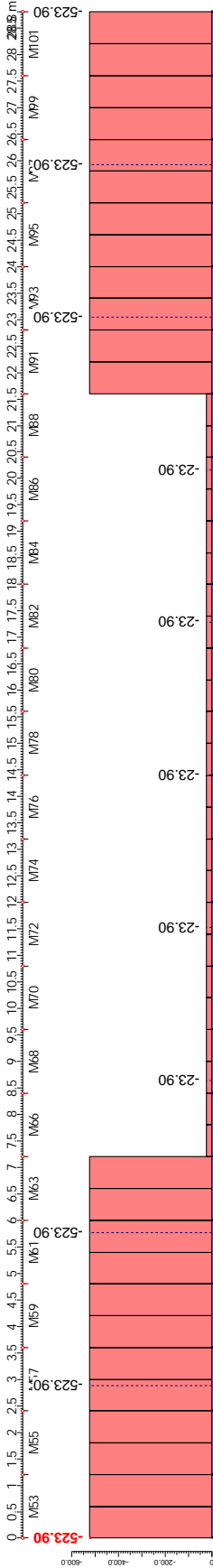


RFEM

LC2: Pre-Stress

Internal forces - N

	x	N
	[m]	[kN]
max	--	-523.90
min	0.000	-523.90

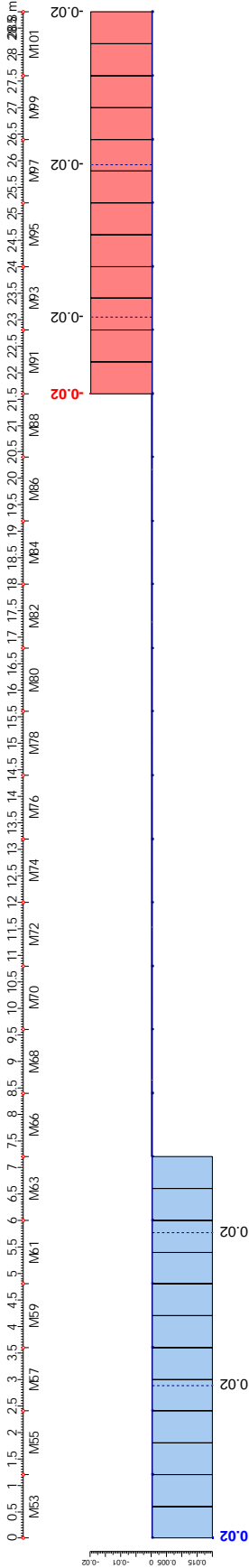


RFEM

LC2: Pre-Stress

Internal forces - V-z

	x	V-z
	[m]	[kN]
max	0.000	0.02
min	21.600	-0.02



Phase 2

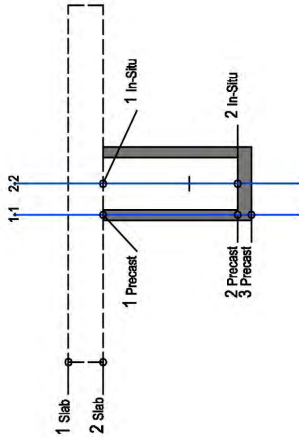
Factor	P	Self Weight		Pre-Stress	Stress P	Stresses Phase 2										Sum Stresses				σ ≤ 0.45 fck							
		M	Q			Slab 1	Slab 2	In-Situ 1	In-Situ 2	Precast 1	Precast 2	Precast 3	Slab 1	Slab 2	In-Situ 1	In-Situ 2	Precast 1	Precast 2	Precast 3	Sum σ Precast 1	Sum σ Precast 2	Sum σ Precast 3	Sum σ In-Situ 1	Sum σ In-Situ 2	Sum σ Precast 1	Sum σ Precast 2	Sum σ Precast 3
x	0	-559.42	-523.90	142.49	M.p	σ Slab 1 [MN/m²]	σ Slab 2 [MN/m²]	σ In-Situ 1 [MN/m²]	σ In-Situ 2 [MN/m²]	σ Precast 1 [MN/m²]	σ Precast 2 [MN/m²]	σ Precast 3 [MN/m²]	σ Slab 1 [MN/m²]	σ Slab 2 [MN/m²]	σ In-Situ 1 [MN/m²]	σ In-Situ 2 [MN/m²]	σ Precast 1 [MN/m²]	σ Precast 2 [MN/m²]	σ Precast 3 [MN/m²]	Sum σ Precast 1	Sum σ Precast 2	Sum σ Precast 3	Sum σ In-Situ 1	Sum σ In-Situ 2	Sum σ Precast 1	Sum σ Precast 2	Sum σ Precast 3
0	1.2	-410.40	-523.90	142.49		0.00	0.00	0.00	0.00	9.01	-9.24	-11.06	0.00	0.00	0.00	0.00	1.12	-17.12	-18.95	1.12	-17.12	-18.95	0.00	0.00	1.12	-17.12	-18.95
1.2	2.4	-274.33	-523.90	142.54		0.00	0.00	0.00	0.00	4.80	-4.92	-6.09	0.00	0.00	0.00	0.00	-2.59	-15.08	-16.33	-2.59	-15.08	-16.33	0.00	0.00	-2.59	-15.08	-16.33
2.4	3.6	-151.23	-523.90	142.56		0.00	0.00	0.00	0.00	0.96	-4.81	-5.38	0.00	0.00	0.00	0.00	-5.74	-13.24	-14.10	-5.74	-13.24	-14.10	0.00	0.00	-5.74	-13.24	-14.10
3.6	4.8	-41.08	-523.90	142.59		0.00	0.00	0.00	0.00	-2.51	-2.89	-2.93	0.00	0.00	0.00	0.00	-8.33	-11.91	-12.27	-8.33	-11.91	-12.27	0.00	0.00	-8.33	-11.91	-12.27
4.8	6	56.10	-523.90	142.61		0.00	0.00	0.00	0.00	-5.62	-1.18	-0.74	0.00	0.00	0.00	0.00	-10.37	-10.79	-10.83	-10.37	-10.79	-10.83	0.00	0.00	-10.37	-10.79	-10.83
6	7.2	140.33	-523.90	142.64		0.00	0.00	0.00	0.00	-8.36	0.33	1.20	0.00	0.00	0.00	0.00	-11.84	-9.98	-9.79	-11.84	-9.98	-9.79	0.00	0.00	-11.84	-9.98	-9.79
7.2	8.4	211.59	-523.90	142.64		0.00	0.00	0.00	0.00	-10.74	1.94	2.88	0.00	0.00	0.00	0.00	-12.74	-9.48	-9.16	-12.74	-9.48	-9.16	0.00	0.00	-12.74	-9.48	-9.16
8.4	9.6	269.90	-523.90	142.67		0.00	0.00	0.00	0.00	-12.43	1.14	1.50	0.00	0.00	0.00	0.00	-15.50	-9.41	-8.60	-15.50	-9.41	-8.60	0.00	0.00	-15.50	-9.41	-8.60
9.6	10.8	315.24	-523.90	142.69		0.00	0.00	0.00	0.00	-13.00	2.05	2.66	0.00	0.00	0.00	0.00	-16.01	-8.03	-6.65	-16.01	-8.03	-6.65	0.00	0.00	-16.01	-8.03	-6.65
10.8	12	347.62	-523.90	142.71		0.00	0.00	0.00	0.00	-13.00	2.75	3.56	0.00	0.00	0.00	0.00	-17.36	-6.18	-5.66	-17.36	-6.18	-5.66	0.00	0.00	-17.36	-6.18	-5.66
12	13.2	367.05	-523.90	142.73		0.00	0.00	0.00	0.00	-13.00	3.26	4.60	0.00	0.00	0.00	0.00	-18.20	-5.72	-5.07	-18.20	-5.72	-5.07	0.00	0.00	-18.20	-5.72	-5.07
13.2	14.4	373.51	-523.90	142.75		0.00	0.00	0.00	0.00	-13.00	3.56	4.73	0.00	0.00	0.00	0.00	-18.20	-5.56	-4.87	-18.20	-5.56	-4.87	0.00	0.00	-18.20	-5.56	-4.87
14.4	15.6	367.02	-523.90	142.76		0.00	0.00	0.00	0.00	-13.00	3.26	4.60	0.00	0.00	0.00	0.00	-18.20	-5.72	-5.07	-18.20	-5.72	-5.07	0.00	0.00	-18.20	-5.72	-5.07
15.6	16.8	347.56	-523.90	142.78		0.00	0.00	0.00	0.00	-13.00	2.75	4.21	0.00	0.00	0.00	0.00	-17.36	-6.18	-5.66	-17.36	-6.18	-5.66	0.00	0.00	-17.36	-6.18	-5.66
16.8	18	315.15	-523.90	142.80		0.00	0.00	0.00	0.00	-13.00	2.05	3.56	0.00	0.00	0.00	0.00	-16.01	-6.95	-6.65	-16.01	-6.95	-6.65	0.00	0.00	-16.01	-6.95	-6.65
18	19.2	269.77	-523.90	142.81		0.00	0.00	0.00	0.00	-13.00	1.14	2.66	0.00	0.00	0.00	0.00	-15.49	-8.03	-8.03	-15.49	-8.03	-8.03	0.00	0.00	-15.49	-8.03	-8.03
19.2	20.4	211.44	-523.90	142.82		0.00	0.00	0.00	0.00	-13.00	0.33	1.50	0.00	0.00	0.00	0.00	-14.84	-9.41	-8.81	-14.84	-9.41	-8.81	0.00	0.00	-14.84	-9.41	-8.81
20.4	21.6	140.14	-523.90	142.83		0.00	0.00	0.00	0.00	-10.73	1.64	2.88	0.00	0.00	0.00	0.00	-12.73	-9.49	-9.16	-12.73	-9.49	-9.16	0.00	0.00	-12.73	-9.49	-9.16
21.6	22.8	55.89	-523.90	142.84		0.00	0.00	0.00	0.00	-8.36	0.33	1.20	0.00	0.00	0.00	0.00	-11.84	-9.98	-9.80	-11.84	-9.98	-9.80	0.00	0.00	-11.84	-9.98	-9.80
22.8	24	-41.33	-523.90	142.85		0.00	0.00	0.00	0.00	-5.61	-1.18	-0.74	0.00	0.00	0.00	0.00	-10.36	-10.79	-10.84	-10.36	-10.79	-10.84	0.00	0.00	-10.36	-10.79	-10.84
24	25.2	-151.50	-523.90	142.86		0.00	0.00	0.00	0.00	-2.51	-2.90	-2.94	0.00	0.00	0.00	0.00	-8.33	-11.92	-12.28	-8.33	-11.92	-12.28	0.00	0.00	-8.33	-11.92	-12.28
25.2	26.4	-274.64	-523.90	142.87		0.00	0.00	0.00	0.00	0.97	-4.81	-5.39	0.00	0.00	0.00	0.00	-5.73	-13.35	-14.11	-5.73	-13.35	-14.11	0.00	0.00	-5.73	-13.35	-14.11
26.4	27.6	-410.73	-523.90	142.88		0.00	0.00	0.00	0.00	4.81	-6.93	-8.10	0.00	0.00	0.00	0.00	-2.58	-15.08	-16.33	-2.58	-15.08	-16.33	0.00	0.00	-2.58	-15.08	-16.33
27.6	28.8	-559.79	-523.90	142.88		0.00	0.00	0.00	0.00	9.02	-9.24	-11.07	0.00	0.00	0.00	0.00	1.13	-17.13	-18.95	1.13	-17.13	-18.95	0.00	0.00	1.13	-17.13	-18.95
σ ≤ 0.45 fck																											
σ Max																											
σ min																											
< fctm																											
< 0.45 fck																											

A [m²]	Cross-Section 1		Midspan
	Support	Redirection	
0.19			
-0.0354			

A [m²]	0.19
S c.1 [m³]	-0.0354
S c.2 [m³]	0.0643
S c.3 [m³]	0.0502
S c.4 [m³]	0.0000

Cross-Section 1			
Position	Support	Redirection	Midspan
Height	σ [MN/m²]	σ [MN/m²]	σ [MN/m²]
1 Slab	0.00	0.00	0.00
2 Slab	0.00	0.00	0.00
1 Precast	1.12	-12.74	-12.48
2 Precast	-17.12	-9.48	-5.56
3 Precast	-18.95	-9.16	-4.87

Cross-Section 2			
Position	Support	Redirection	Midspan
Height	σ [MN/m²]	σ [MN/m²]	σ [MN/m²]
1 Slab	0.00	0.00	0.00
2 Slab	0.00	0.00	0.00
1 In-Situ	0.00	0.00	0.00
2 In-Situ	0.00	0.00	0.00
2 Precast	-17.12	-9.48	-5.56
3 Precast	-18.95	-9.16	-4.87



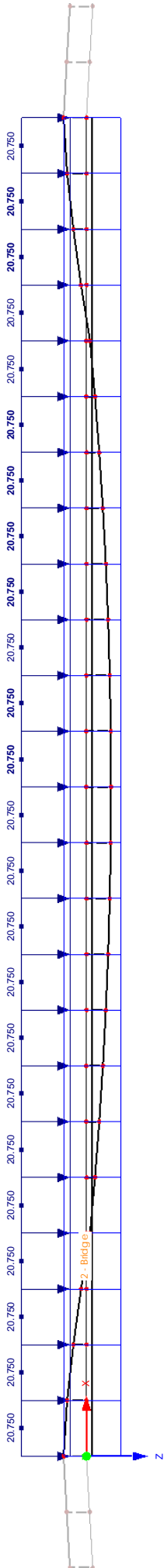
Project: RFEM

Structure: 3D\_Phase 3

LC1: SELF WEIGHT

LC1: Self Weight

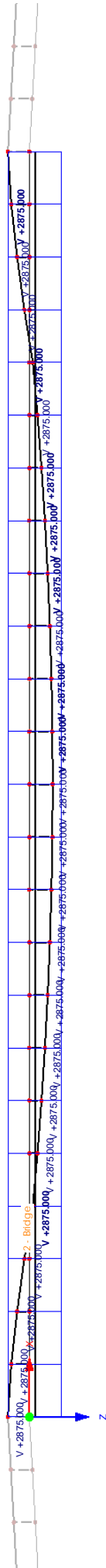
Against Y-direction



LC2: PRE-STRESS

LC2: Pre-Stress

Against Y-direction



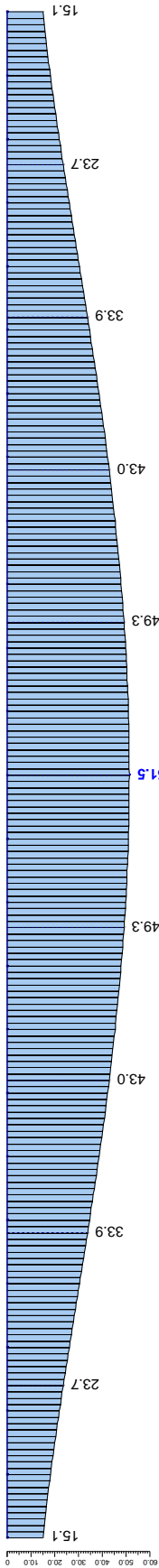
■ RESULT DIAGRAMS FOR CONTINUOUS MEMBERS - SM2

RFEM

LC1: Self Weight

Deformation - u

	x	u
	[m]	[mm]
max	14.400	51.5
min	--	--

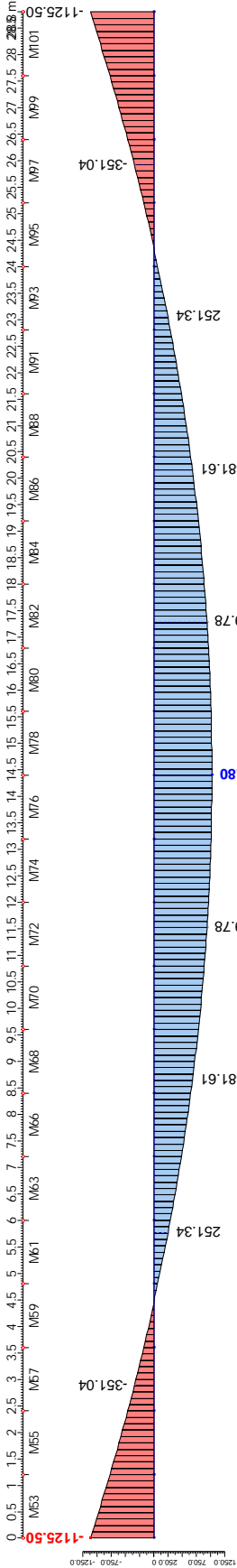


RFEM

LC1: Self Weight

Internal forces - M-y

	x	M-y
	[m]	[kNm]
max	14.400	1025.80
min	0.000	-1125.50

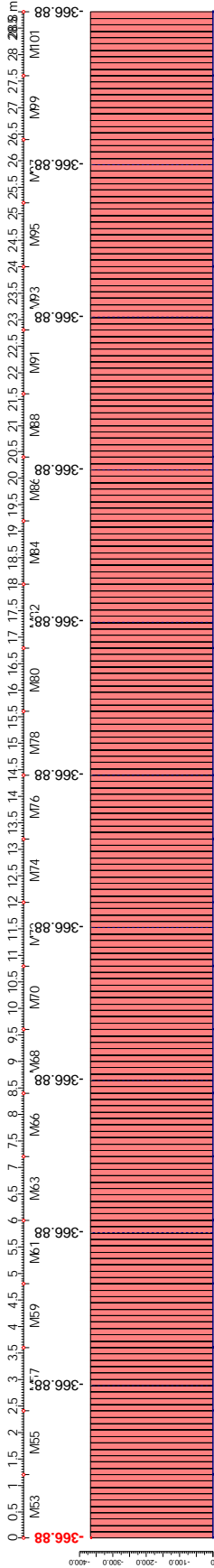


RFEM

LC1: Self Weight

Internal forces - N

	x	N
	[m]	[kN]
max	--	--
min	0.000	-366.88

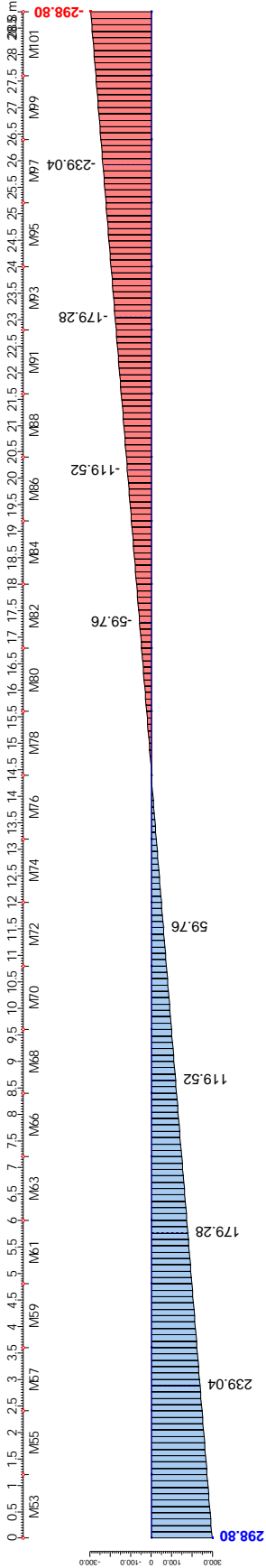


RFEM

LC1: Self Weight

Internal forces - V-z

	x	V-z
	[m]	[kN]
max	0.000	298.80
min	28.800	-298.80



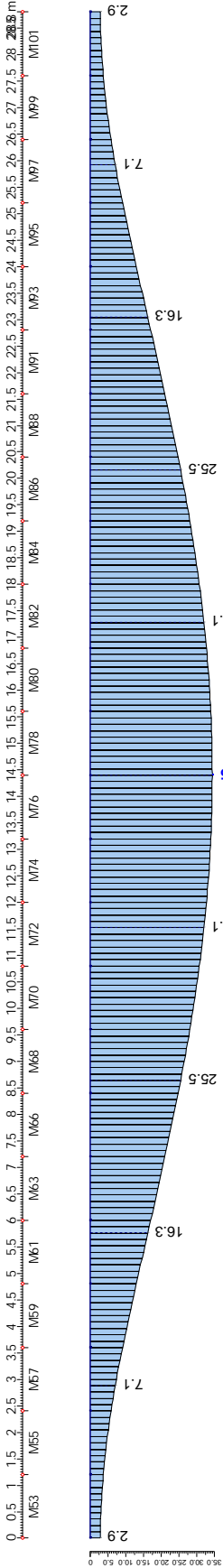
■ RESULT DIAGRAMS FOR CONTINUOUS MEMBERS - SM2

RFEM

LC2: Pre-Stress

Deformation - u

	x	u
	[m]	[mm]
max	14.400	34.5
min	--	--

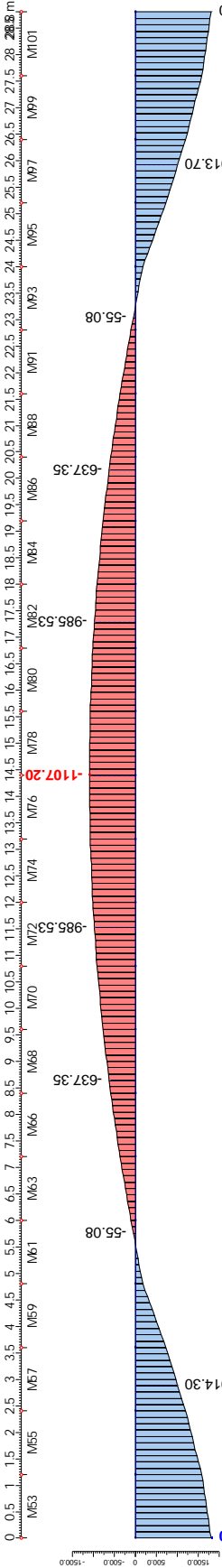


RFEM

LC2: Pre-Stress

Internal forces - M-y

	x	M-y
	[m]	[kNm]
max	0.000	1810.30
min	14.400	-1107.20

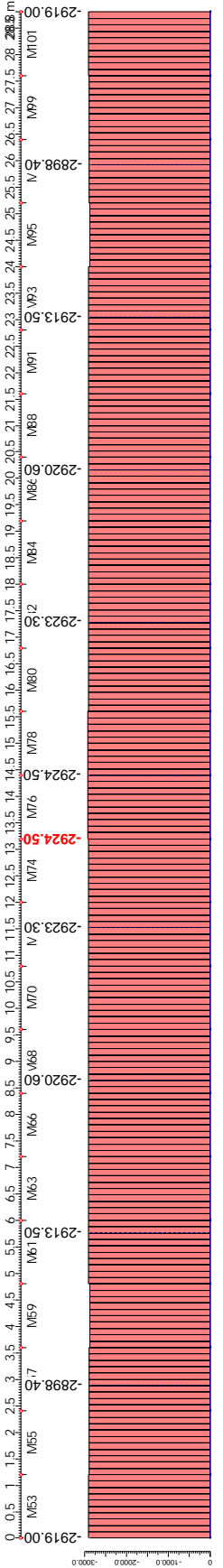


RFEM

LC2: Pre-Stress

Internal forces - N

	x	N
	[m]	[kN]
max	--	--
min	13.200	-2924.50

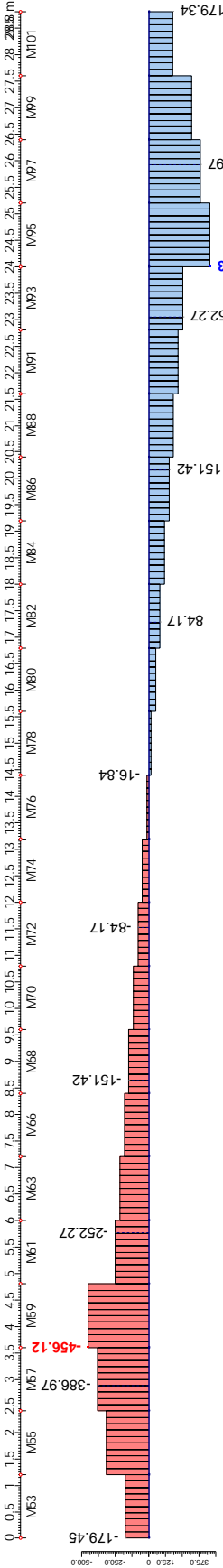


RFEM

LC2: Pre-Stress

Internal forces - V-z

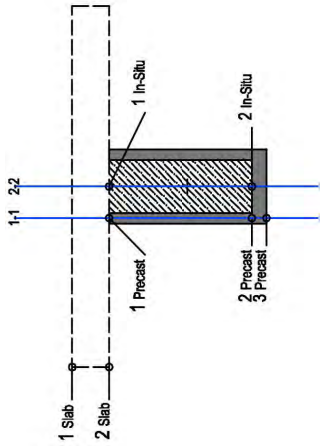
	x	V-z
	[m]	[kN]
max	24.000	455.63
min	3.600	-456.12





Phase 3

Factor	P	Self Weight	-1000		Stresses Phase 3												Sum Stresses				Precast 3				
			Pre-Stress	N	Stress P	Slab 1	Slab 2	In-Situ 1	In-Situ 2	Precast 1	Precast 2	Precast 3	Slab 1	Slab 2	In-Situ 1	In-Situ 2	Precast 1	Precast 2	Precast 3	Sum α	Precast 1	Precast 2	Sum α	Precast 3	
	x	M, g			M, p	σ Slab 1 [MN/m²]	σ Slab 2 [MN/m²]	σ In-Situ 1 [MN/m²]	σ In-Situ 2 [MN/m²]	σ Precast 1 [MN/m²]	σ Precast 2 [MN/m²]	σ Precast 3 [MN/m²]	Sum α Slab 1	Sum α Slab 2	Sum α In-Situ 1	Sum α In-Situ 2	Sum α Precast 1	Sum α Precast 2	Sum α Precast 3						
	0	-1125.50	-2919.00		1810.30	0.00	0.00	-12.10	0.25	-12.10	0.25	1.48	0.00	0.00	-12.10	0.25	-10.98	-16.87	-17.46						
	1.2	-781.91	-2919.00		1595.00	0.00	0.00	-13.37	1.29	-13.37	1.29	2.76	0.00	0.00	-13.37	1.29	-15.96	-13.79	-13.57						
	2.4	-468.17	-2906.60		1203.40	0.00	0.00	-12.58	0.68	-12.58	0.68	2.01	0.00	0.00	-12.58	0.68	-18.32	-12.66	-12.09						
	3.6	-184.31	-2898.40		735.66	0.00	0.00	-10.74	-0.80	-10.74	-0.80	0.20	0.00	0.00	-10.74	-0.80	-19.07	-12.71	-12.07						
	4.8	69.67	-2888.20		185.82	0.00	0.00	-7.79	-3.18	-7.79	-3.18	-2.72	0.00	0.00	-7.79	-3.18	-18.15	-13.97	-13.55						
	6	293.77	-2913.50		-115.63	0.00	0.00	-7.06	-3.85	-7.06	-3.85	-3.53	0.00	0.00	-7.06	-3.85	-18.91	-13.83	-13.52						
	7.2	487.99	-2916.30		-378.17	0.00	0.00	-6.39	-4.41	-6.39	-4.41	-4.21	0.00	0.00	-6.39	-4.41	-19.13	-13.90	-13.57						
	8.4	652.33	-2918.60		-600.56	0.00	0.00	-5.82	-4.89	-5.82	-4.89	-4.79	0.00	0.00	-5.82	-4.89	-11.32	-14.30	-14.59						
	9.6	786.79	-2920.60		-782.71	0.00	0.00	-5.35	-5.28	-5.35	-5.28	-5.27	0.00	0.00	-5.35	-5.28	-13.36	-13.30	-13.30						
	10.8	891.37	-2922.20		-924.53	0.00	0.00	-4.98	-5.58	-4.98	-5.58	-5.64	0.00	0.00	-4.98	-5.58	-14.95	-12.53	-12.29						
	12	966.07	-2923.30		-1025.90	0.00	0.00	-4.72	-5.80	-4.72	-5.80	-5.91	0.00	0.00	-4.72	-5.80	-16.08	-11.98	-11.57						
	13.2	1010.90	-2924.10		-1086.80	0.00	0.00	-4.56	-5.93	-4.56	-5.93	-6.07	0.00	0.00	-4.56	-5.93	-16.76	-11.65	-11.14						
	14.4	1025.80	-2924.50		-1107.20	0.00	0.00	-4.51	-5.98	-4.51	-5.98	-6.12	0.00	0.00	-4.51	-5.98	-16.99	-11.54	-11.00						
	15.6	1010.90	-2924.50		-1086.80	0.00	0.00	-4.56	-5.93	-4.56	-5.93	-6.07	0.00	0.00	-4.56	-5.93	-16.76	-11.65	-11.14						
	16.8	966.07	-2924.10		-1026.20	0.00	0.00	-4.72	-5.80	-4.72	-5.80	-5.91	0.00	0.00	-4.72	-5.80	-14.95	-11.98	-11.58						
	18	891.37	-2923.30		-924.93	0.00	0.00	-4.98	-5.59	-4.98	-5.59	-5.65	0.00	0.00	-4.98	-5.59	-13.36	-12.54	-12.30						
	19.2	786.79	-2922.20		-783.17	0.00	0.00	-5.35	-5.28	-5.35	-5.28	-5.28	0.00	0.00	-5.35	-5.28	-13.36	-13.31	-13.31						
	20.4	652.33	-2920.60		-601.00	0.00	0.00	-5.82	-4.89	-5.82	-4.89	-4.80	0.00	0.00	-5.82	-4.89	-11.31	-14.31	-14.61						
	21.6	487.99	-2918.60		-378.51	0.00	0.00	-6.39	-4.42	-6.39	-4.42	-4.22	0.00	0.00	-6.39	-4.42	-19.13	-13.91	-13.38						
	22.8	293.77	-2916.30		-115.78	0.00	0.00	-7.07	-3.86	-7.07	-3.86	-3.54	0.00	0.00	-7.07	-3.86	-18.91	-13.84	-13.33						
	24	69.67	-2913.50		187.09	0.00	0.00	-7.84	-3.21	-7.84	-3.21	-2.75	0.00	0.00	-7.84	-3.21	-18.21	-14.01	-13.59						
	25.2	-184.31	-2888.20		732.58	0.00	0.00	-10.69	-0.80	-10.69	-0.80	0.19	0.00	0.00	-10.69	-0.80	-19.02	-12.72	-12.09						
	26.4	-468.17	-2898.40		1199.40	0.00	0.00	-12.52	0.66	-12.52	0.66	1.98	0.00	0.00	-12.52	0.66	-18.25	-12.68	-12.13						
	27.6	-781.91	-2906.60		1588.40	0.00	0.00	-13.28	1.26	-13.28	1.26	2.71	0.00	0.00	-13.28	1.26	-15.66	-13.82	-13.62						
	28.8	-1125.50	-2919.00		1810.30	0.00	0.00	-12.10	0.25	-12.10	0.25	1.48	0.00	0.00	-12.10	0.25	-10.97	-16.88	-17.47						
					σ ≤ 0.45 fck	13.50	13.50	13.50	13.50	22.50	22.50	22.50	13.50	13.50	13.50	13.50	22.50	22.50	22.50		22.50	22.50		22.50	
						Cross-Section 1				Cross-Section 2				σ Max				σ Min				σ fck			
						Position	Height	Support	Redirection	Midspan	Support	Redirection	Midspan												
						σ [MN/m²]	σ [MN/m²]	σ [MN/m²]	σ [MN/m²]	σ [MN/m²]	σ [MN/m²]	σ [MN/m²]	σ [MN/m²]												
						1 Slab	0.00	0.00	0.00	0.00	0.00	0.00	0.00												
						2 Slab	0.00	0.00	0.00	0.00	0.00	0.00	0.00												
						1 Precast	-10.98	-10.98	-19.13	-19.13	-16.99	-11.54	-11.00												
						2 Precast	-16.87	-16.87	-13.90	-13.90	-11.54	-11.00	-11.00												
						3 Precast	-17.46	-17.46	-13.37	-13.37	-11.00	-11.00	-11.00												



A [m <sup>2</sup> ]	0.55
S.c.1 [m <sup>3</sup> ]	-0.1008
S.c.2 [m <sup>3</sup> ]	0.1232
S.c.3 [m <sup>3</sup> ]	0.1008
S.c.4 [m <sup>3</sup> ]	0.0000

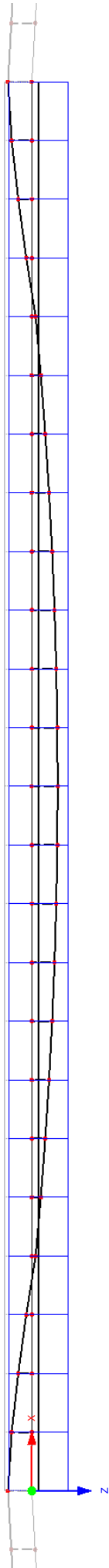
Project: **RFEM**

Structure: **3D\_Phase 4**

■ **LC1: SELF WEIGHT**

LC1: Self Weight

Against Y-direction

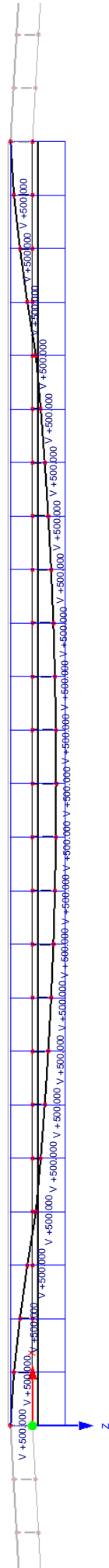


3.00 [m]

■ **LC2: PRE-STRESS**

LC2: Pre-Stress

Against Y-direction



3.00 [m]

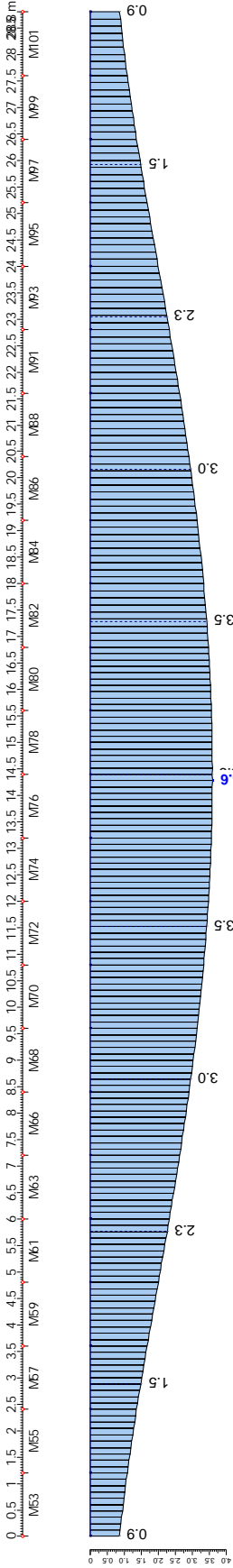
■ RESULT DIAGRAMS FOR CONTINUOUS MEMBERS - SM2

RFEM

LP2: Pre-Stress

Deformation - u

	x	u
	[m]	[mm]
max	14.280	3.6
min	--	--

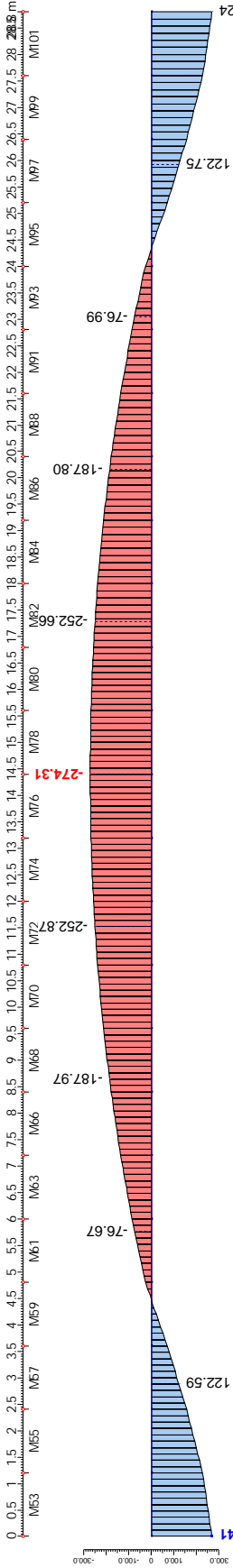


RFEM

LP2: Pre-Stress

Internal forces - M-y

	x	M-y
	[m]	[kNm]
max	0.000	269.41
min	14.400	-274.31

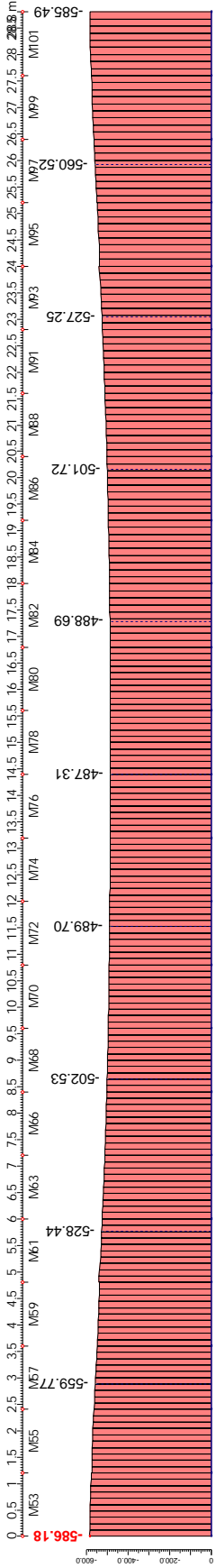


RFEM

LP2: Pre-Stress

Internal forces - N

	x	N
	[m]	[kN]
max	--	--
min	0.000	-586.18

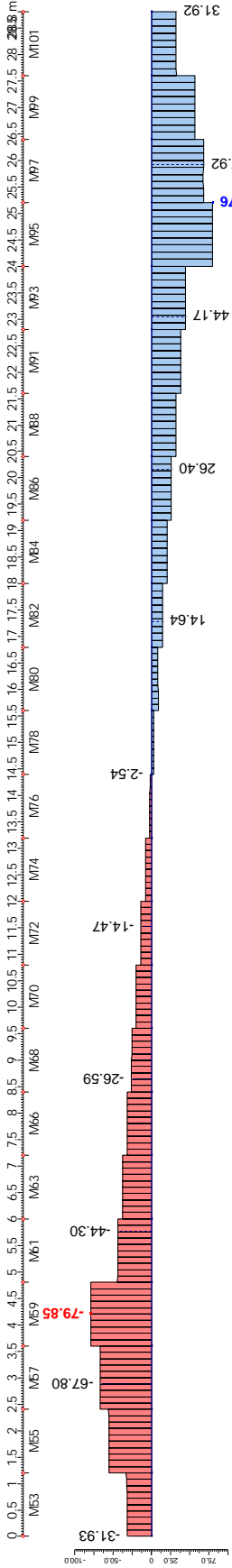


RFEM

LP2: Pre-Stress

Internal forces - V-z

	x	V-z
	[m]	[kN]
max	25.200	79.76
min	4.200	-79.85

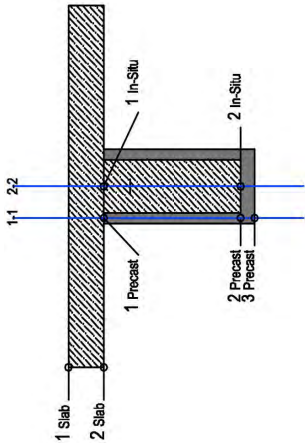


Phase 4

Pre-Stressed Factor		1		Stresses Phase 4														Sum Stresses																
x	P	Self Weight	Pre-Stress	N	M.p	Stress P	Slab 1		Slab 2		In-Situ 1		In-Situ 2		Precast 1		Precast 2		Precast 3		Slab 1		Slab 2		In-Situ 1		In-Situ 2		Precast 1		Precast 2		Precast 3	
							σ Slab 1 [MN/m²]	σ Slab 2 [MN/m²]	σ Slab 2 [MN/m²]	σ In-Situ 1 [MN/m²]	σ In-Situ 1 [MN/m²]	σ In-Situ 2 [MN/m²]	σ In-Situ 2 [MN/m²]	σ Precast 1 [MN/m²]	σ Precast 1 [MN/m²]	σ Precast 2 [MN/m²]	σ Precast 2 [MN/m²]	σ Precast 3 [MN/m²]	Sum σ Slab 1	Sum σ Slab 1	Sum σ Slab 2	Sum σ Slab 2	Sum σ In-Situ 1	Sum σ In-Situ 1	Sum σ In-Situ 2	Sum σ In-Situ 2	Sum σ Precast 1	Sum σ Precast 1	Sum σ Precast 2	Sum σ Precast 2	Sum σ Precast 3	Sum σ Precast 3		
0	0.00	-586.18	-269.41	-1000	-269.41	-269.41	-1.12	-0.76	-0.76	-0.76	-0.76	-0.76	0.63	0.63	-0.76	-0.76	0.63	0.63	0.77	0.77	-1.12	-1.12	-0.76	-0.76	-12.86	-12.86	0.88	0.88	-11.74	-11.74	-16.24	-16.24	-16.69	-16.69
1.2	0.00	-577.26	-227.72		-227.72	-227.72	-0.84	-0.63	-0.63	-0.63	-0.63	-0.63	0.18	0.18	-0.63	-0.63	0.18	0.18	0.26	0.26	-0.84	-0.84	-0.63	-0.63	-13.21	-13.21	0.86	0.86	-18.95	-18.95	-12.48	-12.48	-11.84	-11.84
2.4	0.00	-564.97	-156.43		-156.43	-156.43	-0.63	-0.54	-0.54	-0.54	-0.54	-0.54	-0.17	-0.17	-0.54	-0.54	-0.17	-0.17	-0.14	-0.14	-0.63	-0.63	-0.54	-0.54	-11.27	-11.27	-0.97	-0.97	-19.61	-19.61	-12.88	-12.88	-12.21	-12.21
3.6	0.00	-549.73	-70.52		-70.52	-70.52	-0.39	-0.43	-0.43	-0.43	-0.43	-0.43	-0.57	-0.57	-0.43	-0.43	-0.57	-0.57	-0.59	-0.59	-0.39	-0.39	-0.43	-0.43	-8.22	-8.22	-3.75	-3.75	-18.58	-18.58	-14.54	-14.54	-14.14	-14.14
4.8	0.00	-538.98	-27.87		-27.87	-27.87	-0.24	-0.36	-0.36	-0.36	-0.36	-0.36	-0.82	-0.82	-0.36	-0.36	-0.82	-0.82	-0.86	-0.86	-0.24	-0.24	-0.36	-0.36	-7.42	-7.42	-4.67	-4.67	-19.27	-19.27	-14.65	-14.65	-14.18	-14.18
6	0.00	-528.01	-88.08		-88.08	-88.08	-0.12	-0.30	-0.30	-0.30	-0.30	-0.30	-1.02	-1.02	-0.30	-0.30	-1.02	-1.02	-1.09	-1.09	-0.12	-0.12	-0.30	-0.30	-6.69	-6.69	-5.43	-5.43	-19.43	-19.43	-14.91	-14.91	-14.46	-14.46
7.2	0.00	-513.77	-138.43		-138.43	-138.43	-0.01	-0.25	-0.25	-0.25	-0.25	-0.25	-1.19	-1.19	-0.25	-0.25	-1.19	-1.19	-1.28	-1.28	-0.01	-0.01	-0.25	-0.25	-6.07	-6.07	-6.07	-6.07	-11.57	-11.57	-15.48	-15.48	-15.87	-15.87
8.4	0.00	-504.25	-180.73		-180.73	-180.73	0.07	-0.21	-0.21	-0.21	-0.21	-0.21	-1.32	-1.32	-0.21	-0.21	-1.32	-1.32	-1.43	-1.43	0.07	0.07	-0.21	-0.21	-5.56	-5.56	-6.60	-6.60	-13.58	-13.58	-14.63	-14.63	-14.73	-14.73
9.6	0.00	-497.22	-215.03		-215.03	-215.03	0.14	-0.18	-0.18	-0.18	-0.18	-0.18	-1.43	-1.43	-0.18	-0.18	-1.43	-1.43	-1.55	-1.55	0.14	0.14	-0.18	-0.18	-5.17	-5.17	-7.01	-7.01	-15.13	-15.13	-13.96	-13.96	-13.84	-13.84
10.8	0.00	-492.39	-241.37		-241.37	-241.37	0.18	-0.16	-0.16	-0.16	-0.16	-0.16	-1.50	-1.50	-0.16	-0.16	-1.50	-1.50	-1.64	-1.64	0.18	0.18	-0.16	-0.16	-4.88	-4.88	-7.31	-7.31	-16.25	-16.25	-13.48	-13.48	-13.21	-13.21
12	0.00	-489.35	-259.89		-259.89	-259.89	0.21	-0.15	-0.15	-0.15	-0.15	-0.15	-1.55	-1.55	-0.15	-0.15	-1.55	-1.55	-1.69	-1.69	0.21	0.21	-0.15	-0.15	-4.71	-4.71	-7.48	-7.48	-16.91	-16.91	-13.20	-13.20	-12.83	-12.83
13.2	0.00	-487.77	-270.78		-270.78	-270.78	0.22	-0.15	-0.15	-0.15	-0.15	-0.15	-1.56	-1.56	-0.15	-0.15	-1.56	-1.56	-1.71	-1.71	0.22	0.22	-0.15	-0.15	-4.66	-4.66	-7.54	-7.54	-17.14	-17.14	-13.11	-13.11	-12.70	-12.70
14.4	0.00	-487.31	-274.28		-274.28	-274.28	0.21	-0.15	-0.15	-0.15	-0.15	-0.15	-1.55	-1.55	-0.15	-0.15	-1.55	-1.55	-1.69	-1.69	0.21	0.21	-0.15	-0.15	-4.71	-4.71	-7.48	-7.48	-16.91	-16.91	-13.20	-13.20	-12.83	-12.83
15.6	0.00	-487.52	-270.64		-270.64	-270.64	0.21	-0.15	-0.15	-0.15	-0.15	-0.15	-1.55	-1.55	-0.15	-0.15	-1.55	-1.55	-1.64	-1.64	0.21	0.21	-0.15	-0.15	-4.88	-4.88	-7.31	-7.31	-16.24	-16.24	-13.49	-13.49	-13.21	-13.21
16.8	0.00	-488.19	-259.96		-259.96	-259.96	0.18	-0.16	-0.16	-0.16	-0.16	-0.16	-1.43	-1.43	-0.16	-0.16	-1.43	-1.43	-1.55	-1.55	0.18	0.18	-0.16	-0.16	-5.16	-5.16	-7.02	-7.02	-15.13	-15.13	-13.97	-13.97	-13.85	-13.85
18	0.00	-497.35	-241.31		-241.31	-241.31	0.14	-0.18	-0.18	-0.18	-0.18	-0.18	-1.43	-1.43	-0.18	-0.18	-1.43	-1.43	-1.55	-1.55	0.14	0.14	-0.18	-0.18	-5.56	-5.56	-6.61	-6.61	-13.57	-13.57	-14.63	-14.63	-14.74	-14.74
19.2	0.00	-497.07	-214.79		-214.79	-214.79	0.07	-0.21	-0.21	-0.21	-0.21	-0.21	-1.32	-1.32	-0.21	-0.21	-1.32	-1.32	-1.28	-1.28	-0.07	-0.07	-0.21	-0.21	-6.07	-6.07	-6.08	-6.08	-11.57	-11.57	-15.49	-15.49	-15.89	-15.89
20.4	0.00	-503.80	-180.79		-180.79	-180.79	-0.01	-0.25	-0.25	-0.25	-0.25	-0.25	-1.19	-1.19	-0.25	-0.25	-1.19	-1.19	-1.28	-1.28	-0.01	-0.01	-0.25	-0.25	-6.69	-6.69	-5.44	-5.44	-19.43	-19.43	-14.92	-14.92	-14.47	-14.47
21.6	0.00	-513.34	-138.66		-138.66	-138.66	-0.12	-0.30	-0.30	-0.30	-0.30	-0.30	-1.02	-1.02	-0.30	-0.30	-1.02	-1.02	-1.09	-1.09	-0.12	-0.12	-0.30	-0.30	-7.43	-7.43	-6.67	-6.67	-19.27	-19.27	-14.66	-14.66	-14.19	-14.19
22.8	0.00	-525.00	-88.32		-88.32	-88.32	-0.24	-0.36	-0.36	-0.36	-0.36	-0.36	-0.82	-0.82	-0.36	-0.36	-0.82	-0.82	-0.86	-0.86	-0.24	-0.24	-0.36	-0.36	-8.27	-8.27	-3.79	-3.79	-18.63	-18.63	-14.58	-14.58	-14.18	-14.18
24	0.00	-538.11	-28.24		-28.24	-28.24	-0.39	-0.43	-0.43	-0.43	-0.43	-0.43	-0.58	-0.58	-0.43	-0.43	-0.58	-0.58	-0.59	-0.59	-0.39	-0.39	-0.43	-0.43	-11.23	-11.23	-0.97	-0.97	-19.55	-19.55	-12.89	-12.89	-12.22	-12.22
25.2	0.00	-550.97	70.81		70.81	70.81	-0.63	-0.54	-0.54	-0.54	-0.54	-0.54	-0.17	-0.17	-0.54	-0.54	-0.17	-0.17	-0.13	-0.13	-0.63	-0.63	-0.54	-0.54	-13.16	-13.16	0.84	0.84	-18.89	-18.89	-12.51	-12.51	-11.87	-11.87
26.4	0.00	-566.05	156.74		156.74	156.74	-0.84	-0.63	-0.63	-0.63	-0.63	-0.63	0.18	0.18	-0.63	-0.63	0.18	0.18	0.26	0.26	-0.84	-0.84	-0.63	-0.63	-14.00	-14.00	1.72	1.72	-16.58	-16.58	-13.36	-13.36	-13.04	-13.04
27.6	0.00	-578.03	228.24		228.24	228.24	-1.02	-0.71	-0.71	-0.71	-0.71	-0.71	0.47	0.47	-0.71	-0.71	0.47	0.47	0.58	0.58	-1.02	-1.02	-0.71	-0.71	-12.86	-12.86	0.88	0.88	-11.73	-11.73	-16.25	-16.25	-16.70	-16.70
28.8	0.00	-585.49	269.24		269.24	269.24	-1.12	-0.63	-0.63	-0.63	-0.63	-0.63	0.63	0.63	-0.63	-0.63	0.63	0.63	0.77	0.77	-1.12	-1.12	-0.63	-0.63	-13.50	-13.50	13.50	13.50	22.50	22.50	22.50	22.50	22.50	22.50
σ ≤ 0.45 fck							13.50	13.50	13.50	13.50	13.50	13.50	13.50	13.50	22.50	22.50	22.50	22.50	22.50	22.50	13.50	13.50	13.50	13.50	13.50	13.50	13.50	13.50	22.50	22.50	22.50	22.50	22.50	22.50

Δ [m²]	1.1772
S c.1 [m³]	-1.0255
S c.2 [m³]	0.2386
S c.3 [m³]	0.2124
S c.4 [m³]	-0.4353

Gross-Section 1		Support		Redirection		Midspan	
Position	Height	σ [MN/m²]	σ [MN/m²]	σ [MN/m²]	σ [MN/m²]	σ [MN/m²]	σ [MN/m²]
1 Slab		-1.12	-0.12	-0.12	-0.12	0.22	0.22
2 Slab		-0.76	-0.30	-0.30	-0.30	-0.15	-0.15
1 Precast		-11.74	-19.43	-19.43	-19.43	-17.14	-17.14
2 Precast		-16.24	-14.91	-14.91	-14.91	-13.11	-13.11
3 Precast		-16.69	-14.46	-14.46	-14.46	-12.70	-12.70



Gross-Section 2		Support		Redirection		Midspan	
Position	Height	σ [MN/m²]	σ [MN/m²]	σ [MN/m²]	σ [MN/m²]	σ [MN/m²]	σ [MN/m²]
1 Slab		-1.12	-0.12	-0.12	-0.12	0.22	0.22
2 Slab		-0.76	-0.30	-0.30	-0.30	-0.15	-0.15
1 In-Situ		-12.86	-19.43	-19.43	-19.43	-17.14	-17.14
2 In-Situ		-16.24	-14.91	-14.91	-14.91	-13.11	-13.11
3 Precast		-16.69	-14.46	-14.46	-14.46	-12.70	-12.70

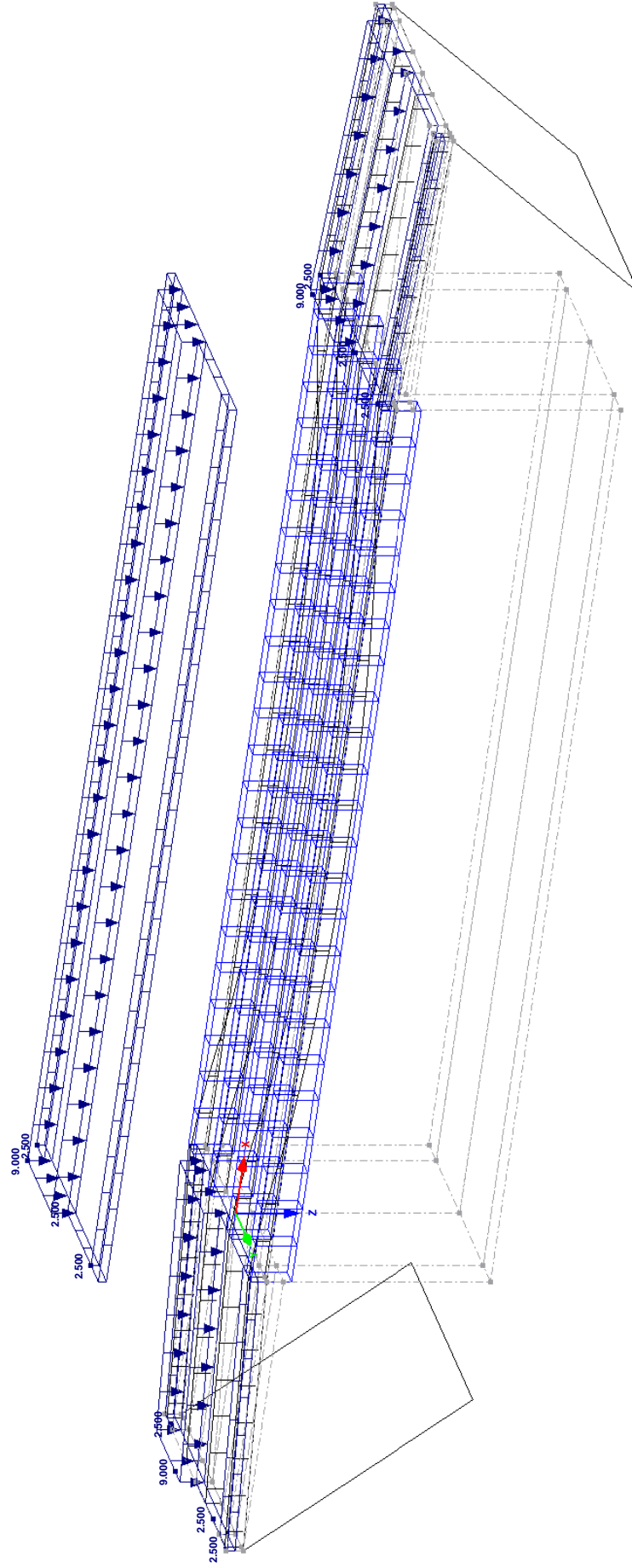
Project: **RFEM**

Structure: **3D\_Phase 5**

■ **LC1: LM1**

LC1: LM1

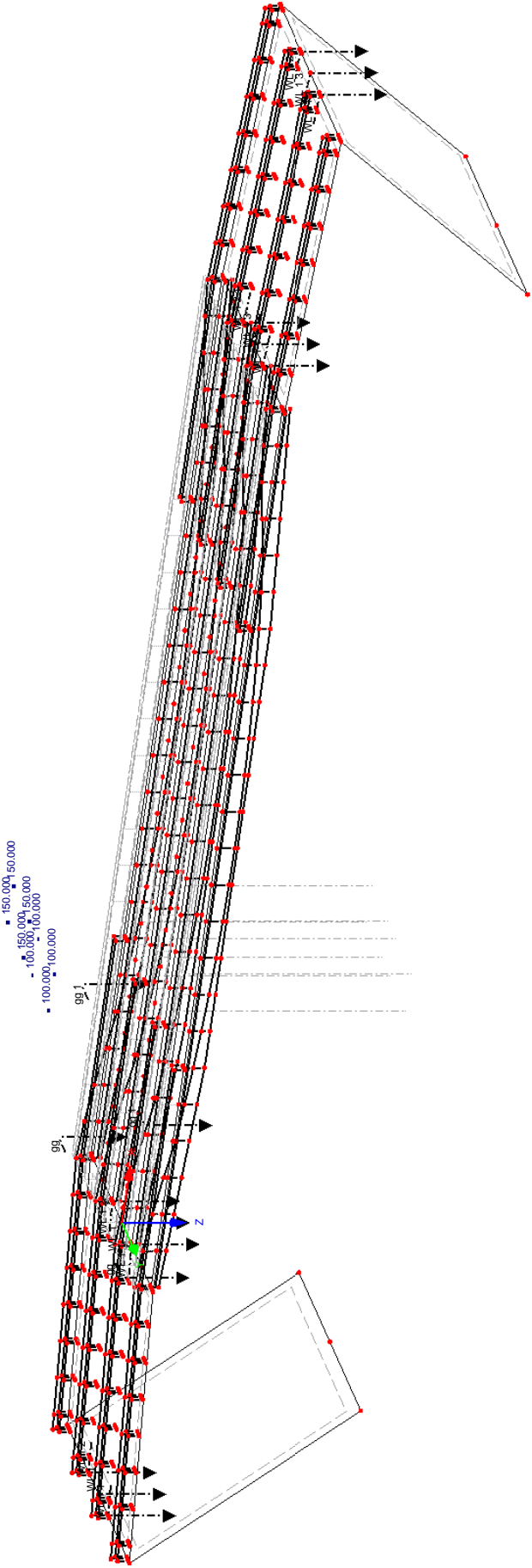
Isometric



Isometrie

■ LC18: Q LM1 POINT LOADS

LF18: Q LM1





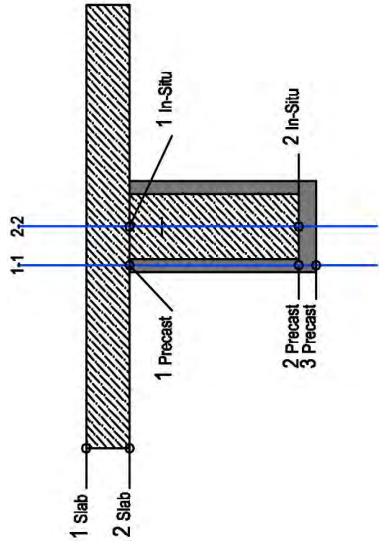
# Phase 5 LM1

Stresses Phase 5										Sum Stresses																		
Self Weight	Slab 1		Slab 2		In-Situ 1		In-Situ 2		Precast 1		Precast 2		Precast 3		Slab 1		Slab 2		In-Situ 1		In-Situ 2		Precast 1		Precast 2		Precast 3	
	σ Slab 1 [MN/m²]	σ Slab 1 [MN/m²]	σ Slab 2 [MN/m²]	σ Slab 2 [MN/m²]	σ In-Situ 1 [MN/m²]	σ In-Situ 1 [MN/m²]	σ In-Situ 2 [MN/m²]	σ In-Situ 2 [MN/m²]	σ Precast 1 [MN/m²]	σ Precast 1 [MN/m²]	σ Precast 2 [MN/m²]	σ Precast 2 [MN/m²]	σ Precast 3 [MN/m²]	σ Precast 3 [MN/m²]	Sum σ Slab 1	Sum σ Slab 2	Sum σ In-Situ 1	Sum σ In-Situ 2	Sum σ Precast 1	Sum σ Precast 2	Sum σ Precast 3							
0	-1219.30	2.80	1.19	1.19	1.19	1.19	-5.11	-5.11	1.19	-5.11	-5.11	-5.11	-5.74	-5.74	1.68	0.43	-11.67	-4.23	-10.55	-21.35	-22.43							
1.2	-816.42	1.88	0.80	0.80	0.80	0.80	-3.42	-3.42	0.80	-3.42	-3.42	-3.42	-3.84	-3.84	0.86	0.08	-13.29	-1.67	-15.88	-16.74	-16.83							
2.4	800.52	-1.84	-0.78	-0.78	-0.78	-0.78	3.35	3.35	-0.78	3.35	3.35	3.35	3.77	3.77	-1.62	-1.41	-13.99	4.21	-19.73	-9.13	-8.07							
3.6	1134.14	-2.61	-1.11	-1.11	-1.11	-1.11	4.75	4.75	-1.11	4.75	4.75	4.75	5.34	5.34	-1.73	-1.41	-12.38	3.79	-20.71	-8.13	-7.45							
4.8	1422.13	-3.27	-1.39	-1.39	-1.39	-1.39	5.96	5.96	-1.39	5.96	5.96	5.96	6.69	6.69	-1.78	-1.82	-9.60	2.21	-19.97	-8.58	-7.45							
6	1665.78	-3.83	-1.62	-1.62	-1.62	-1.62	6.98	6.98	-1.62	6.98	6.98	6.98	7.84	7.84	-1.87	-1.99	-9.05	2.31	-20.89	-7.66	-6.34							
7.2	1868.65	-4.29	-1.82	-1.82	-1.82	-1.82	7.83	7.83	-1.82	7.83	7.83	7.83	8.80	8.80	-4.41	-2.12	-8.52	2.40	-21.25	-7.08	-5.66							
8.4	2034.20	-4.67	-1.98	-1.98	-1.98	-1.98	8.52	8.52	-1.98	8.52	8.52	8.52	9.58	9.58	-4.69	-2.24	-8.06	2.45	-13.55	-6.96	-6.30							
9.6	2165.26	-4.97	-2.11	-2.11	-2.11	-2.11	9.07	9.07	-2.11	9.07	9.07	9.07	10.19	10.19	-2.07	-2.32	-7.67	2.47	-15.69	-5.55	-4.54							
10.8	2264.30	-5.20	-2.21	-2.21	-2.21	-2.21	9.49	9.49	-2.21	9.49	9.49	9.49	10.66	10.66	-2.07	-2.39	-7.38	2.48	-17.34	-4.47	-3.18							
12	2333.61	-5.36	-2.28	-2.28	-2.28	-2.28	9.78	9.78	-2.28	9.78	9.78	9.78	10.98	10.98	-2.09	-2.44	-7.16	2.47	-18.52	-3.71	-2.22							
13.2	2374.67	-5.46	-2.32	-2.32	-2.32	-2.32	9.95	9.95	-2.32	9.95	9.95	9.95	11.18	11.18	-2.11	-2.47	-7.03	2.47	-19.23	-3.25	-1.65							
14.4	2388.10	-5.49	-2.33	-2.33	-2.33	-2.33	10.01	10.01	-2.33	10.01	10.01	10.01	11.24	11.24	-2.11	-2.48	-6.99	2.47	-19.46	-3.10	-1.46							
15.6	2374.79	-5.46	-2.32	-2.32	-2.32	-2.32	9.95	9.95	-2.32	9.95	9.95	9.95	11.18	11.18	-2.10	-2.47	-7.03	2.47	-19.23	-3.25	-1.65							
16.8	2338.04	-5.37	-2.28	-2.28	-2.28	-2.28	9.80	9.80	-2.28	9.80	9.80	9.80	11.01	11.01	-2.10	-2.44	-7.16	2.49	-18.52	-3.69	-2.21							
18	2272.42	-5.22	-2.22	-2.22	-2.22	-2.22	9.52	9.52	-2.22	9.52	9.52	9.52	10.70	10.70	-2.08	-2.40	-7.38	2.51	-17.34	-4.44	-3.15							
19.2	2174.79	-5.00	-2.12	-2.12	-2.12	-2.12	9.11	9.11	-2.12	9.11	9.11	9.11	10.24	10.24	-2.05	-2.33	-7.68	2.51	-15.69	-5.52	-4.50							
20.4	2044.35	-4.70	-1.99	-1.99	-1.99	-1.99	8.57	8.57	-1.99	8.57	8.57	8.57	9.62	9.62	-2.01	-2.25	-8.06	2.49	-13.56	-6.93	-6.26							
21.6	1878.62	-4.32	-1.83	-1.83	-1.83	-1.83	7.87	7.87	-1.83	7.87	7.87	7.87	8.84	8.84	-4.43	-2.13	-8.53	2.44	-21.26	-7.05	-5.63							
22.8	1674.95	-3.85	-1.63	-1.63	-1.63	-1.63	7.02	7.02	-1.63	7.02	7.02	7.02	7.88	7.88	-4.09	-1.99	-9.06	2.34	-20.90	-7.64	-6.31							
24	1430.62	-3.29	-1.40	-1.40	-1.40	-1.40	6.00	6.00	-1.40	6.00	6.00	6.00	6.73	6.73	-1.79	-1.82	-9.67	2.21	-20.03	-8.59	-7.45							
25.2	1142.35	-2.62	-1.11	-1.11	-1.11	-1.11	4.79	4.79	-1.11	4.79	4.79	4.79	5.38	5.38	-1.74	-1.65	-12.34	3.81	-20.67	-8.10	-6.85							
26.4	808.18	-1.86	-0.79	-0.79	-0.79	-0.79	3.39	3.39	-0.79	3.39	3.39	3.39	3.80	3.80	-1.63	-1.42	-13.94	4.23	-19.68	-9.12	-8.06							
27.6	-816.66	1.88	0.80	0.80	0.80	0.80	-3.42	-3.42	0.80	-3.42	-3.42	-3.42	-3.84	-3.84	-0.22	0.08	-13.20	-1.70	-15.78	-16.78	-16.88							
28.8	-1218.00	2.80	1.19	1.19	1.19	1.19	-5.10	-5.10	1.19	-5.10	-5.10	-5.10	-5.73	-5.73	1.68	0.43	-11.67	-4.22	-10.54	-21.35	-22.43							
σ < 0.60 fck	18.00	18.00	18.00	18.00	18.00	18.00	18.00	18.00	30.00	30.00	30.00	30.00	30.00	30.00	18.00	18.00	18.00	18.00	30.00	30.00	30.00							

σ Max	4.23
σ min	-22.43
< 0.45 fck	

Cross-Section 1			
Position	Support	Redirection	Midspan
Height	σ [MN/m²]	σ [MN/m²]	σ [MN/m²]
1 Slab	1.68	-4.41	-5.27
2 Slab	0.43	-2.12	-2.48
1 Precast	-10.55	-21.25	-19.46
2 Precast	-21.35	-7.08	-3.10
3 Precast	-22.43	-5.66	-1.46

Cross-Section 2			
Position	Support	Redirection	Midspan
Height	σ [MN/m²]	σ [MN/m²]	σ [MN/m²]
1 Slab	1.68	-4.41	-5.27
2 Slab	0.43	-2.12	-2.48
1 In-Situ	-11.67	-8.52	-6.99
2 In-Situ	-4.23	2.40	2.47
2 Precast	-21.35	-7.08	-3.10
3 Precast	-22.43	-5.66	-1.46





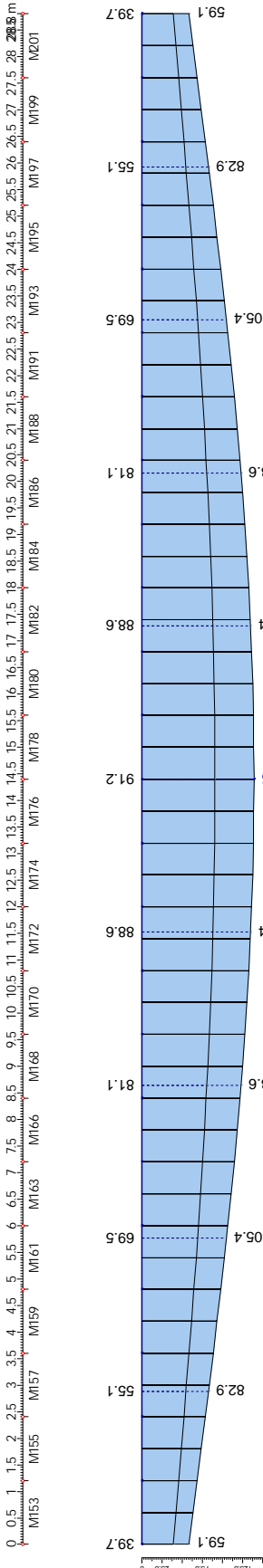
RESULT DIAGRAMS FOR CONTINUOUS MEMBERS - SM1

RFEM

LC3: ULS g+q

Deformation - u-z

	x [m]	u-z [mm]
max	14.400	139.5
min	--	--

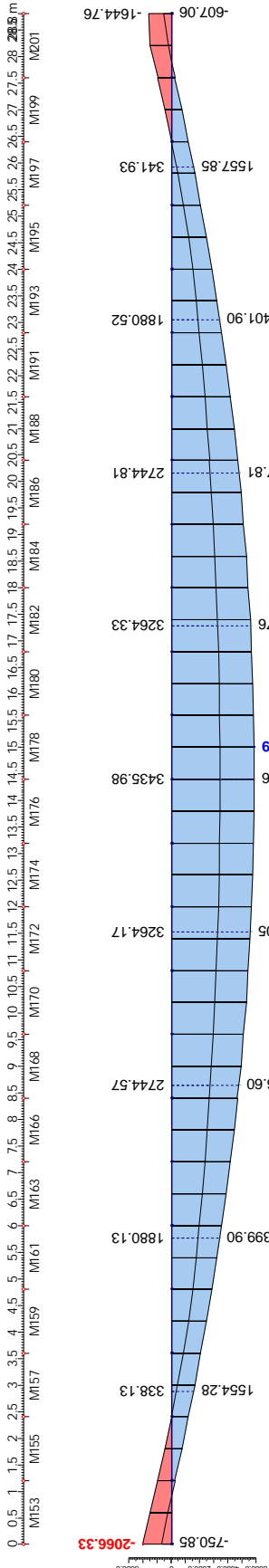


RFEM

LC3: ULS g+q

Internal forces - M-y

	x [m]	M-y [kNm]
max	15.000	5859.39
min	0.000	-2066.33

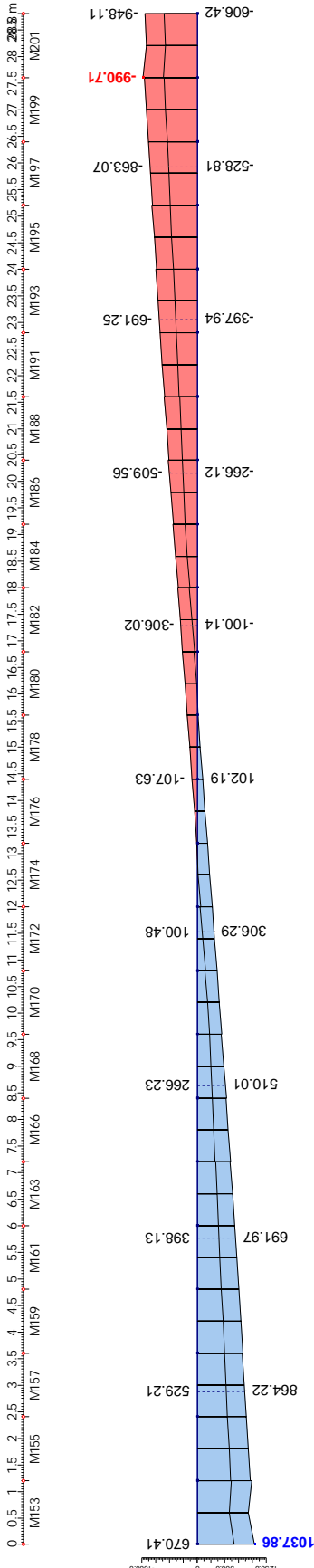


RFEM

LC3: ULS g+q

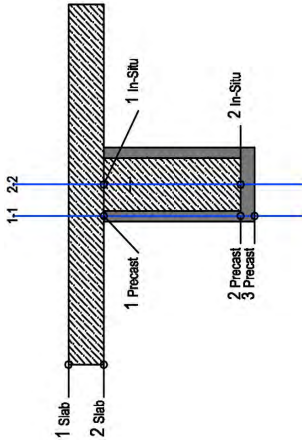
Internal forces - V-z

	x [m]	V-z [kN]
max	0.000	1037.86
min	28.200	-990.71



Phase 4 Falsework

Pre-Stressed Factor			1		Stresses Phase 4																Sum Stresses				Precast 3			
P	Self Weight	Pre-Stress	Stress P	Slab 1	Slab 2	In-Situ 1	In-Situ 2	Precast 1	Precast 2	Precast 3	Slab 1	Slab 2	In-Situ 1	In-Situ 2	Sum σ Precast 1	Sum σ Precast 2	Sum σ Precast 3	Sum σ In-Situ 1	Sum σ In-Situ 2	Precast 1	Precast 2	Precast 3	Sum σ Precast 1	Sum σ Precast 2	Sum σ Precast 3	Sum σ In-Situ 1	Sum σ In-Situ 2	
σ	M (kN.m)	N (mm²)	M (kN.m)	σ Slab 1 (MPa)	σ Slab 2 (MPa)	σ In-Situ 1 (MPa)	σ In-Situ 2 (MPa)	σ Precast 1 (MPa)	σ Precast 2 (MPa)	σ Precast 3 (MPa)	σ Slab 1 (MPa)	σ Slab 2 (MPa)	σ In-Situ 1 (MPa)	σ In-Situ 2 (MPa)	σ Precast 1 (MPa)	σ Precast 2 (MPa)	σ Precast 3 (MPa)	σ Slab 1 (MPa)	σ Slab 2 (MPa)	σ In-Situ 1 (MPa)	σ In-Situ 2 (MPa)	σ Precast 1 (MPa)	σ Precast 2 (MPa)	σ Precast 3 (MPa)	σ Slab 1 (MPa)	σ Slab 2 (MPa)	σ In-Situ 1 (MPa)	σ In-Situ 2 (MPa)
0	-797.44	-6033.35	2047.29	-8.00	-6.34	-6.34	0.11	-6.34	0.11	0.76	-8.00	-6.34	-6.34	0.11	-6.34	0.11	0.76	-8.00	-6.34	-6.34	0.11	-6.34	0.11	0.76	-8.00	-6.34	-6.34	0.11
1.2	-206.80	-5973.34	1656.96	-8.41	-6.49	-6.49	1.01	-6.49	1.01	1.76	-8.41	-6.49	-6.49	1.01	-6.49	1.01	1.76	-8.41	-6.49	-6.49	1.01	-6.49	1.01	1.76	-8.41	-6.49	-6.49	1.01
2.4	-348.85	-5903.20	1080.34	-8.30	-6.41	-6.41	0.97	-6.41	0.97	1.71	-8.30	-6.41	-6.41	0.97	-6.41	0.97	1.71	-8.30	-6.41	-6.41	0.97	-6.41	0.97	1.71	-8.30	-6.41	-6.41	0.97
3.6	-854.99	-5800.85	400.28	-7.81	-6.15	-6.15	0.33	-6.15	0.33	0.98	-7.81	-6.15	-6.15	0.33	-6.15	0.33	0.98	-7.81	-6.15	-6.15	0.33	-6.15	0.33	0.98	-7.81	-6.15	-6.15	0.33
4.8	1313.65	-5698.80	-371.85	-7.00	-5.76	-5.76	-0.89	-5.76	-0.89	-0.41	-7.00	-5.76	-5.76	-0.89	-5.76	-0.89	-0.41	-7.00	-5.76	-5.76	-0.89	-5.76	-0.89	-0.41	-7.00	-5.76	-5.76	-0.89
6	1715.15	-5584.10	-893.53	-6.65	-5.55	-5.55	-1.26	-5.55	-1.26	-0.83	-6.65	-5.55	-5.55	-1.26	-5.55	-1.26	-0.83	-6.65	-5.55	-5.55	-1.26	-5.55	-1.26	-0.83	-6.65	-5.55	-5.55	-1.26
7.2	2070.21	-5421.71	-1344.80	-6.27	-5.31	-5.31	-1.57	-5.31	-1.57	-1.19	-6.27	-5.31	-5.31	-1.57	-5.31	-1.57	-1.19	-6.27	-5.31	-5.31	-1.57	-5.31	-1.57	-1.19	-6.27	-5.31	-5.31	-1.57
8.4	2363.84	-4884.70	-1665.18	-5.75	-4.83	-4.83	-1.22	-4.83	-1.22	-0.86	-5.75	-4.83	-4.83	-1.22	-4.83	-1.22	-0.86	-5.75	-4.83	-4.83	-1.22	-4.83	-1.22	-0.86	-5.75	-4.83	-4.83	-1.22
9.6	2605.64	-4817.87	-1903.04	-5.71	-4.78	-4.78	-1.15	-4.78	-1.15	-0.79	-5.71	-4.78	-4.78	-1.15	-4.78	-1.15	-0.79	-5.71	-4.78	-4.78	-1.15	-4.78	-1.15	-0.79	-5.71	-4.78	-4.78	-1.15
10.8	2794.98	-4762.02	-2089.30	-5.67	-4.73	-4.73	-1.09	-4.73	-1.09	-0.72	-5.67	-4.73	-4.73	-1.09	-4.73	-1.09	-0.72	-5.67	-4.73	-4.73	-1.09	-4.73	-1.09	-0.72	-5.67	-4.73	-4.73	-1.09
12	2928.87	-4728.43	-2220.54	-5.64	-4.71	-4.71	-1.05	-4.71	-1.05	-0.68	-5.64	-4.71	-4.71	-1.05	-4.71	-1.05	-0.68	-5.64	-4.71	-4.71	-1.05	-4.71	-1.05	-0.68	-5.64	-4.71	-4.71	-1.05
13.2	3009.56	-4709.07	-2298.17	-5.63	-4.69	-4.69	-1.02	-4.69	-1.02	-0.66	-5.63	-4.69	-4.69	-1.02	-4.69	-1.02	-0.66	-5.63	-4.69	-4.69	-1.02	-4.69	-1.02	-0.66	-5.63	-4.69	-4.69	-1.02
14.4	3036.76	-4702.89	-2325.49	-5.63	-4.69	-4.69	-1.01	-4.69	-1.01	-0.65	-5.63	-4.69	-4.69	-1.01	-4.69	-1.01	-0.65	-5.63	-4.69	-4.69	-1.01	-4.69	-1.01	-0.65	-5.63	-4.69	-4.69	-1.01
15.6	3009.74	-4710.21	-2299.23	-5.63	-4.69	-4.69	-1.02	-4.69	-1.02	-0.66	-5.63	-4.69	-4.69	-1.02	-4.69	-1.02	-0.66	-5.63	-4.69	-4.69	-1.02	-4.69	-1.02	-0.66	-5.63	-4.69	-4.69	-1.02
16.8	2928.76	-4729.59	-2290.99	-5.64	-4.71	-4.71	-1.05	-4.71	-1.05	-0.69	-5.64	-4.71	-4.71	-1.05	-4.71	-1.05	-0.69	-5.64	-4.71	-4.71	-1.05	-4.71	-1.05	-0.69	-5.64	-4.71	-4.71	-1.05
18	2794.24	-4761.09	-2090.63	-5.66	-4.73	-4.73	-1.10	-4.73	-1.10	-0.73	-5.66	-4.73	-4.73	-1.10	-4.73	-1.10	-0.73	-5.66	-4.73	-4.73	-1.10	-4.73	-1.10	-0.73	-5.66	-4.73	-4.73	-1.10
19.2	2604.94	-4816.55	-1904.67	-5.70	-4.77	-4.77	-1.16	-4.77	-1.16	-0.80	-5.70	-4.77	-4.77	-1.16	-4.77	-1.16	-0.80	-5.70	-4.77	-4.77	-1.16	-4.77	-1.16	-0.80	-5.70	-4.77	-4.77	-1.16
20.4	2365.15	-4889.79	-1664.98	-5.76	-4.84	-4.84	-1.22	-4.84	-1.22	-0.86	-5.76	-4.84	-4.84	-1.22	-4.84	-1.22	-0.86	-5.76	-4.84	-4.84	-1.22	-4.84	-1.22	-0.86	-5.76	-4.84	-4.84	-1.22
21.6	2065.42	-5055.40	-1345.05	-6.04	-4.99	-4.99	-1.29	-4.99	-1.29	-0.92	-6.04	-4.99	-4.99	-1.29	-4.99	-1.29	-0.92	-6.04	-4.99	-4.99	-1.29	-4.99	-1.29	-0.92	-6.04	-4.99	-4.99	-1.29
22.8	1714.86	-5582.31	-882.97	-6.65	-5.55	-5.55	-1.26	-5.55	-1.26	-0.83	-6.65	-5.55	-5.55	-1.26	-5.55	-1.26	-0.83	-6.65	-5.55	-5.55	-1.26	-5.55	-1.26	-0.83	-6.65	-5.55	-5.55	-1.26
24	1311.61	-5687.15	-371.02	-7.00	-5.76	-5.76	-0.90	-5.76	-0.90	-0.41	-7.00	-5.76	-5.76	-0.90	-5.76	-0.90	-0.41	-7.00	-5.76	-5.76	-0.90	-5.76	-0.90	-0.41	-7.00	-5.76	-5.76	-0.90
25.2	852.92	-5798.61	400.63	-7.81	-6.15	-6.15	0.33	-6.15	0.33	0.97	-7.81	-6.15	-6.15	0.33	-6.15	0.33	0.97	-7.81	-6.15	-6.15	0.33	-6.15	0.33	0.97	-7.81	-6.15	-6.15	0.33
26.4	348.35	-5901.60	1081.41	-8.30	-6.41	-6.41	0.98	-6.41	0.98	1.72	-8.30	-6.41	-6.41	0.98	-6.41	0.98	1.72	-8.30	-6.41	-6.41	0.98	-6.41	0.98	1.72	-8.30	-6.41	-6.41	0.98
27.6	-200.21	-5973.63	1662.14	-8.43	-6.50	-6.50	1.05	-6.50	1.05	1.81	-8.43	-6.50	-6.50	1.05	-6.50	1.05	1.81	-8.43	-6.50	-6.50	1.05	-6.50	1.05	1.81	-8.43	-6.50	-6.50	1.05
28.8	-797.44	-6033.35	2047.29	-8.00	-6.34	-6.34	0.11	-6.34	0.11	0.76	-8.00	-6.34	-6.34	0.11	-6.34	0.11	0.76	-8.00	-6.34	-6.34	0.11	-6.34	0.11	0.76	-8.00	-6.34	-6.34	0.11
σ ≤ 0.45 fck				13.50	13.50	13.50	13.50	22.50	22.50	22.50	13.50	13.50	13.50	13.50	22.50	22.50	22.50	13.50	13.50	13.50	13.50	22.50	22.50	22.50	13.50	13.50	13.50	13.50
σ Max				1.81	1.81	1.81	1.81	1.81	1.81	1.81	1.81	1.81	1.81	1.81	1.81	1.81	1.81	1.81	1.81	1.81	1.81	1.81	1.81	1.81	1.81	1.81	1.81	1.81
σ min				< 0.45 fck	< 0.45 fck	< 0.45 fck	< 0.45 fck	< 0.45 fck	< 0.45 fck	< 0.45 fck	< 0.45 fck	< 0.45 fck	< 0.45 fck	< 0.45 fck	< 0.45 fck	< 0.45 fck	< 0.45 fck	< 0.45 fck	< 0.45 fck	< 0.45 fck	< 0.45 fck	< 0.45 fck	< 0.45 fck	< 0.45 fck	< 0.45 fck	< 0.45 fck	< 0.45 fck	



A [m²]	1.1772
S.c.1 [m²]	-1.0255
S.c.2 [m²]	0.2396
S.c.3 [m²]	0.2124
S.c.4 [m²]	-0.4333

Cross-Section 1			
Position	Support	Redirection	Mispan
1 Slab	σ [MN/m²]	σ [MN/m²]	σ [MN/m²]
2 Slab	-8.00	-6.27	-5.63
1 Precast	-6.34	-5.31	-4.69
2 Precast	0.11	-1.57	-1.01
3 Precast	0.76	-1.19	-0.65

Cross-Section 2			
Position	Support	Redirection	Mispan
1 Slab	σ [MN/m²]	σ [MN/m²]	σ [MN/m²]
2 Slab	-8.00	-6.27	-5.63
1 Precast	-6.34	-5.31	-4.69
2 Precast	0.11	-1.57	-1.01
3 Precast	0.76	-1.19	-0.65

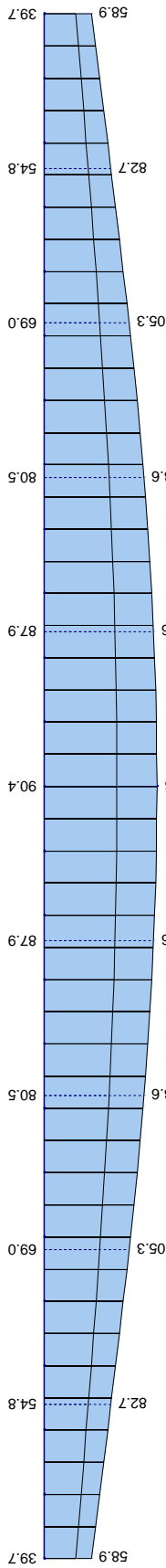
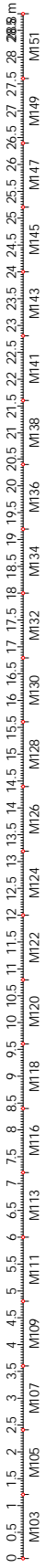
RESULT DIAGRAMS FOR CONTINUOUS MEMBERS - SM2

RFEM

LC3: ULS g+q

Deformation - u-z

x		u-z
[m]		[mm]
max	14.400	139.6
min	--	--

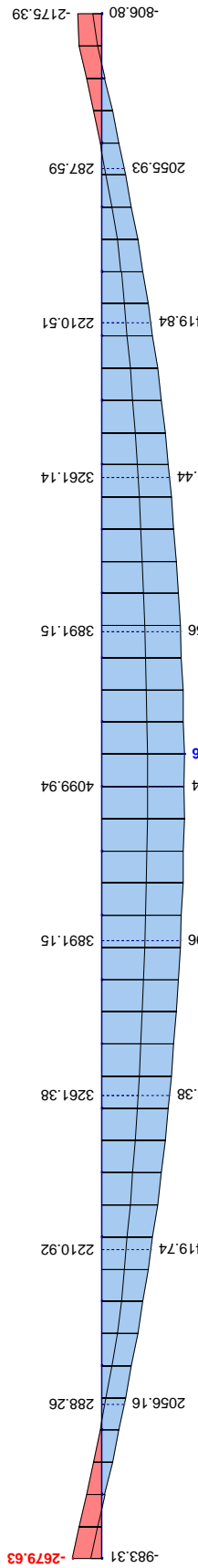
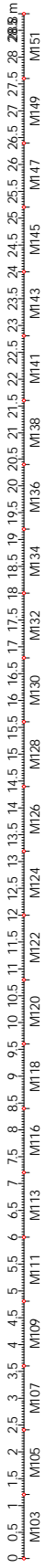


RFEM

LC3: ULS g+q

Internal forces - M-y

x		M-y
[m]		[kNm]
max	15.000	73977.6
min	0.000	-2679.63

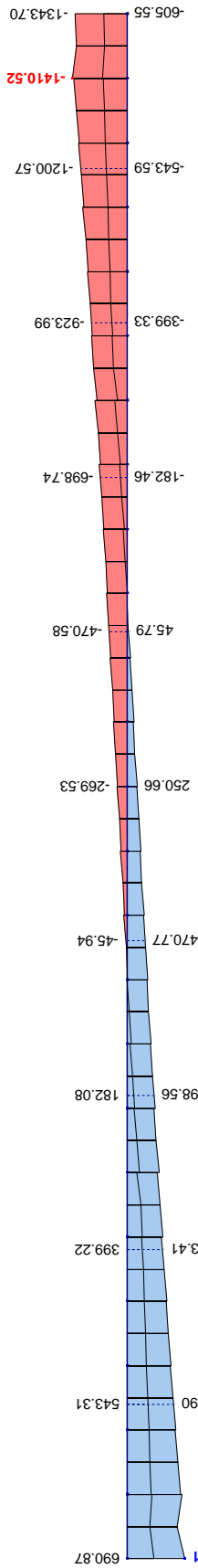
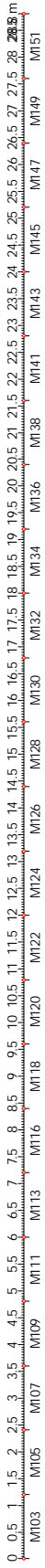


RFEM

LC3: ULS g+q

Internal forces - V-z

x		V-z
[m]		[kN]
max	0.000	1493.81
min	28.200	-1410.52



Phase 5 Falsework (LM1)

Stresses Phase 5														
x	Self Weight		Slab 1		Slab 2		In-Situ 1		In-Situ 2		Precast 1		Precast 2	
	M.g		σ Slab 1 [MN/m²]	σ Slab 1 [MN/m²]	σ Slab 2 [MN/m²]	σ Slab 2 [MN/m²]	σ In-Situ 1 [MN/m²]	σ In-Situ 1 [MN/m²]	σ In-Situ 2 [MN/m²]	σ In-Situ 2 [MN/m²]	σ Precast 1 [MN/m²]	σ Precast 1 [MN/m²]	σ Precast 2 [MN/m²]	σ Precast 2 [MN/m²]
0	-1219.30		2.80	1.19	1.19	1.19	1.19	1.19	-5.11	-5.11	1.19	1.19	-5.11	-5.11
1.2	-816.42		1.88	0.80	0.80	0.80	0.80	0.80	-3.42	-3.42	0.80	0.80	-3.42	-3.42
2.4	-800.52		-1.84	-0.78	-0.78	-0.78	-0.78	-0.78	3.35	3.35	-0.78	-0.78	3.35	3.35
3.6	-1134.14		-2.61	-1.11	-1.11	-1.11	-1.11	-1.11	4.75	4.75	-1.11	-1.11	4.75	4.75
4.8	-1422.13		-3.27	-1.39	-1.39	-1.39	-1.39	-1.39	5.96	5.96	-1.39	-1.39	5.96	5.96
6	-1665.78		-3.93	-1.62	-1.62	-1.62	-1.62	-1.62	6.98	6.98	-1.62	-1.62	6.98	6.98
7.2	-1868.65		-4.29	-1.82	-1.82	-1.82	-1.82	-1.82	7.83	7.83	-1.82	-1.82	7.83	7.83
8.4	-2034.20		-4.67	-1.98	-1.98	-1.98	-1.98	-1.98	8.52	8.52	-1.98	-1.98	8.52	8.52
9.6	-2165.26		-4.97	-2.11	-2.11	-2.11	-2.11	-2.11	9.07	9.07	-2.11	-2.11	9.07	9.07
10.8	-2284.30		-5.20	-2.21	-2.21	-2.21	-2.21	-2.21	9.49	9.49	-2.21	-2.21	9.49	9.49
12	-2333.61		-5.36	-2.28	-2.28	-2.28	-2.28	-2.28	9.78	9.78	-2.28	-2.28	9.78	9.78
13.2	-2374.67		-5.46	-2.32	-2.32	-2.32	-2.32	-2.32	9.95	9.95	-2.32	-2.32	9.95	9.95
14.4	-2388.10		-5.49	-2.33	-2.33	-2.33	-2.33	-2.33	10.01	10.01	-2.33	-2.33	10.01	10.01
15.6	-2374.79		-5.46	-2.32	-2.32	-2.32	-2.32	-2.32	9.95	9.95	-2.32	-2.32	9.95	9.95
16.8	-2338.04		-5.37	-2.28	-2.28	-2.28	-2.28	-2.28	9.80	9.80	-2.28	-2.28	9.80	9.80
18	-2272.42		-5.22	-2.22	-2.22	-2.22	-2.22	-2.22	9.52	9.52	-2.22	-2.22	9.52	9.52
19.2	-2174.79		-5.00	-2.12	-2.12	-2.12	-2.12	-2.12	9.11	9.11	-2.12	-2.12	9.11	9.11
20.4	-2044.35		-4.70	-1.99	-1.99	-1.99	-1.99	-1.99	8.57	8.57	-1.99	-1.99	8.57	8.57
21.6	-1878.62		-4.32	-1.83	-1.83	-1.83	-1.83	-1.83	7.87	7.87	-1.83	-1.83	7.87	7.87
22.8	-1674.95		-3.85	-1.63	-1.63	-1.63	-1.63	-1.63	7.02	7.02	-1.63	-1.63	7.02	7.02
24	-1430.62		-3.29	-1.40	-1.40	-1.40	-1.40	-1.40	6.00	6.00	-1.40	-1.40	6.00	6.00
25.2	-1142.35		-2.62	-1.11	-1.11	-1.11	-1.11	-1.11	4.79	4.79	-1.11	-1.11	4.79	4.79
26.4	-808.18		-1.86	-0.79	-0.79	-0.79	-0.79	-0.79	3.39	3.39	-0.79	-0.79	3.39	3.39
27.6	-816.66		1.88	0.80	0.80	0.80	0.80	0.80	-3.42	-3.42	0.80	0.80	-3.42	-3.42
28.8	-1218.00		2.80	1.19	1.19	1.19	1.19	1.19	-5.10	-5.10	1.19	1.19	-5.10	-5.10
σ < 0.60 fck	18.00		18.00	18.00	18.00	18.00	18.00	18.00	18.00	18.00	30.00	30.00	30.00	30.00

Sum Stresses				
Slab 1	Slab 2	In-Situ 1	In-Situ 2	Precast 3
Sum σ Slab 1	Sum σ Slab 2	Sum σ In-Situ 1	Sum σ In-Situ 2	Sum σ Precast 3
-5.20	-5.15	-5.15	-5.00	-5.74
-6.93	-5.69	-5.69	-2.41	-3.84
-9.08	-7.19	-7.19	4.33	3.77
-8.92	-7.26	-7.26	5.09	5.34
-8.39	-7.15	-7.15	5.07	6.69
-8.28	-7.18	-7.18	5.72	7.84
-10.57	-7.14	-7.14	6.26	8.90
-10.43	-6.81	-6.81	7.30	9.58
-7.82	-6.89	-6.89	7.93	10.19
-7.87	-6.94	-6.94	8.40	10.66
-7.92	-6.98	-6.98	8.73	10.98
-7.95	-7.01	-7.01	8.93	11.18
-11.12	-7.02	-7.02	8.99	11.24
-11.09	-7.01	-7.01	8.93	11.18
-7.92	-6.99	-6.99	8.75	11.01
-7.88	-6.95	-6.95	8.43	10.70
-7.82	-6.90	-6.90	7.96	10.24
-7.76	-6.83	-6.83	7.35	9.62
-10.26	-6.83	-6.83	6.58	8.84
-7.19	-7.19	-7.19	5.76	7.88
-8.40	-7.15	-7.15	5.10	6.73
-8.92	-7.26	-7.26	5.11	5.38
-9.09	-7.20	-7.20	4.36	3.80
-7.64	-5.70	-5.70	-2.37	-3.84
-5.20	-5.16	-5.16	-4.99	-5.73
18.00	18.00	18.00	18.00	30.00

Sum Stresses				
Precast 1	Precast 2	In-Situ 1	In-Situ 2	Precast 3
Sum σ Precast 1	Sum σ Precast 2	Sum σ In-Situ 1	Sum σ In-Situ 2	Sum σ Precast 3
-5.15	-5.00	-5.15	-5.00	-5.74
-5.69	-2.41	-5.69	-2.41	-3.84
-7.19	4.33	-7.19	4.33	3.77
-7.26	5.09	-7.26	5.09	5.34
-7.15	5.07	-7.15	5.07	6.69
-7.18	5.72	-7.18	5.72	7.84
-7.14	6.26	-7.14	6.26	8.90
-6.81	7.30	-6.81	7.30	9.58
-6.89	7.93	-6.89	7.93	10.19
-6.94	8.40	-6.94	8.40	10.66
-6.98	8.73	-6.98	8.73	10.98
-7.01	8.93	-7.01	8.93	11.18
-7.02	8.99	-7.02	8.99	11.24
-7.01	8.93	-7.01	8.93	11.18
-6.99	8.75	-6.99	8.75	11.01
-6.95	8.43	-6.95	8.43	10.70
-6.90	7.96	-6.90	7.96	10.24
-6.83	7.35	-6.83	7.35	9.62
-6.83	6.58	-6.83	6.58	8.84
-7.19	5.76	-7.19	5.76	7.88
-7.15	5.10	-7.15	5.10	6.73
-7.26	5.11	-7.26	5.11	5.38
-7.20	4.36	-7.20	4.36	3.80
-5.70	-2.37	-5.70	-2.37	-3.84
-5.16	-4.99	-5.16	-4.99	-5.73
30.00	30.00	30.00	30.00	30.00

Sum Stresses				
Precast 1	Precast 2	In-Situ 1	In-Situ 2	Precast 3
Sum σ Precast 1	Sum σ Precast 2	Sum σ In-Situ 1	Sum σ In-Situ 2	Sum σ Precast 3
-5.15	-5.00	-5.15	-5.00	-5.74
-5.69	-2.41	-5.69	-2.41	-3.84
-7.19	4.33	-7.19	4.33	3.77
-7.26	5.09	-7.26	5.09	5.34
-7.15	5.07	-7.15	5.07	6.69
-7.18	5.72	-7.18	5.72	7.84
-7.14	6.26	-7.14	6.26	8.90
-6.81	7.30	-6.81	7.30	9.58
-6.89	7.93	-6.89	7.93	10.19
-6.94	8.40	-6.94	8.40	10.66
-6.98	8.73	-6.98	8.73	10.98
-7.01	8.93	-7.01	8.93	11.18
-7.02	8.99	-7.02	8.99	11.24
-7.01	8.93	-7.01	8.93	11.18
-6.99	8.75	-6.99	8.75	11.01
-6.95	8.43	-6.95	8.43	10.70
-6.90	7.96	-6.90	7.96	10.24
-6.83	7.35	-6.83	7.35	9.62
-6.83	6.58	-6.83	6.58	8.84
-7.19	5.76	-7.19	5.76	7.88
-7.15	5.10	-7.15	5.10	6.73
-7.26	5.11	-7.26	5.11	5.38
-7.20	4.36	-7.20	4.36	3.80
-5.70	-2.37	-5.70	-2.37	-3.84
-5.16	-4.99	-5.16	-4.99	-5.73
30.00	30.00	30.00	30.00	30.00

Sum Stresses				
Precast 1	Precast 2	In-Situ 1	In-Situ 2	Precast 3
Sum σ Precast 1	Sum σ Precast 2	Sum σ In-Situ 1	Sum σ In-Situ 2	Sum σ Precast 3
-5.15	-5.00	-5.15	-5.00	-5.74
-5.69	-2.41	-5.69	-2.41	-3.84
-7.19	4.33	-7.19	4.33	3.77
-7.26	5.09	-7.26	5.09	5.34
-7.15	5.07	-7.15	5.07	6.69
-7.18	5.72	-7.18	5.72	7.84
-7.14	6.26	-7.14	6.26	8.90
-6.81	7.30	-6.81	7.30	9.58
-6.89	7.93	-6.89	7.93	10.19
-6.94	8.40	-6.94	8.40	10.66
-6.98	8.73	-6.98	8.73	10.98
-7.01	8.93	-7.01	8.93	11.18
-7.02	8.99	-7.02	8.99	11.24
-7.01	8.93	-7.01	8.93	11.18
-6.99	8.75	-6.99	8.75	11.01
-6.95	8.43	-6.95	8.43	10.70
-6.90	7.96	-6.90	7.96	10.24
-6.83	7.35	-6.83	7.35	9.62
-6.83	6.58	-6.83	6.58	8.84
-7.19	5.76	-7.19	5.76	7.88
-7.15	5.10	-7.15	5.10	6.73
-7.26	5.11	-7.26	5.11	5.38
-7.20	4.36	-7.20	4.36	3.80
-5.70	-2.37	-5.70	-2.37	-3.84
-5.16	-4.99	-5.16	-4.99	-5.73
30.00	30.00	30.00	30.00	30.00

Sum Stresses				
Precast 1	Precast 2	In-Situ 1	In-Situ 2	Precast 3
Sum σ Precast 1	Sum σ Precast 2	Sum σ In-Situ 1	Sum σ In-Situ 2	Sum σ Precast 3
-5.15	-5.00	-5.15	-5.00	-5.74
-5.69	-2.41	-5.69	-2.41	-3.84
-7.19	4.33	-7.19	4.33	3.77
-7.26	5.09	-7.26	5.09	5.34
-7.15	5.07	-7.15	5.07	6.69
-7.18	5.72	-7.18	5.72	7.84
-7.14	6.26	-7.14	6.26	8.90
-6.81	7.30	-6.81	7.30	9.58
-6.89	7.93	-6.89	7.93	10.19
-6.94	8.40	-6.94	8.40	10.66
-6.98	8.73	-6.98	8.73	10.98
-7.01	8.93	-7.01	8.93	11.18
-7.02	8.99	-7.02	8.99	11.24
-7.01	8.93	-7.01	8.93	11.18
-6.99	8.75	-6.99	8.75	11.01
-6.95	8.43	-6.95	8.43	10.70
-6.90	7.96	-6.90	7.96	10.24
-6.83	7.35	-6.83	7.35	9.62
-6.83	6.58	-6.83	6.58	8.84
-7.19	5.76	-7.19	5.76	7.88
-7.15	5.10	-7.15	5.10	6.73
-7.26	5.11	-7.26	5.11	5.38
-7.20	4.36	-7.20	4.36	3.80
-5.70	-2.37	-5.70	-2.37	-3.84
-5.16	-4.99	-5.16	-4.99	-5.73
30.00	30.00	30.00	30.00	30.00

σ Max	10.59
σ min	-11.12
	< 0.45 fck

Cross-Section 1			
Position	Support	Redirection	Midspan
Height			
1 Slab	σ [MN/m²]	σ [MN/m²]	σ [MN/m²]
2 Slab	-5.20	-10.57	-11.12
1 Precast	-5.15	-7.14	-7.02
2 Precast	-5.00	6.26	8.99
3 Precast	-4.98	7.60	10.59

A [m²]	1.1772
S c.1 [m³]	-1.0255
S c.2 [m³]	0.2386
S c.3 [m³]	0.2124
S c.4 [m³]	-0.4353

Cross-Section 2			
Position	Support	Redirection	Midspan
Height			
1 Slab	σ [MN/m²]	σ [MN/m²]	σ [MN/m²]
2 Slab	-5.15	-7.14	-7.02
1 In-Situ	-5.00	6.26	8.99
2 Precast	-5.00	6.26	8.99
3 Precast	-4.98	7.60	10.59

$$\sigma(t) = \sigma_B + (\sigma_L - \sigma_B) \cdot \frac{\varphi_{o\,Total}}{1 + \chi \cdot \varphi_{o\,Total}}$$

$\sigma_B$  Construction Phases  
 $\sigma_L$  Falsework  
 $\sigma_C$  Creep

## Construction Phase 4 (Falsework)

X	0,8
Phi	2,34

Cross-Section 1-1	$\sigma_B$	$\sigma_L$	$\sigma_C$	$\sigma_B$	$\sigma_L$	$\sigma_C$	$\sigma_B$	$\sigma_L$	$\sigma_C$
Position	Support	Support	Support	Redirection	Redirection	Redirection	Midspan	Midspan	Midspan
Height	$\sigma$ [MN/m <sup>2</sup> ]	$\sigma$ [MN/m <sup>2</sup> ]	$\sigma$ [MN/m <sup>2</sup> ]	$\sigma$ [MN/m <sup>2</sup> ]	$\sigma$ [MN/m <sup>2</sup> ]	$\sigma$ [MN/m <sup>2</sup> ]	$\sigma$ [MN/m <sup>2</sup> ]	$\sigma$ [MN/m <sup>2</sup> ]	$\sigma$ [MN/m <sup>2</sup> ]
1 Slab	-1,12	-8,00	-6,72	-0,12	-6,27	-5,13	0,22	-5,63	-4,55
2 Slab	-0,76	-6,34	-5,31	-0,30	-5,31	-4,38	-0,15	-4,69	-3,85
1 Precast	-11,74	-6,34	-7,34	-19,43	-5,31	-7,93	-17,14	-4,69	-6,99
2 Precast	-16,24	0,11	-2,92	-14,91	-1,57	-4,04	-13,11	-1,01	-3,25
3 Precast	-16,69	0,76	-2,47	-14,46	-1,19	-3,65	-12,70	-0,65	-2,88

Cross-Section 2-2	$\sigma_B$	$\sigma_L$	$\sigma_C$	$\sigma_B$	$\sigma_L$	$\sigma_C$	$\sigma_B$	$\sigma_L$	$\sigma_C$
Position	Support	Support	Support	Redirection	Redirection	Redirection	Midspan	Midspan	Midspan
Height	$\sigma$ [MN/m <sup>2</sup> ]	$\sigma$ [MN/m <sup>2</sup> ]	$\sigma$ [MN/m <sup>2</sup> ]	$\sigma$ [MN/m <sup>2</sup> ]	$\sigma$ [MN/m <sup>2</sup> ]	$\sigma$ [MN/m <sup>2</sup> ]	$\sigma$ [MN/m <sup>2</sup> ]	$\sigma$ [MN/m <sup>2</sup> ]	$\sigma$ [MN/m <sup>2</sup> ]
1 Slab	-1,12	-8,00	-6,72	-0,12	-6,27	-5,13	0,22	-5,63	-4,55
2 Slab	-0,76	-6,34	-5,31	-0,30	-5,31	-4,38	-0,15	-4,69	-3,85
1 In-Situ	-12,86	-6,34	-7,55	-6,69	-5,31	-5,57	-4,66	-4,69	-4,68
2 In-Situ	0,88	0,11	0,25	-5,43	-1,57	-2,28	-7,54	-1,01	-2,22
2 Precast	-16,24	0,11	-2,92	-14,91	-1,57	-4,04	-13,11	-1,01	-3,25
3 Precast	-16,69	0,76	-2,47	-14,46	-1,19	-3,65	-12,70	-0,65	-2,88

## Construction Phase 5 (LM1-Falsework)

Cross-Section 1-1	$\sigma_B$	$\sigma_L$	$\sigma_C$	$\sigma_B$	$\sigma_L$	$\sigma_C$	$\sigma_B$	$\sigma_L$	$\sigma_C$
Position	Support	Support	Support	Redirection	Redirection	Redirection	Midspan	Midspan	Midspan
Height	$\sigma$ [MN/m <sup>2</sup> ]	$\sigma$ [MN/m <sup>2</sup> ]	$\sigma$ [MN/m <sup>2</sup> ]	$\sigma$ [MN/m <sup>2</sup> ]	$\sigma$ [MN/m <sup>2</sup> ]	$\sigma$ [MN/m <sup>2</sup> ]	$\sigma$ [MN/m <sup>2</sup> ]	$\sigma$ [MN/m <sup>2</sup> ]	$\sigma$ [MN/m <sup>2</sup> ]
1 Slab	1,68	-5,20	-3,92	-4,41	-10,57	-9,43	-5,27	-11,12	-10,03
2 Slab	0,43	-5,15	-4,12	-2,12	-7,14	-6,21	-2,48	-7,02	-6,18
1 Precast	-10,55	-5,15	-6,15	-21,25	-7,14	-9,75	-19,46	-7,02	-9,32
2 Precast	-21,35	-5,00	-8,03	-7,08	6,26	3,79	-3,10	8,99	6,75
3 Precast	-22,43	-4,98	-8,21	-5,66	7,60	5,15	-1,46	10,59	8,36

Cross-Section 2-2	$\sigma_B$	$\sigma_L$	$\sigma_C$	$\sigma_B$	$\sigma_L$	$\sigma_C$	$\sigma_B$	$\sigma_L$	$\sigma_C$
Position	Support	Support	Support	Redirection	Redirection	Redirection	Midspan	Midspan	Midspan
Height	$\sigma$ [MN/m <sup>2</sup> ]	$\sigma$ [MN/m <sup>2</sup> ]	$\sigma$ [MN/m <sup>2</sup> ]	$\sigma$ [MN/m <sup>2</sup> ]	$\sigma$ [MN/m <sup>2</sup> ]	$\sigma$ [MN/m <sup>2</sup> ]	$\sigma$ [MN/m <sup>2</sup> ]	$\sigma$ [MN/m <sup>2</sup> ]	$\sigma$ [MN/m <sup>2</sup> ]
1 Slab	1,68	-5,20	-3,92	-4,41	-10,57	-9,43	-5,27	-11,12	-10,03
2 Slab	0,43	-5,15	-4,12	-2,12	-7,14	-6,21	-2,48	-7,02	-6,18
1 In-Situ	-11,67	-5,15	-6,36	-8,52	-7,14	-7,39	-6,99	-7,02	-7,01
2 In-Situ	-4,23	-5,00	-4,85	2,40	6,26	5,55	2,47	8,99	7,78
2 Precast	-21,35	-5,00	-8,03	-7,08	6,26	3,79	-3,10	8,99	6,75
3 Precast	-22,43	-4,98	-8,21	-5,66	7,60	5,15	-1,46	10,59	8,36

## 8.4 Creep Coefficient

The creep constant was calculated as an average of the three main parts of the bridge. The first bridge part considered for the calculation of the creep constant is the thin-walled precast beam; the second part is the in-situ concrete being poured inside the thin-walled beams, and finally the bridge slab. The creep constant is then calculated for each of these parts individually and then averaged with its corresponding area values. The creep and shrinkage of the concrete depend on the ambient humidity, the dimensions of the element and the composition of the concrete. Creep is also influenced by the maturity of the concrete.

According to the Eurocode 1992-1-1 Shrinkage and creep are time-dependent properties of concrete. Their effects should generally be taken into account for the verification of serviceability limit states.

Annex B Creep and Shrinkage

$$\varphi_o = \varphi_{RH} \cdot \beta(f_{cm}) \cdot \beta(t_o)$$

$$\varphi_{RH} = \left[ 1 + \frac{1 - RH/100}{0.1 \cdot \sqrt[3]{h_o}} \right] \quad f_{cm} < 35 \text{ N/mm}^2$$

$$\varphi_{RH} = \left[ 1 + \frac{1 - RH/100}{0.1 \cdot \sqrt[3]{h_o}} \cdot \alpha_1 \right] \cdot \alpha_2 \quad f_{cm} > 35 \frac{\text{N}}{\text{mm}^2}$$

$$\beta(f_{cm}) = \frac{16.8}{\sqrt{f_{cm}}} \quad \beta(t_o) = \frac{1}{(0.1 + t_o^{0.2})}$$

$$\alpha_1 = \left[ \frac{35}{f_{cm}} \right]^{0.7} \quad \alpha_2 = \left[ \frac{35}{f_{cm}} \right]^{0.2}$$

$$h_o = \frac{2 \cdot A_c}{u}$$

Creep analysis for the entire bridge cross-section was performed accordingly to the Eurocode 1991-1-1 Annex B

The three different parts of the bridge considered determining the creep coefficient were the following:

- Precast Beam
- In-situ Concrete
- Bridge Slab

#### 8.4.1.1 Creep Coefficient for the precast beam

C 50/60

RH = 70 %

$f_{cm} = 58$  MPa

$t_o = 40$  days

$$\varphi_o = \varphi_{RH} \cdot \beta(f_{cm}) \cdot \beta(t_o)$$

$$\varphi_{RH} = \left[ 1 + \frac{1 - \frac{70}{100}}{0.1 \cdot \sqrt[3]{73}} \cdot 0.7022 \right] \cdot 0.9039 = 1.3595 \quad f_{cm} > 35 \frac{N}{mm^2}$$

$$h_o = \frac{2 \cdot 4 \cdot [(0.5m \cdot 1.1m) - (0.36m \cdot 1m)]}{4 \cdot (0.5m + 1.1m + 0.07m + 1m + 0.36m + 1m + 0.07m + 1.1m)}$$

$$h_o = \frac{2 \cdot 0.19m^2}{5.2m} = 0.073m = 73mm$$

$$\alpha_1 = \left[ \frac{35}{58} \right]^{0.7} = 0.7022 \quad \alpha_1 = \left[ \frac{35}{58} \right]^{0.2} = 0.9039$$

$$\beta(f_{cm}) = \frac{16.8}{\sqrt{58}} = 2.21 \quad \beta(t_o) = \frac{1}{(0.1 + 40^{0.2})} = 0.456$$

$$\varphi_o = 1.3595 \cdot 2.21 \cdot 0.456 = 1.37$$

#### 8.4.1.2 Creep Coefficient for the in-situ concrete filling the precast beam

C 30/37

RH = 70 %

$$f_{cm} = 38 \text{ MPa}$$

$$t_o = 7 \text{ days}$$

$$\varphi_o = \varphi_{RH} \cdot \beta(f_{cm}) \cdot \beta(t_o)$$

$$\varphi_{RH} = \left[ 1 + \frac{1 - 70/100}{0.1 \cdot 265} \right] = 1.467 \quad f_{cm} < 35 \frac{N}{mm^2}$$

$$h_o = \frac{2 \cdot 4 \cdot (0.36 \text{ m} \cdot 1 \text{ m})}{2 \cdot 4 \cdot (0.36 \text{ m} + 1 \text{ m})}$$

$$h_o = \frac{0.72 \text{ m}^2}{2.72 \text{ m}} = 0.265 \text{ m} = 265 \text{ mm}$$

$$\beta(f_{cm}) = \frac{16.8}{\sqrt{38}} = 2.73 \quad \beta(t_o) = \frac{1}{(0.1 + 7^{0.2})} = 0.6346$$

$$\varphi_{o2} = 1.467 \cdot 2.73 \cdot 0.6346 = 2.54$$

#### 8.4.1.3 Creep Coefficient for the bridge slab

$$C 30/37$$

$$RH = 70 \%$$

$$f_{cm} = 38 \text{ MPa}$$

$$t_o = 7 \text{ days}$$

$$\varphi_o = \varphi_{RH} \cdot \beta(f_{cm}) \cdot \beta(t_o)$$

$$\varphi_{RH} = \left[ 1 + \frac{1 - 70/100}{0.1 \cdot \sqrt[3]{248}} \right] = 1.4775 \quad f_{cm} < 35 \frac{N}{mm^2}$$

$$h_o = \frac{2 \cdot (0.36 \text{ m} \cdot 1 \text{ m})}{2 \cdot (0.256 \text{ m} + 8 \text{ m})}$$

$$h_o = \frac{2.048 \text{ m}^2}{8.252 \text{ m}} = 0.248 \text{ m} = 248 \text{ mm}$$



$$\beta(f_{cm}) = \frac{16.8}{\sqrt{38}} = 2.73 \quad \beta(t_o) = \frac{1}{(0.1 + 7^{0.2})} = 0.6346$$

$$\varphi_o = 1.4775 \cdot 2.73 \cdot 0.6346 = 2.54$$

#### 8.4.1.4 Total Creep Coefficient

$$\varphi_{o\,Total} = \frac{\varphi_{o1} \cdot A_{c1} + \varphi_{o2} \cdot A_{c2} + \varphi_{o3} \cdot A_{c3}}{A_{c1} + A_{c2} + A_{c3}}$$

$$\varphi_{o\,Total} = \frac{1.37 \cdot (0.19m^2 \cdot 4) + 2.54 \cdot (0.36m^2 \cdot 4) + 2.56 \cdot 2.048m^2}{(0.19m^2 \cdot 4) + (0.36m^2 \cdot 4) + 2.048m^2}$$

$$\varphi_{o\,Total} = 2.34$$

$$\sigma(t) = \sigma_B + (\sigma_L - \sigma_B) \cdot \frac{\varphi_{o\,Total}}{1 + \chi \cdot \varphi_{o\,Total}}$$

### 8.5 Effective Flange Width $b_{eff}$

In order to do an Ultimate Limit State (ULS) analysis it is important to know the effective geometry of the bridge's beams. The first step is to calculate the effective flange width. This is accomplished following the Eurocode EN 1991-1-1 5.3.2.1 (3) Tables 5.2 and 5.3.

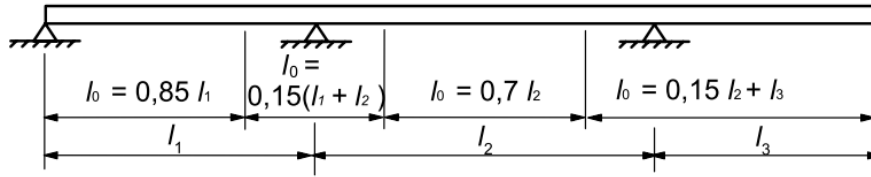


Figure 5.2: Definition of  $l_0$ , for calculation of effective flange width

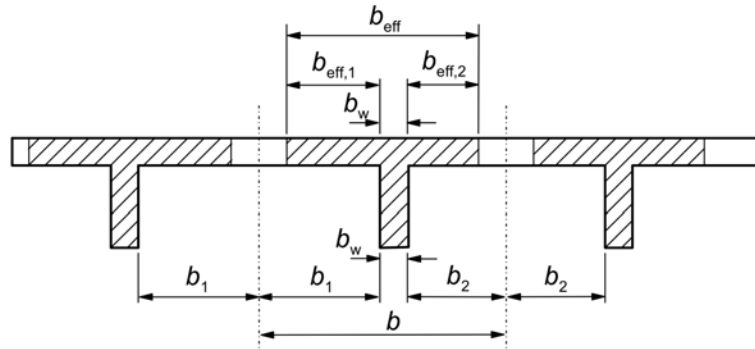
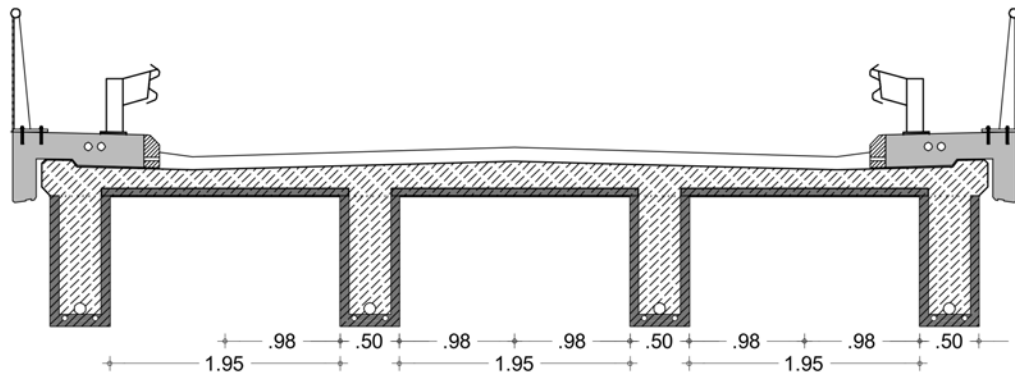


Figure 5.3: Effective flange width parameters

$$b_{eff} = \sum b_{eff,i} + b_w \leq b$$

$$\text{Where: } b_{eff,i} = 0.2 \cdot b_i + 0.1 \cdot l_0 \leq 0.2 \cdot l_0$$

$$\text{And } b_{eff,i} \leq b_i$$



For the geometry of the bridge the values of  $l_0 = 0.7 \cdot l = 0.7 \cdot 28.8 \text{ m} = 20.16 \text{ m}$

$$b_{eff,1} = 0.2 \cdot 0.975 \text{ m} + 0.1 \cdot 20.16 \text{ m} = 2.21 \leq 0.2 \cdot 20.16 \text{ m} = 4.03 \text{ m}$$

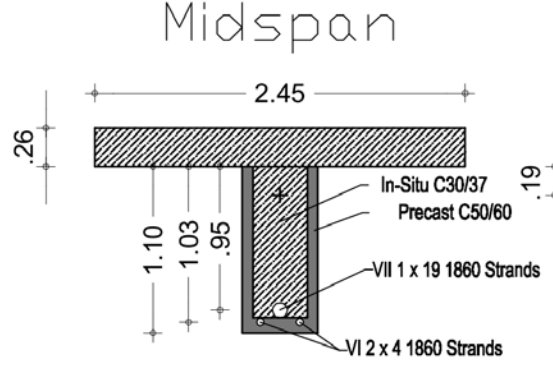
$$b = b_1 + b_2 + 0.50 \text{ m} = 2.45$$

$$b_{eff} = 2 \cdot 2.21 + 0.5 = 4.92 \text{ m}$$

$$b_{eff,i} = 4.92 \text{ m} \geq b = 2.45 \text{ m} \therefore b_{eff} = 2.45 \text{ m}$$

## 8.6 Ultimate Limit State Analysis of Beams

### 8.6.1 Midspan Center Beam Reinforcement Analysis



$$M_{Ed} = 7.398 \text{ MNm}$$

$$A_p = 19 \text{ strands} + 8 \text{ strands} = 2850 + 1200 = 4050 \text{ mm}^2 = 0.00405 \text{ m}^2$$

$$d_p = \frac{2850 \cdot 0.952 + 1200 \cdot 1.03}{2850 + 1200} = 0.974 \text{ m}$$

$$f_{pk} = 1860 \frac{\text{MN}}{\text{m}^2} \quad f_{p0.1k} = 1674 \frac{\text{MN}}{\text{m}^2} \quad f_{pd} = 1455 \frac{\text{MN}}{\text{m}^2}$$

$$F_p = A_p \cdot f_{pd} = 0.00405 \text{ mm}^2 \cdot 1455 \frac{\text{MN}}{\text{m}^2} = 5.893 \text{ MN}$$

$$\sigma_{pm0} = \min \left\{ \frac{0.7 f_{pk}}{0.8 f_{p0.1k}} \right\} P_{to}^{(0)} = \sigma_{pm0} \cdot A_p = 5.273 \text{ MN}$$

with 15% Loss of Prestress

$$P_{\infty} = P_{to}^{(0)} \cdot (1 - 0.15) \cong 4.482 \text{ MN}$$

$$\varepsilon_{py}^{(1)} = \frac{F_p - P_{\infty}}{A_p \cdot E_p} = \frac{5.893 - 4.482}{0.00405 \cdot 195000} = 0.001786 \text{ ‰}$$

$$x_{lim} = \frac{3.5 \cdot 1.23}{3.5 + 1.786} = 0.8144 \text{ m} \quad x_{B \text{ lim}} = 0.6515$$

## Block Diagram

$$x_B = \frac{A_p \cdot f_{yp}}{b \cdot f_{cd}} = \frac{0.00405 \cdot 1455}{2.45 \cdot 20} = 0.120 \text{ m} < h_f = 0.256$$

$$x_B < x_{B \text{ lim}} = 0.149 \text{ m} < 0.6515 \text{ m}$$

$$M_{Rd} = x_B \cdot b \cdot f_{cd} \cdot (d_p - 0.5 \cdot x_B)$$

$$M_{Rd} = 0.120 \cdot 2.45 \cdot 20 \cdot (1.23 - 0.5 \cdot 0.120) = 6.903 \text{ MNm}$$

$$M_{Rd} = 6.88 \text{ MNm} < M_{Ed} = 7.398 \text{ MNm}$$

Additional reinforcement required

Adapt moment to additional  $A_{s1}$  reinforcement

$$d_{p1} = d - d_p = 1.291 - 1.23 = 0.061 \text{ m}$$

$$M_{Ed,s1} = 7.398 + 0.061 \cdot 5.893 = 7.757 \text{ MNm}$$

$$x = 1.202 \cdot \left( d - \sqrt{d^2 - \frac{2.055 \cdot M_{Ed,s1}}{b \cdot f_{cd}}} \right)$$

$$x = 1.202 \cdot \left( 1.23 - \sqrt{1.23^2 - \frac{2.055 \cdot 7.757}{2.45 \cdot 20}} \right) = 0.168 \text{ m}$$

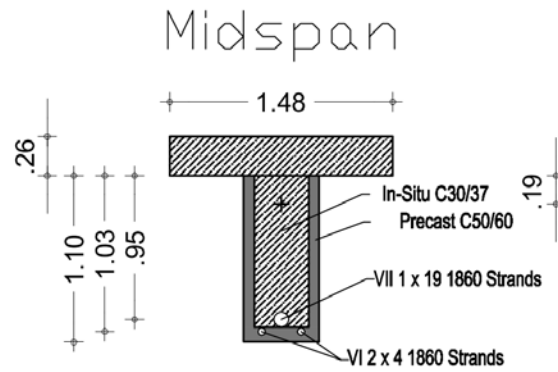
$$A_{s1} = \frac{0.8095 \cdot x \cdot b \cdot f_{cd} - A_p \cdot f_{pd}}{f_{yd}}$$

$$A_{s1} = \frac{0.8095 \cdot 0.168 \cdot 2.45 \cdot 20 - 0.00405 \cdot 1455}{478.3}$$

$$A_{s1} = 0.00166 \text{ m}^2 = 16.61 \text{ cm}^2$$

4Ø26 or 3Ø30

### Midspan Corner Beam Reinforcement Analysis



$$M_{Ed} = 5.859 \text{ MNm}$$

$$A_p = 19 \text{ strands} + 8 \text{ strands} = 2850 + 1200 = 4050 \text{ mm}^2 = 0.00405 \text{ m}^2$$

$$d_p = \frac{2850 \cdot 0.95 + 1200 \cdot 1.03}{2850 + 1200} = 0.974 \text{ m}$$

$$f_{pk} = 1860 \frac{\text{MN}}{\text{m}^2} \quad f_{p0.1k} = 1674 \frac{\text{MN}}{\text{m}^2} \quad f_{pd} = 1455 \frac{\text{MN}}{\text{m}^2}$$

$$F_p = A_p \cdot f_{pd} = 0.00405 \text{ m}^2 \cdot 1455 \frac{\text{MN}}{\text{m}^2} = 5.893 \text{ MN}$$

$$\sigma_{pm0} = \min \left\{ \frac{0.7 f_{pk}}{0.8 f_{p0.1k}} \right\} P_{to}^{(0)} = \sigma_{pm0} \cdot A_p = 5.273 \text{ MN}$$

with 15% Loss of Prestress

$$P_{\infty} = P_{to}^{(0)} \cdot (1 - 0.15) \cong 4.482 \text{ MN}$$

$$\varepsilon_{py}^{(1)} = \frac{F_p - P_{\infty}}{A_p \cdot E_p} = \frac{5.893 - 4.482}{0.00405 \cdot 195000} = 0.001786 \text{ ‰}$$

$$x_{lim} = \frac{3.5 \cdot 1.23}{3.5 + 1.786} = 0.8144 \text{ m} \quad x_{B \text{ lim}} = 6515$$

---

Block Diagram

$$x_B = \frac{A_p \cdot f_{yp}}{b \cdot f_{cd}} = \frac{0.00405 \cdot 1455}{1.475 \cdot 20} = 0.200m < h_f = 0.256$$

$$x_B < x_{lim} = 0.200 \text{ m} < 0.8144 \text{ m}$$

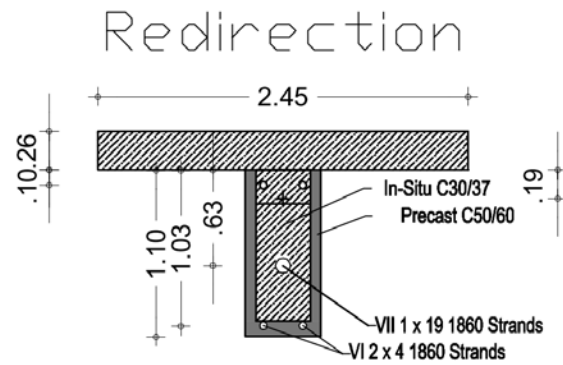
$$M_{Rd} = x_B \cdot b \cdot f_{cd} \cdot (d_p - 0.5 \cdot x_B)$$

$$M_{Rd} = 0.200 \cdot 1.475 \cdot 20 \cdot (1.23 - 0.5 \cdot .200) = 6.649 \text{ MNm}$$

$$M_{Rd} = 6.67 \text{ MNm} > M_{Ed} = 5.859 \text{ MNm}$$

Additional reinforcement is not required

Redirection:



$$M_{Ed} = 5.33 \text{ MNm}$$

$$A_p = 19 \text{ strands} + 8 \text{ strands} + 4 \text{ strands} = 2850 + 1200 + 600 = 4650 \text{ mm}^2 = 0.00465 \text{ m}^2$$

$$d_p = \frac{2850 \cdot (0.256 + 0.63) + 1200 \cdot (0.256 + 1.03) + 600 \cdot (0.256 + 0.10)}{2850 + 1200 + 600} = 0.92 \text{ m}$$

$$f_{pk} = 1860 \frac{\text{MN}}{\text{m}^2} \quad f_{p0.1k} = 1674 \frac{\text{MN}}{\text{m}^2} \quad f_{pd} = 1455 \frac{\text{MN}}{\text{m}^2}$$

$$F_p = A_p \cdot f_{pd} = 0.00465 \text{ m}^2 \cdot 1455 \frac{\text{MN}}{\text{m}^2} = 6.765 \text{ MN}$$

$$\sigma_{pm0} = \min \left\{ \frac{0.7 f_{pk}}{0.8 f_{p0.1k}} \right\} P_{to}^{(0)} = \sigma_{pm0} \cdot A_p = 6.05 \text{ MN}$$

with 15% Loss of Prestress

$$P_{\infty} = P_{to}^{(0)} \cdot (1 - 0.15) \cong 5.146 \text{ MN}$$

$$\varepsilon_{py}^{(1)} = \frac{F_p - P_{\infty}}{A_p \cdot E_p} = \frac{6.765 - 5.146}{0.00465 \cdot 195000} = 0.001786 \text{ ‰}$$

$$x_{lim} = \frac{3.5 \cdot 0.92}{3.5 + 1.786} = 0.609 \text{ m and } x_{B \text{ lim}} = 0.487 \text{ m}$$



---

Block Diagram

$$x_B = \frac{A_p \cdot f_{yp}}{b \cdot f_{cd}} = \frac{0.00465 \cdot 1455}{2.45 \cdot 20} = 0.138 \text{ m} < h_f = 0.256$$

$$x_B < x_{B \text{ lim}} = 0.138 \text{ m} < 0.0487 \text{ m}$$

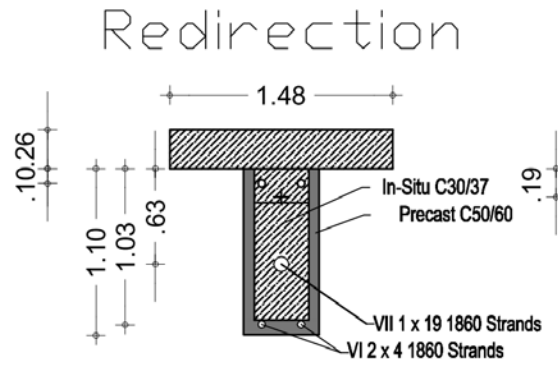
$$M_{Rd} = x_B \cdot b \cdot f_{cd} \cdot (d_p - 0.5 \cdot x_B)$$

$$M_{Rd} = 0.138 \cdot 2.45 \cdot 20 \cdot (0.92 - 0.5 \cdot 0.138) = 5.75 \text{ MNm}$$

$$M_{Rd} = 5.75 \text{ MNm} > M_{Ed} = 5.33 \text{ MNm}$$

Additional reinforcement is not required

Redirection Corner Beam:



$$M_{Ed} = 4.15 \text{ MNm}$$

$$A_p = 19 \text{ strands} + 8 \text{ strands} + 4 \text{ strands} = 2850 + 1200 + 600 = 4650 \text{ mm}^2 = 0.00465 \text{ m}^2$$

$$d_p = \frac{2850 \cdot (0.256 + 0.63) + 1200 \cdot (0.256 + 1.03) + 600 \cdot (0.256 + 0.10)}{2850 + 1200 + 600} = 0.92 \text{ m}$$

$$f_{pk} = 1860 \frac{\text{MN}}{\text{m}^2} \quad f_{p0.1k} = 1674 \frac{\text{MN}}{\text{m}^2} \quad f_{pd} = 1455 \frac{\text{MN}}{\text{m}^2}$$

$$F_p = A_p \cdot f_{pd} = 0.00465 \text{ m}^2 \cdot 1455 \frac{\text{MN}}{\text{m}^2} = 6.765 \text{ MN}$$

$$\sigma_{pm0} = \min \left\{ \frac{0.7 f_{pk}}{0.8 f_{p0.1k}} \right\} P_{to}^{(0)} = \sigma_{pm0} \cdot A_p = 6.05 \text{ MN}$$

with 15% Loss of Prestress

$$P_{\infty} = P_{to}^{(0)} \cdot (1 - 0.15) \cong 5.146 \text{ MN}$$

$$\varepsilon_{py}^{(1)} = \frac{F_p - P_{\infty}}{A_p \cdot E_p} = \frac{6.765 - 5.146}{0.00465 \cdot 195000} = 0.001786 \text{ ‰}$$

$$x_{lim} = \frac{3.5 \cdot 0.92}{3.5 + 1.786} = 0.609 \text{ m and } x_{B \text{ lim}} = 0.487 \text{ m}$$

Block Diagram

$$x_B = \frac{A_p \cdot f_{yp}}{b \cdot f_{cd}} = \frac{0.00465 \cdot 1455}{1.475 \cdot 20} = 0.229 \text{ m} < h_f = 0.256$$

$$x_B < x_{B \text{ lim}} = 0.229 \text{ m} < 0.0487 \text{ m}$$

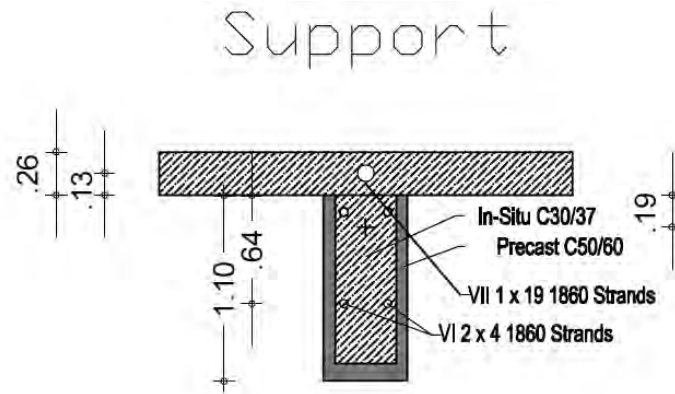
$$M_{Rd} = x_B \cdot b \cdot f_{cd} \cdot (d_p - 0.5 \cdot x_B)$$

$$M_{Rd} = 0.229 \cdot 1.475 \cdot 20 \cdot (0.92 - 0.5 \cdot 0.229) = 5.44 \text{ MNm}$$

$$M_{Rd} = 5.44 \text{ MNm} > M_{Ed} = 4.15 \text{ MNm}$$

Additional reinforcement is not required

Support:



$$M_{Ed} = -2.68 \text{ MNm}$$

$$A_p = 19 \text{ strands} + 8 \text{ strands} + 4 \text{ strands} = 2850 + 1200 + 600 = 4650 \text{ mm}^2 = 0.00465 \text{ m}^2$$

$$d_p = \frac{2850 \cdot (1.10 + 0.13) + 1200 \cdot (1.10 - 0.64) + 600 \cdot (1.1 - 0.10)}{2850 + 1200 + 600} = 1.00 \text{ m}$$

$$f_{pk} = 1860 \frac{\text{MN}}{\text{m}^2} \quad f_{p0.1k} = 1674 \frac{\text{MN}}{\text{m}^2} \quad f_{pd} = 1455 \frac{\text{MN}}{\text{m}^2}$$

$$F_p = A_p \cdot f_{pd} = 0.00465 \text{ m}^2 \cdot 1455 \frac{\text{MN}}{\text{m}^2} = 6.765 \text{ MN}$$

$$\sigma_{pm0} = \min \left\{ \frac{0.7 f_{pk}}{0.8 f_{p0.1k}} \right\} P_{to}^{(0)} = \sigma_{pm0} \cdot A_p = 6.05 \text{ MN}$$

with 15% Loss of Prestress

$$P_{\infty} = P_{to}^{(0)} \cdot (1 - 0.15) \cong 5.146 \text{ MN}$$

$$\varepsilon_{py}^{(1)} = \frac{F_p - P_{\infty}}{A_p \cdot E_p} = \frac{6.765 - 5.146}{0.00465 \cdot 195000} = 0.001786 \text{ ‰}$$

$$x_{lim} = \frac{3.5 \cdot 1.00}{3.5 + 1.786} = 0.662 \text{ m and } x_{B \text{ lim}} = 0.530 \text{ m}$$

Block Diagram

$$x_B = x_{precast} + x_{mixed}$$

$$x_{mixed} = \frac{A_p \cdot f_{yp} - b \cdot x_{precast} \cdot f_{cd}}{b_{in-situ} \cdot f_{cd} + b_{precast} \cdot f_{cd}}$$

$$\frac{0.00465 \cdot 1455 - 0.5 \cdot 0.1 \cdot 33.33}{0.36 \cdot 20 + 0.14 \cdot 33.33} = 0.429 \text{ m}$$

$$x_B = 0.10 + 0.429 = 0.529 \text{ m}$$

$$x_B < x_{B \text{ lim}} = 0.529 \text{ m} < 0.530 \text{ m}$$

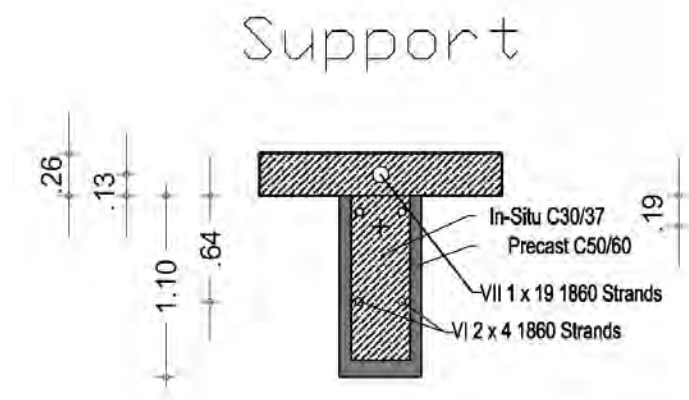
$$M_{Rd} = x_B \cdot b \cdot f_{cd} \cdot (d_p - 0.5 \cdot x_B)$$

$$M_{Rd} = 0.529 \cdot 0.50 \cdot 20 \cdot (1.0 - 0.5 \cdot 0.529) = 3.89 \text{ MNm}$$

$$M_{Rd} = 3.89 \text{ MNm} > M_{Ed} = 2.68 \text{ MNm}$$

Additional reinforcement is not required

Support Corner Beam:



$$M_{Ed} = -2.10 \text{ MNm}$$

$$A_p = 19 \text{ strands} + 8 \text{ strands} + 4 \text{ strands} = 2850 + 1200 + 600 = 4650 \text{ mm}^2 = 0.00465 \text{ m}^2$$

$$d_p = \frac{2850 \cdot (1.10 + 0.13) + 1200 \cdot (1.10 - 0.64) + 600 \cdot (1.1 - 0.10)}{2850 + 1200 + 600} = 1.00 \text{ m}$$

$$f_{pk} = 1860 \frac{\text{MN}}{\text{m}^2} \quad f_{p0.1k} = 1674 \frac{\text{MN}}{\text{m}^2} \quad f_{pd} = 1455 \frac{\text{MN}}{\text{m}^2}$$

$$F_p = A_p \cdot f_{pd} = 0.00465 \text{ m}^2 \cdot 1455 \frac{\text{MN}}{\text{m}^2} = 6.765 \text{ MN}$$

$$\sigma_{pm0} = \min \left\{ \frac{0.7 f_{pk}}{0.8 f_{p0.1k}} \right\} P_{to}^{(0)} = \sigma_{pm0} \cdot A_p = 6.05 \text{ MN}$$

with 15% Loss of Prestress

$$P_{\infty} = P_{to}^{(0)} \cdot (1 - 0.15) \cong 5.146 \text{ MN}$$

$$\varepsilon_{py}^{(1)} = \frac{F_p - P_{\infty}}{A_p \cdot E_p} = \frac{6.765 - 5.146}{0.00465 \cdot 195000} = 0.001786 \text{ ‰}$$

$$x_{lim} = \frac{3.5 \cdot 1.00}{3.5 + 1.786} = 0.662 \text{ m and } x_{B \text{ lim}} = 0.530 \text{ m}$$

Block Diagram

$$x_B = x_{precast} + x_{mixed}$$

$$x_{mixed} = \frac{A_p \cdot f_{yp} - b \cdot x_{precast} \cdot f_{cd}}{b_{in-situ} \cdot f_{cd} + b_{precast} \cdot f_{cd}}$$

$$\frac{0.00465 \cdot 1455 - 0.5 \cdot 0.1 \cdot 33.33}{0.36 \cdot 20 + 0.14 \cdot 33.33} = 0.429 \text{ m}$$

$$x_B = 0.10 + 0.429 = 0.529 \text{ m}$$

$$x_B < x_{B \text{ lim}} = 0.529 \text{ m} < 0.530 \text{ m}$$

$$M_{Rd} = x_B \cdot b \cdot f_{cd} \cdot (d_p - 0.5 \cdot x_B)$$

$$M_{Rd} = 0.529 \cdot 0.5 \cdot 20 \cdot (1.0 - 0.5 \cdot 0.529) = 3.89 \text{ MNm}$$

$$M_{Rd} = 3.89 \text{ MNm} > M_{Ed} = 2.10 \text{ MNm}$$

Additional reinforcement is not required

### 8.6.2 Longitudinal Reinforcement in girders

According to EN 1992-1 (9.1N)

Assuming all concrete is concrete C30/37

$$A_{s,min} = 0.26 \cdot \frac{f_{ctm}}{f_{yk}} \cdot b_t \cdot d \geq 0.0013 \cdot b_t \cdot d$$

$$A_{s,min} = 0.26 \cdot \frac{2.9}{550} \cdot 0.50 \cdot 1.306 = 8.95 \text{ cm}^2$$

$$0.0013 \cdot 0.50 \cdot 1.306 = 8.49 \text{ cm}^2$$

$$A_{s,min} = 8.95 \text{ cm}^2 \geq 8.49 \text{ cm}^2$$

$$A_{s,min} = 8.95 \text{ cm}^2 \leq A_{s,chosen} \text{ 4}\varnothing 26 = 21.24 \text{ cm}^2$$



### 8.6.3 Shear Reinforcement

Geometrical values:

$$\alpha = 90^\circ$$

$$d = h_{deck} + h_{beam} - h_{shear\ stirrup} = 1.306\ m$$

$$z = 0.9 \cdot d = 0.9 \cdot 1.306\ m = 1.18\ m$$

$$\tan \Theta = 0.60 \quad \cot \Theta = 1.66$$

Values taken from RFEM:

$$V_{\max} = 1500\ \text{kN}$$

$$V_p = 300\ \text{kN}$$

$$V_{Ed} = V_{\max} - V_p = 1500\ \text{kN} - 300\ \text{kN} = 1200\ \text{kN}$$

Stirrup reinforcement for maximum shear

$$a_{sw} = \frac{A_{sw}}{s} = \frac{V_{Ed}}{z \cdot f_{yd} \cdot \cot \Theta} = \frac{1200\ \text{kN}}{1.18\ m \cdot 47.8\ \frac{\text{kN}}{\text{cm}^2} \cdot 1.66} = 12.81\ \text{cm}^2/\text{m}$$

Minimum shear reinforcement

$$\rho_{w,min} = 0.15 \cdot \frac{f_{ctm}}{f_{yd}} = 0.15 \cdot \frac{2.9}{47.8} = 0.00091$$

$$a_{sw,min} = \rho_{w,min} \cdot b_w = 0.00091 \cdot 0.50 = 4.55\ \frac{\text{cm}^2}{\text{m}}$$

$$a_{sw} = 12.81\ \text{cm}^2/\text{m} \geq a_{sw,min} = 4.55\ \text{cm}^2/\text{m}$$

$$a_{sw} = \emptyset 16/15\ \text{cm}^2/\text{m}$$

**8.6.4 Slab Reinforcement:**

According to EN 1992-1 (9.1N)

C30/37

$M_{Ed} = 50 \text{ kNm}$

$$A_{s,1} = 4.75 \frac{\text{cm}^2}{\text{m}}$$

$$A_{s,min} = 0.26 \cdot \frac{f_{ctm}}{f_{yk}} \cdot b_t \cdot d \geq 0.0013 \cdot b_t \cdot d$$

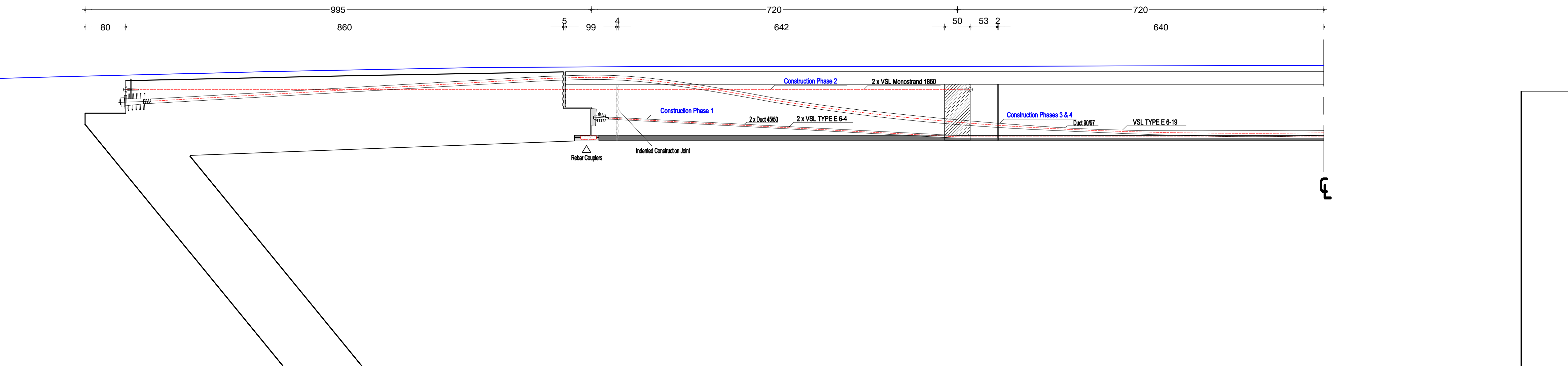
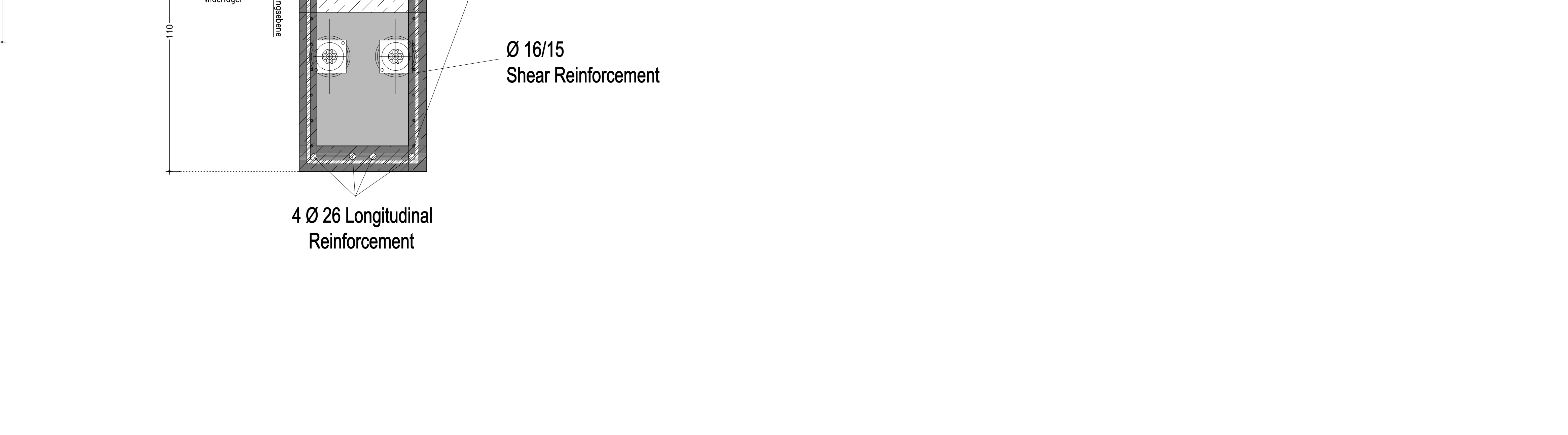
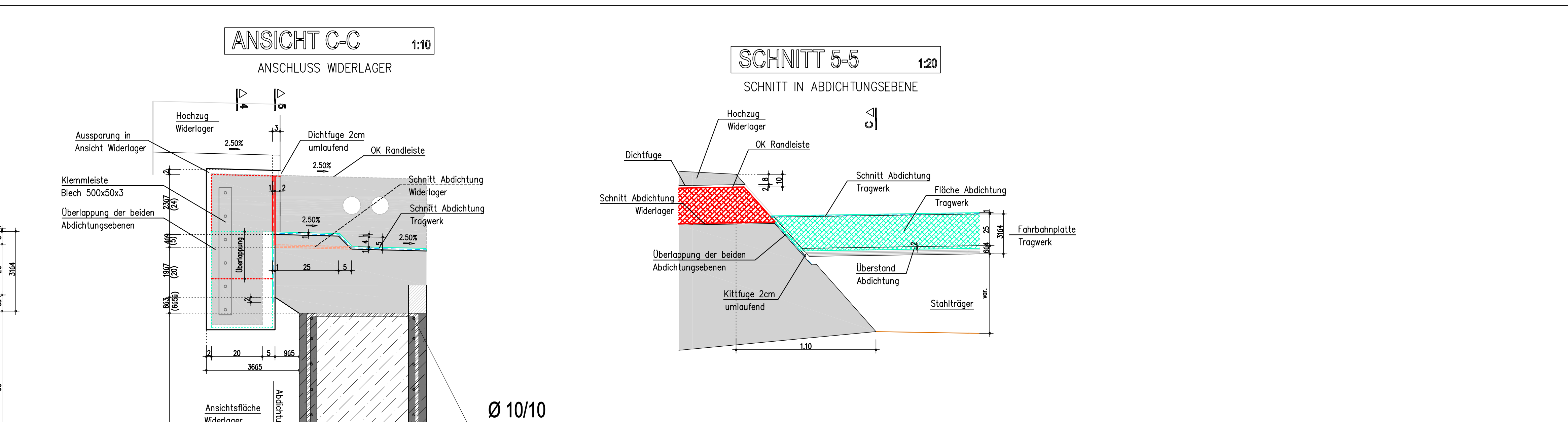
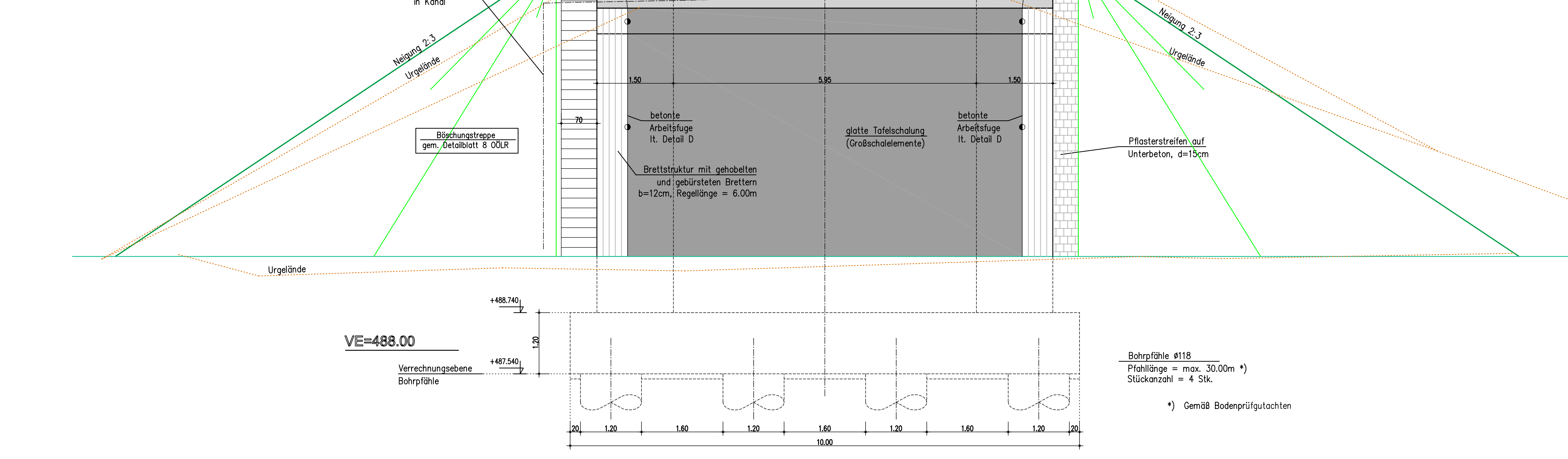
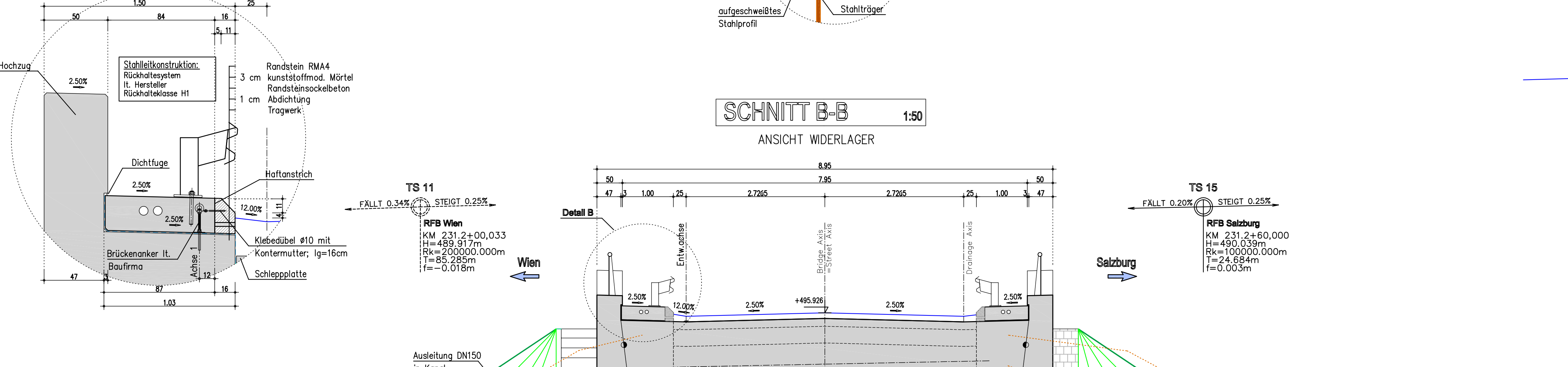
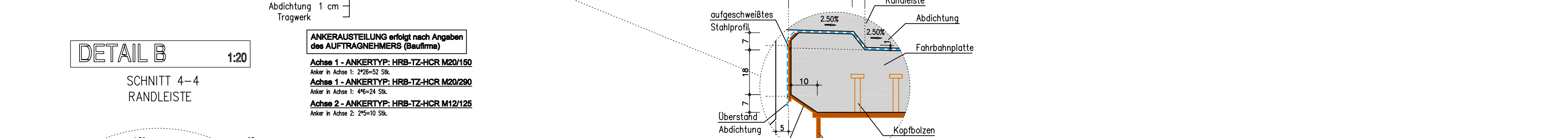
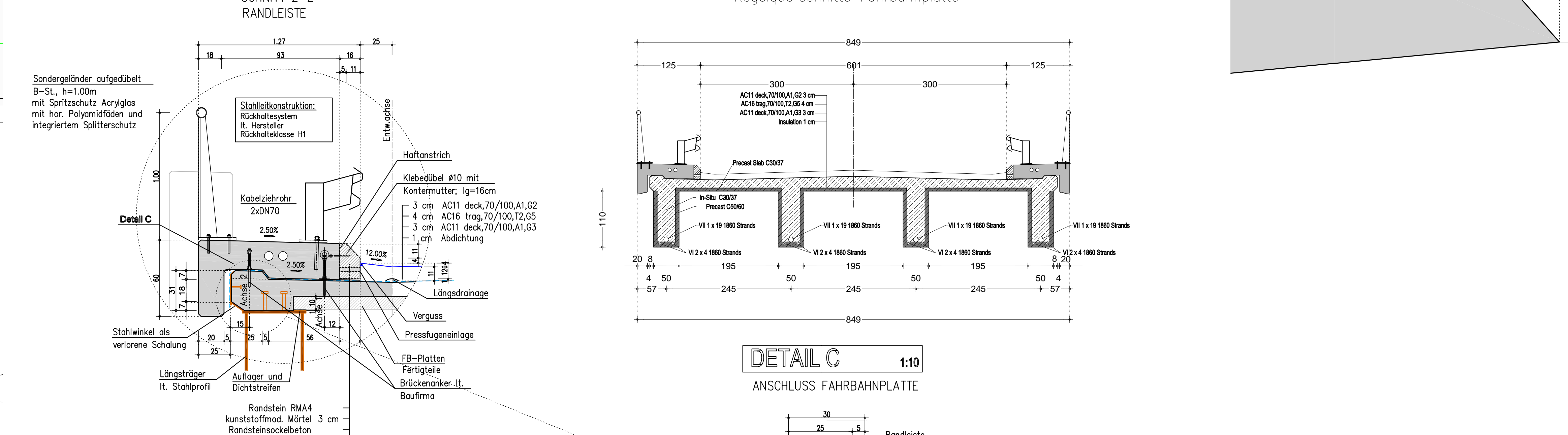
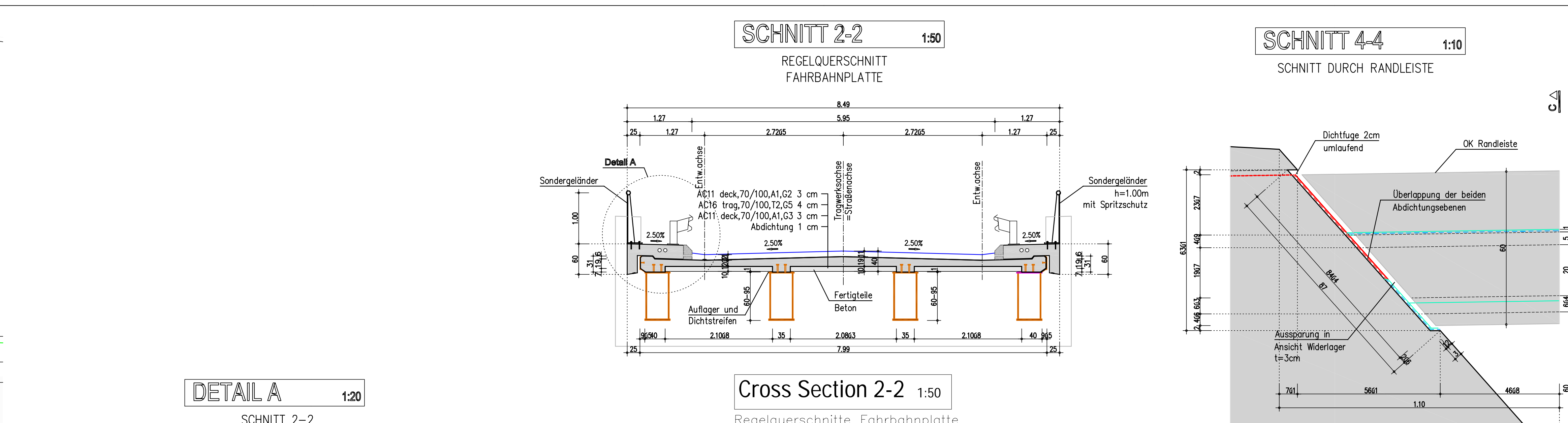
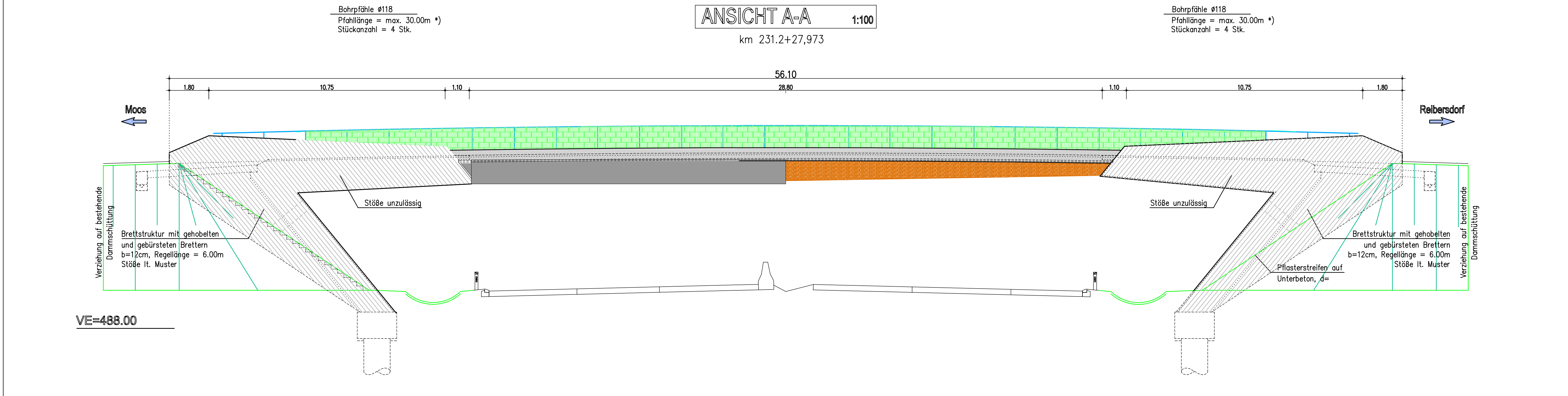
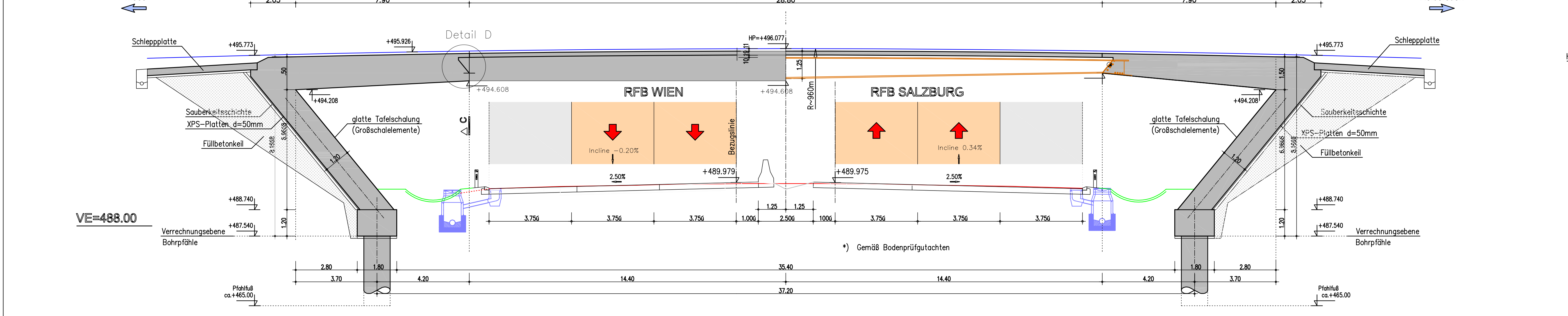
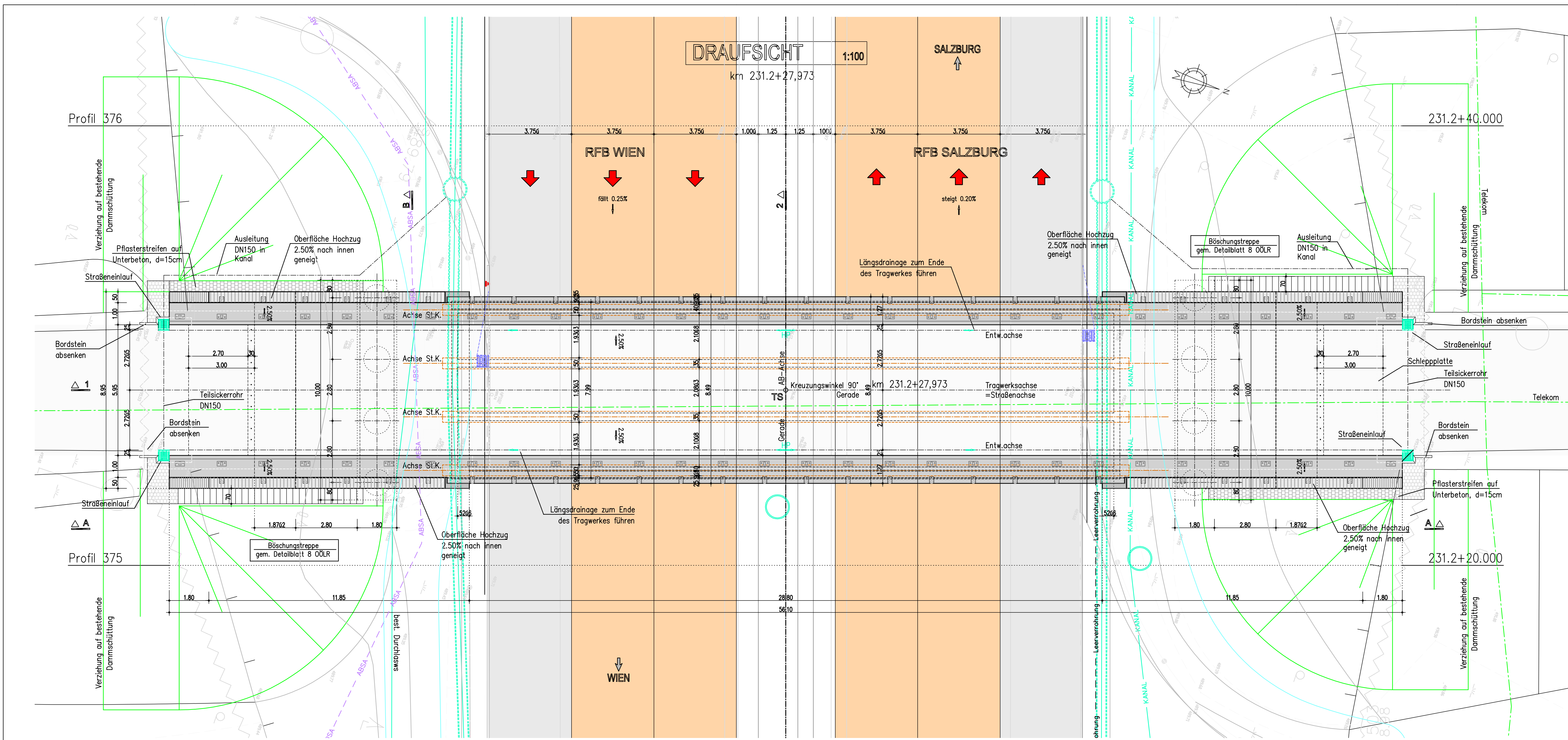
$$A_{s,min} = 0.26 \cdot \frac{2.9}{550} \cdot 1.0 \cdot 0.226 = 3.09 \text{ cm}^2$$

$$0.0013 \cdot 1.0 \cdot 0.226 = 2.94 \text{ cm}^2$$

$$A_{s,min} = 3.09 \text{ cm}^2 \geq 2.94 \text{ cm}^2$$

$$A_{s,1} = 4.75 \text{ cm}^2 \leq A_{s,chosen} \text{ } \emptyset 10/15 = 5.24 \text{ cm}^2/\text{m}$$





Stahlgüte S355J0W

Darstellung von Leitungen und Einbauten nur nachrichtlich!  
Eine Kontrolle der Lage und der Vollständigkeit  
durch den AN mit den Leitungsträgern ist notwendig!

ZUGEHÖRIGE PLÄNE	
S101/D0210	Bestandsdarstellung
S101/D0220	Brückenschnitt
S101/D0400	Abstreifen
S101/D0401	Abstreifen
S101/D0450	Schulung & Bewehrung Bohrpfähle
S101/D04100	Rb. Salzburg: Schulung WL Reibendorf
S101/D04101	Rb. Wien: Schulung WL Mone
S101/D04200	Schulung Fahrbahnplatte (OB) WL Schulungskoten
S101/D04201	Schulung & Bewehrung Fahrbahnplattenfertigteile
S101/D04300	Schulung & Bewehrung Schlepplatten
S101/D04300	Bewehrung Planinspektionsbohle WL
S101/D04100	Bewehrung Widerlager Aufgehendes - Teil 1
S101/D04101	Bewehrung Widerlager Aufgehendes - Teil 2
S101/D04102	Bewehrung Widerlager - Deckblatt zu Pl. S100 und S101
S101/D04300	Bewehrung Fahrbahnplatte (Orbitalen)
S101/D04100	Schulung & Bewehrung Randstreifen
S101/D04300	Führungselemente Brückengelenke
S101/D07001	Stahlbau Führungselemente mit Details

Betongüter:	
Unterlagelager	XO/F38 (A)
Ausgleichsbelag	XO/F38 (A)
Bohrpfähle	C25/S0/B5/GK32
Planinspektionsbohle	C30/S7/B5/GK32
Widerlager	C30/S7/B5
Fertigbeton Fahrbahnplatte	C30/S7/B5/GK32
Fahrbahnplatte	C25/S0/GK32/B7
Schlepplatten	C25/S0/GK32/B7/F45
Betonträger	C50/60

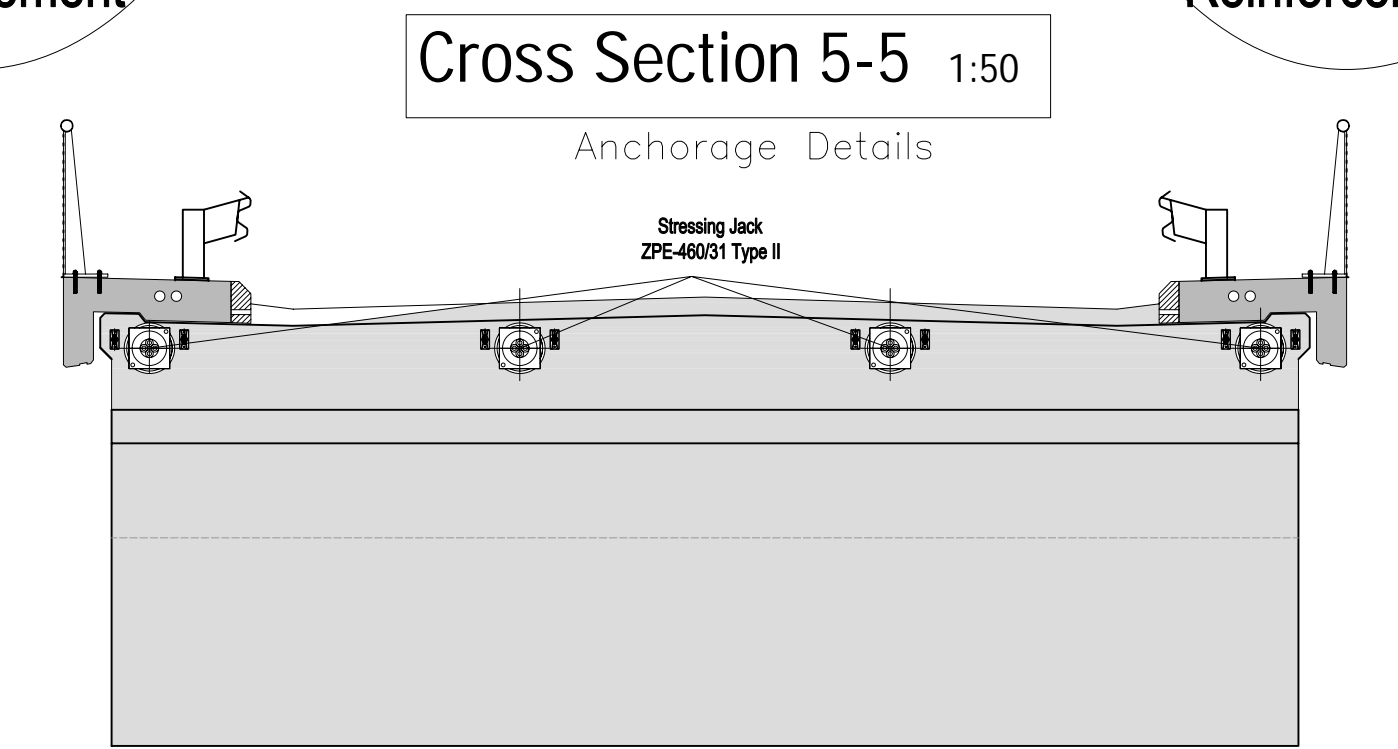
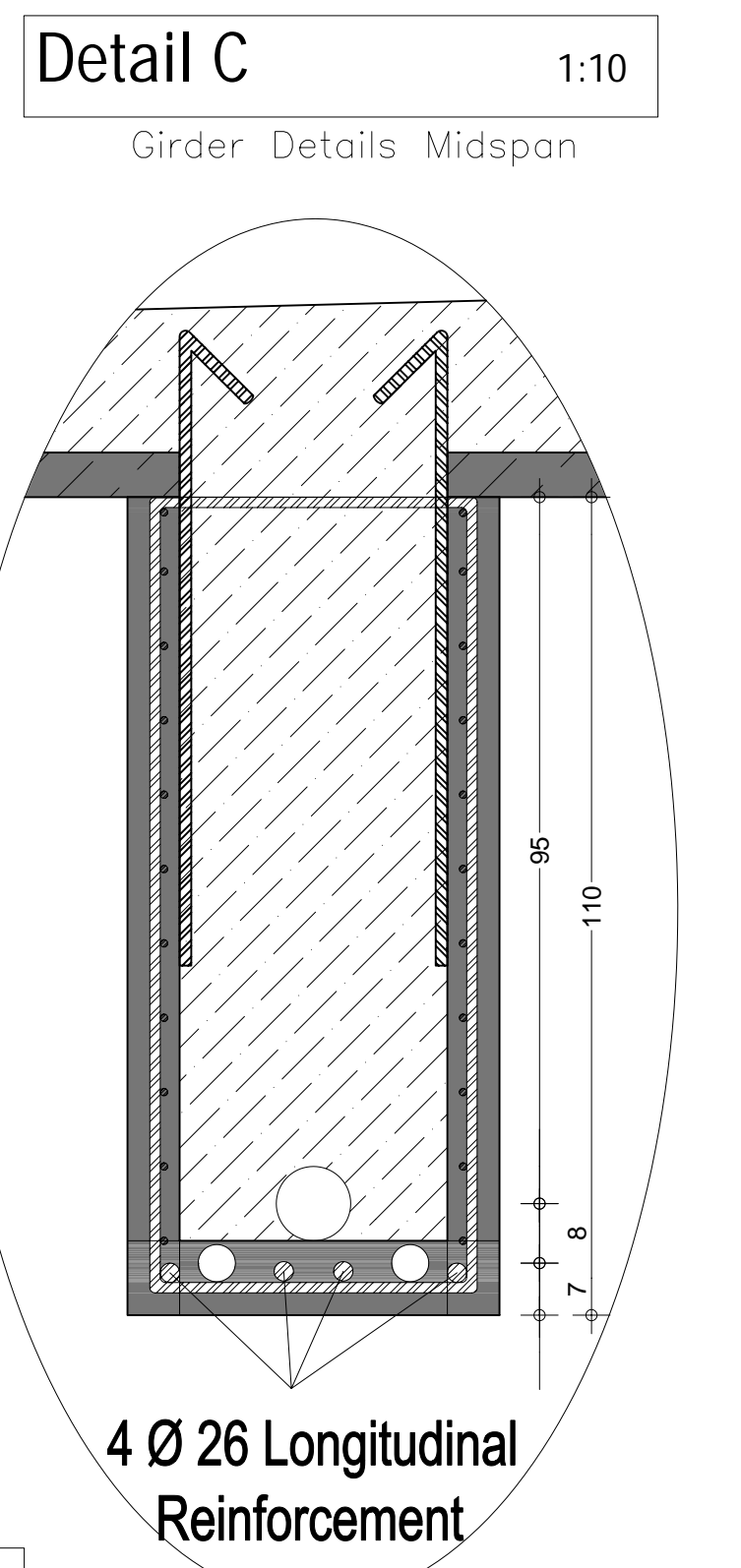
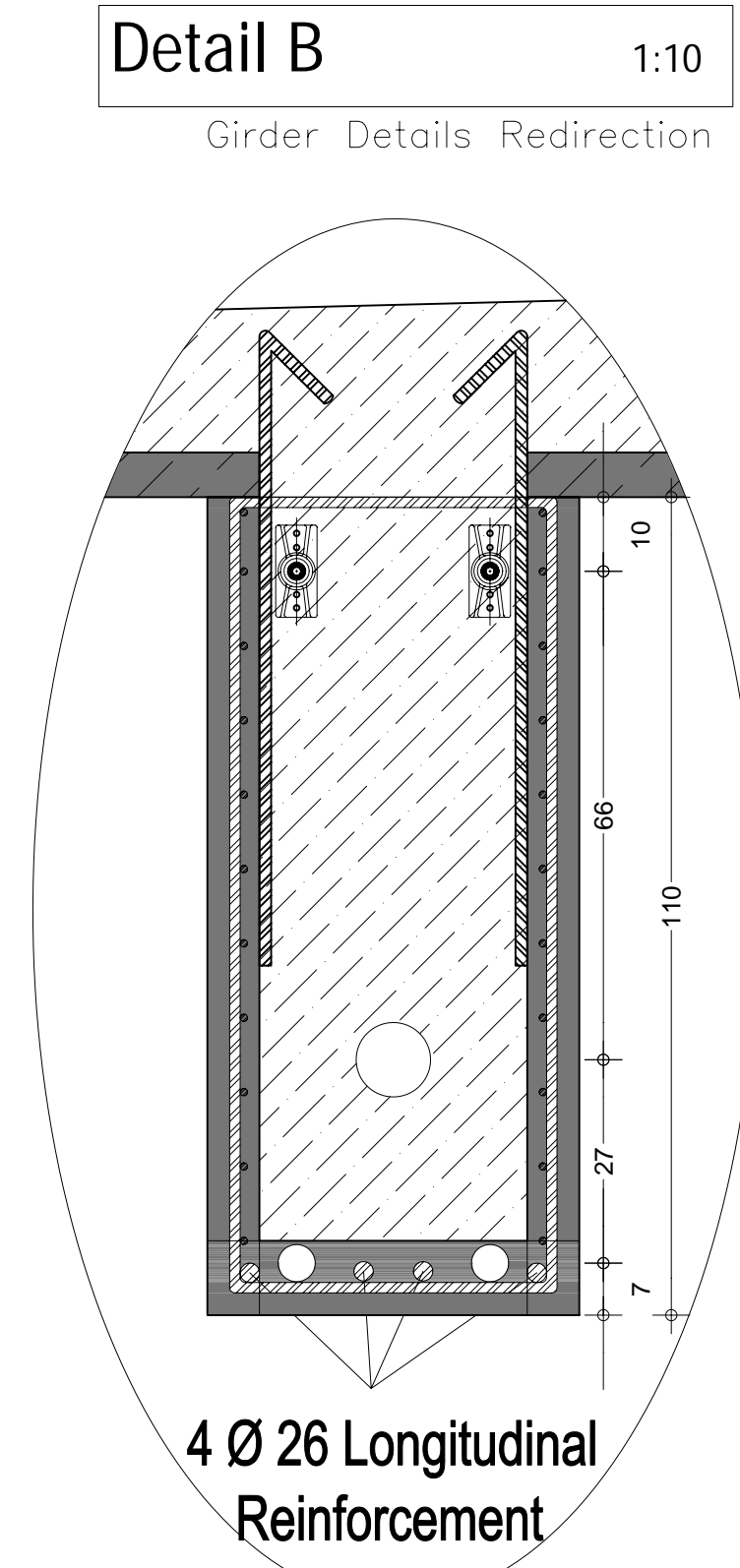
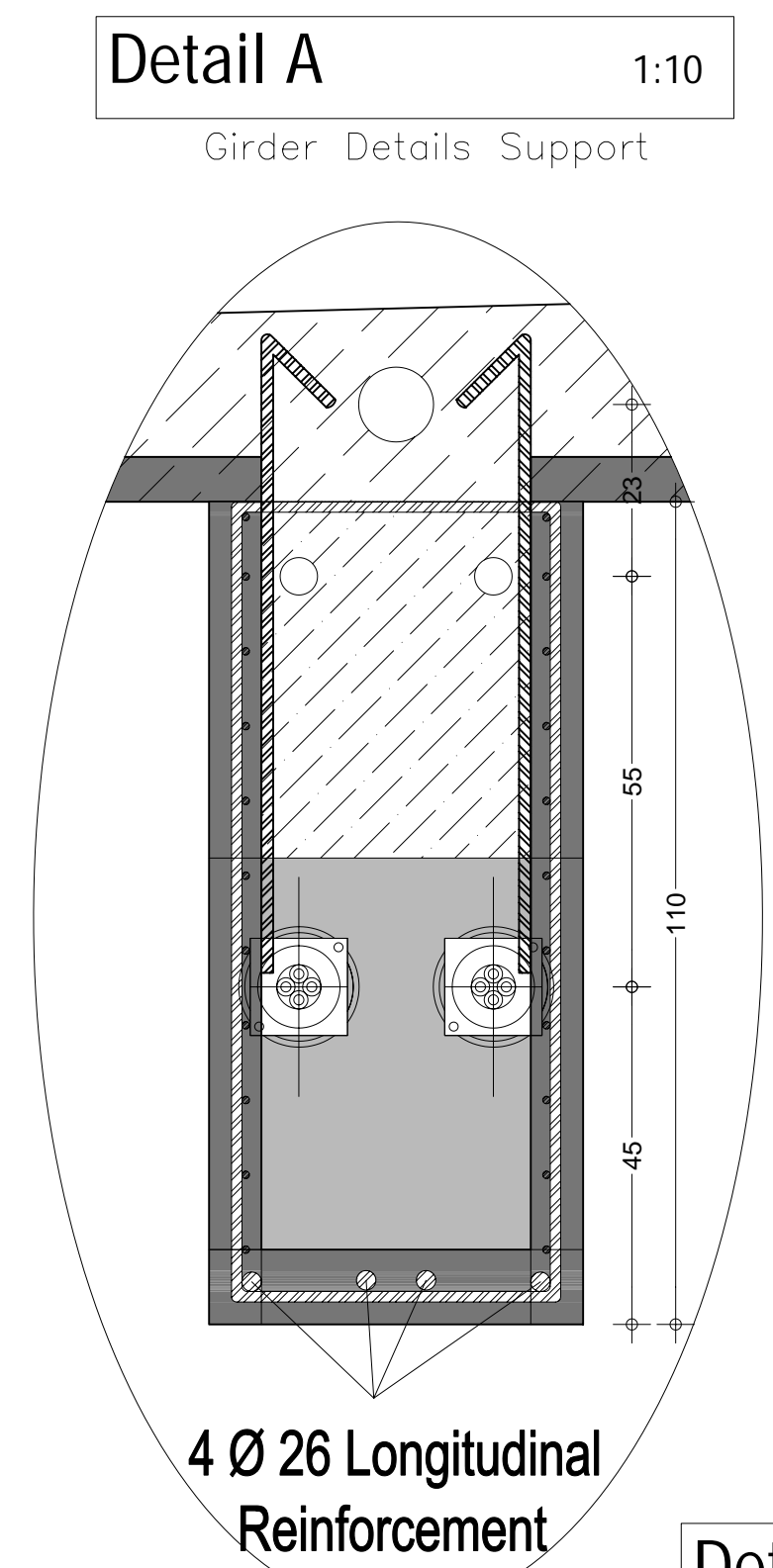
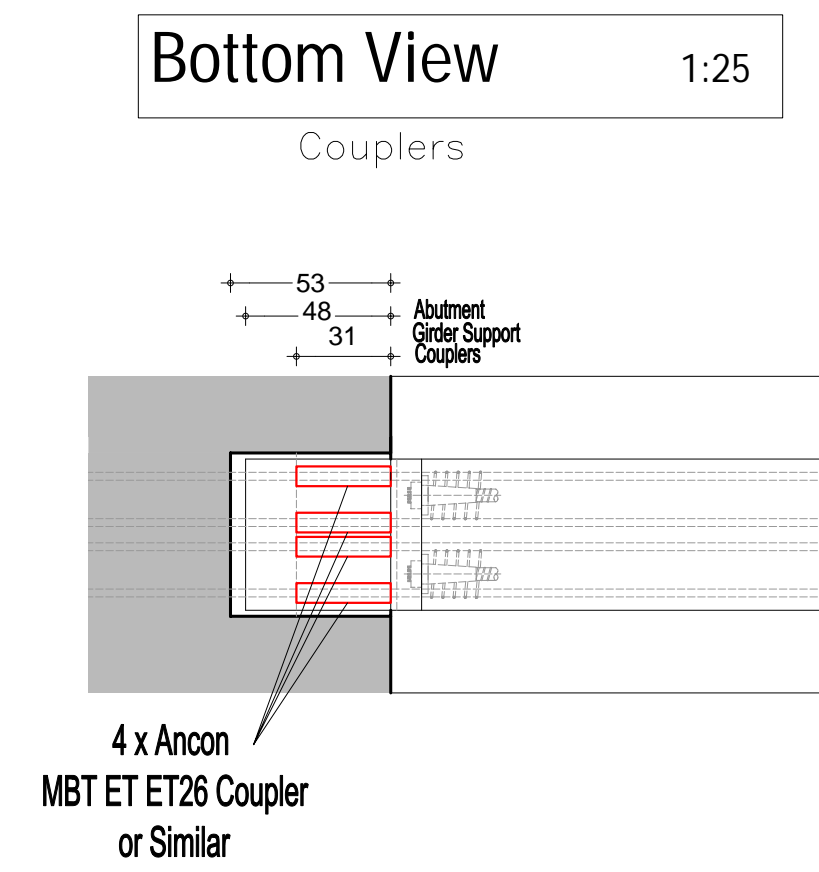
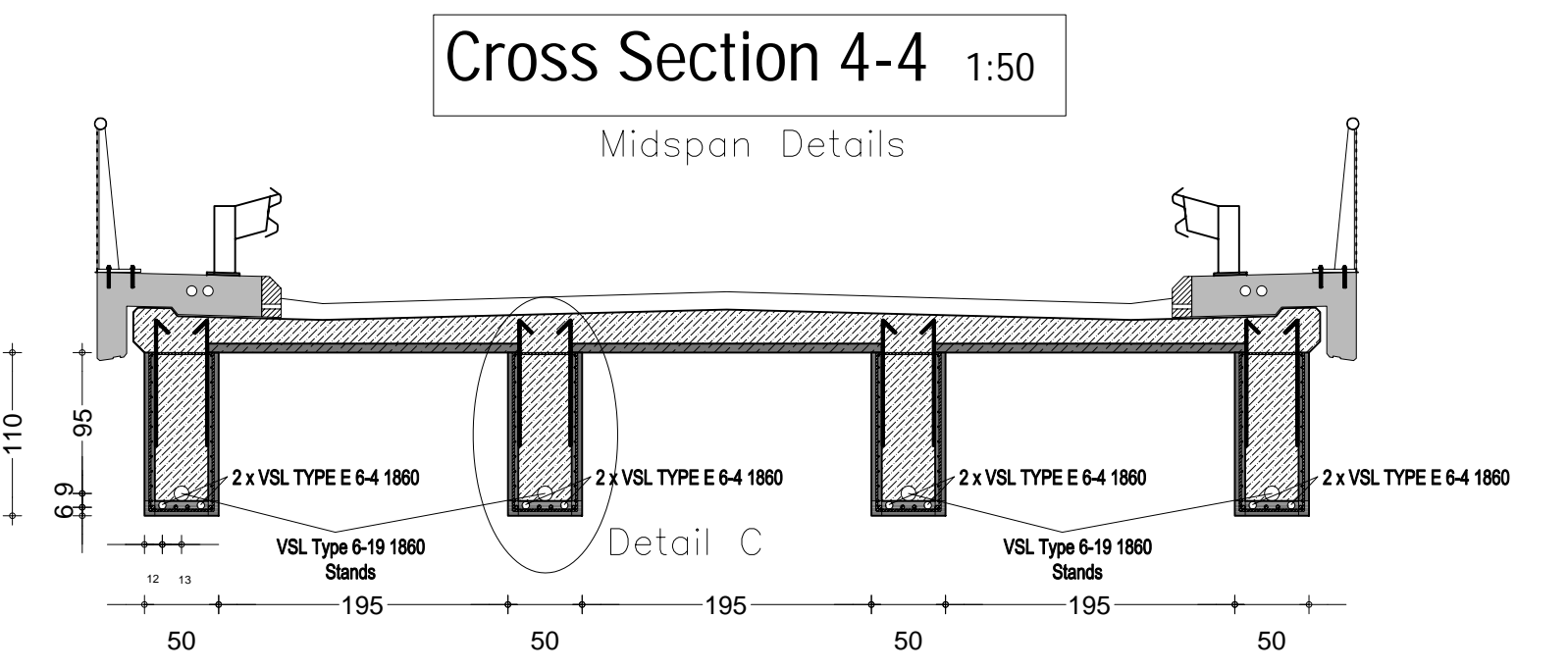
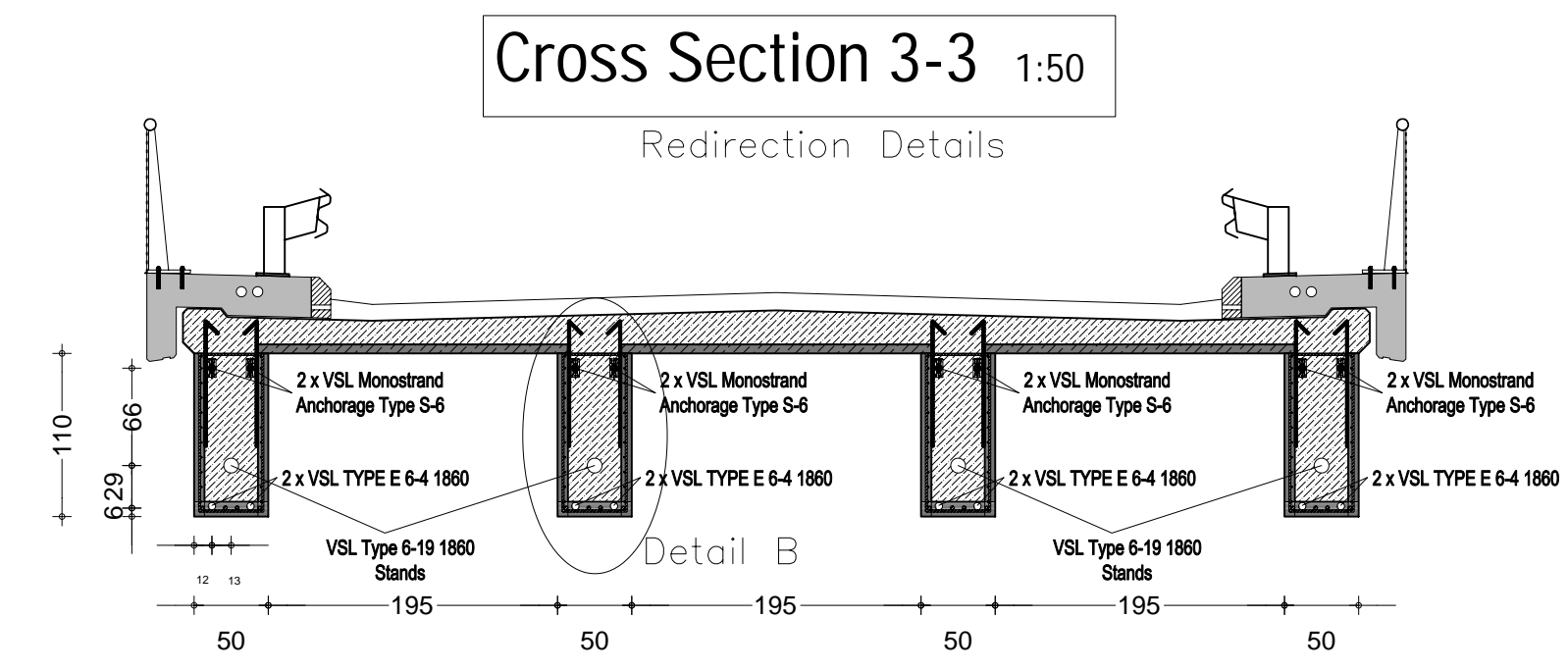
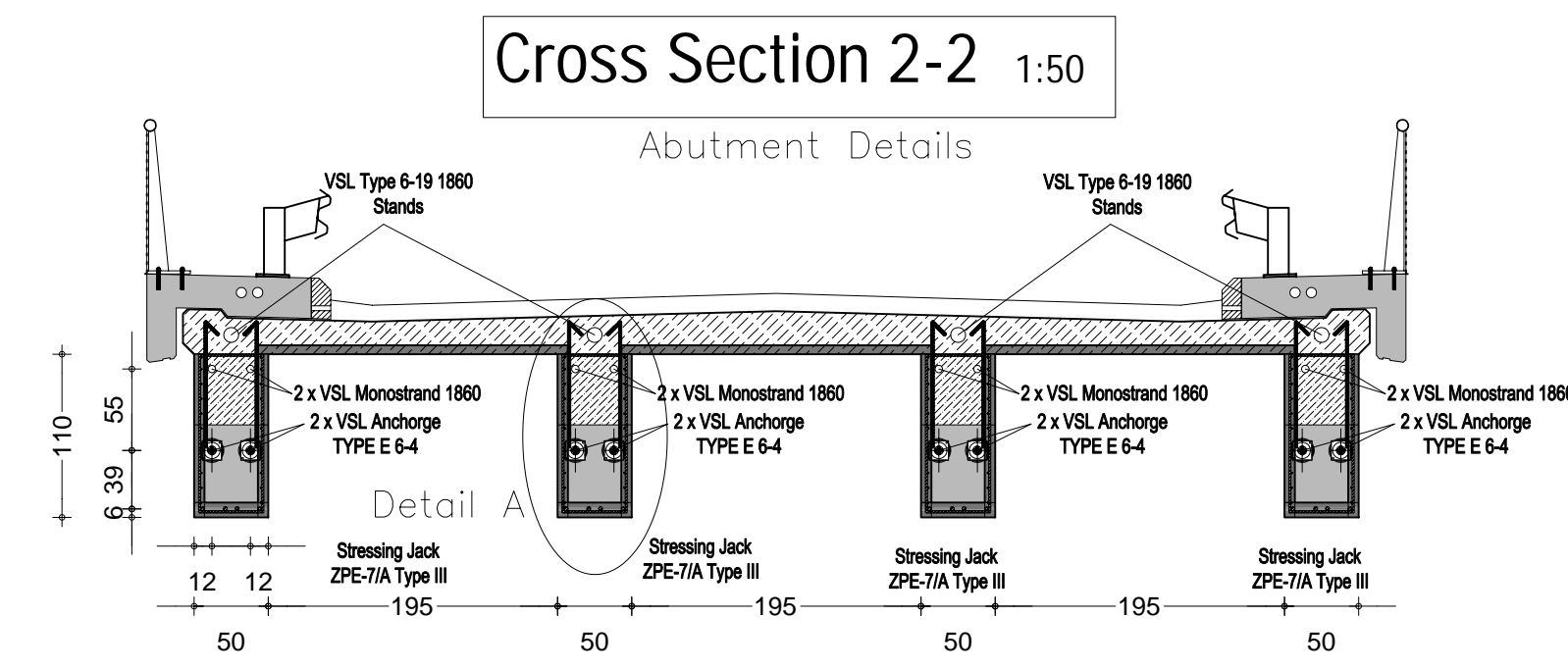
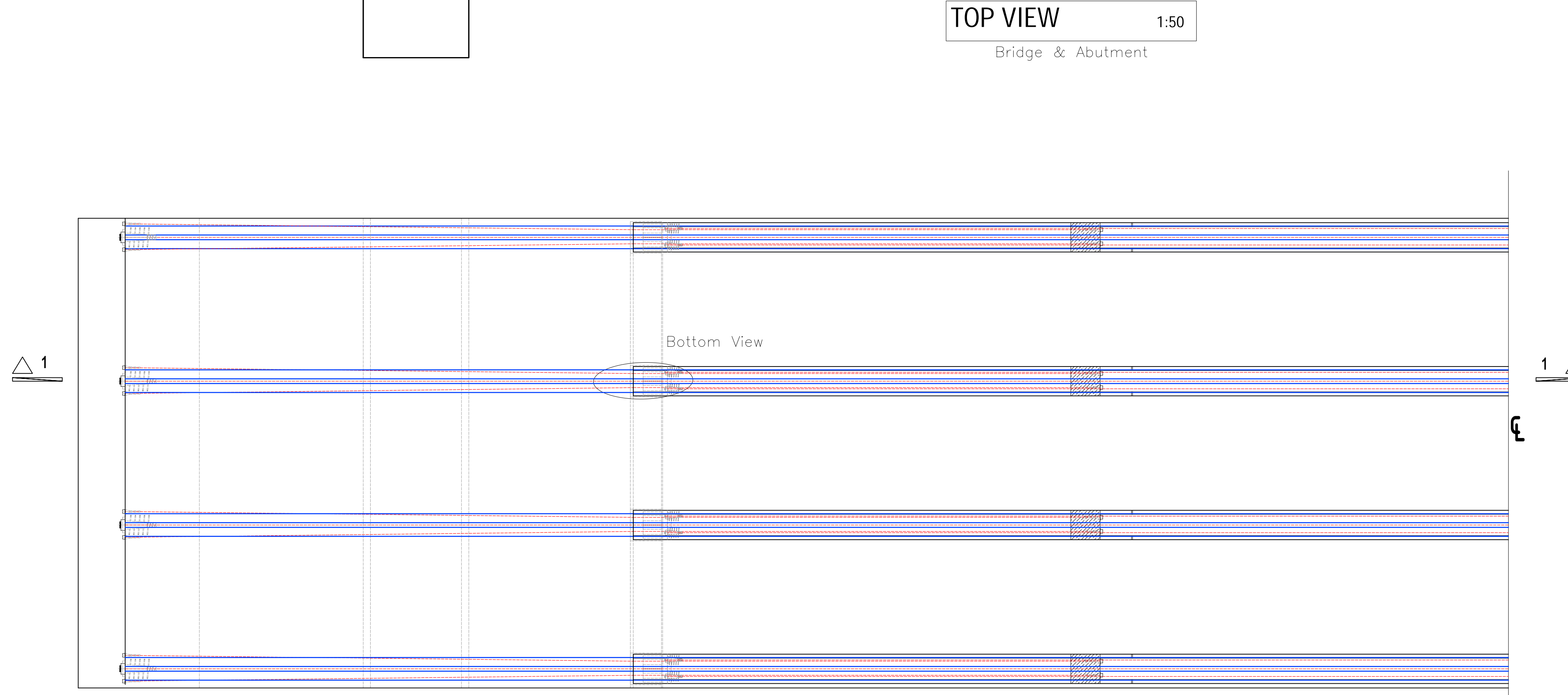
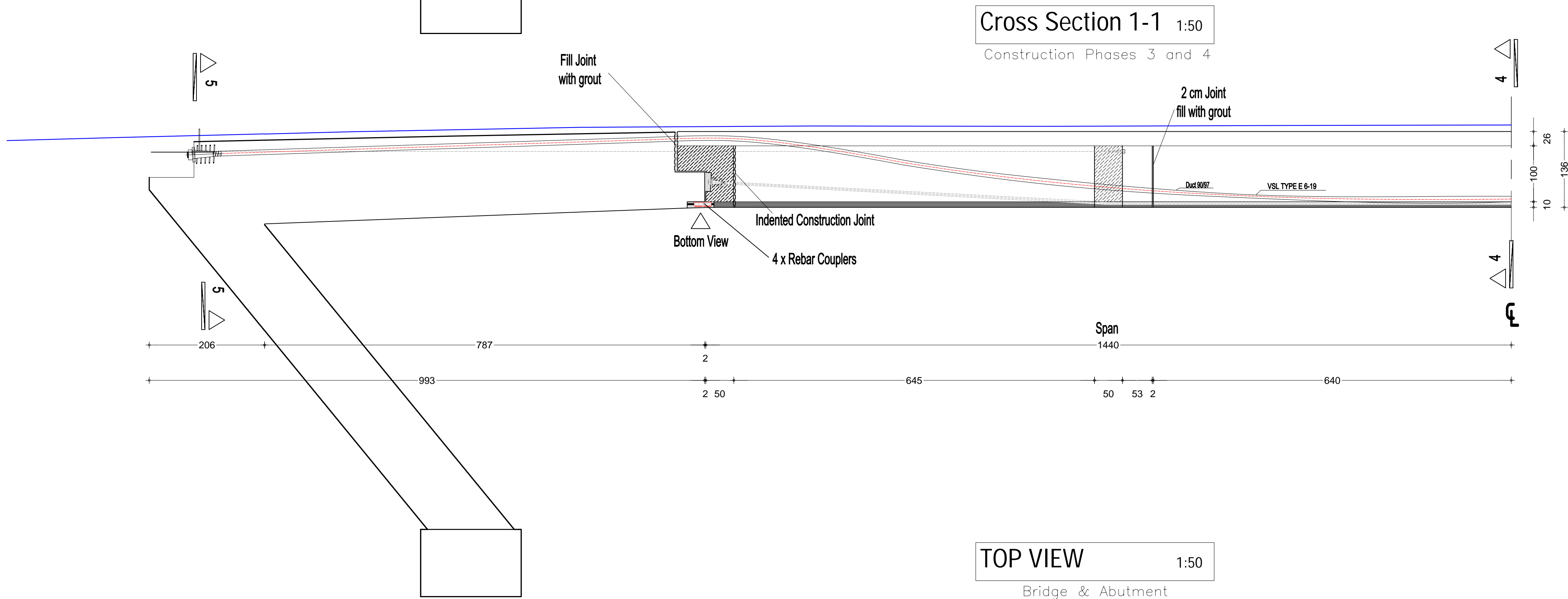
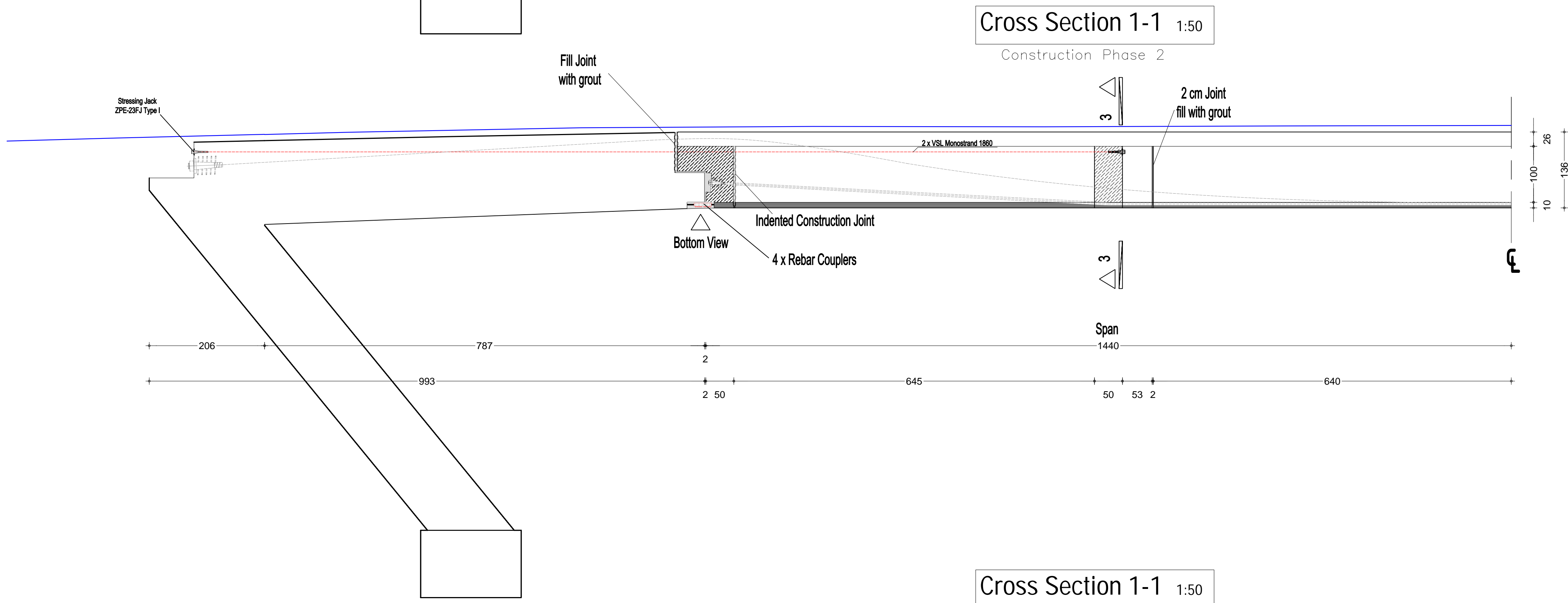
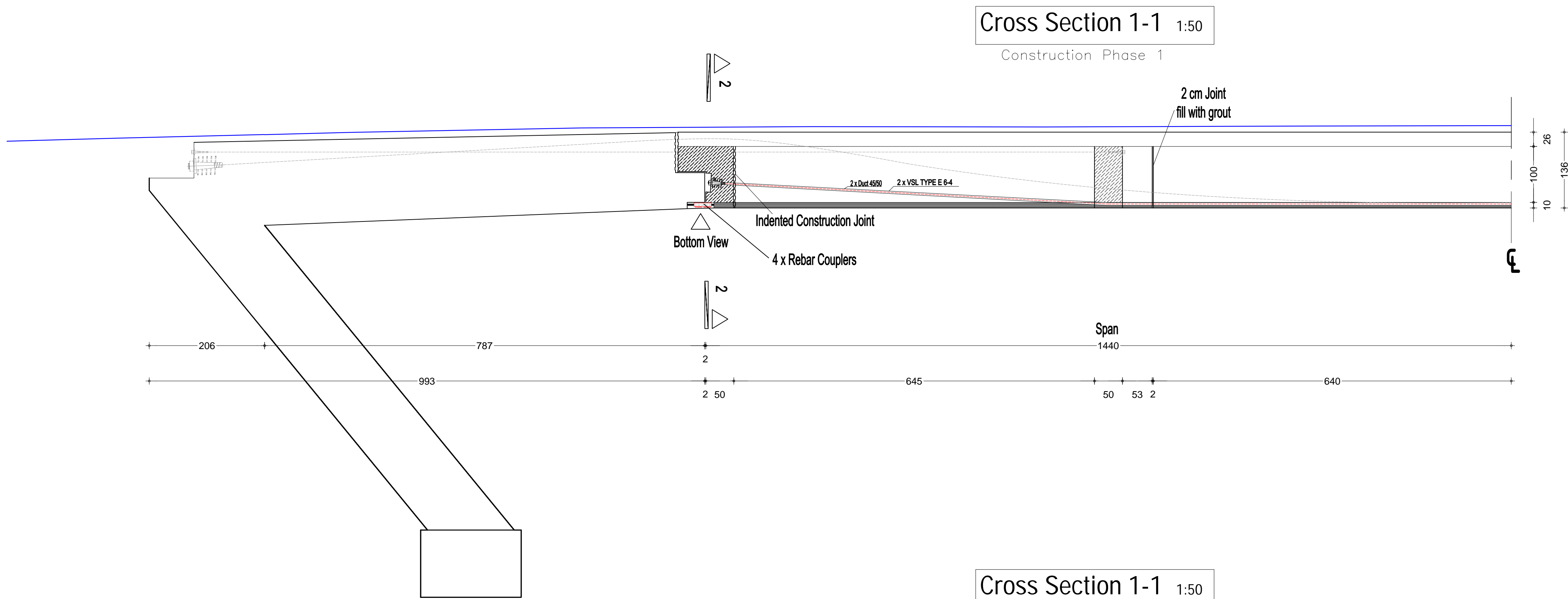
VERKEHRSLASTEN

gemäß ÖNORM-EN 1991-2 (Ausg. 2004-08-01) und ÖNORM-B  
1991-2 (Ausg. 2004-08-01) unter Berücksichtigung der im  
Technischen Bericht beschriebenen Einschränkungen

PROJECT	
Drawn	Rescon
Date	Jan. 2014
Size	1.58 m <sup>2</sup>
Content	Integral Bridge Construction Phases
SCALE	1 : 50
PLAN	1/2

[1] ASFINAG Autobahn Service GmbH  
Nordbestandsübersichtspläne A1 Westautobahn, 2010





PROJECT				
Drawn		Date	Size	
Rascon		Jan. 2014	A0	
Content	Integral Bridge Construction Phases			SCALE
				1 : 50
				PLAN
				2/2